



SAPIENZA
UNIVERSITÀ DI ROMA

Università degli Studi di Roma "La Sapienza"

DIPARTIMENTO DI INGEGNERIA CHIMICA, MATERIALI, AMBIENTE

Corso di Dottorato di ricerca in Ingegneria chimica XXX ciclo

Buccal and Topical drug delivery

Candidato:

Gabriele Varani

Relatore:

Chiar.ma Prof.ssa

Alessandra Adrover

Buccal and Topical drug delivery

Ph.D Thesis. Sapienza-University of Rome

Author: Gabriele Varani, Roma, 2017

email: gabriele.varani@uniroma1.it

This thesis has been typeset by L^AT_EX and the Book class.

A thesis submitted in partial fulfillment of the requirements for the degree
of Doctor of Philosophy in Ingegneria chimica.

Ottobre 2017

Thesis not yet defended.

Dedicated to ***Riccardo***.....
.....*perchè vorrei portarti in tutti i
posti che sogni.*

Abstract

The aim of this work is to investigate new and classical techniques, methods and formulations for topical and buccal release.

All the formulations proposed are based on natural and biocompatible polymer matrices such as gellan gum, scleroglucan and hydroxypropylmethylcellulose.

The proposed formulations are tested by in vitro release tests. In fact they represent a valid support and a useful starting point for the realization of a potentially usable in-vivo pharmaceutical formulation that may have commercial utility.

The research work is both experimental and theoretical. Each topic presents a more chemical-pharmaceutical part, based on the formulation preparation and release experiments, and a more theoretical-numerical approach that allows a correct interpretation and description of the experimental data obtained.

Release from hydrogels and thin films require different modelling approaches. Also the physico-mathematical description of different release experiments (different release devices such as Franz cell, millifluidic device and USP II) requires different theoretical and numerical techniques.

The outcome of an accurate model development is of fundamental importance for future design of pharmaceutical formulations with prescribed release properties.

In addition the formulations are investigated through rheological, mechanical, thermo-analytic and mucoadhesive tests in order to have a more comprehensive picture of their practical utilization.

Contents

1	General Introduction	1
1.1	Thin films for buccal drug delivery	1
1.1.1	Anatomy of the oral mucosa	2
1.1.2	Oral thin films: a general presentation	6
1.1.3	Polymers for the preparation of thin films	8
1.1.4	Mucoadhesive properties of buccal films	9
1.1.5	Films evaluation	10
1.1.6	Manufacturing techniques	13
1.1.7	In vitro dissolution testing of buccal thin films	15
1.2	Hydrogels for topical drug delivery	19
1.2.1	Anatomy of skin	20
1.2.2	Formulation design of Hydrogels	23
1.2.3	Hydrogels evaluation	27
1.2.4	In vitro release from Hydrogels	29
1.3	Oral thin films and Hydrogels in this work	33
1.3.1	Gellan gum, HPMC, Scleroglucan	33
1.3.2	Cyclodextrins(CD)	36
2	Aim of the work	41
3	Scleroglucan based hydrogel for topical drug delivery	43
3.1	Introduction	43
3.2	Materials and methods	44
3.2.1	Chemicals	44
3.2.2	Synthesis of carboxymethyl scleroglucan (<i>Scl</i> – <i>CM</i> ₃₀₀)	44
3.2.3	Hydrogel preparation	44
3.2.4	Rheological characterization	45
3.2.5	Release studies with Franz diffusion cell	45
3.2.6	Mathematical models of permeation experiments in a vertical Franz cell	46
3.2.7	Primary skin irritation experiments	48
3.3	Results	49
3.3.1	Physical hydrogel preparation and characterization	49
3.3.2	Rheological characterization of drug loaded <i>Scl</i> – <i>CM</i> ₃₀₀ physical hydrogels	49
3.3.3	Release studies	53
3.3.4	Primary skin irritation experiments	57
3.4	Conclusion	58
4	Drug delivery from Oral thin films	59
4.1	Introduction	59
4.2	Materials and method	59
4.2.1	Chemicals	59
4.2.2	Film forming technology	60

4.2.3	Thermogravimetric analysis	60
4.2.4	Swelling	61
4.2.5	USP II, Paddle apparatus	62
4.2.6	Novel millifluidic device	62
4.3	Results	65
4.3.1	Swelling model for OTF	65
4.3.2	Drug release time scales	69
4.3.3	Model of release	71
4.3.4	2D-Model	75
4.4	Conclusion	79
5	Release analysis from HPMC based erodible thin films	81
5.1	Introduction	81
5.1.1	Rapid disintegrating film (RDF)	81
5.1.2	Furosemide features	82
5.2	Materials and method	83
5.3	Results and discussion	84
5.3.1	Preliminary analysis	84
5.3.2	Release from Franz Cell	85
5.3.3	Swelling-Erosion tests	95
5.3.4	Sotax Vs Millifluidic device	96
5.4	Conclusion	98
6	Preventing drug crystallization in glycerol-plasticized gellan gum thin films	99
6.1	Introduction	99
6.2	Materials and method	100
6.2.1	Materials	100
6.2.2	Preparation of polymeric films	100
6.2.3	Preparation of inclusion complex cyclodextrins-drug	101
6.2.4	Rheological studies	101
6.2.5	Thickness measurements	101
6.2.6	Thermogravimetric analysis	101
6.2.7	Differential scanning calorimetry	101
6.2.8	Tensile tests	102
6.2.9	Swelling studies	102
6.2.10	Mucoadhesion tests	102
6.2.11	Uniformity of drug content tests	102
6.2.12	In vitro release studies	103
6.3	Results and discussion	103
6.3.1	Preparation of GG:Gly thin films	103
6.3.2	Mechanical properties of GG:Gly thin films	106
6.3.3	Swelling studies	108
6.3.4	Evaluation of the mucoadhesive properties of GG:Gly thin films	108
6.3.5	Drug loaded films	109
6.3.6	Release studies	113
6.4	Conclusion	115
7	General conclusions	117
	Bibliography	119

Chapter 1

General Introduction

1.1 Thin films for buccal drug delivery

The oral route is the most important method of administration for systemic effect, due to low cost, ease of administration and high level of patient compliance. Among the pharmaceutical dosage form for oral delivery, the conventional tablet seems to be most popular, because of its ease of transportability and comparatively low manufacturing cost [1]. Nonetheless, two main types of disadvantages can be ascribed to the oral route: first pass drug metabolism in the liver and pre-systemic elimination of the drug in the gastrointestinal tract (GI first pass) could lessen the effective bioavailability to an unacceptable level, or even destroy the drug, as it is the case of biological active ingredients as proteins and peptides; moreover, a fast administration of emergency drugs and agents with a rapid onset action could not be possible [2]. In these cases, the traditional choice is parenteral drug administration, which is, on the patient side, uncomfortable, uneasy and undesired. Difficulties associated with parenteral delivery and poor drug availability, together with substantial efforts focused on placing a drug or drug delivery system in a particular region of the body for extended periods of time, provided the impetus for exploring alternative routes, such as the mucosal layer lining a number of regions of the gastrointestinal tract, the airways, mouth, the ear, nose, and the eye.

Mucosal tissues can interact with the hydrophilic macromolecules of drug matrices, bringing about an adhesive attachment called mucoadhesion. This interaction retains a formulation in intimate contact with the adsorption site. The buccal region of oral cavity is the most attractive site for the delivery of drugs. Buccal drug delivery involves the administration of desired drug through the buccal mucosal membrane lining of the oral cavity. This route is useful for mucosal (local effect) and transmucosal (systemic effect) drug administration. In the first case, the aim is to achieve a site-specific release of the drug on the mucosa, whereas the second case involves drug absorption through the mucosal barrier to reach the systemic circulation [3-7].

The buccal mucosa is permeable, with a rich blood supply, more robust and have more tolerance to potential sensitizers in comparison to the other mucosal tissues. No activation of the drug absorption is required. Local modification of tissue permeability, inhibition of protease activity and reduction in immunogenic response are allowed.

On the other hand, the environment of the oral cavity presents some significant challenges for systemic drug delivery, given that the mucosa has barrier properties. The principle physiological environment of the oral cavity, in terms of pH, fluid volume and composition, is shaped by the secretion of saliva. Saliva covers the surface area of the mouth (around 217 cm^2) with a layer of average thickness 70-100 μm for adults and 60-90 μm for children. It is continuously secreted at average flow rate of 0.3-1 ml/min, but can be elicited up to 7.07 ml/min by stimulating agents; flow rates $< 0.1 \text{ ml/min}$ must be considered pathological. The volume of saliva in the mouth ranges from 0.8 ml, after swallowing, to 1.1 ml just before swallowing [8-11]. The continuous secretion of saliva

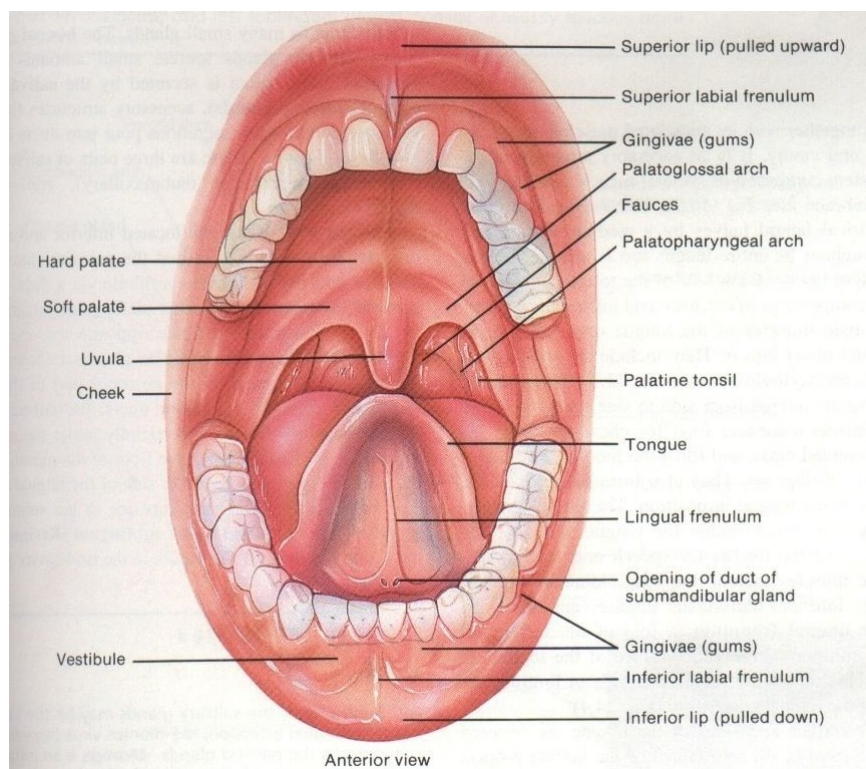


Figure 1.1: Structure of oral cavity.

leads to subsequent dilution of the drug; saliva swallowing can provoke the partial or total removal of the dosage form. The volume of saliva constantly present in the mouth, around 1 ml, provides a relatively low fluid volume available for drug release from delivery systems compared to the GI tract [12, 13].

The different types of buccal dosage forms are buccal tablets, ointments, gels, patches and thin films [14]. Over and above the mentioned demands, oral delivery systems alternative to tablets and syrups have been of interest since the latest 1970's, as a possible improvement for a particular, and not so small, class of patients who have difficulties in swallowing. This disorder affects more frequently for old people, children and mentally illness, but the oral administration without swallowing could be helpful also for travelling or military patients who may not have ready access to water [15, 16].

1.1.1 Anatomy of the oral mucosa

Buccal region is that part of the mouth bounded anteriorly and laterally by the lips and the cheeks, posteriorly and medianly by the teeth and/or gums, and above and below by the reflections of the mucosa from the lips and cheeks to the gums.

Numerous racemose, mucous, or serous glands are present in the sub mucous tissue of the cheeks. The buccal glands are placed between the mucous membrane and buccinator muscle: they are similar in structure to the labial glands, but smaller (figure 1.1).

About five, of a larger size than the rest, are placed between the masseter and buccinator muscles around the distal extremity of the parotid duct; their ducts open in the mouth opposite the last molar tooth. They are called molar glands. Maxillary artery supplies blood to buccal mucosa and blood flow is faster and richer (2.4ml/min/cm²) than that in the sub lingual, gingival and palatal regions, thus facilitates passive diffusion of drug molecules across the mucosa.

The thickness of the buccal mucosa is measured to be 500–800 μm and is rough textured, hence suitable for retentive delivery systems. The turnover time for the buccal

epithelium has been estimated at 5–6 days. Buccal mucosa composed of several layers of different cells as shown in figure 1.2. The epithelium is similar to stratified squamous epithelia found in rest of the body and is about 40–50 cell layers thick.

Lining epithelium of buccal mucosa is the nonkeratinized stratified squamous epithelium that has thickness of approximately 500–600 μm and surface area of 50.2 cm^2 . Basement membrane, lamina propria followed by the sub mucosa is present below the epithelial layer. Lamina propria is rich with blood vessels and capillaries that open to the internal jugular vein [17].

The barriers such as saliva, mucus, membrane coating granules, basement membrane etc retard the rate and extent of drug absorption through the buccal mucosa. The main penetration barrier exists in the outermost quarter to one third of the epithelium.

Oral mucosa, a barrier to permeability

The effective permeability coefficient (P_{eff}) values reported in the literature across the buccal mucosa for different molecules range from a lower limit of $2.2 \cdot 10^{-9}$ cm/s for dextran 4000 across rabbit buccal membrane to an upper limit of $1.5 \cdot 10^{-5}$ cm/s for both benzylamine and amphetamine across rabbit and dog buccal mucosa, respectively. This range clearly demonstrates the presence of a permeability barrier in the oral mucosa, which is mostly imposed by the oral epithelium acting as a protective layer for the tissues beneath, and as a barrier to the entry of foreign material and microorganisms. However, this range is estimated to be 4–4000 times more permeable than that of skin. The permeability barrier property of the oral mucosa is predominantly due to inter cellular materials derived from the so-called "membrane coating granules" (MCGs). MCGs are spherical or oval organelles that are 100–300 nm in diameter and found in both keratinized and non-keratinized epithelia.

These organelles have also been referred to as "small spherically shaped granules", "corpusula", "small dense granules", "small lamellated bodies", "lamellated dense bodies", "keratinosomes", "transitor dense bodies", and "cementsomes". However, most of these descriptive names have not fully defined the functions of this cellular species. MCGs were first named as such because it was believed that they were subject to exocytosis from the cytoplasm of the stratum spinosum of keratinized epithelia following thickening of these cells. Nonetheless, it is actually the contents of MCGs that are subject to exocytosis prior to the onset of membrane thickening.

The main mechanisms responsible for the penetration of various substances include simple diffusion (paracellular, transcellular), carrier-mediated diffusion, active transport, and pinocytosis or endocytosis. Recent evidence has shown that passive diffusion is the primary mechanism for the transport of drugs across the buccal mucosa, although carrier-mediated transport has been reported to have a small role.

Two routes of passive transport are available in the buccal epithelium (figure 1.3); one involves the transport of compounds through the inter cellular spaces between the cells (paracellular), and the other involves passage into and across the cells (transcellular). Depending on the nature of the permeant, the molecular geometry, lipophilicity, and charge, either of the transport pathways across buccal epithelium can be selected. While considerable evidence has been presented to document that most compounds diffuse through the buccal mucosa by passive diffusion or simple Fickian diffusion, some are transported by a carrier mediated process across the buccal mucosa. Glucose, monocarboxylic acids and salicylic acid, and nicotinic acid, are examples of substances which utilize a carrier-mediated diffusion mechanism for permeation across buccal epithelium [18].

Mucus

The epithelial cells of buccal mucosa are surrounded by the intercellular ground substance called mucus with the thickness varies from 40 μm to 300 μm . Though the sublingual glands and minor salivary glands contribute only about 10% of all saliva, together they produce the majority of mucus and are critical in maintaining the mucin layer over the

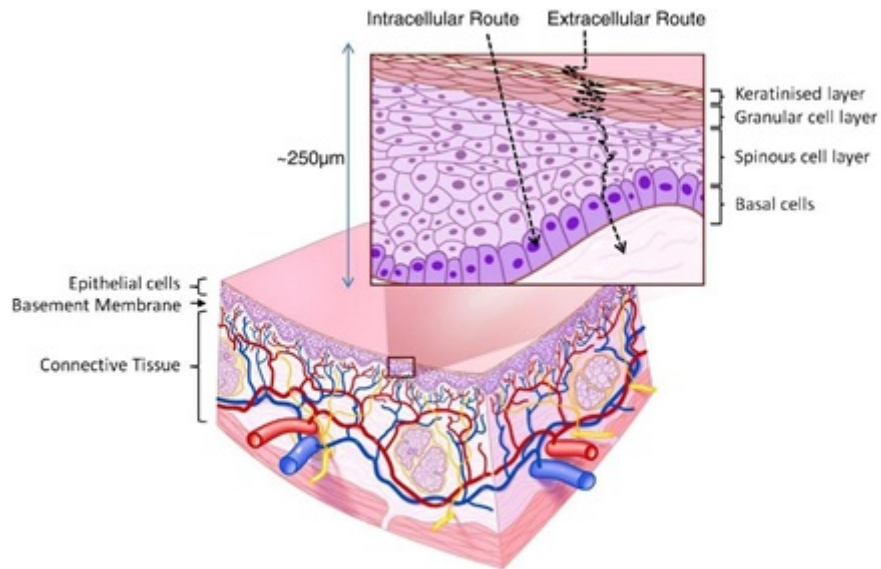


Figure 1.2: A sketch of the buccal mucosa.

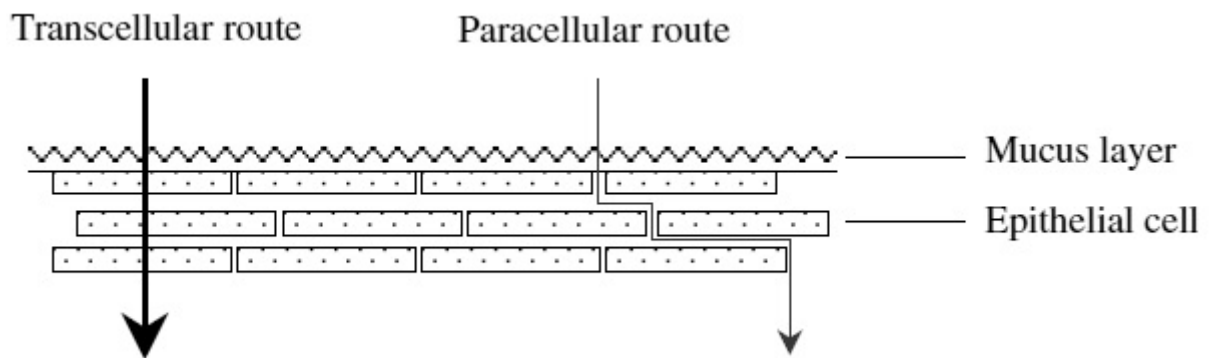


Figure 1.3: Schematic representation of penetration routes in buccal drug delivery.

oral mucosa. It serves as an effective delivery vehicle by acting as a lubricant allowing cells to move relative to one another and is believed to play a major role in adhesion of mucoadhesive drug delivery systems.

At buccal pH, mucus can form a strongly cohesive gel structure that binds to the epithelial cell surface as a gelatinous layer. Mucus molecules are able to join together to make polymers or an extended three-dimensional network. Different types of mucus are produced, for example G, L, S, P and F mucus, which form different network of gels. Other substances such as ions, protein chains, and enzymes are also able to modify the interaction of the mucus molecules and, as a consequence, their bio-physical properties.

Mucus is composed chiefly of mucins and inorganic salts suspended in water. Mucins are a family of large, heavily glycosylated proteins composed of oligosaccharide chains attached to a protein core. Three quarters of the protein core are heavily glycosylated and impart a gel like characteristic to mucus. Mucins contain approximately 70–80% carbohydrate, 12–25% protein and up to 5% ester sulphate.

The dense sugar coating of mucins gives them considerable water-holding capacity and also makes them resistant to proteolysis, which may be important in maintaining mucosal barriers. Mucins are secreted as massive aggregates by prostaglandins with molecular masses of roughly 1 to 10 million Da. Within these aggregates, monomers are linked to one another mostly by non covalent interactions, although intermolecular disulphide bonds also play a role in this process.

Oligosaccharide side chains contain an average of about 8–10 monosaccharide residues of five different types namely L-fucose, D-galactose, N-acetyl-D-glucosamine, N-acetyl-D-galactosamine and sialic acid. Amino acids present are serine, threonine and proline. Because of the presence of sialic acids and ester sulfates, mucus is negatively charged at physiological salivary pH of 5.8–7.4 [19–21].

Saliva

The mucosal surface has a salivary coating estimated to be 70 μm thick, which act as unstirred layer. Within the saliva there is a high molecular weight mucin named MG1 that can bind to the surface of the oral mucosa so as to maintain hydration, provide lubrication, concentrate protective molecules such as secretory immunoglobulins, and limit the attachment of microorganisms. Several independent lines of evidence suggest that saliva and salivarymucin contribute to the barrier properties of oral mucosa.

The major salivary glands consist of lobules of cells that secrete saliva; parotids through salivary ducts near the upper teeth, submandibular under the tongue, and the sublingual through many ducts in the floor of the mouth. Besides these glands, there are 600–1000 tiny glands called minor salivary glands located in the lips, inner cheek area (buccal mucosa), and extensively in other linings of the mouth and throat.

Total output from the major and minor salivary glands is termed as whole saliva, which at normal conditions has flow rate of 1–2 ml/min. Greater salivary output avoids potential harm to acid-sensitive tooth enamel by bathing the mouth in copious neutralizing fluid.

With stimulation of salivary secretion, oxygen is consumed and vasodilator substances are produced; and the glandular blood flow increases, due to increased glandular metabolism.

Saliva is composed of 99.5% water in addition to proteins, glycoproteins and electrolytes. It is high in potassium (7·plasma), bicarbonate (3·plasma), calcium, phosphorous, chloride, thiocyanate and urea and low in sodium(1/10·plasma).

The normal pH of saliva is 5.6–7. Saliva contains enzymes namely α -amylase (breaks 1–4 glycosidic bonds), lysozyme (protective, digests bacterial cell walls) and lingual lipase (break down the fats). Saliva serves multiple important functions. It moistens the mouth, initiates digestion and protects the teeth from decay. It also controls bacterial flora of the oral cavity. Because saliva is high in calcium and phosphate, it plays a role in mineralization of new teeth repair and precarious enamel lesions. It protects the teeth

by forming “protective pellicle”. This signifies a saliva protein coat on the teeth, which contains antibacterial compounds.

However, salivary flow rate may play role in oral hygiene. Intraoral complications of salivary hypofunction may cause candidiasis, oral lichen planus, burning mouth syndrome, recurrent aphthous ulcers and dental caries.

A constant flowing down of saliva within the oral cavity makes it very difficult for drugs to be retained for a significant amount of time in order to facilitate absorption in this site.

In general, intercellular spaces pose as the major barrier to permeation of lipophilic compounds, and the cell membrane which is lipophilic in nature acts as the major transport barrier for hydrophilic compounds because it is difficult to permeate through the cell membrane due to a low partition coefficient. Permeabilities between different regions of the oral cavity vary greatly because of the diverse structures and functions. In general, the permeability is based on the relative thickness and degree of keratinization of these tissues in the order of sublingual > buccal > palatal. The permeability of the buccal mucosa was estimated to be 4–4000 times greater than that of the skin [13,17,18,22,23].

1.1.2 Oral thin films: a general presentation

Similar in size, shape and thickness to a postage stamp, pharmaceutical thin films (figure 1.4) were developed from skin patches technology. They firstly appeared in the 1970’s as breath mint in the confectionery industry and gradually spread in cosmetics, nutraceutical and over-the-counter products. After the approval of Zuplenz and Ondasetron from the Food and Drug Administration (USA) in 2010, they can be considered now as the most advanced oral solid dosage form [24,25]. Pharmaceutical thin films are equivalently called in literature “strips”, “dissolving films” and “orodispersible films” by the European Medicines Agency [26,27]. Also the term “wafer” is improperly used, although this word refers to a similar kind of dosage form. Pharmaceutical films are typically designed to be placed on or under the tongue for oral administration, but they can be used in principle for any other mucosal tissue [28].

Films for oral administration are equivalently called “buccal” or “oral” films. Depending on thickness and disintegration time, three categories can be qualitatively identified. In order of size (increasing): flash release films, mucoadhesive melt-away wafers and mucoadhesive sustained release wafers [29]. Disintegration time is usually scaled to thickness. In the present default of any standardized definition or method, this classification should be considered merely suggestive. Focus of this work is mainly on films with thickness < 100 μ m.



Figure 1.4: Oral thin films(OTF).

In contact with biological fluids, films rapidly disintegrate and dissolve to release the medication, in the mouth (buccally or sublingually) and/or via the small intestines (enterically), without the need of water and improving the efficacy of the active ingredients. In the mouth, a thin film gets instantly wet by saliva, rapidly hydrates and adheres onto the site of application. [30]. Unlike other rapid dissolving dosage forms, films can be produced with a manufacturing process that is competitive with the manufacturing costs of conventional tablets [31]. Just few drugs have been already commercialized in this form because of the complexity associated mainly with its novelty. Among marketed products, there are anti-emetic, antihistaminic, analgesic. The first marketed product under medical prescription has been Zuplenz/Ondasetron.

An extensive pioneer medical work exploring the administration of this drug in oral strips is [32]. Strips have been recognized as an effective and highly patient compliant drug delivery system [33]. Compliance is significant in particular when considering cases of mental-illness, emesis, or children, geriatric, dysphagic patients. In addition, pharmaceutical industries show an increasing interest in oral films, as they can be used to elongate patent-life of existing active principles by a new administration form [34,35].

In summary, the principal advantages of oral strips are [36–38,55]:

- unobstructivity, high compliance for patients with swallowing problems, no special training is required for the administration of dosage form;
- no need of water, drug is wet by saliva;
- quick dissolution and release, with a relatively large surface area and a very high ratio area/thickness, for rapid wetting;
- precision in the administered dose is ensured from each of the strips;
- systemic and local action;
- they can be mucoadhesive;
- overcoming of first pass effect;
- to be not so brittle as oral dissolving tablets, and so there are less transport and storage difficulties;
- no special set up for industries are required and production costs are competitive;
- new business opportunities, like patent extension, product promotion and product differentiation.

On the other hand, most significant disadvantages are:

- expensive packaging, since the dosage form is moisture sensitive;
- taste masking of drug should be done and there are limited taste masking options;
- drugs which irritate the mucosa are forbidden;
- high doses of drug cannot be incorporated.

OTF are typically made of [39]:

- a film-forming hydrophilic polymer (around 45% by weight);
- an active pharmaceutical ingredient (API, up to 30 %);
- plasticizer (0-20 %);
- other additives, such as fillers, surfactants, saliva stimulating agents and sweetening agents (up to % 40).

Drug and polymer are the essential components of OS. Knowledge and techniques about including drugs in thin films have been continuously increasing in the last ten years [40–54]. Desiderable characteristics are a low required dose (< 40 mg), low molecular weight, possibly good taste.

The drug should also be stable and soluble both in saliva and water and partially unionized in water. The active component must be able to pass the mucosa barrier, not provoking irritations. Eligible API are anti emetic, neuroleptics, cardiovascular agents, analgesics, anti allergic, anti epileptics, anxiolytics, sedatives, hypnotics, diuretics, antiparkinsonism agents, anti-bacterial agents and drugs used for erectile dysfunction, antialzheimers, expectorants, antitussive. For mucosal and transmucosal administration, conventional dosage forms are not able to assure therapeutic drug levels in the mucosa and circulation because of the physiological removal of the oral cavity (washing effect of saliva and mechanical stress), which take the formulation away from the mucosa, resulting in a very short exposure time and unpredictable distribution of the drug on the site of action/absorption. To obtain the therapeutic action, it is therefore necessary to prolong and improve the contact between the active substance and the mucosa [20].

1.1.3 Polymers for the preparation of thin films

Polymers are the backbone of film formulations and various polymers are available for the preparation of thin films [55]. The polymers can be used alone or in combination with other polymers to achieve the desired film properties. The polymers employed should be non-toxic, non-irritant, and absence of leachable impurities is required. Water-soluble polymers are used as film formers to produce a thin film with rapid disintegration, good mechanical strength, and good mouth feel effects. Both natural and synthetic polymers are used for film preparation [56, 57]. Availability of diverse polymers allows imparting specific properties in the thin films. For instance, gelatine are available in different molecular weights, and thus the appealing and glossy films could be obtained with the gelatin having a high molecular weight. Pullulan is frequently used for producing a thin film with great solubility, high mechanical strength and they are stable over a wide range of temperatures. The blending of chitosan and high methoxy pectin (HMP) or low methoxy pectin (LMP) resulted in a thin film exhibiting an excellent mechanical strength. The film forming polymers such as hydroxypropyl cellulose (HPC), methyl cellulose, and carboxymethyl cellulose (CMC) produce a thin film with less water vapor barrier due to hydrophilic nature which aids in water retention [58, 59].

The basic idea of pharmaceutical thin strips is exactly that a dissolved component could be immobilized in a solid film, and be released from a gel as soon as the dosage form comes in contact with biological fluids.

Natural and semi-natural polymers have also been reported in the literature as mucoadhesive. Chitosan was first introduced in 1994 by Guo for its use in mucoadhesive film formulations [68]. Following Carbopol and HPMC as polymeric matrices for mucoadhesive films, chitosan exhibited better adhesion than acacia in a peeling test using an Instron 4201.

Mucoadhesive films are thin and flexible retentive dosage forms, and release drug directly into a biological substrate. They facilitate in extending residence time at the application site leading to prolonged therapeutic effects [65]. Majority of the thin film having mucoadhesive properties are hydrophilic in nature and undergoes swelling and form a chain interaction with the mucin. Among the several studied polymers, the most compelling mucoadhesion properties are exhibited by chitosan, hyaluronan, cellulose derivatives, polyacrylates, alginate, gelatin and pectin [66]. Compared with non-ionic polymers, the cationic and anionic polymers facilitate strong interaction with mucus [67].

Plasticizers can significantly help OTF formulation. They improve mechanical properties such as flexibility and brittleness, by reducing the glass transition temperature of the filming polymer. Plasticizers should be compatible with the drug, as well as other additives used in the preparation of OTF. Most attractive plasticizers for OTF are glycerol, propylene glycol, low molecular weight polyethylene glycols, phthalate derivatives

like dibutyl phthalate, citrate derivatives such as tributyl, triethyl, acetyl citrate, castor oil [60, 61]. Improving palatability is probably the first reason that why additives are added in OTF. A simple obscuration technique, which means mixing and blending bitter tasting API with pleasurable taste substances, can be used. Also, barrier techniques, which includes complexation, polymeric coating and coated particle, have recently appeared. Sweetening and flavoring agents are typical additives for palatability improvement. Sweetening agents are the most major part of the food product or in pharmaceutical dosage forms proposed to be disintegrated or dissolved in the oral cavity. Natural as well as artificial sweetening agents are used to improve the palatability of the formulation. Common agents are sugar, dextrose, lactose, mannitol, sucrose, xylitol, malitol, acesulfame potassium, talin, glycyrrhizin, sucralose, aspartame, saccharin, essential oils or water soluble extracts of menthol, wintergreen, peppermint, sweet mint, spearmint, vanillin, cherry, chocolate, cinnamon, clove, lemon, orange. Sweetening agent are generally used either alone as in combination between the concentrations of 3 to 6 % by weight of the film. Selection of flavoring agents is depending on which type of drug is to be incorporated in the formulation. The recognition of the oral disintegrating / dissolving formulation by an individual, depends on the initial flavor quality, which is observed in the first few seconds after the product has been consumed, and on the after taste of the formulation, which lasts for at least about 10 min.

Other functional additives are surfactants and saliva stimulating agents. Surfactants are used as a solubilizing or wetting dispersing agent so that the film gets dissolved within seconds and releases active agent immediately. Some of the commonly used are sodium lauryl sulfate, benzalkonium chloride, tweens, poloxamer 407. Saliva stimulating agents, as citric acid, malic acid, lactic acid, ascorbic acid and tartaric acid, are used to increase the rate of production of saliva. This would aid in the more rapidly disintegration of fast dissolving film formation. Saliva stimulating agents are used alone as well as in combination between 2 to 6 % w/w by weight. Finally, fillers and colorants can be added to improve film's aspect and handling. Typical colorants are natural coloring agents, and natural juice concentrates, pigments such as titanium oxide, silicon dioxide and zinc oxide. Maximum colorants's concentration is 1 % by weight [62-64].

In common terms, polymers are understood as excipients, but it has become an essential component while designing and formulating thin films. Therefore, understanding the properties of polymers such as chemistry, rheology, and physicochemical properties of polymer seems to be imminent for maximizing their uses to develop a thin film. The selection of appropriate polymer during the development of polymeric thin films may be critical; thereby, several points should be considered according to the requirements. Therefore, it is imperative to consider the appropriate polymer for producing a thin film with a better performance that assures high therapeutic success.

1.1.4 Mucoadhesive properties of buccal films

Bioadhesion is the general term describing adhesion between any biological and synthetic surface. Mucoadhesion is a specific term describing the particular interaction of a mucosal membrane with a synthetic surface [69]. The phenomenon of mucoadhesion has been explained by applying any of the five theories of adhesion into the interaction of the dosage form and the biological substrate [70, 71]: electronic [72], adsorption [73, 74], wetting [75], diffusion [76], and fracture theory [77]; here, we briefly summarize theories related to mucoadhesion theory. Since mucoadhesive buccal films include the interaction of a dry polymeric matrix that undergoes hydration, drug release, and sometimes erosion, the phenomenon is very complex. Smart has defined four possible scenarios for the analysis of the mucoadhesion process based on the hydration state of the dosage form and on the amount of mucus layer available for mucoadhesion [78].

Mucoadhesive buccal films can be classified as a "case 3" scenario since they are solid dry substrates that come in contact with a mucosa having thin or discontinuous mucus layers. Relevant to the analysis of the mucoadhesion of polymeric films on the buccal mucosa are the adhesion theories of adsorption and diffusion. The adsorption

theory states that the main contributors to the adhesive bond are the inter-polymer interactions, such as hydrogen bonds and van der Waals forces [79]. The diffusion theory assumes that polymeric chains from the solid substrate, i.e. the mucoadhesive film, and the biological substrate, i.e. mucin in the mucosa layer, interdiffuse across the adhesive interface. Important variables in this process are the diffusion coefficient of the polymer into the mucin layer and vice versa, the contact time, and the molecular chain length and their mobility [79,80].

Most of the mucoadhesive phenomena have two main stages that control the performance of the dosage form: the contact stage and the consolidation stage (figure 1.5) [81]. Since mucoadhesive films are dosage forms that are brought in contact with the biological membrane by the patient, the contact stage is initiated by the patient. During the contact process, the film will start dehydrating the mucus gel layer and will itself hydrate, initiating the interpenetration of the polymeric chains into the mucus and vice versa.

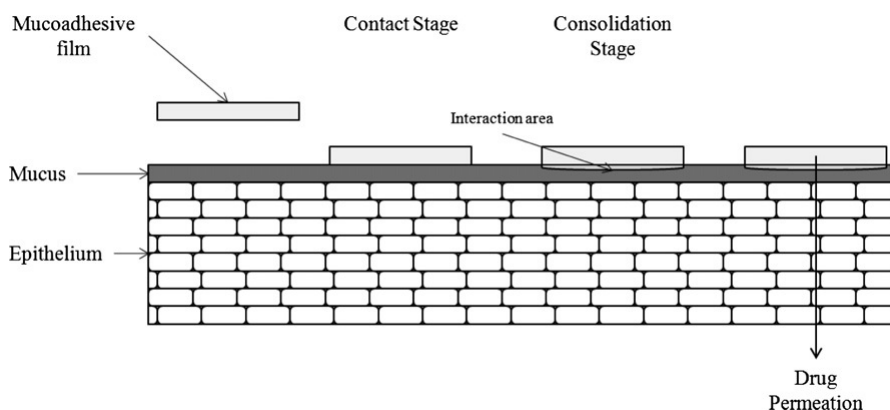


Figure 1.5: Contact and consolidation stage of mucoadhesion.

For mucoadhesive films, which usually are designed to remain for prolonged times in contact with the buccal mucosa, a second stage, the consolidation stage, needs to take place in order to maintain this bond. In the consolidation stage, the mucoadhesive strength will be determined by the polymer in the formulation, and how readily the dosage form hydrates upon contact with the mucus gel layer. This process is explained by the dehydration theory, which explains that when a material capable of gelation, such as a mucoadhesive polymer in a buccal film, is brought into contact with an aqueous viscous colloid, water will move until equilibrium is reached between the two layers [77]. The strength of the mucoadhesive bond will then be determined by the extent of intermixing that occurs after water migrates and reaches equilibrium. Mucoadhesive films have been designed to remain in contact with the buccal mucosa for therapeutic purposes for prolonged periods of time. The measurement of the mucoadhesive strength and time of mucoadhesion [82] are very important parameters.

1.1.5 Films evaluation

Many different characteristics play a significant role in production and handling of pharmaceutical strips, such as mechanical strength, structure, dissolution or storage behaviour. Tests on films assess basic properties which are meaningful in research and quality control. Here we go into details of the main type of analysis.

Tensile/mechanical properties. Mechanical properties indicate at what extent the film can withstand force or stress during processing, packaging, transport and handling. Tensile testing is usually conducted using a texture analyzer device (figure 1.6,1.7), conceptually similar to a classical stress-strain test. The film is inserted and elongated until it breaks. Tensile strength, percent elongation at break, elastic modulus (Young's modulus), tensile energy to break are measured. Some general behaviors of films observed from stress—strain curves are shown in figure 1.8. Part of the literature suggests to follow

ASTM International Test Method for Thin Plastic Sheeting D882. Moderate tensile strength and low elastic modulus are desired features. The mechanical properties of pharmaceutical strips are mainly determined by the hydrophilic polymer and plasticizer used in formulation. Typical values are tensile strength 1-30 MPa, Young's modulus 10-2000 MPa, elongation at break 1-150 % [83-86,107].

Film forming capacity and appearance. Film forming capacity and appearance

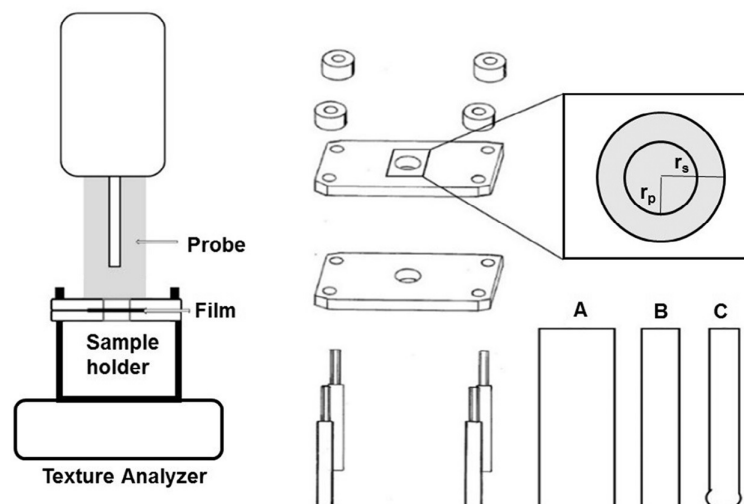


Figure 1.6: Experimental setup (left) and sample holder for the film preparation (right), where r_s indicates radius of samples, and r_p indicates radius of probe. Geometry of cylindrical probes A and B and spherical probe C is shown on the right bottom [105].

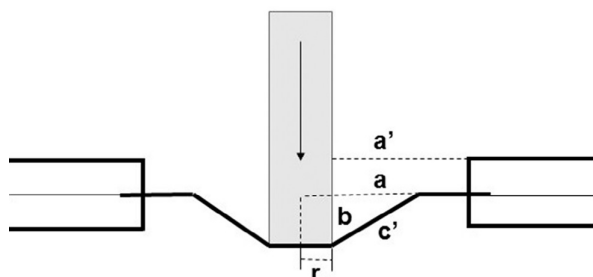


Figure 1.7: Determination of percent elongation of thin films using a texture analyzer, where a = initial length of the film in the sample holder opening, a' = initial length - radius of probe, b = displacement of the probe, $c' + r$ = length after strain, c' = length of a' after strain, r = radius of the probe [105].

of films are two qualitative concepts. Film forming capacity is the ability of film formers to form desired films. It is categorized according to strip forming capacity such as very poor, poor, average, good, very good, excellent. Appearance of strip is evaluated by visual observation such as transparent, semi transparent, opaque [87,88].

Thickness. Thickness is measured at different points (normally 5) by a micrometric screw gauge.

Folding endurance. Folding endurance is determined by folding a film up to it break at the folding point. The number of attempt required to break the film is the folding endurance value [89,90].

Solid state characterization. Solid state properties of films can be analyzed by means of differential scanning calorimetry, Fourier transform infrared spectroscopy, X-Ray diffraction [91].

Swelling properties. Hydrophilic polymers undergo swelling, which is defined as an

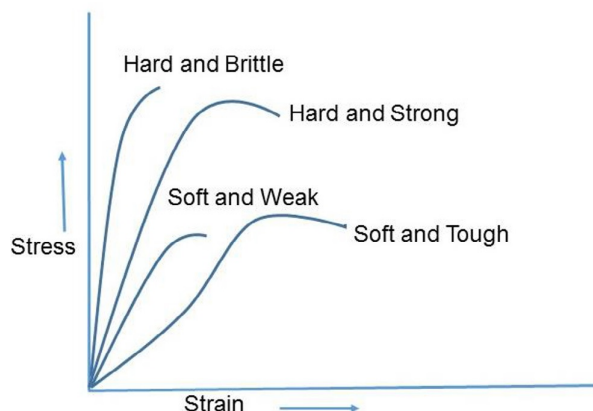


Figure 1.8: Examples of stress–strain curves obtained from polymeric thin films.

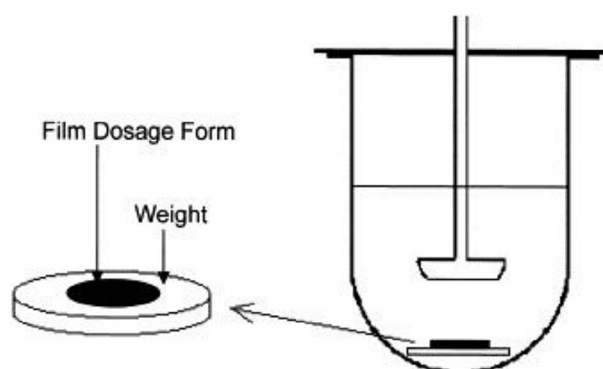


Figure 1.9: Schematic illustration of the apparatus used for dissolution studies of films.

expansion of the matrix in aqueous media. This phenomenon is simultaneous to the set-up of a gel phase. These polymers form physical-linked gels and are bio erodible. So as, a true swelling equilibrium, as in the sense of cross-linked gel such as Poly-methyl-metacrilate, does not exist. Nonetheless, a pseudo-swelling equilibrium can be individuated [92]. Swell is measured by immersing a sample in a swelling medium (generally saliva or water at fixed pH and temperature), then weighing the sample, time by time, until an equilibrium weight is reached. The film can be put in a Petri dish, in a net wire or a beaker. The swelling degree S is usually calculated as (equation (4.10)):

$$S = \frac{M - M_0}{M_0} \quad (1.1)$$

where M is the measured weight and M_0 is the initial weight. Common polymers for OTF can swell from 0.2 to 50 times, depending on the formulation [93,94].

In-vitro dissolution testing. Dissolution testing evaluates the duration of drug release from the dosage form and its pace. Dissolution tests for OTF have been performed in diffusion cells [95], USP paddle II (figure 1.9) or basket (I) apparatus, USP IV flow-through apparatus [96]. In the literature, many authors have done some improvisation on the dissolution apparatus, while others have employed Franz diffusion cells (FDC) for testing the drug release from the polymeric films. A major barrier with respect to film in dissolution testing is the placing of the samples. Several methods have been practiced, where the film is attached on the inner side of the glass vessels or the stirring element using an adhesive tape [106].

Uniformity of drug content. A prerequisite for therapeutic efficacy, safety, and regulatory approval of a medicine is drug content uniformity. Failure to achieve a high degree of accuracy with respect to the amount of drug in individual unit doses of the film

can result in therapeutic failure, non reproducible effects, and, importantly, toxic effects to the patient. Drug content is measured by dissolving a known weight of the film for analysis. An assay of film area rather than weight would be more appropriate for assessing drug content uniformity. Drug uniformity in OTF can normally have a variation of $\pm 15\%$. Drug content uniformity is a crucial aspect in film manufacturing [97].

In vitro Bioadhesion measurement. In vitro bioadhesion measurement method was first reported [98] in evaluation of the adhesive properties of patches using a microprocessor based on advanced force gauge equipment with porcine buccal membrane as a model tissue under simulated buccal conditions. Data collection and calculations were performed using the Data Plot software package of the instrument. Two parameters, namely the work of adhesion and peak detachment force were used to study the buccal adhesiveness of patches. The work of adhesion was determined from the area under force-distance curve while the peak detachment force was the maximum force required to detach the film from the tissue [107].

1.1.6 Manufacturing techniques

Manufacturing processes for OTF preparation have thrived in the last two decades. Solvent casting, semi solid casting, hot-melt extrusion, solid-dispersion extrusion, and rolling are the main technological families. An overview is presented here [99–104].

Casting solution. This technique require raw materials with few trivial prerequisites: the polymer must be soluble in a volatile solvent or water, a stable solution with a reasonable minimum solid content and medium viscosity is sought, formation of a homogeneous film and release from the casting support must be possible. Water soluble polymers-hydrocolloids good to prepare OTF include: hydroxypropylmethyl cellulose (HPMC), hydroxypropyl cellulose (HPC), Pullulan, sodium alginate, pectin, carboxymethyl cellulose (CMC), Poly-vinyl alcohol (PVA). Water-soluble ingredients are dissolved to form a clear, viscous solution. The API and other agents are dissolved apart in a suitable solvent. This second mixture is later vigorously mixed with the water solution. The entrapped air is removed by vacuum. Deaeration is necessary to obtain uniform film property and thickness. The resulting solution is cast as a film, allowed to dry, and cut into pieces to the desired size (figure 1.10). Specific types of equipment, such as rollers, are required for pouring the solution on an inert base. The clearance between the roller and the substrate determines the required thickness of the film. Drying the film, removes the solvent and helps to obtain the finished product. Usually, glass, plastic, inox or teflon plates are used as an inert base for film casting.

This manufacturing technology is the most frequent in laboratory. When transferred to production scale, several problems can be encountered, that include how casting the film, obtaining uniform thickness, and proper drying [108, 109]. Air entrapment may tend to produce non- uniform films. Deaeration step is imperative to get a uniform film which may be achieved by vacuum assisted machines.

Hot-melt extrusion. In the hot-melt extrusion (HME) process, appropriate amounts of polymer, drug, plasticizer and additives are blended into an uniform powdered mixture, prior to feeding through the hopper of the preheated extruder and be transferred into the heated barrel by a rotating extruder screw (figure 1.11). The API and other excipients are mixed in a dry state. An advantage of this process is the complete elimination of the solvent. Films cool and are cut to the desired size. The high temperature makes the process suitable only for thermostable drugs. Homogeneous films are obtained, with thickness < 1 mm [110, 111].

Semi-solid casting. Firstly, a water solution of film forming polymer is prepared. This mixture is added to a solution of an acid insoluble polymer (e.g. cellulose acetate phthalate, cellulose acetate butyrate), which was prepared in ammonium or sodium hydroxide. The appropriate amount of plasticizer is added to obtain a gel mass. Finally, the gel mass is casted in films or ribbons, using heat controlled drums. The thickness of the film is about 0.1-1.1 mm. The ratio of the acid insoluble polymer to film forming polymer should be 1:4 [112].

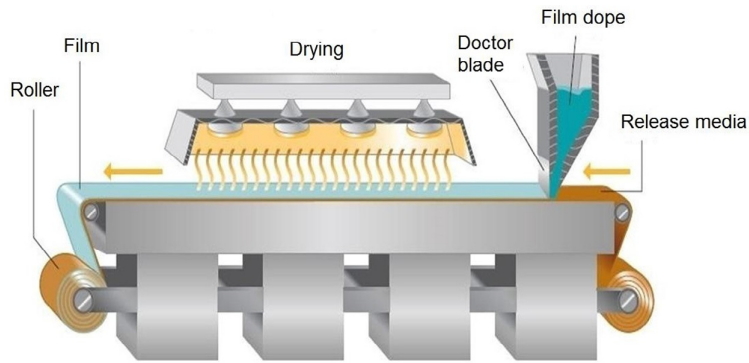


Figure 1.10: Commercial manufacturing of film based on solvent-casting [55].

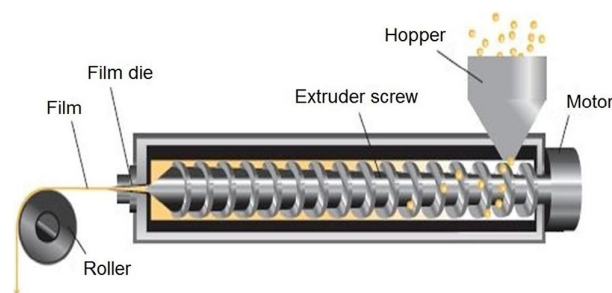


Figure 1.11: Hot-melt extrusion system for the preparation of films [55].

Solid dispersion extrusion. Immiscible components are extruded with drug, preparing solid dispersions. The latter are shaped into films by means of dies [112].

Rolling-method. The film is prepared by pre-mixing of an active ingredient and excipients, followed by subsequent addition of the solvent. The pre-mix or master batch, which includes the film-forming polymer, polar solvent, and any other additives except drug is added to the master batch feed tank. A pre-determined amount of the master batch is controllably fed via a metering pump and control valve to first and second mixers. The required amount of the drug is added through an opening in each of the mixers. After the drug has been blended with the master batch pre-mix for a sufficient time to provide a uniform matrix, a specific amount of the uniform matrix is then fed to the pan through the second metering pump. The film is finally formed on the inert substrate and carried away via the support roller (figure 1.12). Thus the wet film is then dried using controlled bottom drying, desirably in the absence of external air currents or heat on the top (exposed) surface of the film [113].

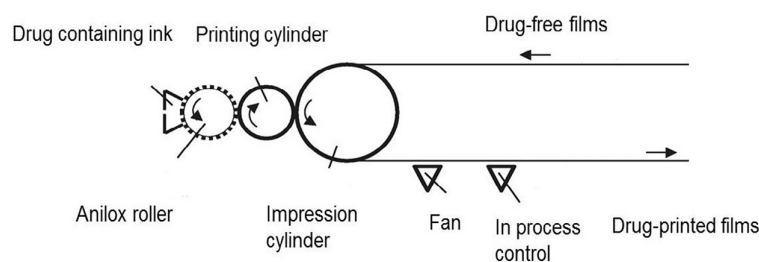


Figure 1.12: Schematic overview of Rolling-print technology for the preparation of films [55].

1.1.7 In vitro dissolution testing of buccal thin films

Absorption of drugs in living organisms schematically depends on three steps [114]:

- release from the dosage form;
- dissolution or solubilization of the drug under physiological conditions;
- permeability across targeted tissues.

The purpose of in-vitro dissolution testing is to offer substantial information about steps 1 and 2, without resorting to test animals. Because of the critical nature of the first two of these steps, in-vitro dissolution testing may be relevant to the prediction of in-vivo performance. It concerns all solid pharmaceutical dosage forms. Most common applications of dissolution testing are:

- assess the lot-to-lot quality of a drug product;
- guide development of new formulations;
- ensure continuing product quality and performance after certain changes, such as changes in the formulation, the manufacturing process, the site of manufacture, and the scale-up of the manufacturing process.

New drug applications (NDAs) submitted to the Food and Drug Administration (FDA) contain bio availability data and in-vitro dissolution data, that, together with chemistry, manufacturing, and controls (CMC) data, characterize the quality and performance of the drug product. In-vitro specifications for generic products should be established based on a dissolution profile. For new drug applications, as well as generic drug applications, dissolution specifications should be based on acceptable clinical, bio availability, and/or bio equivalence batches. Dissolution specifications are set depending on the class of the active substance, with the aim of predicting the likelihood of achieving a successful in vivo-in vitro correlation (IVIVC). FDA Bio pharmaceuticals Classification System (BCS) divides active substances in four classes high permeability-high solubility (1), low solubility - high permeability (2), high solubility - low permeability (3), low solubility - low permeability (4). This classification is focused on oral administration and it is derived from a classical mathematical model of drug absorption through the bowels [115].

Considering the release time, drugs are classified as "immediate release" if 85 % of the substance is released from the dosage form in 30-45 min. Slower dissolution corresponds to modified release dosage forms, such as extended and delayed release [116]. The agencies responsible of dissolution testing standardization are the national Pharmacopeias.

In the last thirty years, European Pharmacopeia, Japanese Pharmacopeia and US Pharmacopeia have been working for a common harmonization of dissolution testing procedures. Thanks to this, regulatory requirements have progressively reached a good grade of agreement [117, 118].

Buccal films have not been included yet in any standardization. At present all literature works have assumed traditional oral dissolution as a starting point [119].

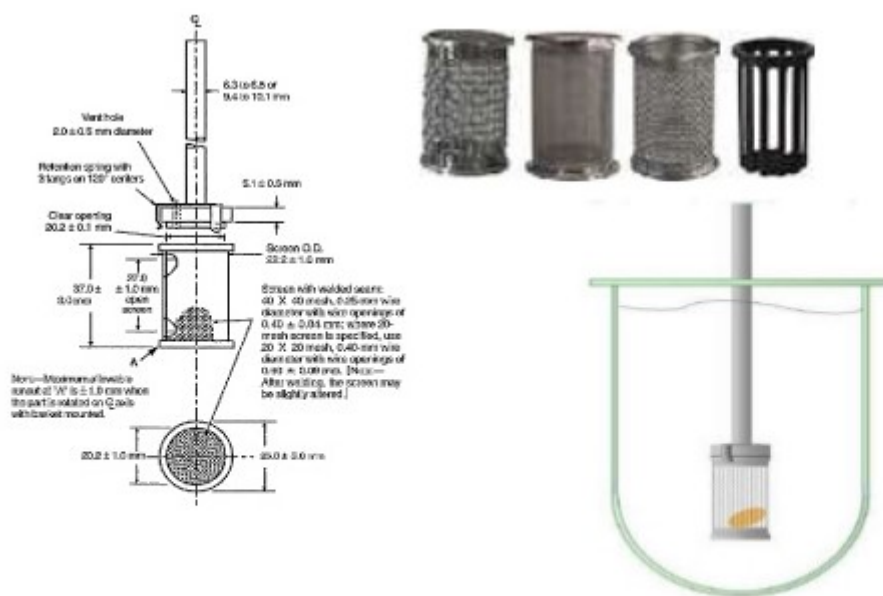
Some words in the nomenclature of dissolution testing [120]:

- **apparatus:** the basic unit for the in-vitro performance testing of dosage units. The apparatus consists of a container (vessel) for the dosage unit and dissolution medium, a device for promoting motion of the dissolution medium (stirring element), temperature control and support to hold the vessel and stirring element in a fixed orientation. Typically, six to eight apparatuses are grouped in a dissolution test assembly.
- **stirring element:** a paddle, rotating basket and shaft, or other device for promoting the movement of dissolution medium relative to the dosage unit under test.

- **assembly:** a combination of multiple apparatuses providing temperature control, controlled unified motion of stirring elements, and providing the opportunity for simultaneous or individual start of the apparatuses.
- **dissolution system:** test assembly connected to sampling and filter unit but without instrumentation such as UV/VIS spectrophotometer or HPLC chromatograph.

Four different apparatuses are in use [121]:

- Basket apparatus (USP 1), figure 1.13;
- Paddle apparatus (USP 2), figure 1.14;
- Reciprocating Cylinder (USP 3), not accepted in the Japanese Pharmacopeia, figure 1.15;
- Flow through cell (USP 4), figure 1.16.



USP TYPE I: BASKET TYPE APPARATUS

Figure 1.13: USP1-Basket apparatus.

Immediate-release, modified release and extended release tablets are usually tested in dissolution baths, using USP 2 paddles. Floating capsules and tablets generally prefer USP 1 baskets [122, 123]. Both USP 1 and UPS 2 apparatuses comprehend a stirred vessel with nominal capacity from 1 to 4 liters. They differ only in the stirring element. USP 2 is generally recommended as the first choice in dissolution apparatuses.

Despite of its universal diffusion, USP 2 have been deeply criticized [124]. Its hydrodynamic conditions have been judged highly unreliable and great part of the uncontrolled variability typical of the dissolution test have been ascribed to hydrodynamic effects. Tests is conducted in a small agitated vessel operated at Reynolds numbers in the transitional regime ($2100 < Re < 10000$): under such conditions, flow behavior in stirred-tanks is known to be both time-dependent and strongly heterogeneous. Consequently, the hydrodynamics in the vicinity of a tablet would likely be both position



Figure 1.14: USP2-Paddle apparatus.

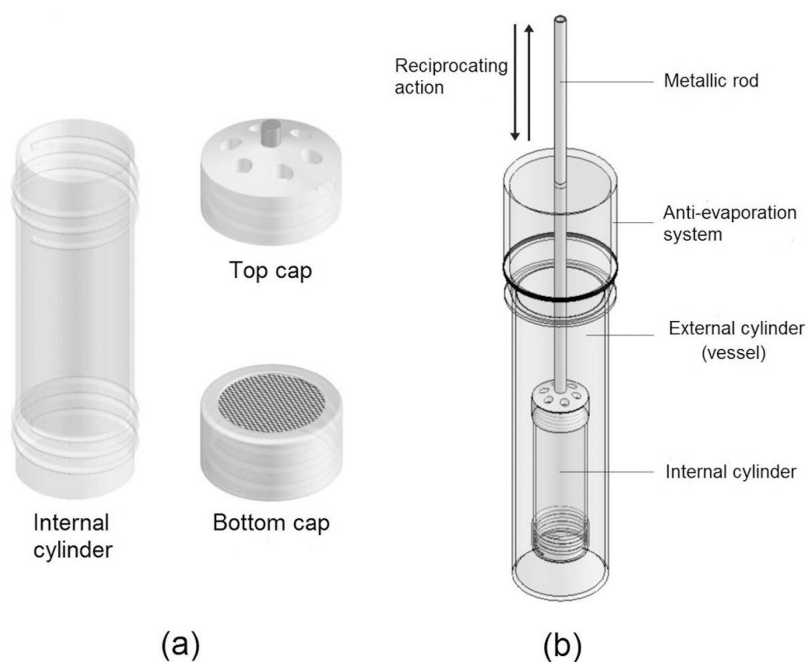


Figure 1.15: USP3-Reciprocating cylinder.

and time-dependent. Fluctuations in the flow introduce variability in the evolution of processes that are affected by hydrodynamics, such as shearing of the tablet surface, de-agglomeration of particles, mass transfer from the solid to the liquid, suspension and mixing of tablet fragments. Changes in the agitation speed can alter the measured dissolution rates and impact the ability to correlate *in vitro* dissolution tests with *in vivo* performance [125, 126].

In experimental and computational fluid dynamics studies, a low recirculation zone was observed in the lower part of the hemispherical vessel bottom, where the tablet dissolution process takes place. This region is the most critical, considering that the

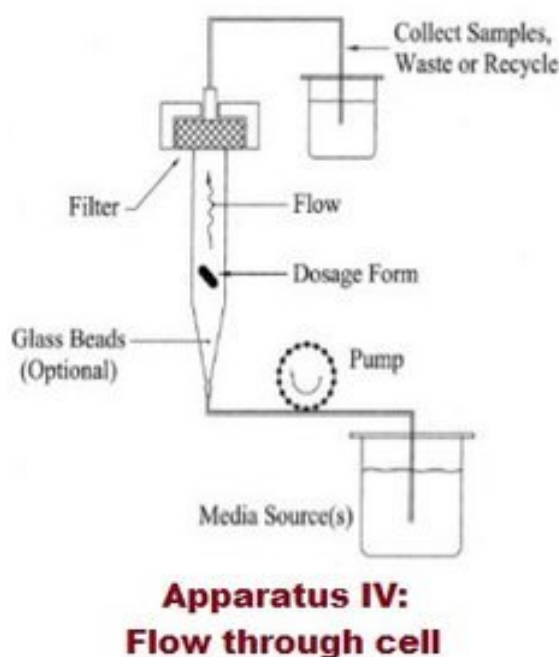


Figure 1.16: USP4-Flow through cell.

dissolving tablet will likely be at this location during the dissolution test. The exact tablet location has a significant impact on the dissolution profile [127, 128].

Drug release in USP 3 can be significantly affected by different agitation patterns [129].

The flow-through cell (USP 4), also referred to as the column (-type) method and USP 4 apparatus, was born of the need to overcome some of the limitations set by existing compendial methods, particularly the USP 1 and USP 2 apparatuses. It is now in widespread use. The flow-through cell offers definite advantages in regards to its low volume hold-up, the ability to maintain sink conditions (particularly for sparingly soluble drugs), and the ease of changing dissolution media (by analogy with physiological changes along the gastro-intestinal tract). Flow-through is also called the "infinite sink" condition. The flow-through cell is claimed to possess ideal hydrodynamic conditions for mild agitation, homogeneity and mathematically definable solvent flow pattern. Different types of cells are available for testing tablets, powders, suppositories, hard- and soft-gelatin capsules, implants, semisolids, suppositories, and drug-eluting stents. For orally administered solid dosage forms, two different cells are described: the large cell (22.6-mm internal diameter) and the small cell (12-mm internal diameter) that provide approximate volumes of 19 ml and 8 ml, respectively, for dissolution (cell volumes without glass beads).

Usually the bottom cone of the cell is filled with small glass beads (about 1-mm diameter), and one bead (about 5-mm diameter) is positioned at the apex to prevent material from descending into the inlet tubing. Different amounts of small glass beads can be used according to the experimental setup. The sample can be placed upon a holder, but also on or within the glass-bead bed. For dispersed systems (i.e., suspensions, powders), mixing of the sample within the glass-bead bed has also been reported [130–133].

1.2 Hydrogels for topical drug delivery

Topical preparations are used for the localized effects at the site of their application by virtue of drug penetration into the underlying layers of skin or mucous membranes. The main advantage of topical delivery system is to bypass first pass metabolism. Avoidance of the risks and inconveniences of intravenous therapy and of the varied conditions of absorption, like pH changes, presence of enzymes, gastric emptying time are other advantage of topical preparations. Semi-solid formulation in all their diversity dominate the system for topical delivery, but foams, spray, medicated powders, solution, and even medicated adhesive systems are in use.

The topical drug delivery system is generally used where the others system of drug administration fails or it is mainly used in pain management, contraception, and urinary incontinence. Over the last decades the treatment of illness has been accomplished by administrating drugs to human body via various routes namely oral, sublingual, rectal, parental, topical, inhalation etc.

Topical drug delivery can be defined as the application of a drug containing formulation to the skin to directly treat cutaneous disorders (e.g. acne) or the cutaneous manifestations of a general disease (e.g. psoriasis) with the intent of confining the pharmacological or other effect of the drug to the surface of the skin or within the skin. Topical activities may or may not require intra-cutaneous penetration or deposition [134, 135]. Topical drug delivery systems include a large variety of pharmaceutical dosage form like semisolids, liquid preparation, sprays and solid powders. Most widely used semisolid preparation for topical drug delivery includes gels, creams and ointments [136].

The advantages of topical drug administration are [137]

- Avoids gastrointestinal (GI) drug absorption difficulties caused by GI pH, enzymatic activity and drug interactions with food, drink, and other orally administered drugs.
- A substitute for other routes of administration (e.g. oral administration, intravenous injection) when that route is unsuitable, as with vomiting, swallowing problems, resistant children and diarrhoea.
- Patient acceptability is better as this drug delivery system is non-invasive, avoiding the inconvenience of parenteral therapy.
- Avoids the first-pass effect, possibly avoiding the deactivation by digestive and liver enzymes.
- Reduction of doses as compare to oral dosage forms.
- Ability to dissolve a wide range of medications with different chemical properties, making combination therapy with one transdermal cream possible.
- Provides extended therapy with a single application, improving compliance.
- Drug therapy may be terminated rapidly by removal of the application from the skin surface.
- Less greasy and can be easily removed from the skin.

On the other hand, the limitations of transdermal drug delivery (TDD) are functions of skin physiology and drug bio-activity [141]. The excellent barrier properties of skin are well known [138, 139], and currently limit TDD to only the most potent drugs.

In terms of dosage, this criterion implies that drugs, the daily dose of which is 10-20 mg or less, are potential candidates for TDD.

There are, in addition, further constraints determined by the physicochemical properties of the drug. For a drug molecule to reach the cutaneous microvasculature, and, hence, the systemic circulation, it must traverse both the lipophilic stratum corneum and the much more hydrophilic viable epidermis [140]. Therefore, drugs with a reasonable

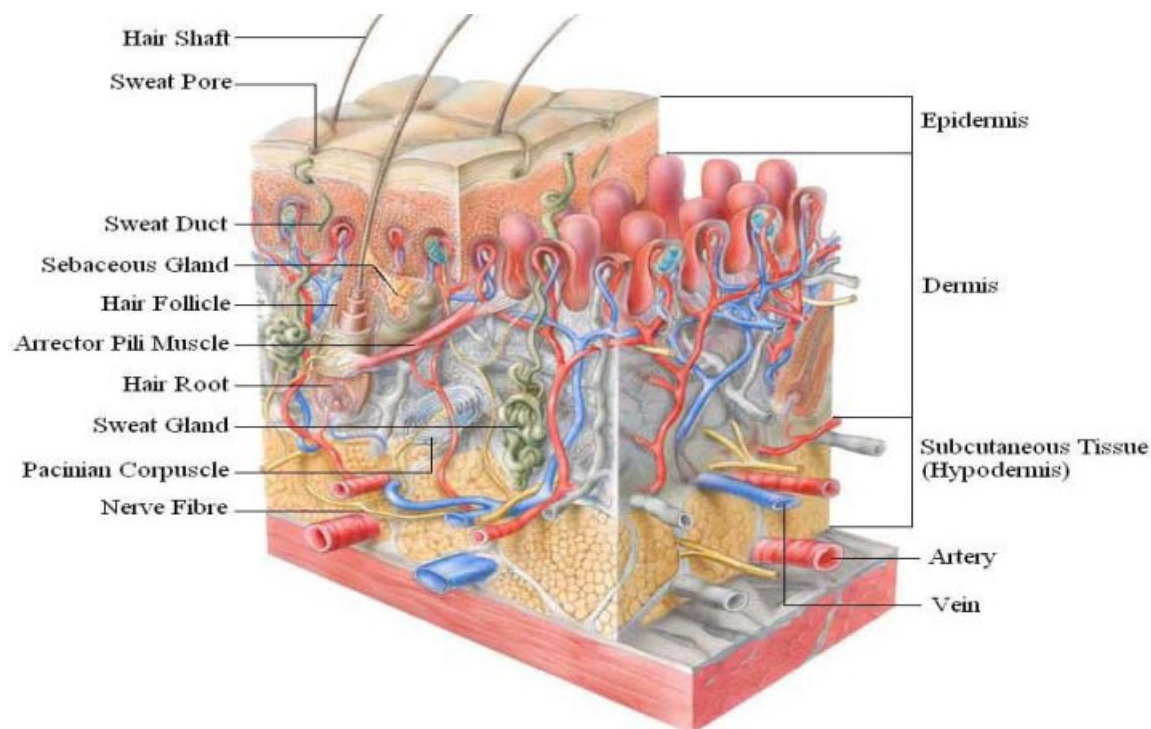


Figure 1.17: Longitudinal section of skin.

partition coefficient and possessing solubility both in oil and in water are most ideal. A highly lipophilic compound, for example, may readily enter and diffuse within the stratum corneum but be unable to penetrate deeper into the skin. The other major disadvantage of TDD is the potential elicitation of either allergic or irritant responses by the drug or the adhesive of the device.

1.2.1 Anatomy of skin

The human body has two systems that protect it from the harmful organisms existing in the environment. The internal defense system destroys microorganisms and bacteria that have already attacked the body. The external defense system prevents microbial microorganisms to enter the body. Skin is biggest external defense system. Skin covers the outside of the body but has other functions beside the defense mechanism. It serves as a mechanical barrier between the inner part of the body and the external world [142]. Temperature of skin varies in a range of 30 °C to 40 °C degree depending on the environmental conditions [143].

Skin is the largest organ in the body. It consists of three layers (figure 1.17). The outer layer is called epidermis, the middle layer is dermis and the inner most layer is hypodermis [147–149].

Epidermis

Consists of epithelial cells. Among these cells, both living cells and dead cells can be found. These new cells at the bottom of epidermis divide fast and push the older cells upward. The epidermis does not have any direct source of blood veins to provide nutrition. It takes its nutrients from the diffusion of necessary molecules from a rich vascular network in the underlying dermis. Epidermal cells are connected very strongly by desmosomes. Desmosomes are in contact with the intracellular keratin filaments. Keratin filaments produce keratin. Keratin cells accumulate and crosslink with the other keratin cells in the cytosol during their maturation. Afterward when the older cells die, this

network of keratin fibres remains and provides a tough and hard protective layer in epidermis, called protective keratinized layer. This layer is waterproof and airtight. It prevents most substances to enter the body or leave from the body. In diseased skin, particularly burns, epidermis is destroyed causing potential loss of body fluid and an increase in susceptibility to microbial infections, leading to fatal consequences untreated.

Cell types that exist in the epidermis are (figure 1.19):

- Keratinocytes; these are the main cell types in epidermis (95% of cells);
- Melanocytes; these are the pigment producer cells and found in the basal layers of epidermis;
- Langerhans cells; these cells are important immunological cells and can be found in the mid dermis as well Merkel cells; these cells are found in the basal layer of epidermis and are one part of amine precursor and decarboxylation system [144, 145].

Epidermis consists of five layers, namely from inside to outside(figure 1.18):

- stratum germinativum (basal layer);
- stratum spinosum;
- stratum granulosum;
- stratum lucidum;
- stratum corneum.

Stratum corneum is the outer most layer of epidermis and has a thickness of 10-20 μm when it is dry and 40 μm when it is hydrated and becomes swollen [145].

Stratum corneum has a structure of "bricks and mortar" arrangement. In this model the keratin rich corneocytes (bricks) are sitting in the intracellular lipid rich matrix (mortar) [145].

Corneocytes (the bricks) create 85 % of stratum corneum and intracellular lipids (15%) are arranged in 15-20 layers. Stratum corneum consists of 70% proteins, 15% lipids and only 15% water [146].

Molecules can basically permeate through skin by two different pathways(figure 1.20).The first pathway is called the transappendeal route. In this route the molecules should permeate through skin by permeation through sweat glands and across the hair follicles. The number of molecules which can penetrate through this pathway is very limited. The second pathway of penetration through skin is the transepidermal pathway. In this pathway molecules should pass through stratum corneum as multilayered barrier. This pathway has two micro pathways: the intracellular micro pathway and the transcellular micro pathway [145].

Dermis

Dermis is positioned under epidermis and is characterized by lots of elastin fibres that provide the stretching ability as well as lots of collagen that provides the strength to the skin. Blood vessels found in dermis provide nutrients for both dermis and epidermis. Dermis also plays a major role in temperature regulation. Nerves present there are responsible for pressure and pain sensations. Dermis has a thickness of 3-5 mm. In addition to elastin fibres, blood vessels and nerves, an interfibrillar gel of glycosaminoglycan, salt, water, lymphatic cells and sweat glands are parts of dermis [145]. Cell types found in dermis are:

- Fibroblasts: collagen producing cells;
- Macrophages: scavenger cells

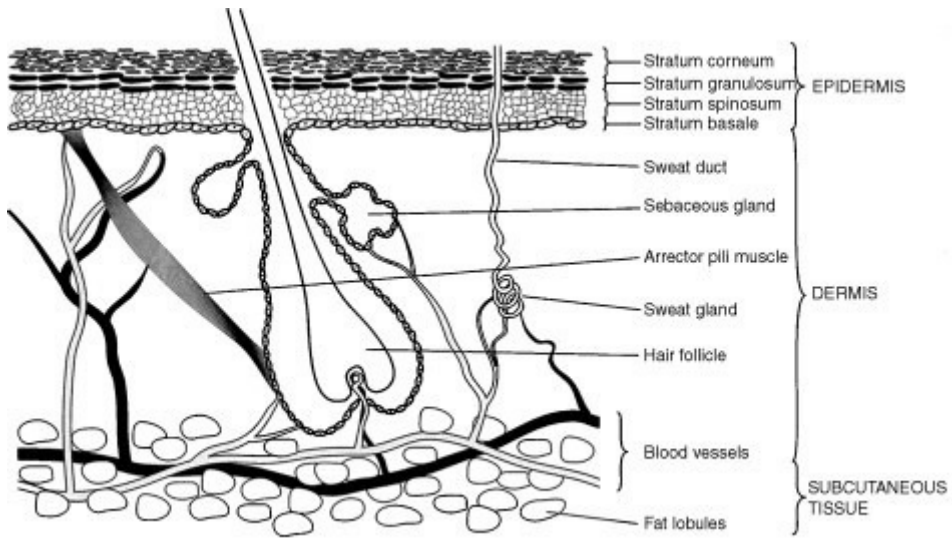


Figure 1.18: Epidermal and skin layer.

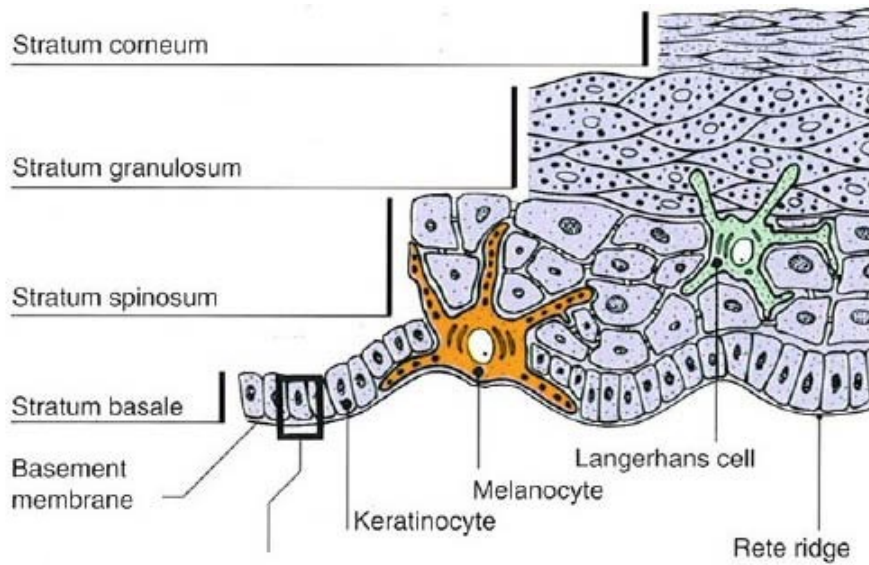


Figure 1.19: Layers of epidermis.

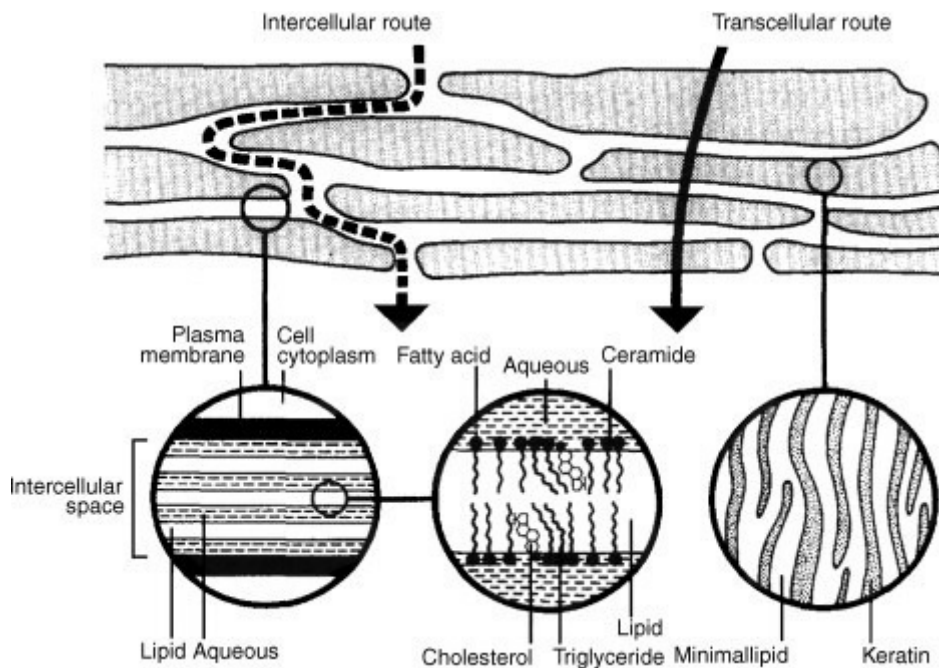


Figure 1.20: Structure of stratum corneum and penetration pathways.

- Mast cells: responsible for immunological reactions and interactions with eosinophils [144]

Dermis plays an important role as connection to other skin layers also. Changes in the metabolism in dermis can influence growth integrity of the epidermis, hair follicles and skin glands [143].

Hypodermis

Hypodermis is the inner layer of skin. It is the contact layer between skin and the underlying tissues in body such as muscles and bone [137]. Sweat glands, sebaceous glands and hair follicles enfold in epidermis but they stem from dermis. Sweat glands release a dilute salt solution into the surface of skin. The evaporation of this solution makes skin cool and this is important for temperature regulation of both body and skin. Sweet glands are present all over the body. The amount of dilutions (sweet) that gets produced depends on environmental temperature, the amount of heat generating skeletal muscle activity and various emotional factors. The sebaceous glands produce sebum. Sebum is an oily liquid released into hair follicles and from there onto the skin surface. Sebum protects both hair and skin from drying out and provides waterproof layer [142].

1.2.2 Formulation design of Hydrogels

To treat skin infection various hydrogels based formulations are prepare and apply topically for local action. Hydrogels have been used to deliver active component. Instead of conventional creams, the hydrogels have been formulated for better patient compliance [150].

Gels that consist of an aqueous dispersion medium that is gelled with a suitable hydrophilic gelling agent are known as hydrogels. Hydrogels are three-dimensional hydrophilic polymer networks, which have the ability to absorb large quantities of water [154]. Hydrophilic polymers such as hydroxypropyl methylcellulose (HPMC), Carbopol and sodium alginate have been previously investigated as gelling agents [155,156].

Hydrogels can be formed via chemical or physical crosslinks, which provide a networked structure and physical stability. These physical crosslinks include entanglements, crystallites, Van der Waals interactions or hydrogen bonding. Hydrogels formed from physical crosslinks are known as "reversible" or "physical" hydrogels [153,157]. In contrast, hydrogels known as "chemical" or "permanent" gels are formed via covalently bonded crosslinked networks [151,152].

Some of the topically applied preparations are shown in figure 1.21. Topically applied gels are classified by two schemes [158]. The first scheme divides gels in two types of gel systems. These are called as inorganic and organic gel systems. Most inorganic hydrogels

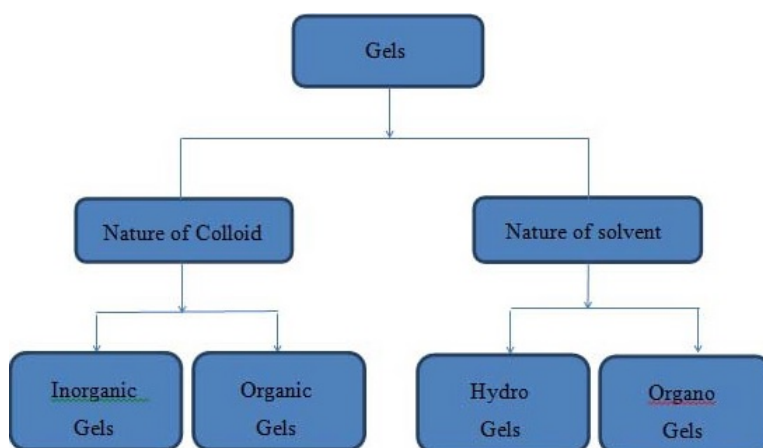


Figure 1.21: General classification of gel.

are two-phase systems, such as aluminum hydroxide gel and bentonite magma. Bentonite has also been used as an ointment base in about 10% to 25% concentrations. Most organic gels are single-phase systems and may include such gelling agents as carbomer and tragacanth and those that contain an organic liquid, such as Plastibase.

The second classification scheme divides gels into hydrogels and organogels with some additional sub categories. Hydrogels include ingredients that are soluble in water; they include organic hydrogels, natural and synthetic gums, and inorganic hydrogels. Examples include hydrophilic colloids such as silica, bentonite, tragacanth, pectin, sodium alginate, methylcellulose carboxymethyl cellulose sodium, and alumina, which in high concentration form semisolid gels. Sodium alginate has been used to produce gels that can be employed as ointment bases. In concentrations greater than 2.5% and in the presence of soluble calcium salts, a firm gel, stable between pH 5 and 10, is formed.

Methylcellulose, hydroxy ethylcellulose, and sodium CMC are among the commercial cellulose products used in ointments. They are available in various viscosity types, usually high, medium, and low. Organogels include the hydrocarbons, animal and vegetable fats, soap base greases, and the hydrophilic organogels.

Topical gel may include the following components:

- Gel forming agent or polymer;
- Drug Substance;
- Penetration Enhancers;

Gel forming agent or Polymer [159–170]. Different classes of polymeric materials have been used to achieve rate controlled drug delivery. The mechanism of drug release depends upon the physicochemical properties of the drug and polymer. The following criteria should be satisfied for a polymer to be used in a topical system:

- Molecular weight, chemical functionality of polymer must allow diffusion and release of the specific drug.

- The polymer should permit the incorporation of a large amount of drug.
- The polymer should not react, physically or chemically with the drug.
- The polymer should be easily manufactured and fabricated into the desired product and inexpensive.
- The polymer must be stable and must not decompose in the presence of drug and other excipients used in the formulation, at high humidity conditions, or at body temperature.
- Polymers and its degradation products must be nontoxic. No single material may have all these attributes, certain excipients may be incorporated to alter some properties for example Co-solvents such as ethanol, propylene glycol, PEG 400 could be added to increase drug solubility.

Gel forming polymers are classified as below:

- Natural Polymers:
 - Proteins-E.g. Collagen, Gelatin, Xanthin, Gellum Gum;
 - Polysaccharides-E.g. Agar, Alginic acid, Sodium or potassium carrageenan, Tragacanth, Pectin, Guar Gum, Cassia tora;
- Semi synthetic Polymers:
 - Cellulose Derivatives-E.g. Carboxymethyl cellulose Methylcellulose, Hydroxypropyl cellulose, Hydroxypropyl methylcellulose, Hydroxyethyl cellulose;
- Synthetic Polymers:
 - Carbomer-E.g. Carbopol-940, Carbopol-934, Carbopol -941;
 - Poloxamer;
 - Polyacrylamide;
 - Polyvinyl Alcohol;
 - Polyethylene and its copolymers;
- Inorganic Substances-E.g. Aluminum Hydroxide bentonite;
- Surfactants-E.g. Cetosteryl alcohol, Brij-96;

Drug Substance [159–170]. Drug Substance plays a very important role in the successful development of a topical product. The important drug properties that effect its diffusion through gels as well as through skin are as follows.

- Physicochemical properties:
 - Drug should have a molecular weight of less than 500 Daltons.
 - Drugs highly acidic or alkaline in solution are not suitable for topical delivery.
 - Drug must have adequate lipophilicity.
 - A saturated aqueous solution of the drug should have a pH value between 5 and 9.
- Biological properties:
 - The drug should not be directly irritated to the skin.
 - Drugs, which degrade in gastrointestinal tract or are inactivated by hepatic first pass effect, are suitable for topical delivery.

- Tolerance to the drug must not develop under the near zero order release profile of topical delivery.
- The drug should not stimulate an immune reaction in the skin.
- Drugs which have to be administered for a long time or which cause adverse effects to non-target tissue can also be formulated for topical delivery.

Penetration Enhancer [171–183]. Penetration enhancers (also called accelerants or sorption promoters) are defined as substances that are capable of promoting penetration of drugs into skin, or their permeation through skin, by reversibly reducing the skin barrier resistance. Percutaneous absorption involves the passage of the drug molecule from the skin surface into the stratum corneum under the influence of a concentration gradient and its subsequent diffusion through the stratum corneum and underlying epidermis, through the dermis, and into the blood circulation. The skin behaves as a passive barrier to the penetrant molecule. The stratum corneum provides the greatest resistance to penetration, and it is the rate-limiting step in percutaneous absorption.

A penetration enhancer acts by altering the skin as a barrier to the flux of a desired penetrant and are considered as an integral part of most topical formulations. To achieve and maintain therapeutic concentration of drug in the blood, the resistance of skin (stratum corneum) to diffusion of drugs has to be reduced in order to allow drug molecules to cross skin and to maintain therapeutic levels in blood. They can modify the skin's barrier to penetration either by interacting with the formulation that applied or with the skin itself. Ideally, these materials should be pharmacologically inert, nontoxic, non-irritating, non-allergenic, and compatible with the drug and excipients, odorless, tasteless, colorless, and inexpensive and have good solvent properties. The enhancer should not lead to the loss of body fluids, electrolytes, and other endogenous materials, and skin should immediately regain its barrier properties on its removal.

An ideal penetration enhancer should have the following properties:

- It should be pharmacologically and chemically inert, and chemically stable.
- It should be non-toxic, non-irritant, noncomedogenic and non-allergenic.
- It should have a rapid onset of action, predictable duration of activity, as well as a reproducible and reversible effect.
- It should be chemically and physically compatible with the formulation ingredients.
- After it is removed from the skin, the stratum corneum should rapidly and fully recover its normal barrier property.
- It should be odorless, tasteless, colorless, and inexpensive.
- It should be pharmaceutically and cosmetically acceptable.
- It should have a solubility parameter similar to that of skin.

In spite of the fact that a variety of compounds have been proposed as skin penetration enhancers, to date, no substance has been found to possess all the aforementioned ideal properties. Nevertheless, many known and newly developed compounds have been assessed for their enhancing abilities and some have shown more promising characteristics.

Preparation methods of Hydrogels

Hydrogels are polymeric networks. This implies that crosslinks have to be present in order to avoid dissolution of the hydrophilic polymer chain in aqueous solution. The various methods for crosslinking are as follows:

Crosslinking of Polymers.In this method chemically crosslinked gels are formed by radical polymerization of low molecular weight monomers, or branched homopolymers, or copolymers in the presence of crosslinking agent. This reaction is mostly carried out in solution for biomedical applications.

Copolymerization/Crosslinking Reactions.Copolymerization reactions are used to produce polymer gels, many hydrogels are produced in this fashion, for example poly (hydroxyalkyl methylacrylates).

Crosslinking by High Energy Radiation.High energy radiation, such as gamma and electron beam radiation can be used to polymerize unsaturated compounds. Water soluble polymers derivatized with vinyl groups can be converted into hydrogels using high energy radiation.

Crosslinking Using Enzymes.Recently a new method was published using an enzyme to synthesize PEGbased hydrogels. A tetrahydroxy PEG was functionalized with addition of glutaminyl groups and networks were formed by addition of transglutaminase into solution of PEG and poly (lysinecophenylalanine). The synthesis of hydrogel in industry is Consist of solution and reversed suspension and reversed emulsion polymerizations [184–187].

1.2.3 Hydrogels evaluation

Gels should possess the following properties:

- Ideally, the gelling agent for pharmaceutical or cosmetic use should be inert, safe, and should not react with other formulation components;
- The gelling agent included in the preparation should produce a reasonable solid-like nature during storage that can be easily broken when subjected to shear forces generated by shaking the bottle, squeezing the tube, or during topical application;
- It should possess suitable anti-microbial activity against microbial attack;
- The topical gel should not be tacky;
- The gels intended for ophthalmic use should be sterile; [188, 189]

Hydrogels are water swollen polymer matrices, with a tendency to imbibe water when placed in aqueous environment. This ability to swell, under biological conditions, makes it an ideal material for use in drug delivery and immobilization of proteins, peptides, and other biological compounds. Due to their high water content, these gels resemble natural living tissue more than any other type of synthetic biomaterial. These networks, have a three dimensional structure, crosslinked together either physically (entanglements, crystallites), or chemically (tie-points, junctions). This insoluble crosslinked structure allows immobilization of active agents, biomolecules effectively, and allows for its release in well-defined specific manner.

Thus the hydrogels biocompatibility and crosslinked structure are responsible for its varied applications [196, 197].Due to their hydrophilicity, hydrogels can imbibe large amounts of water. Therefore, the molecule release mechanisms from hydrogels are very different from hydrophobic polymers. Both simple and sophisticated models have been previously developed to predict the release of an active agent from a hydrogel device as a function of time. These models are based on the rate limiting step for controlled release and are therefore categorized as diffusion, swelling et chemically controlled mechanism.

Diffusion controlled.It is most widely applicable mechanism relating to drug release. Fick's law of diffusion is commonly used in modeling this release. Types of diffusion-controlled hydrogel delivery systems are as follows:

- Reservoir system(Drug depot is surrounded by a polymeric hydrogel membrane. Fick's first law describes drug release through the membrane);
- Matrix system(Drug uniformly dispersed throughout the matrix, unsteady state drug diffusion in a one dimensional slab-shaped matrix may be described using Fick's second law);

Drug diffusion coefficient is assumed to be of diffusion constant. Other assumptions are sink condition and a thin planar geometry where the release through the edges is neglected. Drug diffusion coefficient is a function of drug concentration except in very dilute solutions.

Diffusivities of encapsulated molecules depend on the degree of swelling and cross linking density of the gels for hydrogel devices. Diffusion coefficient used to describe drug release is sensitive to environmental changes or degradation of the polymer network and varies over the time scale of release [149,195].

Swelling controlled.It occurs when diffusion of drug is faster than hydrogel swelling. In this condition the modeling of drug involves moving boundary, where molecules are released at the interface of the rubbery and glassy phases of swollen hydrogels. Transition occurs from a glassy state where entrapped molecules remain immobile to a rubbery state where molecules rapidly diffuse. Release of small molecule drugs from HPMC hydrogel tablets are based on this mechanism.

Chemically controlled.It characterizes molecule release based on reactions occurring within a delivery matrix. Most commonly occurring reactions are:

- Cleavage of polymer chains via hydrolytic or enzymatic degradation;
- Reversible or irreversible reactions occurring between the polymer network and releasable drug.

Diffusion mechanism is regulated by movement through the polymer matrix or by bulk erosion of the hydrogel. Chemical stimulated gels swell in response to external cues like pH and temperature or by enzymatic action¹⁵ and effectively open their pores for release of the entrapped drug. This type of mechanism can be used for targeted drug release only for diseased tissues. Drug release via diffusion is more common for localized and non specific drug release whereas drug release by chemical stimulation have seen its more application for oral drug delivery and can offer control for selective treatment [192,193].

Generally hydrogels are characterized for their morphology, swelling property, chemical structure and elasticity. Morphological study gives us information about porous structure of hydrogels. Swelling determines the release mechanisms of the drug from the swollen polymeric mass while elasticity affects the mechanical strength of the network and determines the stability of these drug carriers [194]. Some of the important features for characterization of hydrogels are as follows.

General properties of hydrogel [190, 191]

The gel is a state that is neither completely liquid nor completely solid. These half liquid-like and half solid-like properties cause many interesting relaxation behaviors that are not found in either a pure solid or a pure liquid. From the point of view of their mechanical properties, the hydrogels are characterized by an elastic modulus which exhibits a pronounced plateau extending to times at least of the order of seconds, and by a viscous modulus which is considerably smaller than the elastic modulus in the plateau region.

Swelling. When a gelling agent is kept in contact with liquid that solvates it, then an appreciable amount of liquid is taken up by the agent and the volume increases. This process is referred to as swelling. This phenomenon occurs as the solvent penetrates the matrix. Gel-gel interactions are replaced by gel solvent interactions. The degree of

swelling depends on the number of linkages between individual molecules of gelling agent and on the strength of these linkages.

Syneresis. Many gels often contract spontaneously on standing and exude some fluid medium. This effect is known as syneresis. The degree to which syneresis occurs, increases as the concentration of gelling agent decreases. The occurrence of syneresis indicates that the original gel was thermodynamically unstable. The mechanism of contraction has been related to the relaxation of elastic stress developed during the setting of the gels. As these stresses are relieved, the interstitial space available for the solvent is reduced, forcing the liquid out.

Ageing. Colloidal systems usually exhibit slow spontaneous aggregation. This process is referred to as ageing. In gels, ageing results in gradual formation of a denser network of the gelling agent. This process is similar to the original gelling process and continues after the initial gelation, since fluid medium is lost from the newly formed gel.

Structure. The rigidity of a gel arises from the presence of a network formed by the interlinking of particles gelling agent. The nature of the particles and the type of force that is responsible for the linkages, which determines the structure of the network and the properties of gel. The individual particles of hydrophilic colloid may consist of either spherical or an isometric aggregates of small molecules, or single macromolecules.

Rheology. Solutions of the gelling agents and dispersion of flocculated solid are pseudo plastic i.e. exhibiting Non-Newtonian flow behaviour, characterized by a decrease in viscosity with increase in shear rate. The tenuous structure of inorganic particles dispersed in water is disrupted by n gels, ageing results in gradual formation of a denser network of the gelling agent.

1.2.4 In vitro release from Hydrogels

In vitro methods:Overview [198–204]

The vast majority of mathematical estimates of percutaneous absorption use, as their primary input, information on the rate of passage, or permeability, of a chemical across the skin. This is usually the permeability coefficient, k_p , or the more infrequently used (in the context of model development) maximum steady-state flux, J_{max} . In addition, a number of the physicochemical descriptors also modelled are measured experimentally, including measures of lipophilicity (commonly referred to as the octanol–water partition coefficient, $\log P$) and melting point.

It should be first commented that the vast majority of mathematical models for percutaneous absorption used data from, and therefore most closely reflect, in vitro laboratory experiments. These are physical experiments that use membranes, which are either mammalian or synthetic in nature, across which the permeation of a chemical is measured experimentally. Such experiments are widely carried out and are an area of substantial interest across a range of industries. They have been used to measure the percutaneous absorption of pharmaceuticals, materials in cosmetic formulations, for toxicology studies and for estimation of risk assessment and occupational exposure of materials used in a variety of industrial applications.

In vitro methods are commonly used prior to in vivo experiments and in some cases (such as for the assessment of new chemical entities) are solely used to provide an indication of potential toxicity prior to any human exposure. Consequently, in vitro models are widely and commonly employed to assess the risks and hazards associated with exposure of human skin to exogenous chemicals. Classically, in vivo studies have been conducted and provided valuable information on the mechanism of percutaneous absorption.

However, these studies were generally non-invasive in that they measured a response in the skin, such as vasodilatation or skin blanching, rather than taking blood samples or punch biopsies of the skin for subsequent analysis. Despite their advantages, such methods are clearly limited in their applicability to other chemicals, particularly those that do not result in a non-invasively measurable physiological change. In addition, the

non-invasive monitoring of certain topically applied chemicals, such as cosmetic formulations, may be measured in terms of efficacy by a range of biophysical methods, but such methods generally (with the exception of, for example, patch testing) do not provide any indication of cutaneous toxicity.

In vitro methods for the characterization of percutaneous absorption, while ultimately delivering the same outcome, are many and varied in the details of their methods. Selection of the diffusion membrane, type of cell (i.e. the use of either "static" or "flow-through" cell designs, described below), nature of the experiment (e.g. duration, occlusion) and the composition of the phases that sit either side of the diffusion membrane are some of the key parameters that add to the diversity of acceptable experimental protocols from which the data to construct mathematical models is abstracted.

Membrane selection [205–222]

The use of various animal skins is also a commonly accepted constituent of in vitro percutaneous penetration studies. Skin from a wide range of species, including pigs, rats, guinea pigs, monkeys and snakes, among others, has been suggested as a suitable replacement for human skin. Generally, skin from the pig and the rat has found the most widespread use, with the former in particular offering similar barriers to diffusion for the penetration through human skin of a wide range of molecules. Rat or mouse skin may be much more (up to 10 times) permeable than human skin, while pigskin has been claimed to be a better surrogate. However, rodent skin is still widely used as an in vitro membrane, possibly due to the use of such species more broadly in pharmacological research. Several researchers have developed artificial skin equivalents, often known as living skin equivalents (LSEs) in an attempt to address some of the issues associated with using animal tissue in place of human skin (such as the lack of similarity in diffusional characteristics or complexity compared to human skin, and the stratum corneum in particular). LSEs have been used with some success in skin grafting and in the surgical treatment of burns. Such materials aim to replicate the hydrophilic and hydrophobic balance of human stratum corneum, as well as the manifestation of its barrier function in, for example, the control of transepidermal water loss (TEWL) and control of bacterial ingress to the deeper epidermal and dermal tissues.

Artificial membranes have been used when human or animal skin is difficult to obtain, or where a large number of experiments are to be carried out, particularly with regard to pre formulation screening experiments. The most widely used artificial membranes are polydimethylsiloxane (PDMS) and cellulose acetate (porous dialysis tubing). However, these membranes have often been shown to overestimate significantly the flux across skin and their use is significantly limited. For example, Moss et al. (2006) compared the permeability of a series of prodrugs across pigskin and PDMS membranes in vitro. They demonstrated a reasonable relationship for hydrophilic molecules, whereas an increase in hydrophobicity resulted in a significant difference in permeability, with the PDMS showing significant overestimation of permeability compared to pigskin.

The use of human tissue is optimal for in vitro experiments. However, it is not without its problems. Human skin is usually obtained from skin banks or from tissue donated by the patient as a result of surgery—generally, this can range from cosmetic procedures including face lifts, "tummy tucks" and breast reduction or from medical procedures including amputations. The experimenter therefore has little control over the handling and quality of the skin obtained. For example, surgical procedures and protocols used to remove skin may include the use of alcohol-based disinfectants; while this is clearly essential for the surgical procedure and is a central part of infection control policies, it may affect the permeability in subsequent experiments as the alcohol has the potential to remove stratum corneum lipids and potentially affect its barrier properties. Further, the skin may be frozen and stored prior to dispatch and use in experiments, and this may result in damage to, or degradation of, the membrane.

Selection of the diffusion cell apparatus [223–227]

Fundamentally, the aim of an *in vitro* percutaneous absorption study is to determine the amount of permeant that passes into and across the skin. This involves the use of a diffusion chamber in which the membrane (normally human or animal skin, or an artificial membrane) separates the two compartments—the donor compartment is where the formulation containing the permeant of interest is introduced at the start of the experiment; and the receptor compartment is the chamber into which the permeant of interest may diffuse, following passage into and across the membrane.

In addition to measuring the amount, and rate, of permeant that passes across the membrane and into the receptor phase, the experiment also presents the experimenter with the opportunity to determine how much of the material of interest has passed into the skin and has remained there at the end of the experiment. This is usually achieved by using adhesive tape to remove the stratum corneum and by digesting the remaining tissue using acid/solvent mixtures. These samples can then be prepared for quantitative analysis.

Thus, the experiment is essentially a passive diffusion process that is governed by the diffusion gradient across the membrane as well as the experimental protocol and the physicochemical properties of the permeant. Despite various designs, some more complex than others (figure 1.22), the fundamentals of the process are very similar—passage of the permeant of interest from the donor chamber to the receptor chamber while maintaining a viable diffusion gradient and avoiding equilibrium between both compartments. The receptor compartment normally has a sampling port—usually a sidearm—which is occluded during the experiment to stop evaporative loss and from which aliquots of the receptor media may be removed (and replaced with fresh receptor fluid) for analysis.

There are two main types of diffusion cells: static and flow-through cells. The vast majority of *in vitro* percutaneous absorption experiments are conducted using upright static glass diffusion cells, known as Franz or Franz-type cells. These involve the partition of the permeant into a “static” receptor compartment of a fixed volume that is maintained at a controlled temperature and is continually stirred throughout the experiment to ensure complete mixing and to avoid the presence of any “dead” zones or diffusion gradients within the receptor compartment.

Franz-type diffusion cells are found in a range of designs and sizes (figure 1.22) and are therefore very flexible, with particular cells being chosen for particular purposes (e.g. when a different surface area might be required, or when the receptor compartment may need to be varied based on the solubility of a particular permeant). The simple design of the upright cells allows a wide range of formulations to be applied to the skin surface, including solutions, creams, ointments and various other semi-solid materials of a pharmaceutical or cosmetic nature. A variation on the Franz-type cells is the side-by-side cell, which allows both compartments to be stirred at the same time, although the range of formulations suitable for use in such cells is clearly limited. One of the main perceived limitations of the Franz-type cells is their susceptibility to “sink conditions”. As described above, the diffusion process requires a gradient to be established, and maintained, across the membrane that divides the donor and receptor compartments. Thus, in a static diffusion cell, it is important to maintain a concentration gradient such that, normally, the concentration of the permeant of interest is not greater than 10 % of its saturated solution in the receptor compartment.

Flow-through diffusion cells, often called “Bronaugh cells”, offer an alternative approach to the issue of sink conditions and attempt to mimic *in vivo* conditions by utilizing a constantly perfusing receptor compartment, flowing usually at 1–2 ml/h, which aims to mimic the blood flow beneath the skin. This is normally achieved with the use of a peristaltic pump which is connected to tubing that supplies a compartment beneath the membrane. The receptor fluid flows into a receptacle and is analysed, either offline or, more infrequently, via an online flow-through method of analysis. Either arrangement provides the facility for substantial automation of sample collection. This arrangement ensures that sink conditions are maintained throughout the experiment and that the

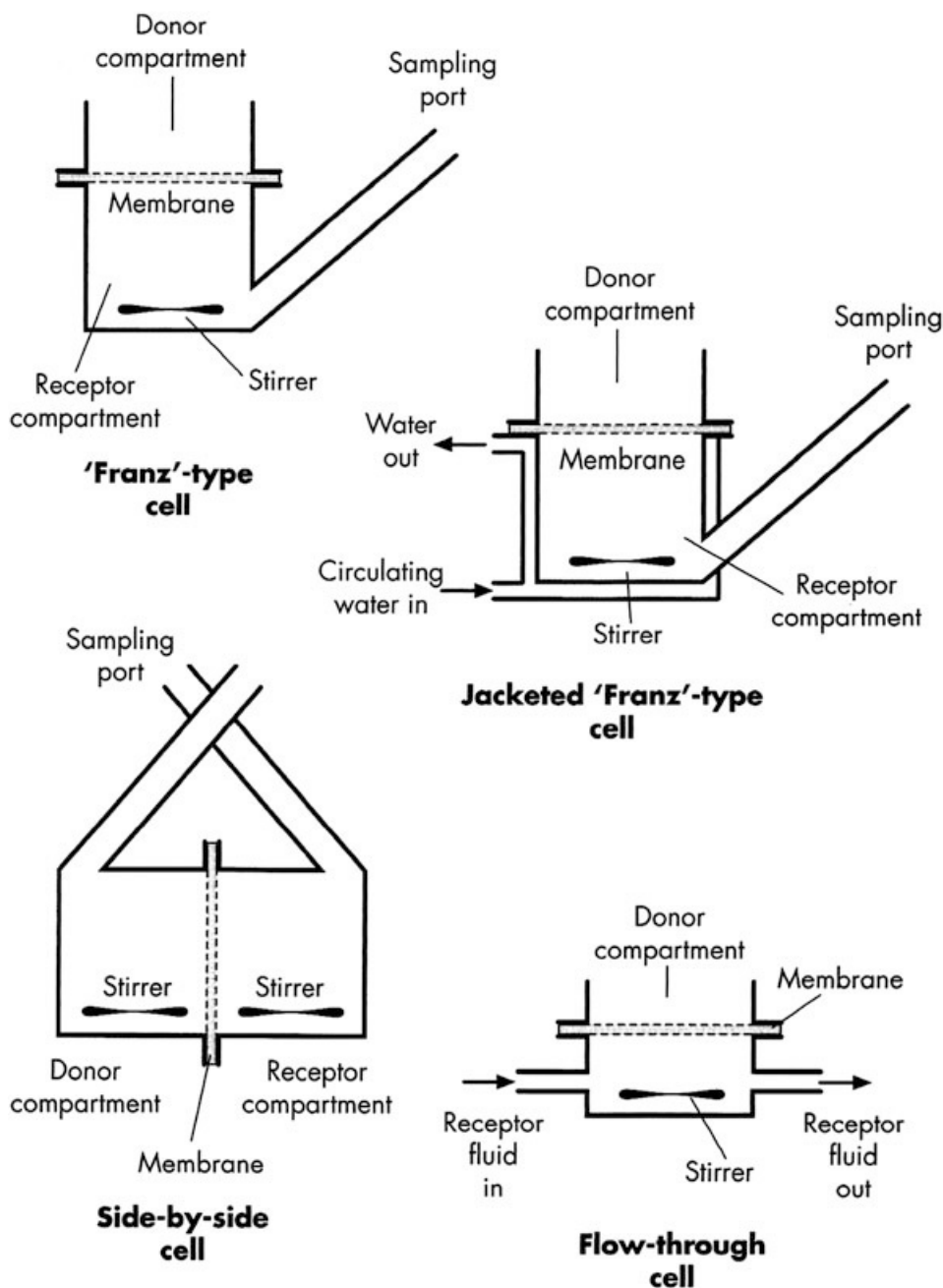


Figure 1.22: Examples of commonly used diffusion cells.

receptor phase does not have to be replaced should a penetrant be rapidly absorbed.

While flow-through cells are more flexible (i.e. in terms of automation), they are more complex and substantially more expensive than Franz cells. Consequently, the use of Franz-type static diffusion cells is more common than the use of flow-through cells. In either case, most experiments use between 6 and 24 cells per experiment in order to ensure reproducibility. As mentioned above, the cell design can influence the formulation type that can be applied to it. For example, the side-by-side cells, while having the advantage of even stirring and mixing in both donor and receptor compartments, are limited in the type of formulation that can be applied—pharmaceutical dosage forms such as creams, gels, ointments and patches are very difficult to apply in this manner.

Thus, the cell design and the protocol used can all affect the outcome—the measure-

ment of percutaneous absorption and the cell design should be considered when considering the uniformity of data that are to be used in the construction of mathematical models of skin absorption.

1.3 Oral thin films and Hydrogels in this work

The next chapters of this paper will cover the description and study of releases from thin films and hydrogels, as well as the characterization of pharmaceutical formulations for potential use in drug delivery.

Chapter 3 will cover the release from hydrogel (Scleroglucan-CM as a polymer matrix) of three types of drugs belonging to 3 different classes: Fluconazole, Diclofenac and Betamethasone.

Chapter 4 will investigate the release from thin films (Gellan gum as a polymer matrix), while in chapter 6 will be presented film GG:Glycerol and the technique for preventing crystallization. In both cases, fluconazole is used as a model drug.

Chapter 5 illustrates the work done at the Pharma Lux Lab in Oslo, where HPMC5 films were analyzed using furosemide as a model drug.

Mathematical models have been developed to understand and analyze the data achieved from the release profiles. Drug diffusion values were estimated in both hydrogels and thin films.

1.3.1 Gellan gum, HPMC, Scleroglucan

It's necessary to spend some words about the polymer used in this work:

- Gellan gum, for the production of swellable thin films;
- HPMC for the realization of erodible-fast dissolving thin films;
- Scleroglucan to make a biocompatible physical hydrogel.

Gellan gum

Gellan gum is an anionic polysaccharide hydrogel-forming polymer produced from the bacteria *Sphingomonas elodea* [239]. Structurally, it comprises a tetrasaccharide repeat unit of two β -D-glucoses, one β -D-glucuronate, and one α -L-rhamnose [228] (figure 1.23).

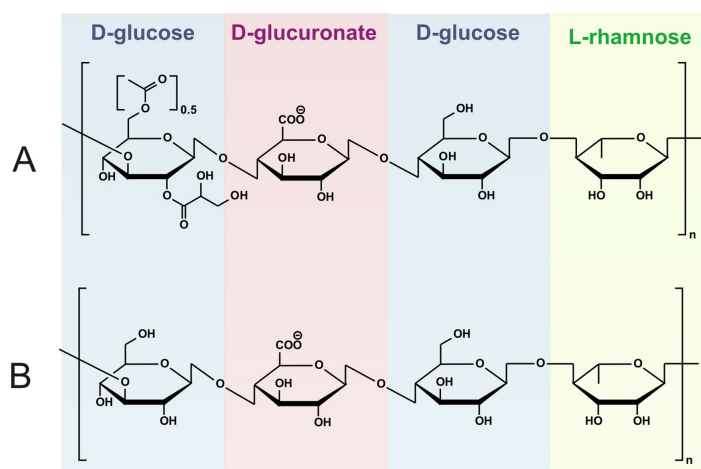


Figure 1.23: The structure of native (A) and low acyl (B) form of gellan gum.

Gellan gum is available commercially under the trade names *Gelrite*[®] and *Kelcogel*[®] in 'high acyl' and 'low acyl' forms with the high acyl form being the native state [229]. Native form of gellan contains two types of acyl substituents, namely L-glyceryl and acetyl [240]. The low acyl gellan gum is prepared via alkali treatment of the native gellan gum and is distinctively different in its gelation behaviour and mechanical properties [230]. The high acyl gellan gum will form a gel upon cooling from 65 °C creating a flexible, soft hydrogel while low acyl gellan gum will form a gel upon cooling below 40 °C creating a rigid and brittle hydrogel [231].

In recent years, low acyl gellan gum has become an attractive biopolymer for applications in tissue engineering as a cellular scaffold because it resembles the natural extracellular matrix (ECM) and is bio-inert [232, 233].

Gellan gum has also been used as an injectable and printable matrix for cellular therapies and 3D tissue scaffold fabrication [234, 235]. There is therefore potential for gellan gum based materials to be used for computer aided tissue engineering [229, 236].

Gellan gum, like many anionic polysaccharides forms a physical gel by undergoing a random coil to double helix transition upon cooling. Stronger gels are formed if cations are present during the sol-gel transition. In this case, divalent cations form particularly strong gels through the aggregation of helices and monovalent cations form intermediate strength hydrogels through electrostatic interactions with carboxylate groups [228]. The presence of divalent cations also inhibits the ability of the un-hydrated gellan gum to become hydrated [237]. In the food industry, it is common practice to add calcium sequestrants (citrate and phosphates) to water to improve the ability of low acyl gellan gum to be hydrated [238].

The presence of cations in commercially provided gellan gum is ordinarily minimal and may not impede their use in food and pharmaceutical applications. However, very small amounts of calcium present in commercial gellan gums may still affect the more sophisticated chemistries used to modify gellan gum for tissue engineering applications [229]. Calcium may also affect the gel transition temperature so significantly that it precludes it from being utilised in rapid prototyping technology.

A method for the rapid purification of gellan gum was established two decades ago which employed an ion-exchange resin to capture the cations present in commercial gellan gum. They reported that after purifying the gellan gum of divalent cations, the acid form gellan gum could be converted to a monovalent salt using a corresponding hydroxide salt. Sodium or potassium gellanate salts were able to be hydrated at much lower temperatures and formed gels of comparable strengths to un-purified gellan gum hydrogels. [230, 237]

HPMC

Hydroxypropyl Methylcellulose (HPMC) is probably the most widespread employed polymer for drug release. Hydroxypropyl methylcellulose is a semi-synthetic material derived from cellulose. It is a linear polymer comprised of etherified anhydroglucose rings (figure 1.24). Its polymeric backbone is made of cellulose, a natural carbohydrate that contains a basic repeating structure of anhydroglucose units. In the industrial production of HPMC, cellulose fibers are heated with a caustic solution which in turn is treated with methyl chloride and propylene oxide to obtain hydroxypropyl substitution on the anhydroglucose units. The amount of substituent groups on the anhydroglucose units of cellulose can be designated by the weight percent or by the average number of substituent groups attached to the ring, a concept known as "degree of substitution"(D.S.).

Like all polymers, HPMC macromolecules exist as a distribution and may be characterized by parameters such as the number average molecular weight (M_n), the weight average molecular weight (M_w), and the polydispersity (M_w/M_n). These molecular weight moments may be determined by a number of techniques, such as osmometry, light scattering, or size exclusion chromatography.

The chemical modification to obtain HPMC is generally conducted under heterogeneous conditions and the substituents within a specific glucose unit, as well as along the cellulose backbone, can be introduced within a large variation. This lack of control

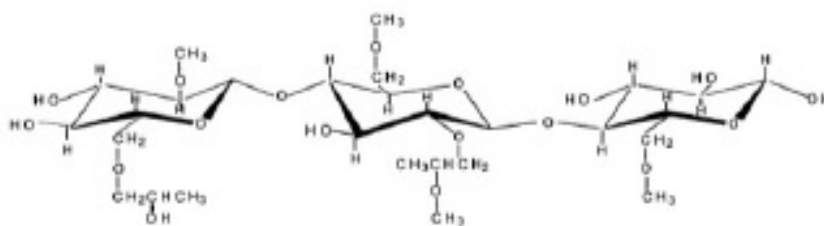


Figure 1.24: Structural formula of HPMC.

over the chemical composition within and between commercial HPMC batches results in chemically inhomogeneous materials. This is undesired, and this heterogeneity sometimes affects the functionality of HPMC in pharmaceutical applications. A selection of a proper grade has not always proven to give predictable release rates from hydrophilic matrix tablets and batch-to-batch variations are frequently seen. Because of this variability, a recent study shows the molecular sizes of the polymer chains cannot alone predict the release and swelling, and it does not matter whether the polymer sizes are described in terms of chain lengths (molecular weights), resistance against shear forces (viscosities) or sizes of the polymer coils (intrinsic viscosity or radius of gyration).

The average values of parameters describing the hydrophilic/hydrophobic characters such as the degree of substitution or cloud points can be related to the water transport through the gel layer into the hydrophilic matrix and thus also to the macroscopic degree of swelling [241, 242].

Investigation of hydrophilic polymers, in particular cellulose derivatives, has attracted considerable attention for the development of controlled release technology in the formulation of pharmaceutical matrix products. Matrix tablets swell on contact with water, and the release of a drug depends on interactions between water, polymer and drug. In the field of controlled release, the influence of carriers on drug dissolution kinetics, which are the result of differently acting mechanisms, was investigated frequently. Usually, two main mechanisms are studied: diffusion and erosion.

In the case of cellulose ether based matrix tablets, drug release can be described as being controlled by the rate of swelling. However, drug release in general is not purely swelling controlled, since it occurs mostly as the result of a combination of polymer relaxation and Fickian diffusion. Previous studies of matrix tablets led to the conclusion that the rate and extension of drug release depend on the type of polymer, its viscosity grade, hydration and polymer proportion in the formulation [243]. The extent and rate of matrix swelling depends in turn on the viscosity grade of HPMC and the agitation rate of the dissolving medium [244, 245].

Moreover, swelling shows to be pH-dependent [246]. Erosion shows a cubic dependence on time and, contrary to t_{rep} theories, no lag time was observed [247]. Interesting results on swelling and erosion can be obtained using a simple optical method [248]. A new and very promising approach for a deeper characterization of HPMC compacts behaviour is presented in [247] and involves UV-imaging in a buffer solution.

A statistical approach -QRS (Quantitative-Structure Property Relationship) technique identifies the aqueous solubility of drug (dipole moment), the size of the drug molecule and the matrix erosion rate as the most significant parameters for drug release [249].

Scleroglucan

Scleroglucan (Scl) is an example of a natural polysaccharide produced by the fungi of the genus *Sclerotium* [250], which possesses several structural properties particularly useful

for the design of physical hydrogels for topical applications. Specifically, the polymer consists of a main backbone of (1-3)-linked- β -D-glucopyranosyl residues with a single (1-6)-linked- β -D-glucopyranosyl unit linked in side chain every third sugar molecule of the main chain. In aqueous solutions, Scl reassembles in a triple helix conformation that can only be broken into random coil chains at pH 12 or in dimethylsulfoxide(DMSO) [251,252]. Scl finds application in the industrial and pharmaceutical field as a thickening agent and for the preparation of modified release dosage forms for oral and topical delivery [253–255].

In addition, Scl can be easily modified with pH-responsive groups, which have a profound effect on the main characteristics of the polymer [256,257]. For example, a carboxymethyl derivative of Scleroglucan (Scl-CM, figure 1.25) is obtained by reaction with chloroacetic acid in a basic medium, and the number of carboxylic groups introduced has a significant influence on the corresponding gel properties. Specifically, a Scl-CM

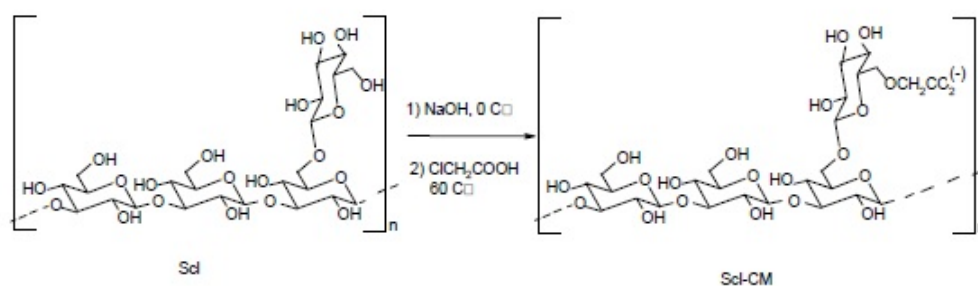


Figure 1.25: Scheme of Scl-CM synthesis.

derivative with a high degree of functionalization is capable of forming physical hydrogels without the addition of any salt. These physical gels have been already proposed as carriers for the oral administration of anti-inflammatory drugs proving to adequately protect the gastrointestinal mucosa from any drug-induced damage while modulating the release rate of the loaded molecules [258].

The peculiar physico-chemical properties of Scl suggested its suitability as a slow release matrix; tablets prepared with the polymer show a remarkable swelling process, that can slow down the diffusion of molecules previously loaded in the system [259].

1.3.2 Cyclodextrins(CD)

Cyclodextrins (CD), or cycloglucans, first discovered by A. Villiers in 1891 and also called "cellulosines" are cyclic oligosaccharides consisting of α -D-glucopyranose monomer units joined by α -1,4-glycosidic bond. Cyclodextrins originate from the hydrolysis degradation of potato or corn starch by cyclodextrin-glycosyl-transferase, an amylase secreted by numerous microorganisms such as *Bacillus macerans*. The reaction of enzymatic degradation produces a mixture containing three types of natural CD classified according to the number of monomeric units of α -D-glucopyranosion in α -CD (6 units), β -CD (7 units) and γ -CD (8 units) (figure 1.26).

Due to the "chair" configuration of α -D-glucopyranose units, the CDs have a truncated cone shape [260]. The primary hydroxyl functions on the C-6 of the saccharides units are oriented towards the narrowest side of the cavity and are the most reactive, nucleophilic, and most easily accessible for poor steric impediment. They are also more "mobile" than the -OH secondary ones, giving the cavity flexibility so that it can accommodate hydrophobic molecules. The secondary hydroxyl functions are located on the wider side of the cavity. In particular, the -OH group present on the C-2 is more acidic and reactive than the C-3 hydroxyl, which is also less accessible within the cavity. In solution, the hydroxyl groups establish hydrogen bonds with the surrounding water molecules forming a hydration sphere that envelops the cyclodextrin [261].

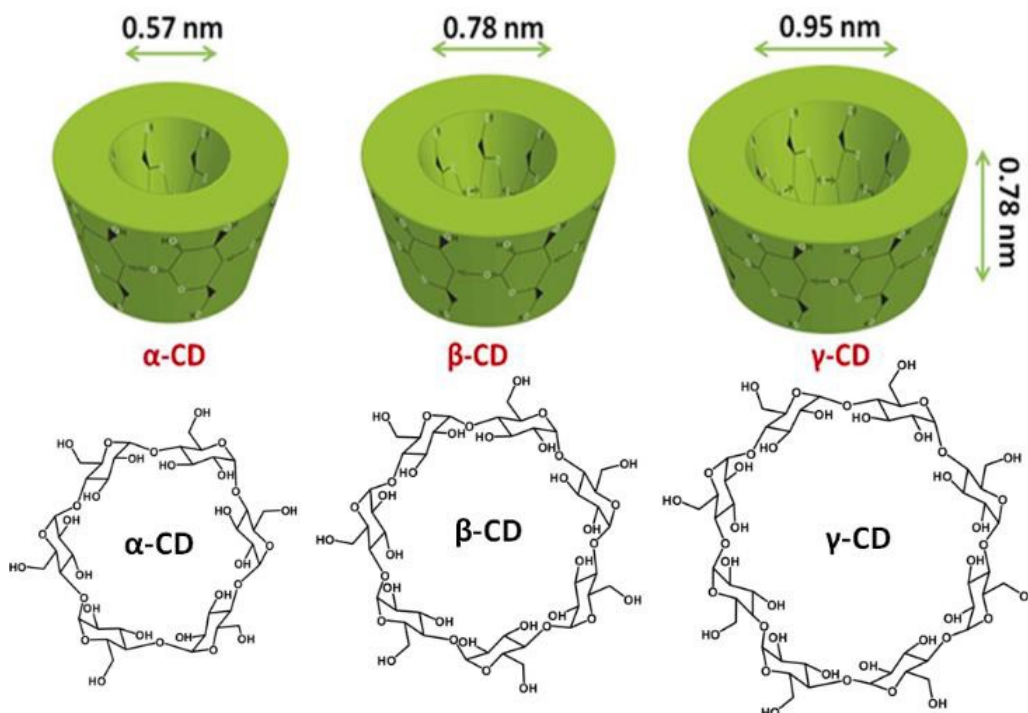


Figure 1.26: α -CD, β -CD and γ -CD.

The carbonaceous skeleton and the ethereal oxygen molecules of the glucose residues form the central cavity and give it a relatively lipophilic character with a polarity that has been estimated to be similar to that of an aqueous ethanol solution (figure 1.27).

The dual nature, inside lipophilic and hydrophilic on the outer surface, shape and structure give the cyclodextrine solution the unique ability to trap inside a host molecule forming an inclusion complex. The dynamic complexation equilibrium that regulates this process does not involve the formation and / or break of covalent bonds. The displacement of the water molecules from the apolar cavity of the cyclodextrin, an increase in the number of hydrogen bonds due to the return in solution of the water molecules from the cavity, a reduction in the repulsive interactions between the hydrophobic host and the aqueous environment and an increase in hydrophobic interactions due to the insertion of the host molecule into the cavity are driving forces that move the equilibrium towards the formation of the inclusion complex (figure 1.28).

Of course, the possibility of forming a stable complex is inevitably related to the size of the cyclodextrin and to the chemical-structural characteristics of the host molecule. This must have adequate molecular weight and steric size, be sufficiently lipophilic and possess good conformational freedom to allow it to settle inside the cavity in such a way as to maximize interactions.

Pharmaceutical application of cyclodextrine

The ability of cyclodextrine to form inclusion complexes makes them particularly promising in the pharmaceutical technology. In particular, in the case of lipophilic or poorly soluble drugs, the formation of a complex allows for an increase in the apparent solubility of the drug itself [262]. In this way, it is both possible to bring into solution drugs that are poorly soluble, allowing for parenteral administration, and also to obtain an increase in dissolution rate as predicted by the Noyes-Whitney equation (equation (1.2)):

$$\frac{dq}{dt} = kS_s(C_s - C) \quad (1.2)$$

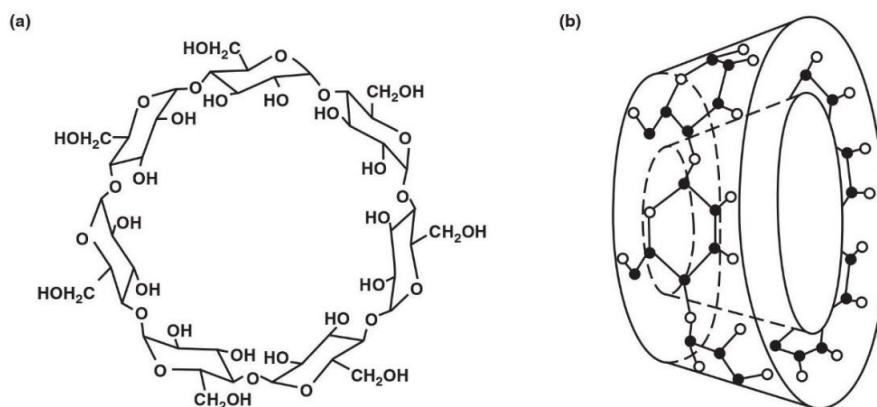


Figure 1.27: Structure of cyclodextrin.

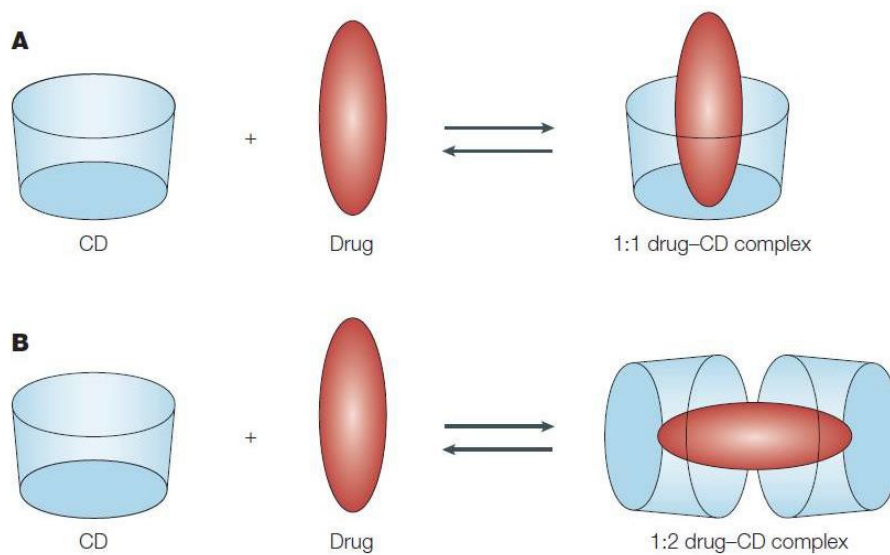


Figure 1.28: Complexation equilibrium.

where q is the amount of solid released in time t , k is the proportionality coefficient, S_s is the specific surface area of dissolved particles, C_s is the max concentration of saturation (solubility of the drug), C is the drug concentration in biological fluid (between 0 and C_s). Another benefit of using CD in the pharmaceutical field is related to increased drug stability. Cyclodextrin provides greater protection to oxidative degradation reactions, hydrolysis and thermal degradation by increasing its stability.

Finally, thanks to the formation of inclusion complexes with cyclodextrin, it is possible to produce modified release formulations: is the complexity constant and related factors that regulate the dynamic equilibrium between free drug and complex drug, defining the kinetics release of the active ingredient.

In general, the use of CDs in the pharmaceutical field allows to obtain:

- an increase in drug solubility;
- an increase in the rate of dissolution;
- an increase in the bioavailability of the drug;
- a reduction in side effects;
- an increase in the stability of the pharmaceutical formulation;
- elimination of incompatibility: in multicomponent pharmaceutical forms
- masking odors and unpleasant flavors.

Hp- β -CD

Natural cyclodextrine, particularly β -CD, have limited solubility in water (18.5 mg / ml) due to the numerous molecular hydrogen bonds present in the crystalline state and do not have great versatility. In order to overcome these problems, which make these cyclodextrine poorly usable in the pharmaceutical field, their derivatives have been prepared and characterized. Among these, a particularly interesting is the (2-hydroxypropyl)- β -cyclodextrin (HP- β -CD), a semi synthetic derivative of β -CD obtained by reaction of the latter with propylene oxide and subsequent replacement of the hydroxyl group with a hydroxypropyl chain (figure 1.29) [263]. There are many reasons why HP- β -CDs are beneficial:

- High solubility in water: HP- β -CDs have good solubility in water at 25 °C;
- ease of complexation: with HP- β -CDs is possible the formation of an inclusion complex for simple addition of the drug to an HP- β -CD aqueous solution and subsequent agitation of the system;
- reduced toxicity: HP- β -CDs are not toxic if administered low and moderate doses. Due to its high solubility, HP- β -CDs are not nephrotoxic and can be administered either oral or parenterally.

Within the OTF, the introduction of HP- β -CD allows to increase the stability and solubility of the active principle present in the formulation and, at the same time, to obtain a modified release of the drug.

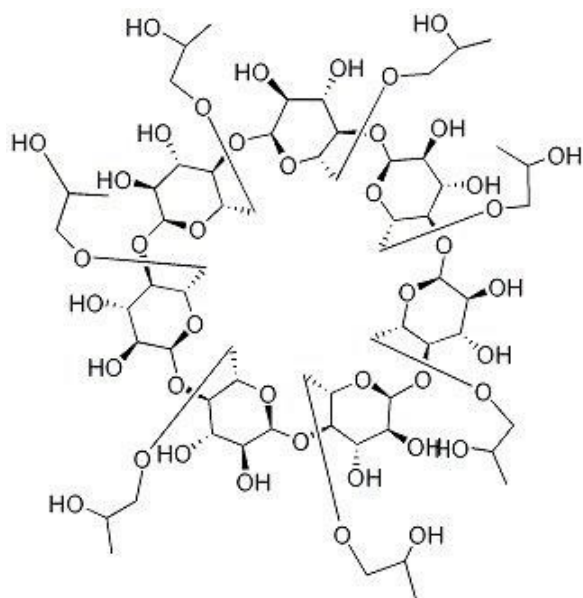


Figure 1.29: Structure of HP- β -CD.

Chapter 2

Aim of the work

The aim of this work is to develop innovative pharmaceutical formulations in the form of hydrogels and thin films that can improve existing solutions in the field of topical and oral drug delivery.

The main objectives can be summarized as follows:

- to realize innovative pharmaceutical formulations with biocompatible polymers;
- to optimize concentrations and proportions of the various components to obtain the best performances in terms of mechanical properties, workability, controlled or modulated drug release;
- to prepare versatile pharmaceutical formulations for fast or sustained release of drugs belonging to different pharmaceutical classes;
- to choose the dissolution apparatus most suitable for topical or buccal in-vitro release experiment in order to reproduce release conditions as close as possible to real/physiological ones;
- to critically evaluate already existing and commonly used apparatuses and to test new or recently proposed ones.
- to develop mathematical models to properly describe the physics of release experiments with the aim to:
 - estimate the physical parameters (such as diffusivity values of the drug and -or solvent within the polymeric matrix), which are essential for a proper formulation design and development;
 - predict the release time scales when changing the operating conditions or changing from in-vitro to ex-vivo experiments.

Chapter 3

Scleroglucan based hydrogel for topical drug delivery

3.1 Introduction

Topical formulations are a valid strategy to treat common disorders, including acute and chronic inflammations, skin infections and acute pain [265]. The use of the skin as a portal of entry for drugs is particularly attractive since it can overcome the challenges associated with other administration routes [266]. However, beside its great accessibility, the skin possesses highly efficient barrier properties, which frequently hamper drug delivery through it. In this context, hydrogels represent a primary solution to design innovative topical formulations [267]. In fact, their soft consistency combined with their ability to swell, make them the perfect candidate for topical applications. Moreover, they possess a pleasant texture, which does not create any greasy residue on the skin compared to creams and ointments [268].

Hydrogels properties can be modulated by varying the type of polymer and the crosslinking step during their fabrication. Chemical or physical bonds can hold the polymeric matrix together, and its swelling behavior can be tuned by introducing pH-sensitive functional groups [269].

For all these reasons, hydrogels offer a versatile platform as carriers of a variety of drugs for topical delivery. This concept particularly holds true for physical hydrogels made of bio compatible polysaccharides where the presence of hydrogen bonds, ion-dipole, and electrostatic interactions are the driving forces responsible for the hydrogel formation. The same interactions can influence the hydrogel strength and elasticity as well as the release behavior of the loaded drugs from the hydrophilic matrix.

Among polysaccharides, scleroglucan (Scl) has been proposed for the preparation of effective modified drug delivery systems. Scl is a water-soluble extra-cellular polysaccharide produced by fungi of the genus *Sclerotium*.

The carboxymethyl derivative (Scl-CM) of scleroglucan is able to form physical hydrogels with divalent ions, such as Ca^{+2} . The release rate of the drug critically depended on the concentration of the salt and the molar ratio carboxylated repetitive units of the polymer/ Ca^{+2} .

To further extend the potentiality of high carboxymethylated Scl-based hydrogels in the pharmaceutical field, their use as a topical formulation for a variety of drugs including anti fungal, steroidal and non-steroidal anti-inflammatory molecules, was here attempted.

Specifically, three different therapeutic drugs, namely diclofenac, betamethasone, and fluconazole, were tested in this work. Flow curves and frequency sweep tests were carried out on the loaded *Scl - CM*₃₀₀ hydrogels along with release studies in a vertical Franz cell. Particular attention was paid to possible interactions between the hydrogel matrix and the loaded drugs, and how their presence could influence both the rheological and release properties of the corresponding physical hydrogels.

Mathematical models, describing transport and possible interactions between the selected drugs and $Scl - CM_{300}$, were adopted to estimate the effective diffusion coefficient of these molecules in the polymeric network. Numerical solutions were obtained by COMSOL 3.5 multiphysics.

Finally, preliminary in-vivo experiments were carried out on rabbits to verify the skin tolerability of the $Scl - CM_{300}$ -based formulations.

3.2 Materials and methods

3.2.1 Chemicals

All used reagents were of analytical grade. Scleroglucan with $M_w = 1.4 \cdot 10^6$, as evaluated by viscosimetric measurements in 0.01 M NaOH, was provided by Carbomer (USA). Dimethylsulfoxide (DMSO) and chloroacetic acid were purchased from Fluka (Switzerland). Diclofenac sodium salt, DOWEX 50WX4-50 ion exchange resin, acetonitrile, and methanol were purchased from Sigma-Aldrich (England). Betamethasone phosphate sodium salt and fluconazole were received as gifts from Sigma-Tau (Italy) and Recordati S.p.A. (Italy), respectively. Dialysis membranes with cut-off 12,000-14,000 Da were purchased from Medicell International (UK).

3.2.2 Synthesis of carboxymethyl scleroglucan ($Scl - CM_{300}$)

Scleroglucan was modified into its carboxymethyl derivative ($Scl - CM_{300}$) following a reported procedure [258]. Scleroglucan (1.0 g) was dissolved in water (40 ml) at 60 °C for 24 h. NaOH (28.0 g) was then added to the polymeric solution in an ice bath to disrupt the triple helix. Finally, chloroacetic acid (40.0 g) was added drop wise to start the reaction. The polymeric mixture was kept under stirring at 60 °C for 24 h followed by neutralization with glacial acetic acid. The obtained $Scl - CM_{300}$ was purified by exhaustive dialysis (cellophane membrane, Visking tubing, cut-off 12,000-14,000 Da) to remove the excess of salts and unreacted products. The dialyzed solution was eluted through a DOWEX 50WX4-50 ion-exchange resin column previously treated with 2.0 M HCl, to obtain all the carboxylic groups in the undissociated form.

The number of carboxylic groups added to the backbone of the polymer was quantified by potentiometer titration. Fully protonated $Scl - CM_{300}$ (100 mg) was dissolved in water and submitted to potentiometer titration using $1 \cdot 10^{-2}$ M NaOH. The amount of acid in mmol (equal to the mmol of NaOH used) was inserted in the following equation:

$$Scl - CM_{\text{amount}}(\text{mg}) = X \cdot MW_{\text{repetitive-unit}} + (\text{mmol-of-acid}) MW_{\text{acid-group}} \quad (3.1)$$

allowing the calculation of X which represents the mmoles of repetitive units of the polymer. The ratio between the mmol of acid and the mmol of the repetitive units of the polymer multiplied by 100 is necessary to obtain the degree of derivatization (DD). This value represents the number of carboxylic groups per 100 repetitive units. A derivative having a DD equal to 300 ± 10 was obtained (labeled as $Scl - CM_{300}$) and used for all the studies. The freeze-dried polymer was mixed with KBr and characterized by FT-IR spectroscopy in the range of 4000–650 cm^{-1} (resolution of 1 cm^{-1}), using a FT-IR Perkin Elmer Paragon 1000 spectrophotometer.

3.2.3 Hydrogel preparation

Solutions of $Scl - CM_{300}$ (2.0% w/v) were prepared by solubilizing $Scl - CM_{300}$ (0.1 g) in 5 ml of distilled water. The mixtures were kept under stirring at 60 °C for 30 minutes to allow a complete solubilization of the polymer. The polymeric solutions were then left to cool down at room temperature (20 °C), to obtain the formation of the corresponding physical hydrogels. Hydrogels loaded with drugs were prepared following the same procedure described above. Specifically, fluconazole, diclofenac sodium salt,

and betamethasone phosphate sodium salt were selected as model molecules for the preparation of the medicated physical hydrogels of *Scl* – *CM*₃₀₀. Each drug was mixed with the polymeric solution before the gel formation at 60 °C in the range of concentration from 0.1 up to 0.5% w/v.

3.2.4 Rheological characterization

Rheological experiments were carried out with a Haake RheoStress 300 Rotational Rheometer (Germany) equipped with a Haake DC10 thermostat. Flow curves were recorded with a shear stress in the range of 0.01–100 Pa at 37 °C ± 0,01 °C. Physical hydrogels of *Scl* – *CM*₃₀₀ (2% w/v) with and without drugs were placed on a cone-plate geometry (angle of 1°) in order to completely cover the surface. In addition, frequency sweep tests were carried out on the same samples in the range of 0.01 up to 10 Hz. Mechanical spectra were recorded within the linear viscoelastic region measuring hydrogels response at a strain amplitude of 1%.

3.2.5 Release studies with Franz diffusion cell

Release studies were carried out from hydrogels loaded with fluconazole, diclofenac sodium salt and betamethasone phosphate sodium salt (0.25% w/v) using a vertical Franz cell [270]. The cylindrical donor chamber (cross-section area 0.5 cm²) was loaded with a weighted amount (100 mg) of the drug-carrying hydrogel, gel thickness $L_g = 2$ mm. The donor chamber was separated by the receptor one with a dialysis membrane (cellophane membrane, Visking tubing, cut-off 12,000-14,000 Da) having an area of 0.5 cm² and thickness $L_m = 48$ μm.

The receptor chamber was filled with 4.1 ml of phosphate buffer pH 7.4 under constant stirring (50 rpm). pH 7.4 was chosen for this study because of the dependence of diclofenac solubility from pH ([271]). At pH 7.4 we have the maximum solubility of diclofenac, therefore even if back-diffusion of the release medium towards the donor compartment occurred during the study, no drug precipitation is expected within the gel.

Release experiments were carried out keeping the diffusion cell in a water bath at 37 °C ± 0,01 °C for 24 h. Aliquots of 250 μl were withdrawn at fixed time intervals and replaced with equal volumes of fresh buffer. The release rate of diclofenac from *Scl* – *CM*₃₀₀-based hydrogels was also studied at room temperature (20 °C) following the same experimental set-up. In addition, diffusion profiles of 0.25% w/v aqueous solutions of the three investigated drugs (0.1 ml, solvent thickness in the donor chamber $L_s = L_g = 2$ mm) were used as blanks. Diffusion profiles of 0.25% w/v aqueous solutions of theophylline were also used as blanks to investigate the dependence of the drug diffusion coefficient in the dialysis membrane on the drug molecular weight.

All the drugs were quantified by HPLC analysis carried out with a Perkin-Elmer apparatus equipped with a Perkin Elmer Series 200LC pump and a series 235 Diode Array Detector, using a Merck Hibar LiChrocart (250-4, 5 μm) RP-18 column. The three drugs were determined according to already reported analytical methods, with some modifications. Diclofenac was analyzed using a mixture consisting of methanol and 0.01 M phosphoric acid (80:20, v:v), as the mobile phase, with a flow rate 0.7 ml/min and measuring the drug at 215 nm ([258]). Fluconazole was analyzed using a mobile phase consisting of methanol, water and acetic acid (50:48:2, v:v:v), with a flow rate of 0.9 ml/min and monitoring the drug at 260 nm ([272]). Betamethasone was instead detected using a mobile phase made of methanol and 0.01 M phosphoric acid (60:40, v:v), with a flow rate 0.8 ml/min and detecting the drug at 215 nm ([273]).

All the experiments were repeated in triplicate, and the results reported as mean value ± standard deviation.

3.2.6 Mathematical models of permeation experiments in a vertical Franz cell

We present the time-dependent one-dimensional Fickian and non-Fickian transport models adopted to describe drug permeation in a Franz vertical cell, both accounting for the presence of the cellophane (dialysis) membrane and finite volume of the receptor chamber. Both transport models are numerically solved by Finite Element Method (FEM) using Comsol 3.5 Multiphysics. The Convection-Diffusion Package in Transient Analysis has been used. The linear solver adopted is UMFPACK, with relative tolerance 10^{-3} and absolute tolerance 10^{-6} . The Time Stepping Method adopted is BDF with a Strict policy for Time steps taken by the solver. Lagrangian quadratic elements are chosen. The number of finite elements is $2 \cdot 10^4$ with a non-uniform mesh. Maximum-minimum element sizes $2.5 \cdot 10^{-3} - 2.5 \cdot 10^{-7}$ in dimensionless units (total length of the domain in dimensionless units 1.024). Smaller elements are located in the membrane domain and close to the boundaries gel/membrane and membrane/receptor chamber to guarantee the convergence of the numerical scheme and accurate resolution of concentration gradients.

Fickian diffusion model

Drug release from *Scl* - *CM*₃₀₀ networks can be described as a purely one-dimensional Fickian diffusion process (along the vertical coordinate z spanning the donor chamber), assuming that no drug/hydrogel matrix interaction and no matrix erosion of the fully swollen hydrogel occurs during the release experiments. A purely Fickian transport model can be adopted to describe blank experimental release data as well as release data from *Scl* - *CM*₃₀₀ hydrogels for molecules that exhibit a typical Fickian behavior, i.e. $M_t/M_\infty \sim t^{1/2}$ at short-intermediate time scales. Let us indicate with C_g , D_g , C_m , and D_m the drug concentrations and the effective diffusion coefficients in the hydrogel and the dialysis membrane, respectively. C_0 indicates the initial drug concentration in the hydrogel (thickness $L_g = 2$ mm, volume $V_g = 0.1$ cm³). The dialysis membrane used in the study has a thickness $L_m = 48$ μm and a volume $V_m = 2.4$ mm³. Let C_{res} be the drug concentration in the perfectly mixed receptor chamber of volume $V_{res} = 4.1$ ml.

By introducing the dimensionless time and space variables $\tau, \zeta, \beta, \alpha_m$ and the diffusivity ratio γ_g :

$$\tau = tD_m/L_g^2, \zeta = z/L_g, \alpha_m = L_m/L_g, \beta = V_g/V_{res}, \gamma_g = D_g/D_m \quad (3.2)$$

the transport equations and the boundary/initial conditions can be written as:

$$\frac{\partial C_g}{\partial \tau} = \gamma_g \frac{\partial^2 C_g}{\partial \zeta^2} \quad \text{for } 0 < \zeta < 1, \quad \frac{\partial C_g}{\partial \zeta} = 0 \quad \text{at } \zeta = 0, \quad C_g(0, \zeta) = C_0 \quad (3.3)$$

$$\frac{\partial C_m}{\partial \tau} = \frac{\partial^2 C_m}{\partial \zeta^2} \quad \text{for } 0 < \zeta < 1 + \alpha_m, \quad C_m = C_g \quad \text{at } \zeta = 1 \quad (3.4)$$

$$\gamma_g \frac{\partial C_g}{\partial \zeta} = \frac{\partial C_m}{\partial \zeta} \quad \text{at } \zeta = 1, \quad C_m = C_{res} \quad \text{at } \zeta = 1 + \alpha_m, \quad C_m(0, \zeta) = 0 \quad (3.5)$$

$$\frac{dC_{res}}{d\tau} = -\beta \frac{\partial C_m}{\partial \zeta} \quad \text{at } \zeta = 1 + \alpha_m, \quad C_{res}(0) = 0 \quad (3.6)$$

We assume no mass-transfer resistance at the membrane-receptor chamber interface and unitary partition coefficients at the membrane-receptor chamber interface as well as at the gel membrane interface. The balance equation for C_{res} , equation (3.6), and the boundary condition $C_m = C_{res}$ at $\zeta = 1 + \alpha_m$ account for the finite volume of the receptor chamber. By solving the transport equations eq:(3.3)-(3.6) for C_g , C_m , and C_{res} , the drug-release curve can be computed as follows:

$$\frac{M_\tau}{M_\infty} = \frac{V_{res} C_{res}(\tau)}{V_{res} C_{res}^\infty}, \quad M_\infty = V_{res} \frac{\beta C_0}{1 + \beta(1 + \alpha_m)} = \frac{V_g C_0}{1 + \beta(1 + \alpha_m)} \quad (3.7)$$

where $M_\infty < V_g C_0$ because of the finite volume of the receptor chamber. The same set of transport equations can be used to describe the blanks, representing the drug release studies from the aqueous solutions without the hydrogel. This is possible by simply replacing C_g (drug concentration in the gel) with C_s (drug concentration in the aqueous solution placed in the donor chamber) and considering the diffusivity ratio $\gamma_s = D_s/D_m$ instead of $\gamma_g = D_g/D_m$, where D_s represents the drug diffusivity in the solvent solution.

The Wilke-Chang correlation ([274]) was used to estimate D_s for each model drug:

$$D_s^{drug} \left[\frac{cm^2}{s} \right] = 7.4 \cdot 10^{-8} \frac{\sqrt{\Psi_B M W_B T}}{\eta_B V_{drug}^{0.6}} \quad (3.8)$$

where B indicates the solvent (water, $\Psi_B = 2.26$) and V_{drug} is the LeBas drug molar volume usually obtained from a group contribution approach, considering the contributions of individual atoms, functional groups and cycles composing each molecule [274]. From the blanks, we estimate the effective diffusion coefficient of the different model drugs in the dialysis membrane D_m , by best fitting the only unknown parameter γ_s . Hence, from the release data from *Scl - CM₃₀₀* hydrogel, we estimate the effective diffusion coefficient of each model drug D_g in the hydrogel by best fitting the only unknown parameter $\gamma_g = D_g/D_m$. This model fits well blank experimental release data as well as release data from *Scl - CM₃₀₀* hydrogel for molecules that exhibit a typical Fickian behavior, i.e. $M_\tau/M_\infty \sim \tau^{1/2}$ at short-intermediate time scales.

Drug/hydrogel interaction model

A second mathematical model was introduced to describe possible interactions between a model drug and the hydrogel matrix and their effects on the drug release kinetics. This model can be used to explain the apparent "anomalous" non-Fickian behavior $M_\tau/M_\infty \sim \tau^n$ characterized by an exponent $n \gg 1/2$ that can be observed at short-intermediate time scales in the presence of solute/polymeric matrix interactions (for a fully swollen gel). In this case, a two-phases kinetic model, originally proposed by Adrover [275] for drug release from water swollen scleroglucan matrices, is adopted to describe the system. Specifically, it is possible to define a fraction ϵ of the drug molecules that is capable of interacting with the polymeric network, which can be separated from the other drug molecules that are simply dissolved in the water phase of the hydrogel, where they are free to diffuse with an effective diffusion coefficient D_g . A similar approach has been adopted by Singh et al., modeling drug release from hydrogels via a diffusion transport coupled with adsorption/desorption mechanism [276].

The "two-phases" model adopted in the present work actually describes the adsorption/desorption mechanism in terms of a linear transfer rate from the adsorbed "bounded" phase to the desorbed "free" (or gel-solvent) phase and viceversa. Let us then indicate C_b and C_g as the drug concentrations in the bounded and free (gel-solvent) phases, respectively. By assuming a reversible reaction and a linear transfer rate from the bounded to the free phase $-r_{b \rightarrow g} = K_{bg} C_b$ as well as a linear transfer rate from the free to the bounded phase $-r_{g \rightarrow b} = K_{gb} C_g$, the dynamic equations describing the phenomenon can be written as:

$$\frac{\partial C_g}{\partial \tau} = \gamma_g \frac{\partial^2 C_g}{\partial \zeta^2} + \phi^2 \gamma_g (C_b - C_g / K_{eq}) \quad \text{for } 0 \leq \zeta \leq 1 \quad (3.9)$$

$$\frac{\partial C_b}{\partial \tau} = -\phi^2 \gamma_g (C_b - C_g / K_{eq}) \quad \text{for } 0 \leq \zeta \leq 1 \quad (3.10)$$

$$\frac{\partial C_g}{\partial \zeta} = 0 \quad \text{at } \zeta = 0, \quad C_g = C_m \quad \text{at } \zeta = 1 \quad (3.11)$$

$$C_g(0, \zeta) = (1 - \epsilon) C_0, \quad C_b(0, \zeta) = \epsilon C_0 \quad (3.12)$$

where $K_{eq} = K_{gb}/K_{bg}$ is the equilibrium constant (depending on the temperature of the experiment) and $\phi^2 = \frac{K_{bg}L_g^2}{D_g}$ is a dimensionless parameter, equivalent to a square Thiele modulus, representing the ratio between the characteristic diffusion time L_g^2/D_g in the free(gel-solvent) phase and the characteristic time for the reversible transfer from the bounded to the free phase $1/K_{bg}$. No drug diffusion occurs in the bounded phase. Balance equations for C_m and C_{res} , as well as the boundary conditions for C_g and C_m remain unchanged with respect to the purely Fickian diffusion model.

In this case, the total amount of drug released up to an infinite time reads as:

$$\lim_{\tau \rightarrow \infty} M_\tau = \frac{V_g C_0}{1 + \beta(1 + \alpha_m + K_{eq}^{-1})} \quad (3.13)$$

that can be significantly smaller than M_∞ (see eq:(3.7)), depending on the value of K_{eq} , because for any finite value of K_{eq} , part of the drug, namely the total amount $\frac{V_g C_0 \beta K_{eq}^{-1}}{1 + \beta(1 + \alpha_m + K_{eq}^{-1})}$, get trapped in the bounded phase and never released. The initial partition coefficient ϵ depends on the initial temperature of the gel sample. If the gel sample is kept at constant ambient temperature T_0 prior of the experiment and then, at time $t=0$, placed in the donor chamber in contact with the solvent solution in the receptor chamber kept at constant temperature $37^\circ\text{C} \pm 0,01^\circ\text{C}$ (temperature of the water bath), the initial partition coefficient reads as:

$$\epsilon = \frac{1}{1 + K_{eq}(T_0)} \quad (3.14)$$

The gel sample, initially at temperature T_0 , rapidly warms up (1–3 minutes) to the water bath temperature T and the release process takes place at constant temperature T . The equilibrium constant $K_{eq}(T_0)$ at the initial temperature T_0 , and therefore the initial partition coefficient ϵ , can be estimated from an independent release experiment performed at temperature T_0 of the water bath, by experimentally estimating $\lim_{\tau \rightarrow \infty} M_\tau$ at $T = T_0$ and therefore $K_{eq}(T_0)$ from equation (3.13) and ϵ from equation (3.14).

3.2.7 Primary skin irritation experiments

Three healthy male New Zealand White rabbits were purchased from Charles River (Calco Lecco, Italy) and acclimated to the laboratory for a week. The rabbits were individually housed and received a standard diet and tap water ad libitum. Laboratory animal care guidelines (EEC Directive of 1986; 86/609/EEC) were followed. The back of the animals was clipped free of their fur with an electric clipper 24 h before application of the samples. Clipped rabbit skin was divided into four sites of same area (30 · 30 mm).

Scl, Scl- CM_{300} -based hydrogels were spread on two of the four different locations (500 mg/site), whereas the other two ones were kept free from any material application and used as a visual control. The treated and the control areas were covered with a gauze, and the back of the rabbit was wrapped with a non-occlusive bandage. After the treatment, the animals were returned to their cages. Bandages and the test hydrogels were removed after 4 h and rabbits were examined for skin irritation 1 hour later.

Observation of the different sites was repeated at 24, 48 and 72 h. The reaction, defined as erythema or edema, was evaluated according to the score of the skin reactions already reported. The score of primary irritation (SPI) was calculated for each rabbit as the difference between the sum of the scores of erythema and edema at 24, 48 and 72 h in the treated sites and the control areas. These values were also divided by the number of observations. The primary skin irritation index (PII) was calculated as the arithmetical mean of the SPI values of the three animals. The evaluation of PII was performed according to the categories reported in the literature [277].

3.3 Results

3.3.1 Physical hydrogel preparation and characterization

Scleroglucan carboxymethyl ($Scl - CM_{300}$) with a high degree of derivatization was obtained following a previously established protocol [258]. FT-IR spectra of the polymer prior and after ion exchange were recorded to evaluate the conversion of Scl in its carboxymethyl derivative. As expected, elution through DOWEX resin caused the complete conversion of the polymer to the free acid derivative and a consequent increase in the intensity of the corresponding stretching band at 1725 cm^{-1} could be observed. In fact, a shift in the equilibrium from the carboxylate group ($-COO^-$) to the carboxylic group ($-COOH$) is evident from the overlapping of the FT-IR spectra.

Specifically, the stretching of the carbonyl group shifts from 1590 cm^{-1} (before ionic exchange) to 1725 cm^{-1} (after ionic exchange), thus indicating a higher presence of carboxylic groups in the protonated form. The total amount of carboxylic groups added to the polymer backbone was quantified through potentiometer titration and resulted in being 300 ± 10 . The high number of carboxymethyl functional groups introduced on the Scl backbone promote interaction among the polymeric chains, making possible the formation of physical hydrogels without the addition of any salt. Specifically, the carboxylic groups introduced in the backbone of the polysaccharide can form hydrogen bonds and ion-dipole interactions, responsible for the physical gel formation (figure 3.1A).

Hydrogels were formed at the concentration of 2.0% w/v in the presence and absence of drugs. This concentration was chosen as the optimal one because of the homogeneous consistency of the hydrogels suitable for topical application. The flow curve of the plain hydrogel (without drugs) has been carried out to study the rheological properties of the system at different shear rates (figure 3.1B). $Scl - CM_{300}$ at 2.0% w/v showed a shear-thinning behavior that is typical of a pseudoplastic macromolecular system. It is noteworthy that the viscosity behavior of Scl-CM at a high degree of derivatization resembles the flow properties of native scleroglucan at the same concentration ([258]).

The preservation of the pseudoplastic flow behavior after derivatization is an essential feature allowing the use of this system as a topical formulation, which can be applied to the skin or to the mucosae. Frequency sweep tests carried out in the viscoelastic region showed values of the elastic modulus G' higher than the viscous modulus G'' over the range of frequencies tested (figure 3.1C), indicating the formation of a physical hydrogel. The value of G' slightly changes throughout the test showing the typical behavior of a weak gel, for which the value of G' is influenced by the frequency of the applied deformation.

3.3.2 Rheological characterization of drug loaded $Scl - CM_{300}$ physical hydrogels

A previous report [258] proposing $Scl - CM_{300}$ hydrogels as drug carriers for oral drug administration, showed that a reduction in the pH value can increase the hydrogel strength (higher values of the G' elastic modulus) and reduce the swelling capacity of the matrix.

The focus of our investigation was to determine whether the presence of a loaded drug could affect the rheological properties of $Scl - CM_{300}$ hydrogels as drug carriers for topical administration. To this end, three different therapeutic molecules, such as fluconazole, diclofenac, and betamethasone phosphate were included in the polymeric solution of $Scl - CM_{300}$ 2.0% w/v before hydrogel formation. Different concentrations of the three drugs were tested varying from 0.1% w/v up to 0.5% w/v. Irrespective of the drug considered and its amount, the corresponding physical hydrogels showed shear-thinning behavior similar to the plain system, with almost no significant effects on the viscosity values (see figure 3.2). Results of frequency sweep tests for the hydrogels loaded with the selected drugs (0.25% w/v) showed different behaviors according to the type of molecule loaded in the polymeric network (see figure 3.3).

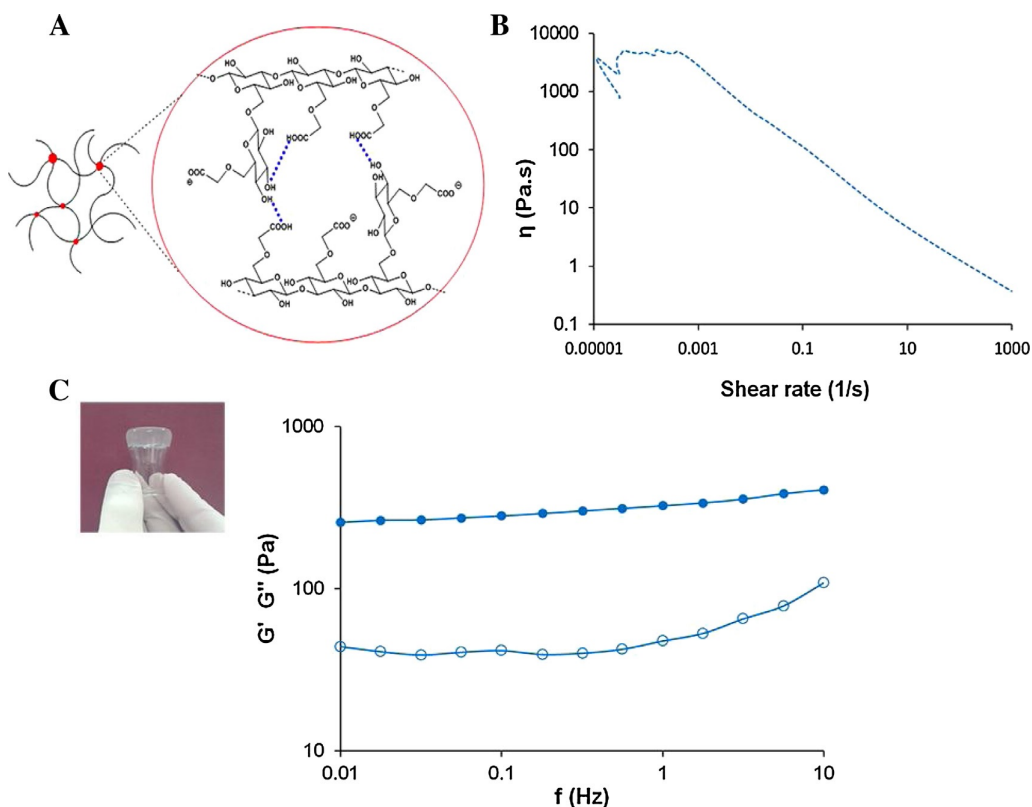


Figure 3.1: Rheological characterization of *Scl*-*CM*₃₀₀ physical hydrogels. A) Schematic representation of hydrogen bond formation among carboxyl and hydroxyl groups. B) Flow curve showing the pseudoplastic behavior of the polymer at $37^{\circ}\text{C} \pm 0,01^{\circ}\text{C}$. C) Representative picture of *Scl*-*CM*₃₀₀ physical hydrogel and the corresponding frequency sweep test carried out in the range of 0.01–10 Hz. Full circles represent the elastic modulus G' and empty circles the viscous modulus G'' .

Fluconazole did not influence the hydrogel properties over the whole range of frequencies investigated, and only a small decrease in the G'' values was observed respect to the hydrogel without the drug. Mechanical spectra of *Scl*-*CM*₃₀₀ hydrogel loaded with betamethasone showed a reduction of both G' and G'' when compared to the plain hydrogel, indicating that the drug partially interferes with the formation of the polymeric network, thus resulting in a softer hydrogel. On the contrary, the presence of diclofenac induced a significant increase of both G' and G'' , thus indicating the formation of a stronger gel (figure 3.3C).

It is possible to assume that the presence of a carboxylic group in the diclofenac molecule leads to additional hydrogen bonding interactions affecting the final rheological properties of the physical hydrogel. Based on these results it may be expected a different ability of the *Scl*-*CM*₃₀₀ network to modulate the release of the three selected molecules. In fact, besides the molecular weight and the chemical structure of the investigated drugs, the strength of the drug-polymer interactions is an additional factor, which may affect the molecular mobility of the incorporated model drug, playing a critical role in controlling the release rate from the polymer matrix. For this reason, these findings were further investigated through in-vitro release tests.

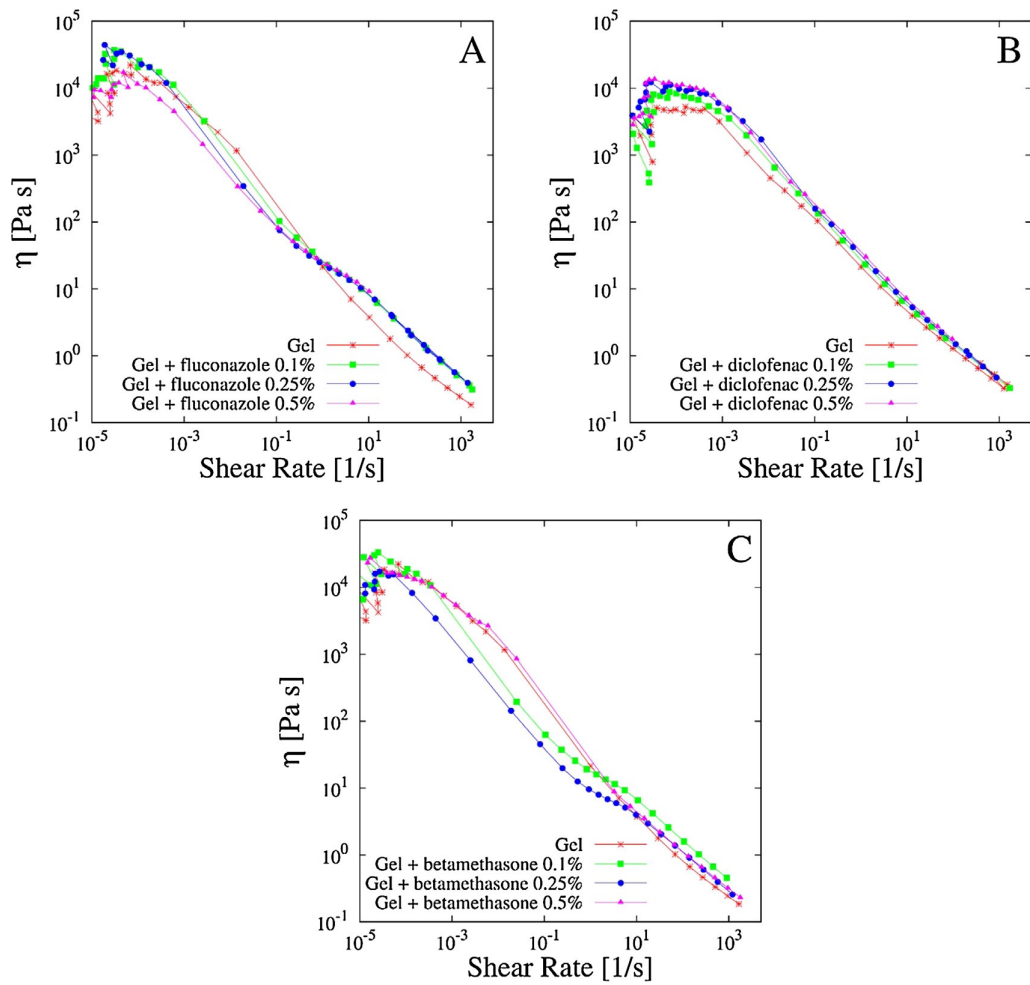


Figure 3.2: Comparison of flow curves of *Scl* - *CM*₃₀₀ physical hydrogels loaded with different concentration (from 0.1% w/v up to 0.5% w/v) of A) fluconazole, B) diclofenac and C) betamethasone. Flow curves were recorded at $37^\circ\text{C} \pm 0,01^\circ\text{C}$.

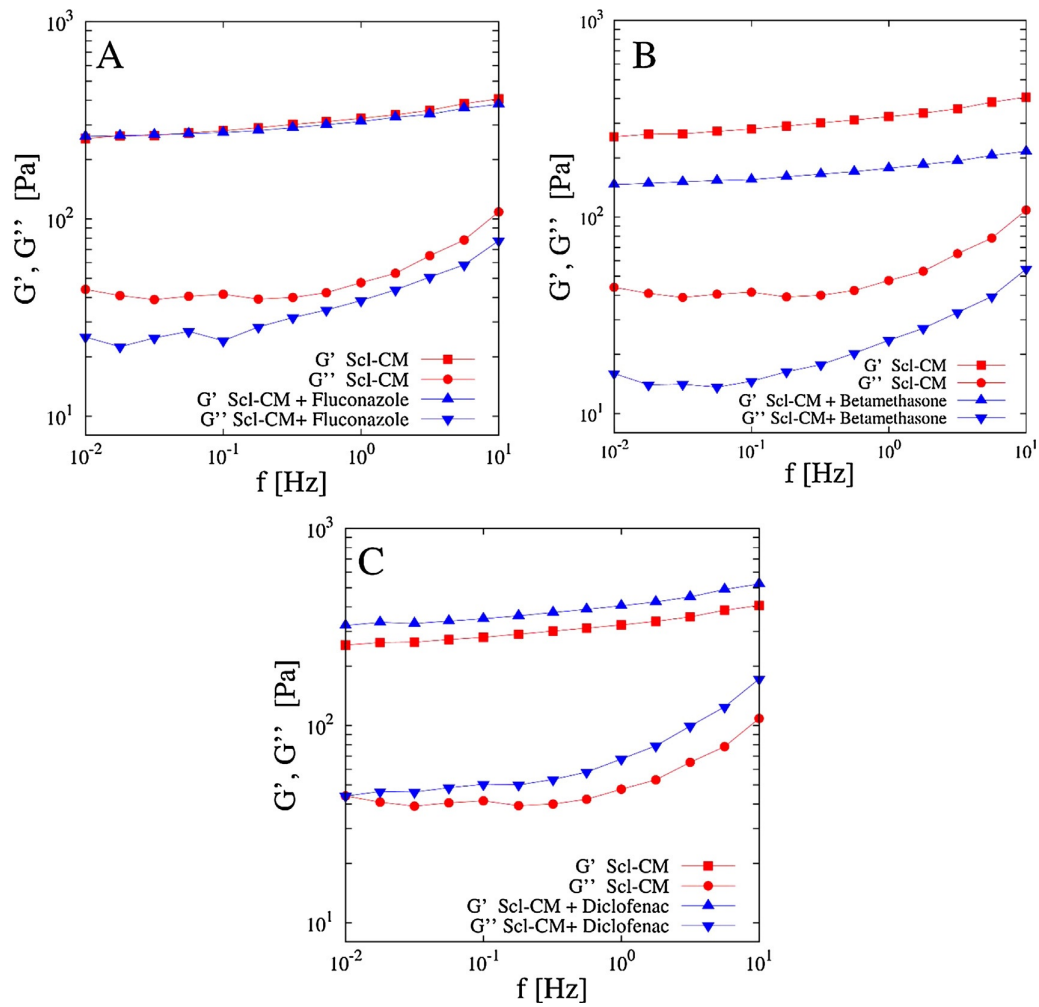


Figure 3.3: Frequency sweep tests carried out in the range of 0.01–10 Hz for plain *Scl* – *CM*₃₀₀ hydrogel (red square and circular points for G' and G'' , respectively) and loaded with different model drugs (upper and lower triangular points for G' and G'' , respectively). A) fluconazole; B) betamethasone; C) diclofenac.

3.3.3 Release studies

Analysis of release data from blanks

Figure 3.4 shows the release profiles of the three model drugs in aqueous solution (blank systems, points with error bars) and the comparison with the Fickian model (continuous lines).

It can be observed that diclofenac and fluconazole exhibit similar blank release curves since they are characterized by very close values of the LeBas volume. A slower release is obtained for betamethasone due to the significantly larger value of its LeBas volume. Model curves were obtained, for each model drug, by estimating D_s from the Wilke-Chang correlation (3.8) and by best fitting the ratio $\gamma_s = D_s/D_m$ in the Fickian transport model (see table 3.1). The values of γ_s are in the order of 10^1 for all the model drugs, thus implying that the effective diffusion coefficient in the dialysis membrane is one order of magnitude smaller than the diffusivity in water solution. Therefore the dialysis cellophane membrane, even if extremely thin ($L_m = 48\mu m$), offers a significant resistance to drug transport from the donor to the receptor compartment and its presence should be necessarily taken into account in the transport model [278]. This is in agreement with other drug release studies from Scleroglucan hydrogels making use of the same cellophane membrane (Visking tubing, cut-off 12,000-14,000 Da) in two or three compartments diffusion cells [279].

This observation is further supported by the analysis of blank release data from a 0.25% w/v aqueous solutions of theophylline (TPH), usually adopted as a model drug and characterized by both a low MW and a small LeBas volume. For TPH, the value of the water diffusivity $D_s = 8.39 \cdot 10^{-6} cm^2/s$ estimated from the Wilke-Chang correlation, is in perfect agreement with experimental literature data $D_s = 8.2 \cdot 10^{-6} cm^2/s$ at 37 °C [279, 280] and the best fit value of the diffusivity ratio is $\gamma_s = 16 \pm 0.2$.

Figure 3.4B shows the effective diffusion coefficient in the dialysis membrane D_m as a function of the molecular weight for all the model drugs analyzed, highlighting how D_m is a linear decreasing function of the molecular weight over the whole range of MW analyzed.

Analysis of release data from *Scl* – *CM*₃₀₀ hydrogels

Figure 3.5 shows experimental release data of the three model drugs under investigation from *Scl* – *CM*₃₀₀ hydrogels at 37 °C. Continuous black lines a-b represent the short-intermediate time-scale Fickian behavior $M_t/M_\infty \sim t^{0.5}$ (in agreement with the release data of fluconazole and betamethasone) while curve c represents the "anomalous" non-Fickian behavior $M_t/M_\infty \sim t^n$ with $n=1.2 \gg 1/2$, in agreement with diclofenac release profile (figure 3.5).

Drug-polymer interactions are here responsible for the time-lag observed in the early-stage release curve of diclofenac that is a typical feature of non-Fickian transport. Similar features have been observed in drug release experiments from sclerox and cross-linked sclerox hydrogels [281]. These results confirmed the trend observed in the frequency sweep tests where diclofenac was the only tested drug capable of increasing the values of G' and G'' due to the formation of drug-polymer hydrogen bonding interactions. The same interactions are here responsible for the observed anomalous release. Specifically, diclofenac is released at a significantly slower rate than fluconazole and betamethasone, despite the fact that its LeBas molar volume is similar or significantly smaller than the ones reported for fluconazole and betamethasone. Moreover, not the whole amount of drug initially loaded is actually released after 24 h.

For these reasons, a Fickian transport model was adopted for fluconazole and betamethasone, whereas the non-Fickian solute transport model taking into account drug - hydrogel interactions, was introduced to describe diclofenac release curves. The half-life time $t^{0.5}$ for drug molecules non interacting with the hydrogel matrix are $t^{0.5} = 45.6$ min for fluconazole (MW=306) and $t^{0.5} = 96$ min for betamethasone (MW=516).

Table 3.1: LeBas molar volumes, diffusion coefficients in water solution, diffusivity ratio γ and effective diffusion coefficient in the dialysis membrane and in *Scl* - *CM*₃₀₀ hydrogel at $37^\circ\text{C} \pm 0,01^\circ\text{C}$ for different model drugs.

-	$V_{LB}[\text{mol}/\text{cm}^3]$	$D_s[\text{cm}^2/\text{s}]$	$\gamma_s = D_s/D_m$	$D_m[\text{cm}^2/\text{s}]$	γ_g	$D_g[\text{cm}^2/\text{s}]$
Theophylline	170.2	$8.39 \cdot 10^{-6}$	$16,0 \pm 0,2$	$5.24 \pm 0.06 \cdot 10^{-7}$	n.e.	n.e.
Diclofenac	294.8	$6.05 \cdot 10^{-6}$	$14,1 \pm 0,2$	$4.29 \pm 0.06 \cdot 10^{-7}$	$14,1 \pm 0,2$	$6.05 \cdot 10^{-6}$
Fluconazole	307.6	$5.89 \cdot 10^{-6}$	$14,0 \pm 0,2$	$4.20 \pm 0.06 \cdot 10^{-7}$	$14,0 \pm 0,2$	$5.89 \cdot 10^{-6}$
Betamethasone	471.2	$4.56 \cdot 10^{-6}$	$19,4 \pm 0,2$	$2.35 \pm 0.02 \cdot 10^{-7}$	$11,5 \pm 0,2$	$2.70 \cdot 10^{-6}$

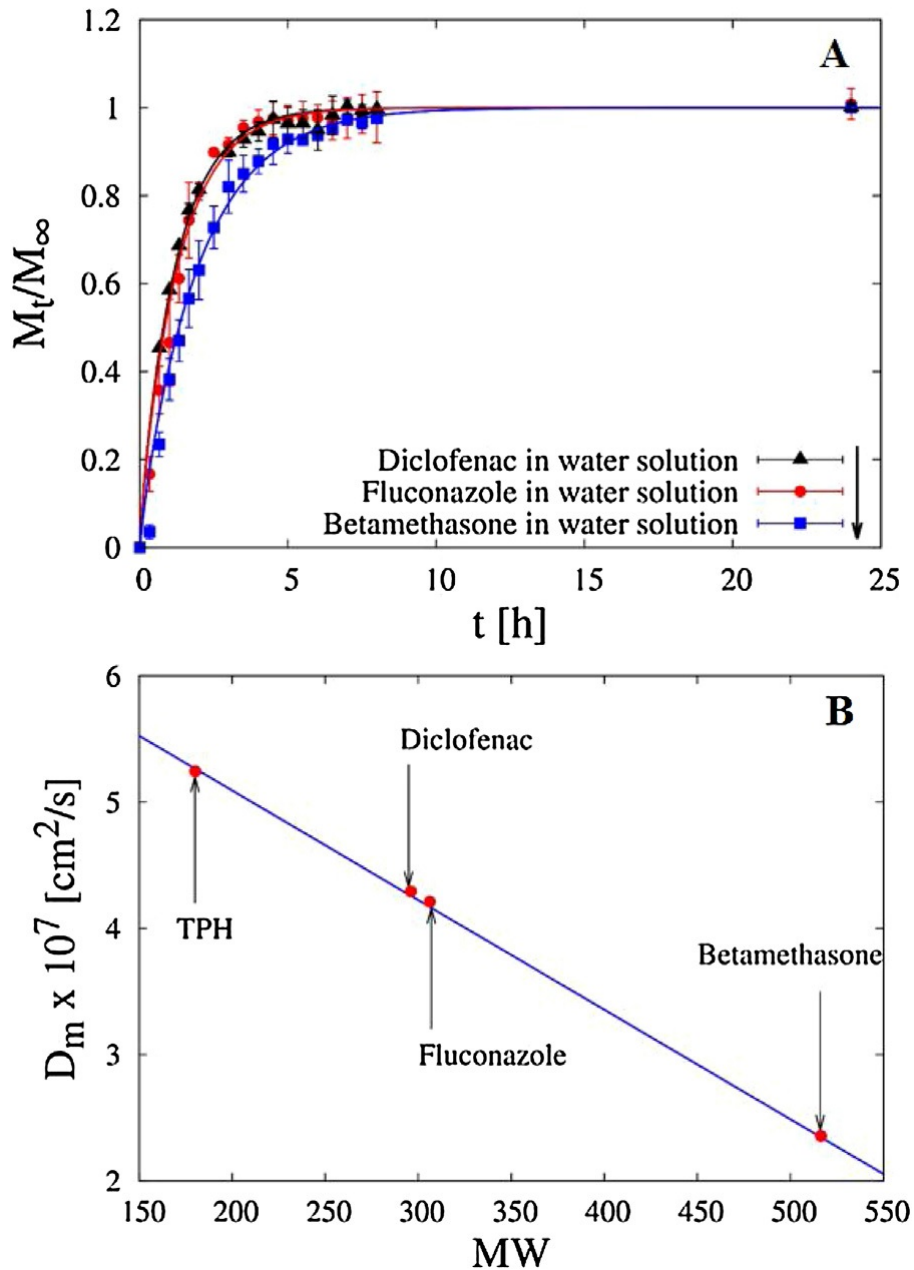


Figure 3.4: A) Experimental release data from 0.1 ml of aqueous solutions (0.25% w/v) (blanks, points with error bars) containing different model drugs and the comparison with the Fickian transport model (continuous lines). Best fit values of the diffusivity ratio $\gamma_s = D_s/D_m$ are reported in table 3.1. The arrow indicates increasing values of the LeBas volume. B) D_m vs MW for different model drugs, including TPH.

Therefore by almost doubling the molecular weight of the loaded drug, also the half-life time doubles. Henceforth the hydrogel *Scl* - *CM*₃₀₀ appears to be suitable for drug delivery as the release is strongly dependent on the dimensions of the model drug and therefore the delivery can be tailored in function of the steric hindrance of the entrapped molecule. Similar release features have been observed by Coviello et al., 2005 for *Scl*/Borax hydrogels, which they proposed as suitable hydrogels for a sustained drug delivery. Coviello et al., 2005 observed a Fickian behaviour for the release curves of TPH (MW=180), Vit. B12 (MW=1355) and myoglobin (MW=17800) from *Scl*/Borax hydro-

gel in distilled water and showed how half-lives for Vit. B12 (about ten times bigger than TPH in terms of MW) and myoglobin (about one hundred times bigger than TPH) were respectively about two and five times bigger than the TPH half-life. Therefore, the hydrogel of *Scl* – *CM*₃₀₀ appears to be more sensitive to the drug molecular weight than Scl/Borax hydrogel.

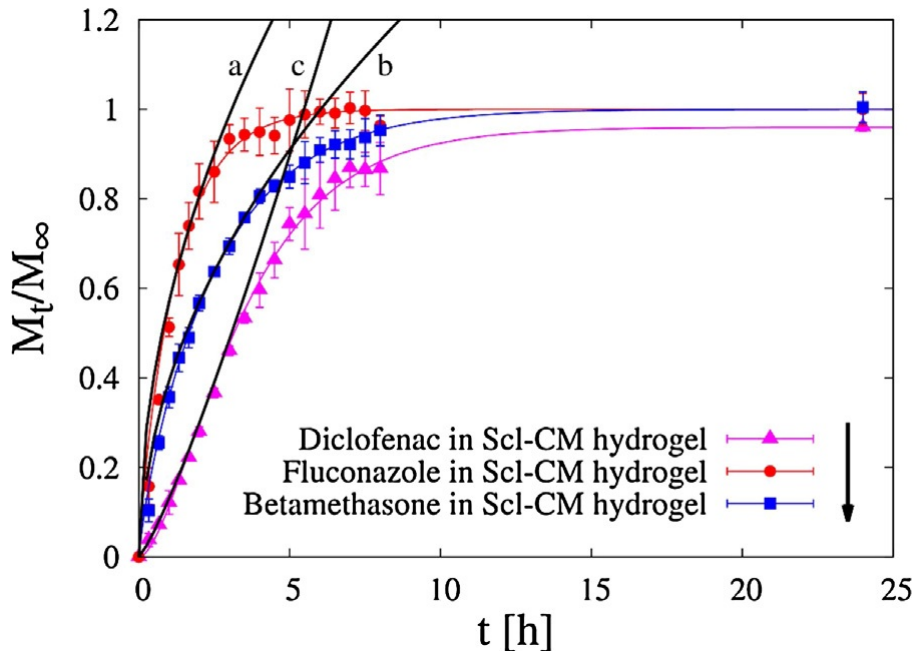


Figure 3.5: Experimental release data from *Scl* – *CM*₃₀₀ hydrogel containing different model drugs and the comparison with the Fickian short-intermediate time-scale behavior $M_t/M_\infty \sim t^{0.5}$ (curves a-b) and the non-Fickian behavior $M_t/M_\infty \sim t^n$ with $n=1.2 \gg 1/2$ (curve c). The arrow indicates increasing values of LeBas molar volumes.

Release data modeling

Fig:3.6A shows fluconazole release data from an aqueous solution and from the hydrogel in excellent agreement with the Fickian transport model with $\gamma_s = \gamma_g$, since release data from the hydrogel and from the aqueous solution are almost coincident. It is therefore a case of an ideal topical release, as this formulation does not offer additional resistance to fluconazole release with respect to an aqueous solution. Figure 3.6B shows betamethasone release data from aqueous solution and hydrogel in excellent agreement with the Fickian transport model with $\gamma_s = 19.4$ and $\gamma_g = 11.5$.

Therefore, the *Scl* – *CM*₃₀₀ formulation offers a small additional resistance to betamethasone transport (larger LeBas molar volume) since $D_g = (\gamma_g/\gamma_s) D_s \sim 0.59 D_s$. For a direct comparison between D_g and D_s for different model drugs see table 3.1.

Figure 3.6C shows diclofenac release data from aqueous solution and hydrogel at $37^\circ\text{C} \pm 0,01^\circ\text{C}$, together with the release data from hydrogel at room temperature 20°C .

The release curve from *Scl* – *CM*₃₀₀ hydrogel is significantly slower than that from water solution although the diclofenac molecule exhibits the smallest LeBas volume among the three model drugs analyzed. Rheological results support the idea of a chemical interaction between diclofenac and the hydrogel matrix. Release data at room temperature are a direct evidence not only for the interaction between diclofenac and *Scl* – *CM*₃₀₀, but they also suggest that a very large amount of drug is bounded to the polymer matrix and is unable to diffuse out from the hydrogel.

In fact, only 10% of the drug is released from the hydrogel after 24 h. From the asymptotic value $\lim_{t \rightarrow \infty} M_t/M_\infty(20^\circ\text{C}) = 0.11 \pm 0.02$ and from equations:(3.13)-(3.14)

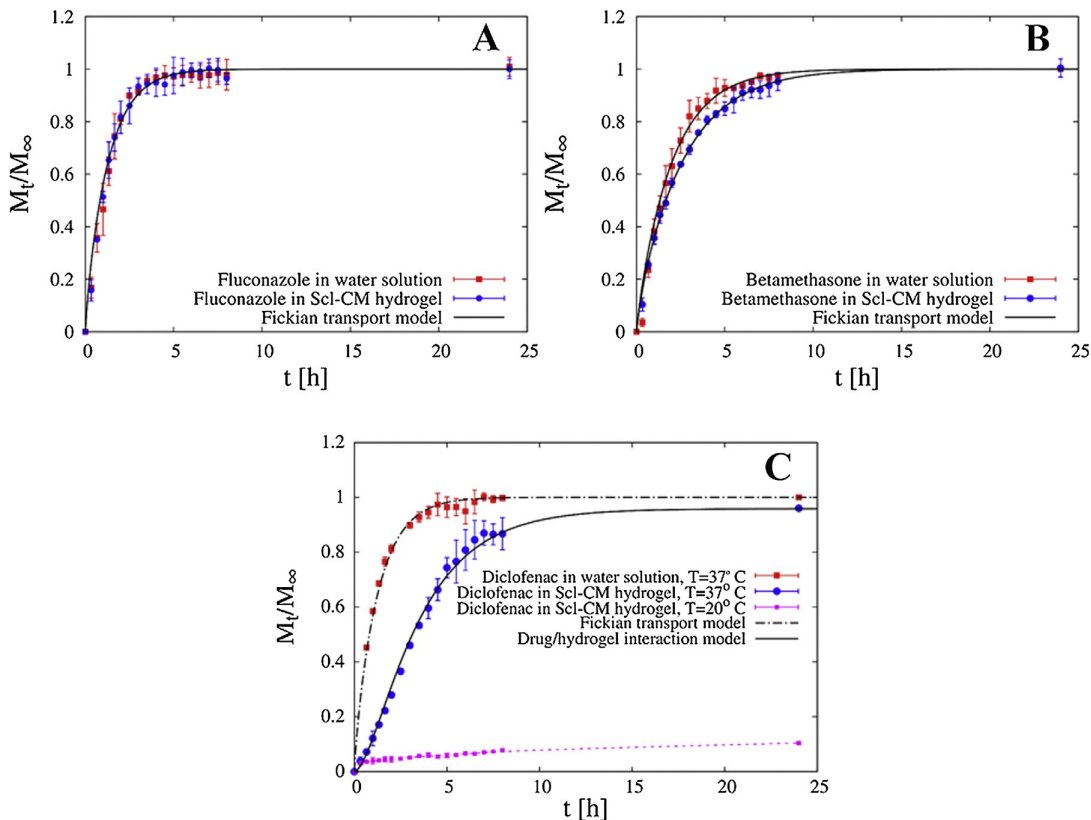


Figure 3.6: Experimental release data of A) fluconazole from water solution and from *Scl* – *CM*₃₀₀ hydrogel and the comparison with the Fickian transport model with $\gamma_s = \gamma_g$; B) betamethasone from water solution and from *Scl* – *CM*₃₀₀ hydrogel and the comparison with the Fickian transport model with $\gamma_s = 19.4$ and $\gamma_g = 11.5$; C) diclofenac from water solution (at 37 °C) and from *Scl* – *CM*₃₀₀ hydrogel at 37 °C and 20 °C. Broken dot-line curve represents the Fickian transport model for blank with $\gamma_s = 14.1$. Continuous line represents the non-Fickian drug/matrix interaction model with $\gamma_g = \gamma_s = 14.1$ and $\phi^2 = 0.74 \pm 0.02$.

we estimate $K_{eq}(20^\circ\text{C}) = 2.9 \cdot 10^{-3}$ and the initial partition coefficient $\epsilon = 0.001$ for the release experiment at the working temperature of 37 °C.

The three other parameters entering the non-Fickian transport model are γ_g , $K_{eq}(37^\circ\text{C})$ and ϕ^2 . From the asymptotic value $\lim_{t \rightarrow \infty} M_t/M_\infty(37^\circ\text{C}) = 0.96 \pm 0.03$ and from equations:(3.13) we estimate $K_{eq}(37^\circ\text{C}) = 0.57$. For γ_g we set $\gamma_g = \gamma_s = 14.1$ because of the small LeBas volume of the drug molecule. The only best fit parameter is the square Thiele modulus ϕ^2 . Figure 3.6C shows the excellent agreement between the release data from the hydrogel and the non-Fickian transport model with $\phi^2 = 0.74 \pm 0.02$.

The best fit value of ϕ^2 , order of unity, indicates that the characteristic time for the irreversible transfer from the bounded to the free-solvent phase is of the same order as the characteristic diffusion time, thus explaining the significant slowing down of the experimental release curve. The data obtained proved that *Scl* – *CM*₃₀₀-based hydrogels are useful for a sustained release of diclofenac, provided that the percentage of drug released after 5 h is less than 80%.

3.3.4 Primary skin irritation experiments

Primary skin irritation experiments were carried out on rabbits, to assess possible use of *Scl* – *CM*₃₀₀-based hydrogels in topical formulations. Individual skin irritation scores, were always equal to 0. No signs of erythema or edema were observed in the animals up

to 72 h after the application of the samples. According to these data, the primary skin irritation index (PII) of the tested materials was negligible, highlighting that *Scl*–*CM*₃₀₀ possesses adequate properties for application as a modified drug delivery system in topical formulations.

3.4 Conclusion

High-carboxymethylated scleroglucan can form physical hydrogels with negligible primary skin irritation index and adequate rheological properties even in the presence of different therapeutic drugs such as fluconazole, diclofenac sodium salt, and betamethasone phosphate sodium.

The shear thinning behavior of the system was not affected by loading these molecules within the polymeric network. A slightly weaker hydrogel was obtained with betamethasone. On the contrary, the carboxylic group of diclofenac made it able to interact with *Scl*–*CM*₃₀₀, thus strengthening the mechanical properties of the corresponding physical gel.

These findings are supported by experimental drug release studies carried out on drug-loaded *Scl*–*CM*₃₀₀ hydrogels and further confirmed by mathematical modeling of the release profiles. In fact, while betamethasone and fluconazole were released according to a Fickian transport model, model analysis applied to diclofenac explained the non-Fickian feature of its release profile. The estimated values of effective drug diffusion coefficients in the hydrogel for betamethasone and fluconazole, compared to those in an aqueous solution, led us to propose *Scl*–*CM*₃₀₀ as an excellent formulation for fast topical release.

The slower release rate observed for diclofenac, due to drug-polymer interactions, made *Scl*–*CM*₃₀₀ useful for a sustained topical release of this drug.

Chapter 4

Drug delivery from Oral thin films

4.1 Introduction

Oral mucosal drug delivery is an alternative and promising method of systemic delivery which offers several advantages [282, 283]. The oral mucosa is highly vascularized; for this reason, drugs that are absorbed through it directly enter the systemic circulation, bypassing the gastrointestinal tract and first-pass metabolism in the liver [284]. When sublingual mucosa administration is chosen, a rapid onset of action results via a more comfortable and convenient delivery route than the intravenous route [285].

Additional advantages include an improved bioavailability for certain drugs and an easy access to the absorption sites so that the delivery system can be applied and removed easily [286, 287].

In this work, novel OTFs were prepared combining Gellan gum, along with Glycerol, used as plasticizer. Gellan gum thin films were fabricated casting aqueous solutions of the polymer containing different concentrations of glycerol and loaded with two different amount of Fluconazole, used as model drug. The manufacturing process was optimized monitoring some critical parameters including the rheological properties of the starting polymeric solutions, air bubbles entrapped, content uniformity, residual water in the final films and drying rate. All these parameters have an important part on the physical appearance, thickness homogeneity, content uniformity, mechanical and release properties of the resulting films and for this reason they were thoroughly investigated.

Moreover, the influence of the plasticizer on the swelling equilibrium and release of the drug is investigated in simulated saliva (pH 6.7) at 37 °C. Release studies were carried out in a novel millifluidic flow-through device that using a laminar tangential flow is able to better mime physiological mouth conditions.

4.2 Materials and method

4.2.1 Chemicals

Fluconazole, Gellan gum and Glycerol used in this work were procured from Sigma Aldrich. Cellulose membrane filters were purchased from Medicell International. Methanol (CH_3OH), glacial acetic acid (CH_3COOH), bidistilled water (for HPLC), potassium dihydrogen phosphate (KH_2PO_4), di-sodium hydrogen phosphate dehydrate (Na_2HPO_4), sodium chloride (NaCl) and hydrochloric acid (HCl), (used to prepare simulated saliva pH = 6.7), were supplied by Carlo Erba Reagents.

Gellan was added to glycerol to confer plasticity to the films. The glycerol is a triol, that is, an organic structure with three -OH groups. Glycerol is a component of lipids and phospholipids from which it is obtained by hydrolysis. At environment temperature

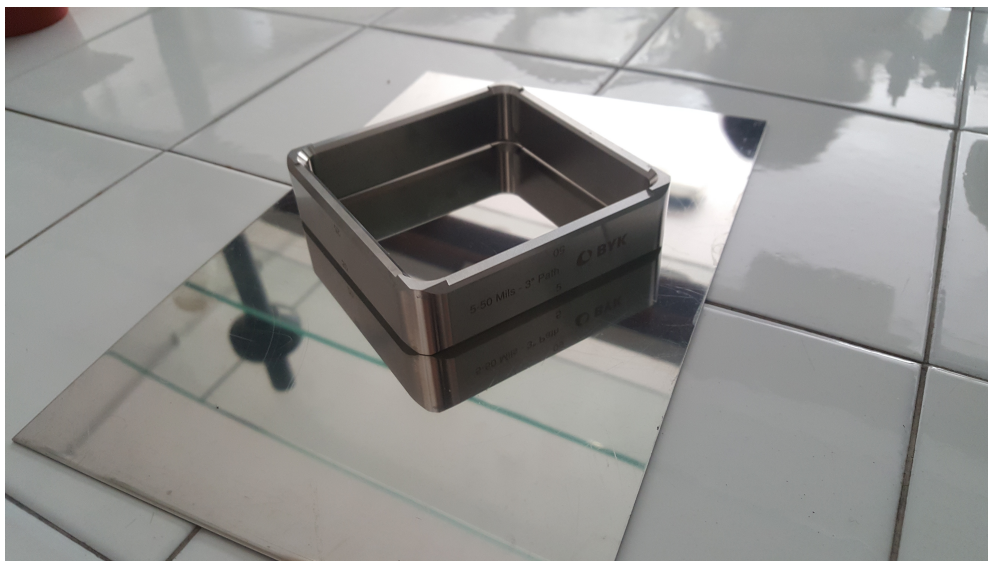


Figure 4.1: BYK-Gardner square film applicator.

appears as a colorless, dense, viscous liquid: the presence of the three Hydroxide groups make it miscible with water in any proportion.

The third component is fluconazole. This is an antimicrobial of the category ofazole drugs. Is Used for prevention and the treatment of superficial and systemic fungal infections. It looks like a crystalline white powder, not soluble in water (8 mg/ml at 37 °C) and soluble in alcohol [288].

4.2.2 Film forming technology

Films were produced by a casting/solvent evaporation technique using different combinations of Gellan (2% w/v) and the plasticizer Glycerol (from 0.5% to 6% w/v). Gellan and Glycerol were dissolved in double distilled water, and the resulting solution was solubilized at 25 °C, under magnetic stirring, for five hours. The mixture was coated onto silicone plate (figure 4.2) or steel plate using BYK square film applicator (figure 4.1) to prepare thin films, then dried by heating in a stove at 60 °C for 15 hours. Fluconazole thin films were produced with the same method by adding a Fluconazole solution (14%w/w) to the casting solution. Thicknesses of OTFs are in the range 40 – 60 μ m for OTFs at 5% Glycerol and 60 – 90 μ m for OTFs at 6% Glycerol.

4.2.3 Thermogravimetric analysis

Thermogravimetric analysis was performed in order to estimate the amount of solvent in the dry films and therefore to estimate a lower bound for the minimum amount of solvent required to initiate the glassy-rubbery transition. Thermogravimetric analysis were performed using a Q600 TGA (TA Instruments), in a temperature range from 25 °C to 120 °C, flowing nitrogen atmosphere (5ml/min), and the thermogravimetric data were recorded at a constant heating rate of 5 °C/min.

Were evaluated three kind of samples (5 and 6% of glycerol):

- empty films (without fluconazole);
- 7%(w/w) fluconazole;
- 14%(w/w) fluconazole.

The picture 4.3 highlight that the content of residual water increase if increase the drug amount in the films.



Figure 4.2: Picture of silicon mold for casting solution.

Moreover films at 5% glycerol have more residual water than films at 6%.

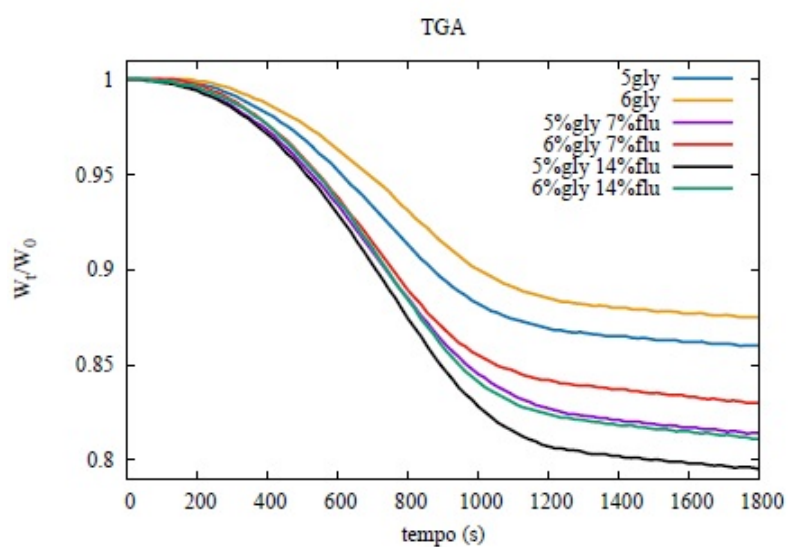


Figure 4.3: Thermogravimetric tests for several kind of films. W_t is the weight of the film at time t , while W_0 is the weight at time 0, at the start of the thermogravimetric test

4.2.4 Swelling

Films were cut, weighted and inserted in a beaker of 5 ml contained simulated saliva pH 6.7. At regular time intervals, non-adsorbed water was drained and wet film was weighted. Tests were performed at 37 °C and repeated in triplicate. From the swelling tests is it possible to calculate the polymer volume fraction at equilibrium and the solvent diffusion coefficient in the completely swollen film.

4.2.5 USP II, Paddle apparatus

Dissolution tests were carried out in a conventional USP type II paddle apparatus. Samples of square shape fluconazole-loaded OTF (surface area 36 cm^2) were placed in different part of the vessel: a) taped on the side wall; b) taped on the bottom; c) anchored to the bottom with a wire mesh. All the release studies were carried out in 500 mL of simulated saliva (phosphate buffer, pH 6.7, containing 0.137M NaCl) at $37^\circ\text{C} \pm 0,1^\circ\text{C}$ with a rotation rate of 50 rpm. Aliquots of the release medium (2 mL) were taken at appropriate time intervals from 1 to 30 min and immediately replenished with the same volume of fresh simulated saliva.

Fluconazole concentrations were assayed by HPLC analysis as reported in the previous chapter. Tests were repeated in triplicate and the results were expressed as mean values \pm the standard deviation.

4.2.6 Novel millifluidic device

Drug release experiments were performed in the newly proposed continuous flow-through device [289, 290].

The existing in-vitro dissolution devices lead to results under expectations if applied to pharmaceutical strips. This subject has been already extensively reviewed in the previous part. A common feature is that the testing apparatuses known in the prior art comprise dissolution chambers in vessels of several cm^3 containing mechanical parts, such as mixing and/or stirring means, beads or sample holders.

Thin films or strips to be tested are allocated in a number of different positions and configurations by using fixing means such as glue or adhesive membranes. Dimensions are here scaled down to cubic millimeter and the resulting flow-pattern deserves, the name of millifluidic (figure 4.4). A new dissolution cell was designed and applied in a new dissolution method [264]. The cell and the dissolution system comprise a channel with an operative volume of a fraction of cubic centimeter, connected with two balancing basins of few cubic millimeters. Therefore the cell and apparatus have a far smaller dissolution volume. The cell and apparatus strictly work in laminar flow conditions between two plates, not in stirred vessels conditions, therefore the residence time is of fraction of minutes or less, depending on the prescribed flow rate, also if the latter is small. Moreover, the dissolution chamber is empty and the desired flow conditions are obtained by the flow-through and the small geometry.

In the cell and the apparatus there is a unique possible set-up for film positioning which completely prevents floating and detachment. The cell and the apparatus may be completely transparent or optionally have a transparent region, as wide as desired, with an optical path for spectrophotometry analysis far shorter than usual dissolution cells. No mechanical mixing devices are required to influence the fluid flow because non-stagnant conditions and laminar flow are obtained by means only of the geometrical design of the objects and of adequate flow rates.

Moreover, there is no need for a sample holder since in the cell the thin film or strip is tightly held during the dissolution, in a controlled layout, by the geometry itself. The thin film or strip is placed in the cell and, when it is closed, a predetermined area part of the film becomes a surface of the dissolution channel. Therefore, the unpredictable and ruinous detachments and floating of the existing devices are avoided.

The picture 4.4 of this device shows:

- a superior plate (1) having an upper face (3) and a lower face (2) with two channels (4) from the upper face (3) to the lower face (2) ending on the lower face (2) in two basins (5) wherein one works as an inflow (4') and the other works as an outflow(4'');
- An inferior plate (6);
- A sheet (7) of slightly deformable material and known thickness, inserted between the plates (1) and (6), wherein a rectangular slit is cut out, deep as the thickness of the sheet itself, and its extremities partially overlap with the two basins;

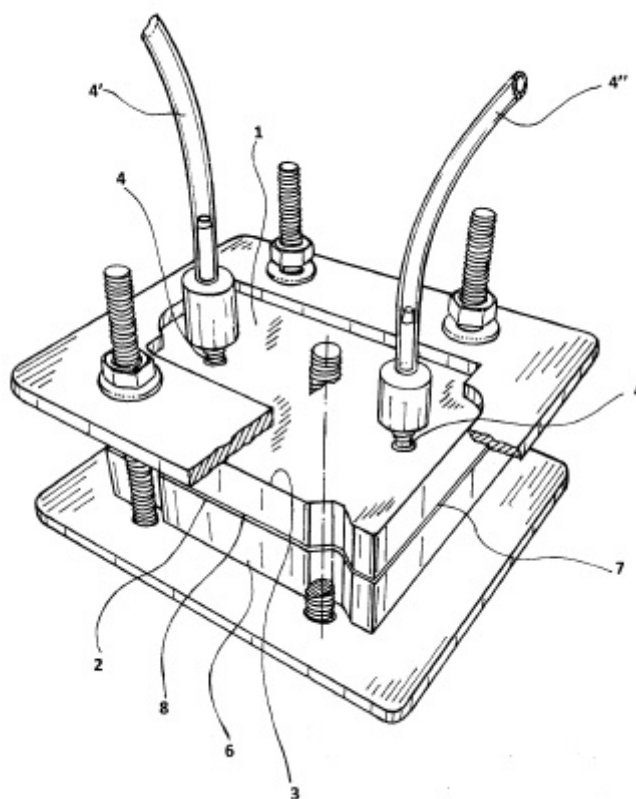


Figure 4.4: Draw of the dissolution cell.

- A dissolution chamber (8) between the lower face (2) of the superior plate (1) and the inferior plate (5), which coincides with the rectangular slit in the sheet (7).

The apparatus comprising the cell connection joints at the exit of each circular channel(4), a closure system, a support system, a thermal insulation system.

A dissolution system is formed by the apparatus, feed pump, a reservoir feeding the feed pump, measurement devices and means for controlling temperature. It is a further object of the present invention a method for testing thin film or strip comprising the following steps:

- Inserting the thin film or strip sample to be tested comprising at least one active ingredient in the dissolution chamber of the cell so that the exposed area is equal to the area of the slit in the sheet (7);
- Feeding a dissolution media at controlled flow rate from the reservoir by the feed pump (4) through the inflow channel and basin (4');
- Continuously contacting the dissolution media with the thin film or strip in the dissolution chamber (8) under laminar and tangential flow conditions;
- Analyzing the dissolution media exiting from the outflow channel (4'') wherein the active ingredient is dissolved by means of a measurement device.

In a preferred embodiment the device is realized in two hard plates made of acrylic polymer and a sheet made of Teflon wherein four screws are realized at the edges of the plates and sheet and the cell is closed by a metallic mask. The inferior plate is smooth and plain. Through the superior plate two circular channels of 2 mm diameter have been drilled. On one face, channels end in two rectangular basins designed to set adequate

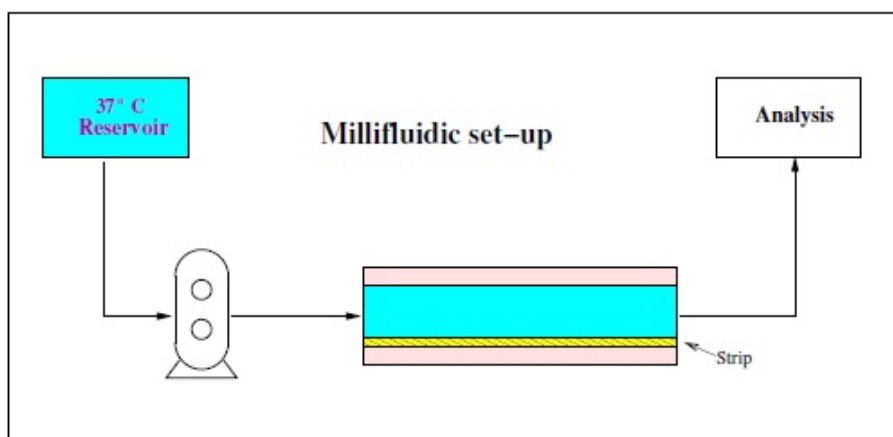


Figure 4.5: Schematic representation of the flow-trough millifluidic device. Instruments of analysis on the outlet flow.

laminar flow conditions. The first couple basin-channel works as inflow and connection volumes, while the other, symmetrically, as outflow and connection volumes.

The device can work either horizontally or vertically. Two connection joints are put at the exit of the cylindrical channels. The dissolution chamber is obtained by the insertion of a sheet, wherein a rectangular slit is cut out, deep as the thickness of the sheet itself, and its extremities partially overlap with the two basins, is inserted between the two plates. The extremities of the rectangular slit overlap with the extremities of the basins.

If plates, sheet and oral strip are tightened together, a single free volume is obtained, from one cylindrical channel to the other, passing over an OS's area equal to the area of the slit. The system is made water-tight by the sheet itself. The device can be easily opened, and the OS substituted. The height of the dissolution chamber is equal to the thickness of the sheet and can be easily changed by substituting the sheet itself. A likely range is in the order of millimeters. The device is connected to a volumetric pump and to a UV-vis spectrophotometer.

The flow rate is set by the rotation speed of the pump. The area exposed to the dissolution media is constant and known in advance, since the strips is tightened by the geometry itself and the exposed area is equal to the area of slit. The dissolution process can be easily monitored through the transparent window. Figure 4.5 is a scheme representing the set-up of the device if working with the analysis instruments on the outlet flow.

Flow rates investigated in this work are in the range $Q \in [2 - 11]$ ml/min corresponding to laminar flow conditions with Reynolds numbers $Re \in [3 - 36]$, based on the hydraulic radius $d = 3.27$ mm. Low flow rates are comparable with salivary flow rates $Q \in [1 - 4]$ ml/min. Solution exiting the cell is sent to the UV/vis analyzer (Perkin Elmer, continuous flow cell, optical path 1 mm) in order to quantify the amount of active ingredient released from the swelling film (figure 4.6,4.7).

Drug concentration values $C_s(t)$ mg/ml are recorded every 0.1 s. The amount of drug released is calculated with a calibration curve. Calibration curve for Fluconazole reference standard (RS) is obtained by measuring the UV absorption ($\lambda = 260nm$) in dissolution medium (simulated saliva). Tests are repeated in triplicate at $37^\circ C$. The differential $F(t)$ and integral $I(t)$ release curves are subsequently computed from the experimental data as follows:

$$F(t) = \frac{QC_s(t)}{\int_0^{t_f} QC_s(t')dt'} = \frac{QC_s(t)}{M_\infty} \quad (4.1)$$



Figure 4.6: Millifluidic device.

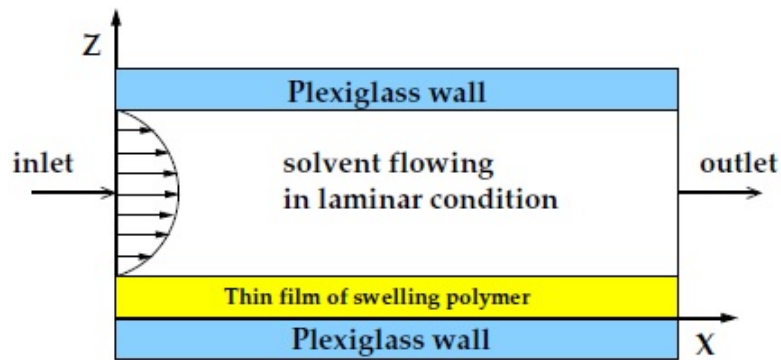


Figure 4.7: Millifluidic model.

$$I(t) = \frac{M_t}{M_\infty} = \frac{\int_0^{t_f} Q C_s(t') dt'}{M_\infty} = \int_0^t F(t') dt' \quad (4.2)$$

t_f being a final time for the experimental test sufficiently long to ensure the complete drug release. The final time t_f depends on the flow rate Q . The smaller is the flow rate Q , the longer is the time interval required for complete drug release.

4.3 Results

4.3.1 Swelling model for OTF

Figure 4.8 and figure 4.9 shows the swelling ratio $Q = \text{weight}(t)/\text{weight}(t = 0)$ as a function of time for OTFs at 5% Glycerol (average thickness $L_0 = 47\mu\text{m}$) and 6% Glycerol (average thickness $L_0 = 86\mu\text{m}$), with and without Fluconazole. A polymer volume fraction at swelling equilibrium is estimated from long term data. It can be calculated as follow:

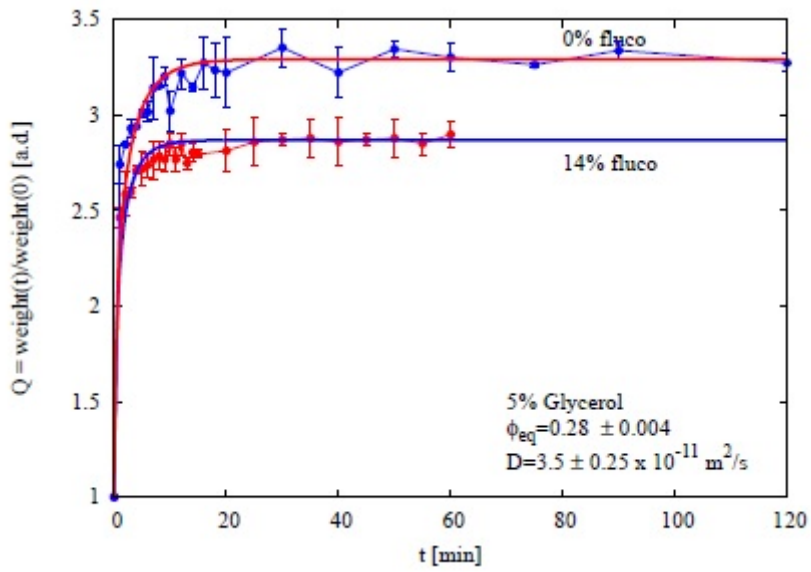


Figure 4.8: Experimental swelling dynamics for OTFs at 5% glycerol.

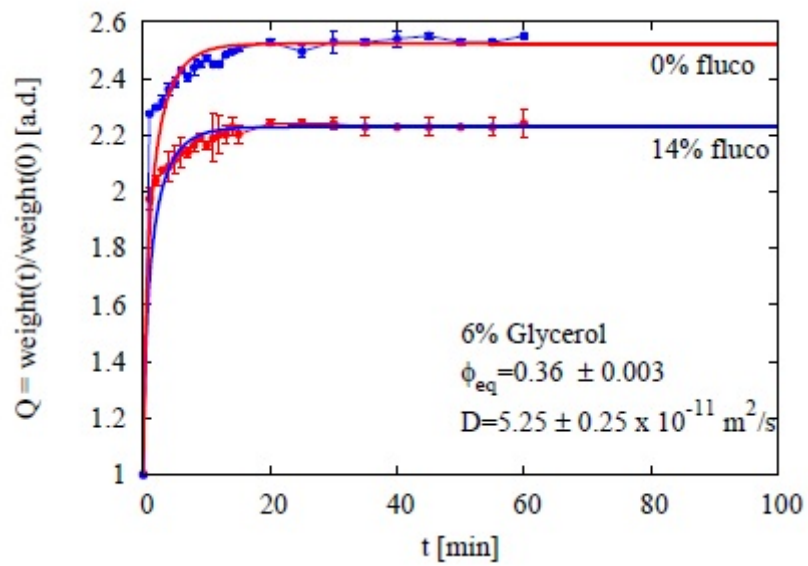


Figure 4.9: Experimental swelling dynamics for OTFs at 6% glycerol.

$$\phi_{polymer}^{\infty} = \frac{\frac{x_{polymer}^{\infty}}{\rho_{polymer}}}{\frac{x_{polymer}^{\infty}}{\rho_{polimero}} + \frac{x_{water}^{\infty}}{\rho_{water}} + \frac{x_{fluconazole}^{\infty}}{\rho_{fluconazole}}} \quad (4.3)$$

where $\rho_{polymer}, \rho_{water}, \rho_{fluconazole}$ are respectively the density of polymer (average based on the weight proportion of gellan gum and glycerol in the film at 5 or 6% glycerol), water and fluconazole. $x_{polymer}^{\infty}, x_{water}^{\infty}$ and $x_{fluconazole}^{\infty}$ can be calculated with the follow equation:

$$x_{polymer}^{\infty} = x_{polymer}^0 \cdot f \quad (4.4)$$

$$x_{water}^{\infty} = 1 - f(x_{polymer}^0 + x_{fluconazole}^0) \quad (4.5)$$

$$x_{fluconazole}^{\infty} = x_{fluconazole}^0 \cdot f \quad (4.6)$$

where $x_{polymer}^0$ and $x_{fluconazole}^0$ are the mass fraction of polymer and fluconazole dried films, while $1/f$ is derived from asymptotic value of experimental data:

$$\frac{1}{f} = \frac{W_{\infty}}{W_0} \quad (4.7)$$

where W_{∞} is the mass of completely swelled film and W_0 is the mass of dried film. The table 4.1 shows the value of $1/f$ and $\phi_{polymer}^{\infty}$ in both cases.

Table 4.1: Value of $1/f$ and $\phi_{polymer}^{\infty}$ at 5 and 6% Gly

-	$1/f$	$\phi_{polymer}^{\infty}$
5%Gly	2.86	0.28
6%Gly	2.24	0.36

Traditionally, gellan gum form solvent-activated films. The drug is immobilized and packaged inside a solid polymeric structure well below its glass transition temperature. In these conditions the diffusivity is very low (tending to zero). In the presence of water the film is soaked and swollen.

There is a transition from the glassy to the rubbery state of the material with relaxation of the polymer chains and dissolution of the loaded drug. Gellan gum generally forms structures with a good degree of derivatization and is crosslinked, so it does not encounter erosion but only swelling. Polymer swelling and drug dissolution are the phenomena that regulate the release of the drug from the matrix.

The kinetics of the problem is actually studied by the analysis of the movement of the fronts of swelling, diffusion and erosion within the matrix. In particular, the position of the erosion and swelling front define the thickness of the gum layer, which is considered to be the key factor in the release kinetics of the drug.

Knowledge of an appropriate mathematical model capable of describing the phenomenon is very important because it allows to simulate the effect of design and design parameters on the release profiles [291–293].

The mathematical model is based on ordinary and partial differential equations (ODE, PDE). To solve, we need the initial condition and the outline conditions. We also need to know the law with which the bounds move. Depending on the complexity of the equation system, we can get an analytical or numeric solution.

At the initial state, the glassy matrix of thickness $S_0 = R_0$ begins to swell due to the penetration of the solvent. Two distinct fronts come to life (figure 4.10):

- swelling front $R(t)$;
- erosion front $S(t)$;

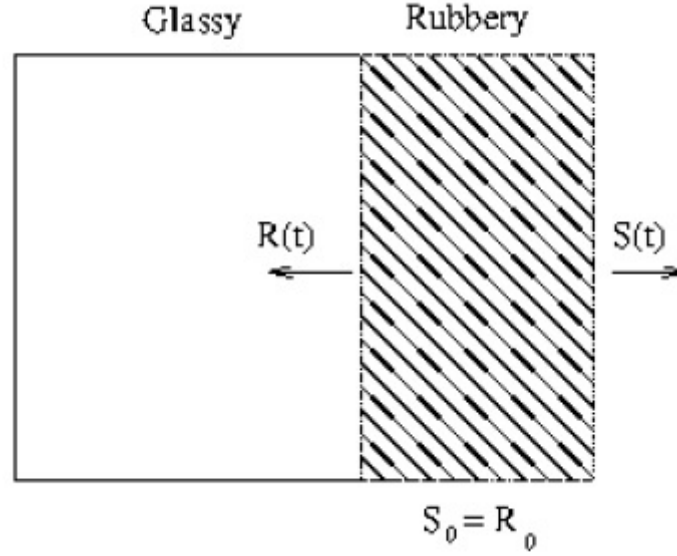


Figure 4.10: Classical scheme of swelling.

Most swelling models are unidimensional. The phenomenon is painted as a Stefan's problem with two $S(t)$ and $R(t)$ mobile boundary. The mass balance for the solvent in the rubbery phase ($R(t) < z < S(t)$) becomes:

$$\frac{\partial c}{\partial t} + \frac{\partial(q + cv)}{\partial z} = 0 \quad (4.8)$$

where c is the solvent concentration, t the time, z the spatial axis, q the diffusive flow and v swelling rate. The total flow thus consists of a diffusive contribution q and a convective term due to the global swelling rate.

The convection term can be calculated from the concentration gradient [294],

$$q = -D(c) \frac{\partial c}{\partial z}, \quad v = -q = D(c) \frac{\partial c}{\partial z}, \quad (4.9)$$

From the study and analysis of scientific literature [295–297] we can derive the one-dimensional axial pattern for thin films. The material balance for the solvent expressed in terms of the volumetric fraction of the polymer ϕ becomes:

$$\frac{\partial \phi}{\partial t} = \frac{\partial}{\partial z} \left(D_s(\phi) \phi \frac{\partial \phi}{\partial z} \right), \quad R(t) < z < S(t), \quad t > 0. \quad (4.10)$$

where $D_s(\phi)$ represents the solvent diffusion coefficient that is the function of the polymer fraction.

$$D_s(\phi) = D_s^{SG} \exp \left[-\beta_s \left(\frac{\phi - \phi_{eq}}{1 - \phi_{eq}} \right) \right] \quad (4.11)$$

where D_s^{SG} is the solvent diffusion coefficient in the fully swelled film, ϕ_{eq} the volumetric fraction at equilibrium and β_s a positive constant.

The movement of the erosion front $S(t)$ and swelling front $R(t)$ is described by Stefan's condition:

$$\phi = \phi_{eq}, \quad \frac{dS(t)}{dt} = -D_s^{SG} \frac{\partial \phi}{\partial z}, \quad z = S(t). \quad (4.12)$$

$$\phi = \phi_g, \quad (\phi_0 - \phi) \frac{dR}{dt} = D_s(\phi) \phi \frac{\partial \phi}{\partial z}, \quad z = R(t). \quad (4.13)$$

where ϕ_g represents the concentration of starting swelling.

When $R(t)$ reaches $z = 0$, the glass phase disappears and the flow is zero (symmetry boundary condition).

$$\frac{\partial \phi}{\partial z} = 0, \quad z = 0. \quad (4.14)$$

The initial condition:

$$R(0) = S(0) = \frac{L_0}{2}, \quad \phi = \phi_0 = 1, \quad 0 \leq z \leq \frac{L_0}{2} \quad (4.15)$$

with $\frac{L_0}{2}$ which is half the thickness of the dry film.

The physical parameters that enter the model are therefore D_s^{SG} , β_s , ϕ_{eq} and ϕ_g available from literature, swelling data obtained from the best fit of experimental data (dynamic swelling).

No significant erosion effect is observed up to 100 min. OTFs at 5% Glycerol exhibit a slightly larger equilibrium swelling ratio (lower equilibrium polymer volume fraction), but the swelling dynamics is slower than that observed for OTFS at 6% Glycerol (see the diffusivity value in the picture4.8 and 4.9). Both swelling dynamics and equilibrium polymer volume fraction are not influenced by the presence of Fluconazole. For both OTFs complete swelling is obtained after 20 min.

Continuous lines represent numerical results obtained by numerical solution of a one-dimensional moving boundary solvent transport problem (swelling along the z direction, orthogonal to the x - y plane representing the flat surface of the thin polymeric film, two moving fronts, the glassy-rubbery and the gel-solvent fronts) adopted for describing the swelling behavior of the thin polymeric film [295], initially in the glassy state, when in contact with simulated saliva (solvent). Glassy-rubbery threshold polymer volume fraction is estimated from thermogravimetric experiments.

The numerical solution of the one-dimensional swelling model furnishes a quite accurate estimate of the effective diffusion D of the solvent in the fully swollen film, confirming a swelling dynamics for OTFs at 5% Glycerol slower than that for OTFs at 6% Glycerol. ($D(5\%) = 3.5 \cdot 10^{-11} m^2/s < D(6\%) = 5.25 \cdot 10^{-11} m^2/s$).

Through the use of Comsol Multiphysics 3.5, using the method of finite elements was possible to solve numerically the swelling problem. Were used the packages ALE(Arbitrary Lagrangian Eulerian) and Convection-diffusion. The linear solver adopted was UMF-PACK with relative tolerance 10^{-3} and absolute tolerance 10^{-6} . In this way it was possible to see gradually how the glassy-rubbery faces (R/L_0) and gel-solvent (S/L_0) evolve in time, depending on the different fraction of glycerol present in the films.

In Figure 4.11 we notice that the dynamics of the glassy-rubbery front is almost equal in both films, while the behavior of the gel-solvent front is the same just in the first few minutes, because films at 6% glycerol swell more quickly. Another aspect to point out is that the transition from the Glassy state to the rubbery occurs in about 1 minute.

4.3.2 Drug release time scales

In vitro dissolution tests were carried out using the novel millifluidic device. The solvent flow rates used are in the range $Q \in [2 - 11] ml/min$.

Differential and integral release curves (and therefore the release time scales) are extremely sensitive to the initial thickness L_0 of the dry film. For example, Figure 4.12 shows the differential curves obtained for $Q=2$ ml/min for three films at 6% Glycerol loaded with the same amount of Fluconazole. The three films differ in their initial thickness ($L_0 = 68, 71, 78 \mu m$). As expected the thicker film exhibits a slower release curve (larger diffusion path). In order to compare different release curves obtained in the same operating conditions and to average over repeated experiments with films with slightly different initial thickness, we need to analyze release data in terms of a dimensionless time t/t_{ref} where $t_{ref} = L_0^2/D$ is the characteristic swelling time, accounting for the initial dry film thickness.

Figure 4.13 shows that the same three release curves, expressed in terms of the dimensionless time t/t_{ref} , are actually consistent and can be taken as representative of the

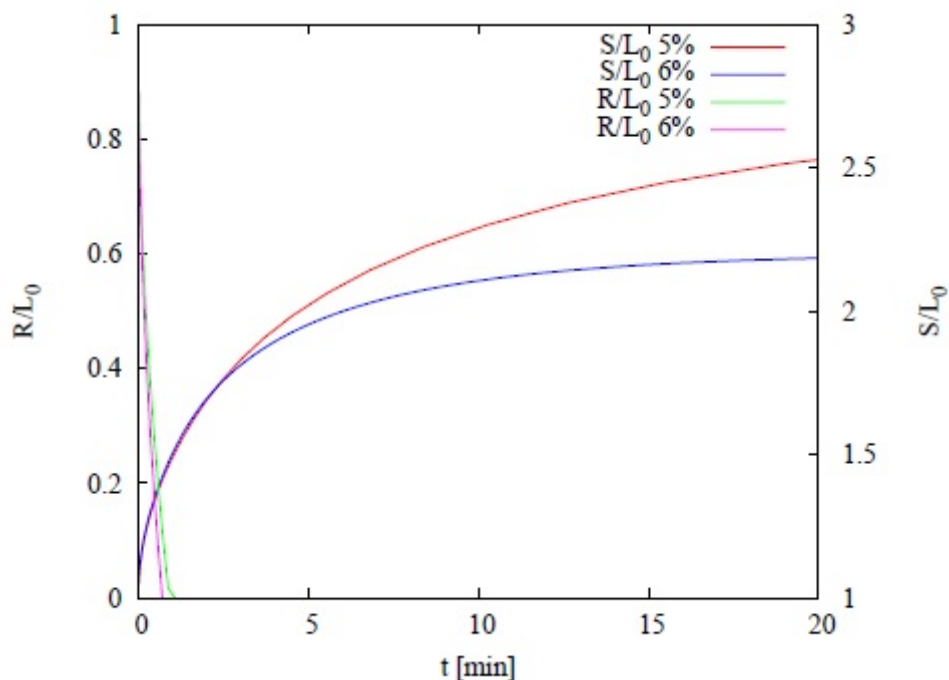


Figure 4.11: Representation of the position of the glassy-rubbery and gel-solvent front depending on the time for the two kind of films.

same experiment, repeated in triplicate and associated to a film with average thickness $\langle L_0 \rangle = (68 + 71 + 78)/3 = 72.3 \mu\text{m}$.

Figure 4.14 and 4.15 shows the corresponding differential and integral release curves, averaged over the three experiments. Error bars represent the standard deviation (STD), supporting a good reliability and reproducibility of the experimental release curves.

Figure 4.16 shows integral release curves (dimensionless time) for OTFs at 6% Glycerol for increasing values of the flow rate Q . Release curves are extremely sensitive to flow rate for low values of Q in the salivary flow range $Q \in [1 - 4] \text{ ml/min}$, while becomes almost independent of Q for $Q > 8 \text{ ml/min}$. In point of fact, the mass transfer resistance at the gel-solvent interface decreases for increasing values of the flow rate.

For flow rates sufficiently high, the dissolved drug is immediately swept away by the solvent flow and diffusion through the polymeric swelling matrix becomes the controlling step. At this point, any further increase in the flow rate does not improve drug release. Figure 4.17 shows the comparison between release curves for OTFs at 5% Glycerol and 6% Glycerol in terms of the dimensionless time ($t/\text{swelling characteristic time}$). The close similarity between the two sets of curves confirms that the release process occurs simultaneously with the swelling process and that the swelling time scales control drug release dynamics. Therefore, drug release from OTFs at 5% Glycerol is slower than release from OTFs at 6% Glycerol, according with the fact that swelling dynamics at 5% Glycerol is slower than 6% Glycerol.

From experimental tests at high flow rates, it was also possible to estimate the drug diffusion coefficient in the swollen gel. The red curve in figure 4.18 shows the differential curve at flow rate of 11 ml/min on adimensional scale, while the blue curve shows the exponential behavior derived from the best fitting data at 11 ml / min. Because the mass fraction of solute released in the time is given by equation (4.16):

$$\frac{M_t}{M_\infty} = 1 - \frac{8}{\pi^2} \sum_{n=0}^{\infty} \frac{1}{(2n+1)^2} \exp\left(-\frac{(2n+1)^2 \pi^2 t D_d^{SG}}{4 L_f^2}\right) \quad (4.16)$$

and as the the differential curve is equal to the derivative of the integral curve, it is

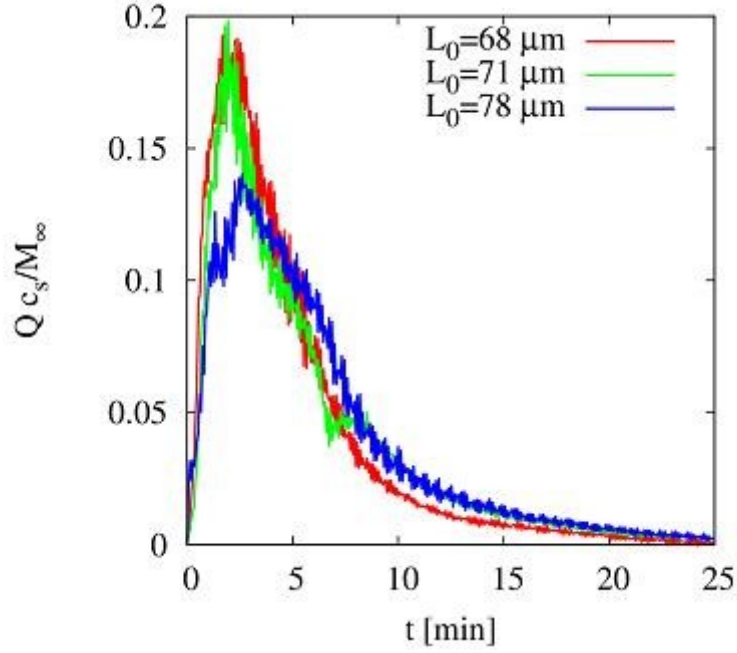


Figure 4.12: Experimental differential release curves for Fluconazole (6% Glycerol) at $Q = 2$ ml/min for three films with different thicknesses.(physical time).

obtained the equation (4.17):

$$\frac{QC_s}{M_\infty} = \frac{d(\frac{M_t}{M_\infty})}{dt} \sim \exp \frac{-\pi^2 t D_d^{SG}}{4L_f^2} \quad (4.17)$$

in which L_f is the thickness of the film, after having completely swelled. From here it was possible to estimate the drug diffusion coefficient in the swollen gel, which was then used in the simulations in Comsol. The same procedure it was done for the D_d^{SG} of film 5% glycerol.

4.3.3 Model of release

The drug release process from the OTFs was schematized according to a 2D model. Fixed the x axis as the direction of the flow, this varies in range $x \in [0 - L_x]$, where $L_x = 30mm$ is the length of the channel. The z axis represents the vertical direction, varies in range $z \in [0 - L_z]$, where $L_z = 2mm$ is the height of channel. L_y is the channel width of 9 mm. Thin film exposed at the flow has an area equal to $L_x \cdot L_y$ and an initial thickness $L_0 \ll L_z$. $c^G(x; z; t)$ and $c^F(x; z; t)$ are respectively the drug concentration in the gel and in the channel.

The mass balance of drug in the gel is:

$$\frac{\partial c^G}{\partial t} = \nabla(D_d^G \nabla c^G), \quad 0 < x < L_x, \quad R(t) < z < S(t). \quad (4.18)$$

where D_d^G is the effective diffusion coefficient of drug in the gel, and it depend on the volumetric fraction of polymer:

$$D_d^G(\phi) = D_d^{SG} \exp \left[-\beta_d \left(\frac{\phi - \phi_{eq}}{1 - \phi_{eq}} \right) \right] \quad (4.19)$$

being D_d^{SG} the drug diffusivity in the completely swollen gel and β_d a positive factor of decay. (4.18) must be resolved with the initial condition:

$$c^G(x, z, 0) = c_0 \quad \text{for} \quad 0 \leq z \leq L_0, \forall x, \quad S(0) = R(0) = L_0 \quad (4.20)$$

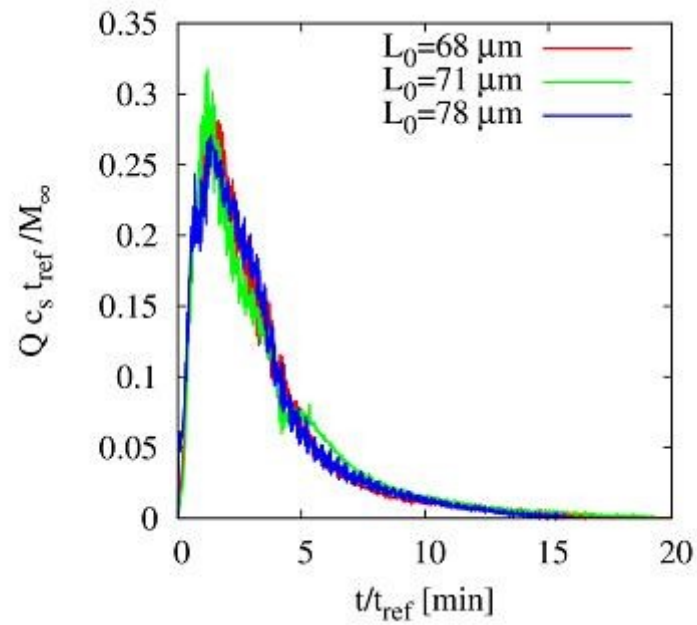


Figure 4.13: Experimental differential release curves for Fluconazole (6% Glycerol) at $Q=2$ ml/min for three films with different thicknesses. (dimensionless time rescaled t/t_{ref} , t_{ref} being the characteristic swelling time).

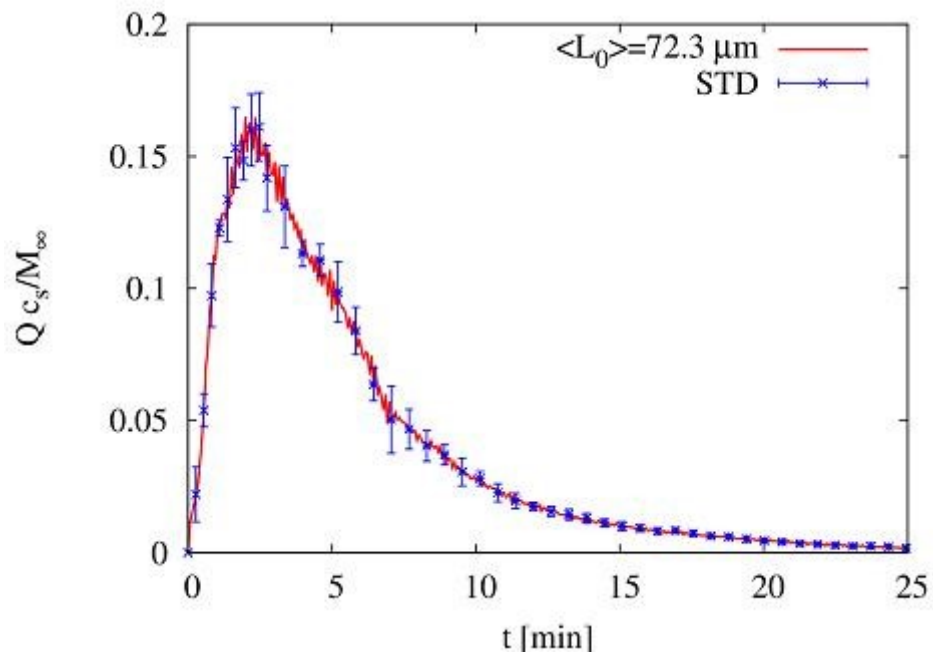


Figure 4.14: Differential release curve averaged over three repeated experiments.

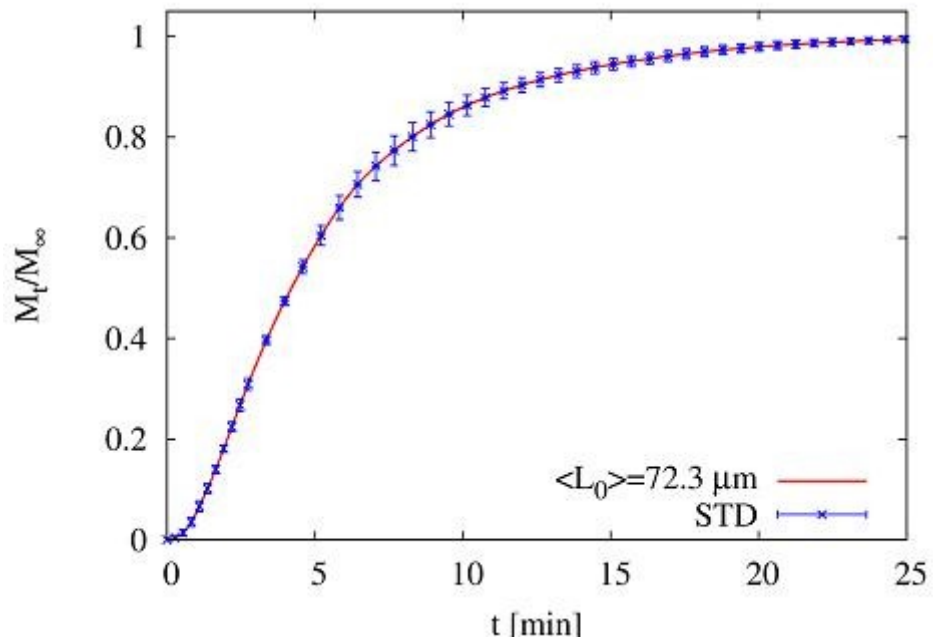


Figure 4.15: Integral release curve averaged over three repeated experiments.

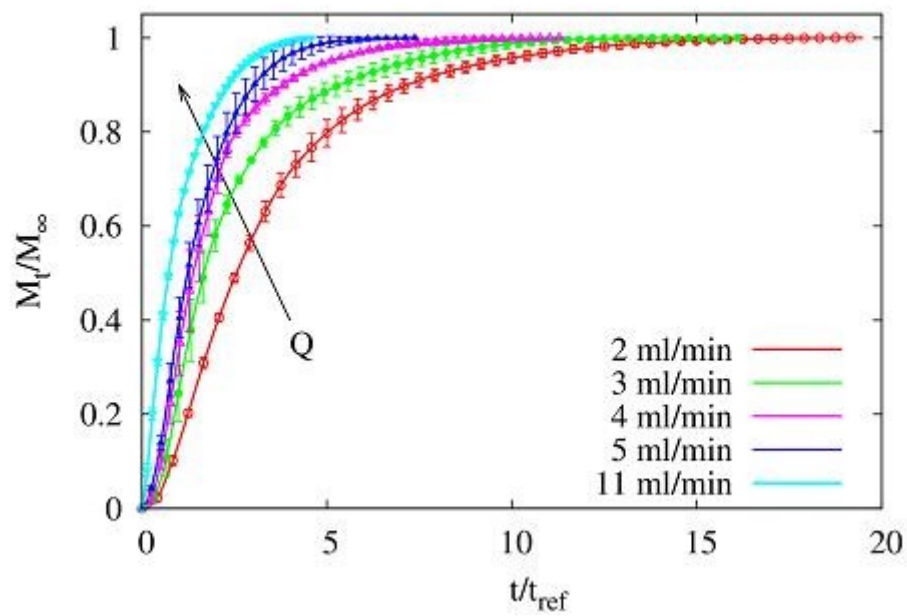


Figure 4.16: Integral release curves (dimensionless time) of Fluconazole for increasing values of the flow rate Q . OTFs at 6% Glycerol. Error bars represent STD over three repeated experiments.

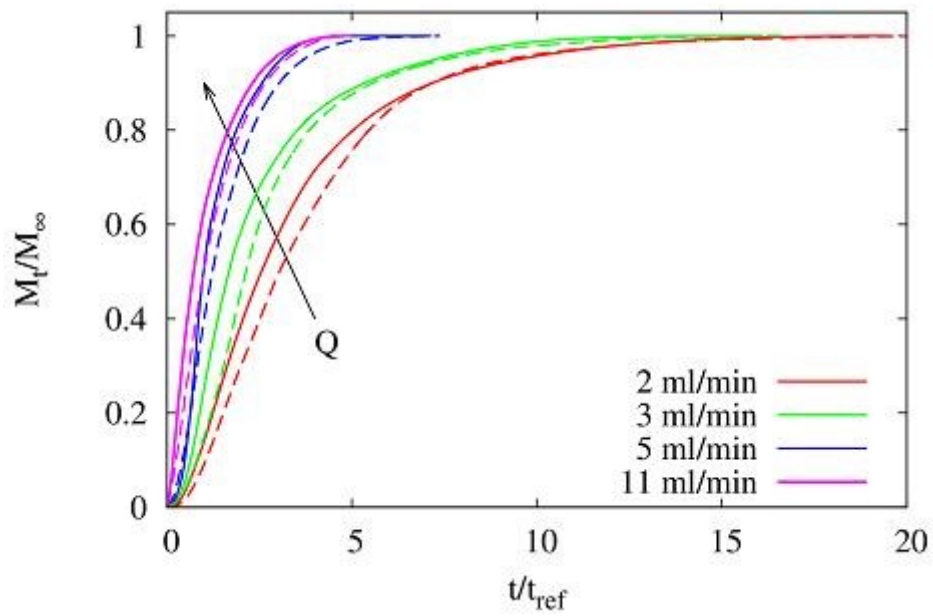


Figure 4.17: Integral release curves (dimensionless time) of Fluconazole for increasing values of the flow rate Q . Comparison between OTFs at 6% Glycerol (continuous lines) and OTFs at 5% Glycerol (dashed lines).

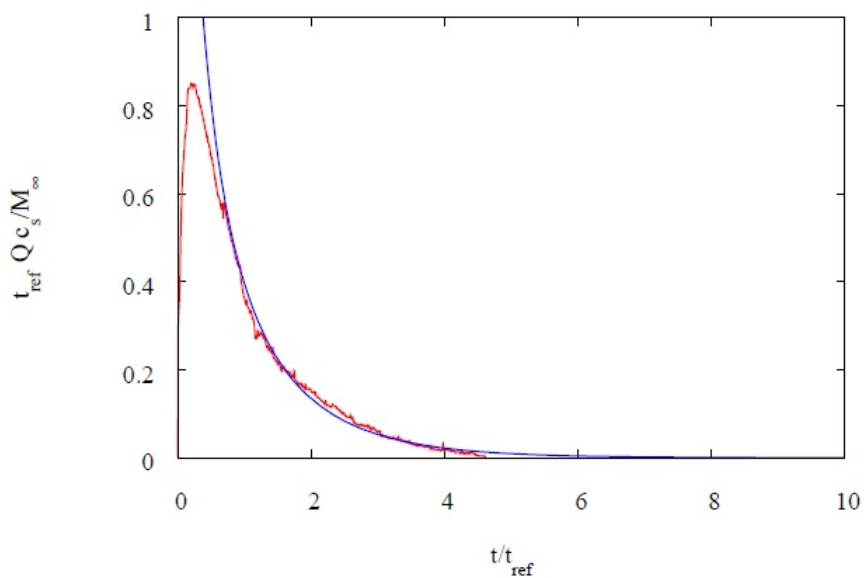


Figure 4.18: Differential curve (the red one) and the exponential behavior derived (the blue one) at flow rate of 11 ml/min on a dimensional scale.

with the boundary condition of impermeable wall at $x = 0, L_x$ and Stefan condition at glassy-rubbery interface $z=R(t)$:

$$\left. \frac{\partial c^G}{\partial x} \right|_{0,z} = \left. \frac{\partial c^G}{\partial x} \right|_{L_x,z} = 0 \quad (4.21)$$

$$\frac{dR(t)}{dt} (c_0 - c^G) \Big|_{x,R(t)} = D_d^G \left. \frac{\partial c^G}{\partial z} \right|_{x,R(t)} \quad (4.22)$$

The mass transport in the channel is characterize by diffusion and convection:

$$\frac{\partial c^F}{\partial t} = D_d^F \nabla^2 c^F - v_x(z, t) \frac{\partial c}{\partial x}, \quad 0 < x < L_x, \quad S(t) < z < L_z. \quad (4.23)$$

where D_d^F is the diffusivity of the drug in the channel and $v_x(z, t)$ is the velocity of the solvent in the channel:

$$v_x(z, t) = \frac{6Q(z - S(t))(L_z - z)}{L_y(L_z - S(t))^3}, \quad \int_{S(t)}^{L_z} v_x(z', t) dz' = \frac{Q}{L_y} \quad (4.24)$$

Equation (4.23) need the boundary condition in the channel to be solved:

$$c^F(x, z, 0) = 0 \quad \text{for } S(0) \leq z \leq L_x, \forall x, \quad S(0) = R(0) = L_0 \quad (4.25)$$

and the Danckwertz condition at the exit of the channel and null flow on the top wall of the channel:

$$\left. \frac{\partial c^F}{\partial x} \right|_{L_x,z} = 0 \quad (4.26)$$

$$\left. \frac{\partial c^F}{\partial z} \right|_{x,L_z} = 0 \quad (4.27)$$

The concentration profiles of drug in the channel and gel are connected by the continuity condition at the gel-solvent interface $S(t)$:

$$c^F|_{x,S(t)} = c^G|_{x,S(t)}, \quad D_d^F \left. \frac{\partial c^F}{\partial z} \right|_{x,S(t)} = D_d^{SG} \left. \frac{\partial c^G}{\partial z} \right|_{x,S(t)} \quad (4.28)$$

the diffusion coefficient at equilibrium in the fully swelled gel was estimated from the asymptotic value of exponential decay of the differential curve of release for high flow rate values, while the diffusion coefficient of the solvent in the gel completely swelled film it was estimated by the swelling tests.

4.3.4 2D-Model

Starting from the solution of the swelling problem, which provides the position of the fronts gel-solvent and glassy-rubbery at any instant of time, was possible to solve the problem of drug release from film. The two-dimensional drug release model from thin films was solved numerically by means of the finite element method in Comsol Multiphysics 3.5 using the convection-diffusion package.

To make easier the resolution of the problem, we have transformed a problem of transport with mobile frontiers to one with static borders, including the motion of boundaries in the transport equations [295].

The following adimensional space/time variables were defined:

$$\chi = \frac{x}{L_x}, \quad \tau = \frac{t}{t_{ref}}, \quad t_{ref} = \frac{L_0^2}{D_s^{SG}} \quad (4.29)$$

$$\lambda_z = \frac{L_z}{L_0} \gg 1, \quad \lambda_x = \frac{L_x}{L_0} \gg 1 \quad (4.30)$$

$$\tilde{R}(\tau) = \frac{R(t/t_{ref})}{L_0}, \quad \tilde{S}(\tau) = \frac{S(t/t_{ref})}{L_0} \quad (4.31)$$

$$\varsigma = \frac{z/L_0 - \tilde{S}(\tau)}{\lambda_z - \tilde{S}(\tau)} \quad \text{for} \quad \tilde{S}(\tau) \leq z/L_0 \leq \lambda_z \quad (4.32)$$

$$\varsigma = \frac{z/L_0 - \tilde{S}(\tau)}{\tilde{S}(\tau) - \tilde{R}(\tau)} \quad \text{for} \quad \tilde{R}(\tau) \leq z/L_0 \leq \tilde{S}(\tau) \quad (4.33)$$

The adimensional concentration in the gel is:

$$C^G(\chi, \varsigma, \tau) = \frac{c^G(x, z, t)}{c_0}, \quad (\chi, \varsigma) = ([0, 1] \cdot [-1, 0]) \quad (4.34)$$

and in the channel:

$$C^F(\chi, \varsigma, \tau) = \frac{c^F(x, z, t)}{c_0}, \quad (\chi, \varsigma) = ([0, 1] \cdot [0, 1]) \quad (4.35)$$

The velocity in the channel from equation (4.24) becomes:

$$v_\chi(\varsigma, \tau) = \frac{6PeD_d^F \varsigma(1-\varsigma)}{L_0(\lambda_z - \tilde{S}(\tau))} \quad (4.36)$$

where Pe is equal to the ratio between the characteristic time of convection of the drug in the channel and the characteristic time of diffusion of drug in the channel.

$$Pe = \frac{Q}{L_y D_d^F} \quad (4.37)$$

Other adimensional parameters entering the transport equation are:

$$\gamma^F = \frac{D_d^F}{D_s^{SG}}, \quad \gamma^{SG} = \frac{D_d^G}{D_s^{SG}} \quad (4.38)$$

Through the adimensionalisations carried out, we have moved from two domains by mobile frontiers, to two square domains with fixed borders. In adimensional terms the transport equation within the gel becomes:

$$\frac{c_0 \partial C^G}{\partial t} = \nabla(D_d^G c_0 \nabla C^G) \quad (4.39)$$

where

$$\frac{\partial C^G}{\partial t} = \frac{\partial C^G}{\partial \tau} \frac{D_s^{SG}}{L_0^2} + \frac{\partial C^G}{\partial \varsigma} \frac{\partial \varsigma}{\partial \tau} \frac{D_s^{SG}}{L_0^2} \quad (4.40)$$

and:

$$\nabla(D_d^G \nabla C^G) = \frac{D_d^G}{L_x^2} \frac{\partial^2 C^G}{\partial \chi^2} + \frac{D_d^{SG}}{L_0^2} \frac{1}{(\tilde{S}(\tau) - \tilde{R}(\tau))^2} \frac{\partial}{\partial \varsigma} \left(f_d(\phi) \frac{\partial C^G}{\partial \varsigma} \right) \quad (4.41)$$

by combining the various terms we get:

$$\frac{\partial C^G}{\partial \tau} \frac{D_s^{SG}}{L_0^2} + \frac{\partial C^G}{\partial \varsigma} \frac{\partial \varsigma}{\partial \tau} \frac{D_s^{SG}}{L_0^2} = \frac{D_d^G}{L_x^2} \frac{\partial^2 C^G}{\partial \chi^2} + \frac{D_d^{SG}}{L_0^2} \frac{1}{(\tilde{S}(\tau) - \tilde{R}(\tau))^2} \frac{\partial}{\partial \varsigma} \left(f_d(\phi) \frac{\partial C^G}{\partial \varsigma} \right) \quad (4.42)$$

and replacing the various terms previously defined we obtain:

$$\frac{\partial C^G}{\partial \tau} + v_\varsigma^G(\varsigma, \tau) \frac{\partial C^G}{\partial \varsigma} = \frac{\gamma^{SG} f_d(\phi)}{\lambda_x^2} \frac{\partial^2 C^G}{\partial \chi^2} + \gamma^{SG} \frac{1}{(\tilde{S}(\tau) - \tilde{R}(\tau))^2} \frac{\partial}{\partial \varsigma} \left(f_d(\phi) \frac{\partial C^G}{\partial \varsigma} \right) \quad (4.43)$$

The boundary conditions in equations(4.21) and (4.22) become:

$$\left. \frac{\partial c^G}{\partial \chi} \right|_{0,\varsigma} = \left. \frac{\partial c^G}{\partial \chi} \right|_{1,\varsigma} = 0 \quad (4.44)$$

$$\left. \frac{\partial \tilde{R}(\tau)}{\partial \tau} (1 - C^G) \right|_{\chi,-1} = \left. \frac{\gamma^{SG} f_d(\phi_G)}{(\tilde{S}(\tau) - \tilde{R}(\tau))} \frac{\partial C^G}{\partial \varsigma} \right|_{\chi,-1} \quad (4.45)$$

In adimensional terms, the transport equation (4.23) within the channel becomes:

$$c_0 \frac{\partial C^F}{\partial t} = -v_x(z, t) c_0 \frac{\partial C^F}{\partial x} + D_d^F c_0 \nabla^2 C^F \quad (4.46)$$

where

$$\frac{\partial C^F}{\partial t} = \frac{D_s^{SG}}{L_0^2} \frac{\partial C^F}{\partial \tau} + v_\varsigma^F(\varsigma, \tau) \frac{D_s^{SG}}{L_0^2} \frac{\partial C^F}{\partial \varsigma} \quad (4.47)$$

$$D_d^F \nabla^2 C^F = \frac{D_d^F}{L_x^2} \frac{\partial^2 C^F}{\partial \chi^2} + \frac{D_d^F}{L_0^2 (\lambda_z - \tilde{S}(\tau))^2} \frac{\partial^2 C^F}{\partial \varsigma^2} \quad (4.48)$$

$$v_x(z, t) \frac{\partial C^F}{\partial x} = \frac{6Pe}{L_x} \frac{D_d^F \varsigma (1 - \varsigma)}{L_0 (\lambda_z - \tilde{S}(\tau))} \frac{\partial C^F}{\partial \chi} \quad (4.49)$$

by combining the various terms and replacing the terms defined before you get it:

$$\frac{\partial C^F}{\partial \tau} + v_\varsigma^F(\varsigma, \tau) \frac{\partial C^F}{\partial \varsigma} = \frac{\gamma^F}{\lambda_x^2} \frac{\partial^2 C^F}{\partial \chi^2} + \frac{\gamma^F}{(\lambda_z - \tilde{S}(\tau))^2} \frac{\partial^2 C^F}{\partial \varsigma^2} - \frac{6Pe}{\lambda_x} \frac{\gamma^F \varsigma (1 - \varsigma)}{(\lambda_z - \tilde{S}(\tau))} \frac{\partial C^F}{\partial \chi} \quad (4.50)$$

The initial condition in equation (4.25) and the boundary conditions (4.26) and (4.27) becomes:

$$C^F|_{0,\varsigma} = 0 \quad (4.51)$$

$$\left. \frac{\partial C^F}{\partial \varsigma} \right|_{\chi,1} = 0 \quad (4.52)$$

$$\left. \frac{\partial C^F}{\partial \chi} \right|_{1,\varsigma} = 0 \quad (4.53)$$

The terms $v_\varsigma^G(\varsigma, \tau)$ $v_\varsigma^F(\varsigma, \tau)$ in equations (4.43) and (4.50) are equal to:

$$v_\varsigma^G(\varsigma, \tau) = \frac{-\frac{\partial \tilde{S}(\tau)}{\partial \tau} (1 + \varsigma) + \varsigma \frac{\partial \tilde{R}(\tau)}{\partial \tau}}{\tilde{S}(\tau) - \tilde{R}(\tau)} \quad (4.54)$$

$$v_\varsigma^F(\varsigma, \tau) = \frac{1}{\lambda_z - \tilde{S}(\tau)} \left(-\frac{\partial \tilde{S}(\tau)}{\partial \tau} (1 - \varsigma) \right) \quad (4.55)$$

where the evolution in time of front positions $\tilde{S}(\tau)$ and $\tilde{R}(\tau)$ are given by the solution of swelling model 1D. There to avoid any singularity a for the spatial variable ς , the position of the erosion and swelling faces are set to $\tilde{S}(0) = 1$ and $\tilde{R}(0) = 0.99$. In this way we identify the two different fronts and define the corresponding domain of swollen gel $0.99 \leq z/L_0 \leq 1$ at time $\tau = 0$. Initial conditions for concentrations are $C^G(\chi, \varsigma, 0) = 0$ and $C^F(\chi, \varsigma, 0) = 0$.

The continuity condition at interface gel-solvent (equation (4.28)) becomes a discontinuity condition of flows, due to the different rescaling of ς in the gel and in the channel:

$$C^F|_{\chi,0} = C^G|_{\chi,0} \quad (4.56)$$

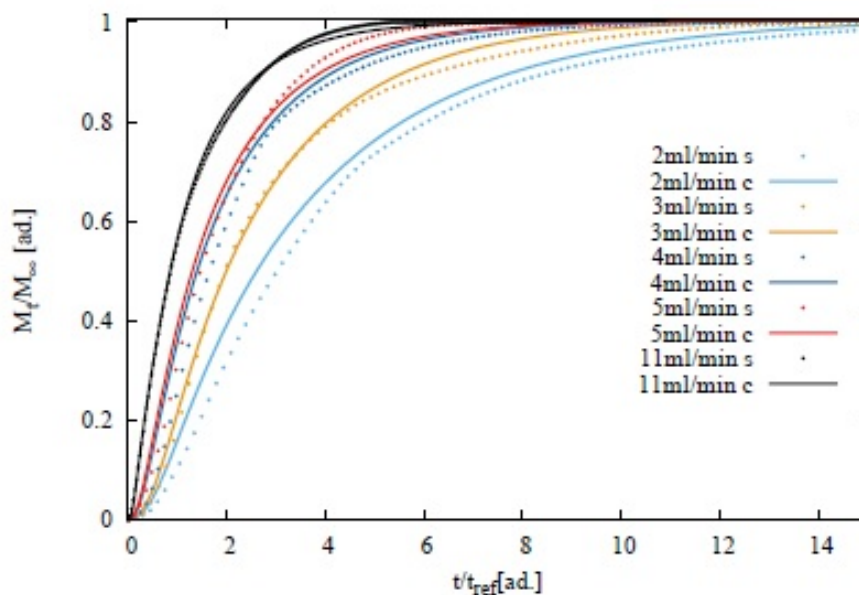


Figure 4.19: Comparison between the experimental results and numerical solution at 6% glycerol.

Table 4.2: Summary table of the most significant data.

-	5%Glycerol	6%Glycerol
ϕ_{water}^0	0.195	0.184
$\phi_{polymer}^\infty$	0.28	0.36
ϕ_{water}^∞	0.72	0.64
ϕ_g	0.7	0.7
D_s^{SG}	$2.1 \cdot 10^{-5} [cm^2/min]$	$3.75 \cdot 10^{-5} [cm^2/min]$
β_s	0	0
D_d^{SG}	$5.528 \cdot 10^{-5} [cm^2/min]$	$6.75 \cdot 10^{-5} [cm^2/min]$
β_d	0	0
D_d^F	$6.925 \cdot 10^{-5} [cm^2/min]$	$6.925 \cdot 10^{-5} [cm^2/min]$

$$\gamma^F \frac{1}{(\lambda_z - \tilde{S}(\tau))} \frac{\partial C^F}{\partial \varsigma} \Big|_{x,0} = \gamma^{SG} \frac{1}{\tilde{S}(\tau) - \tilde{R}(\tau)} \frac{\partial C^G}{\partial \varsigma} \Big|_{x,0} \quad (4.57)$$

Table 4.2 shows the most significant data deriving from the experimental tests and numerical solution. From the comparison of the experimental results in integral terms has been shown that the curves at 5% and 6% glycerol are perfectly coincident if we use the adimensional variable through the time of swelling. For this reason it is decided to show just the problem solution at 6% glycerol (figure 4.19).

In the end figure 4.20 shows a comparison between the release profiles from millifluidic device and Sotax paddle apparatus (always 6% of glycerol) just to highlight as USP II made an overestimating the time scale of release. In fact release data from millifluidic device are more reliable than USP II release data because can better mime the physiological condition of the mouth, with laminar tangential flow rate that reproduce the fluidodynamic buccal behavior, instead of Sotax that is useful to simulate the gastro intestinal tract and gastroenteric release.

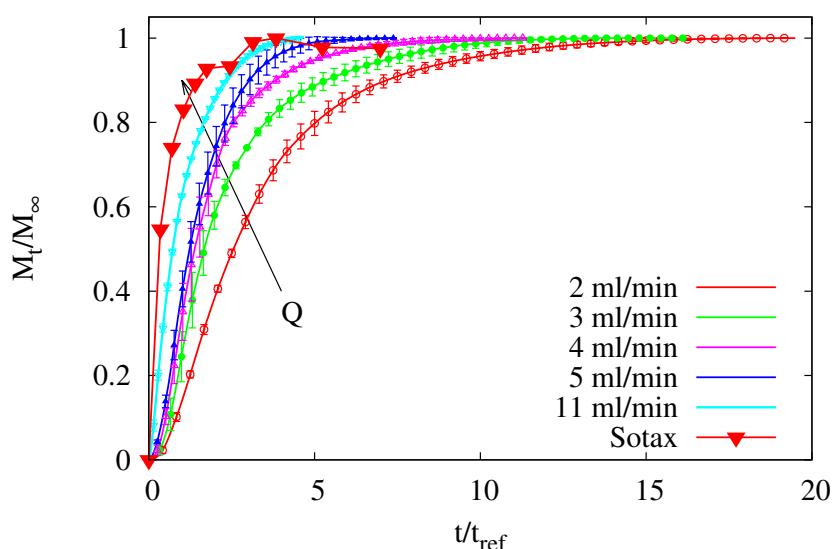


Figure 4.20: Comparison between the release data from USP II and millifluidic device (6% glycerol).

4.4 Conclusion

Through this work it was possible to study a new polymeric thin buccal films (thickness less than $100\mu\text{m}$) made up to gellan gum (2%), fluconazole (14%) and 5-6% glycerol useful for drug administration. Before studying film from the point of view of release times, were analyzed in terms of mechanical strength, residual water quantity in dry film and typical times of swelling.

Specifically, from TGA tests, it was possible to detect residual water in the dry film. At 5% glycerol the amount of residual water is greater than in the case at 6%. From swelling tests have been obtained that film at 5% need much time than those at 6% to swell completely and these tests have allowed to estimate the solvent diffusion coefficient in the swollen gel.

We have studied the dynamic of release with the use of the novel millifluidic device, that can better mime the physiological fluidodynamic condition of the mouth. This device is characterized by a laminar tangential flow of simulated saliva, that lays only the upper surface of the film, while the lower surface adheres perfectly to the bottom plate. In this way the drug and the solvent can diffuse just from one side, as is the case within the oral cavity.

It was noted that release kinetics is strongly influenced by the thickness of the dry film and solvent flow, but for high flow rates the resistance to the mass transfer to the gel-solvent interface is reduced drastically, so the integral release curves become almost independent of flow. A model has been developed to simulate both the swelling process as well as the release. The swelling model shows the evolution of glassy-rubbery and gel-solvent fronts in function of the time and is then embedded in the release process, to see how the release dynamics is dependent on the characteristic times of swelling through the diffusion coefficient in the swollen gel.

The release of drug is modeled as a non-stationary process of Fickian diffusion, characterized by mobile boundary that describe the swelling to which it is subject the film, initially in the glassy state, once in contact with simulated saliva.

Chapter 5

Release analysis from HPMC based erodible thin films

5.1 Introduction

5.1.1 Rapid disintegrating film (RDF)

Many pharmaceutical dosages are administered in the form of pills, granules, powders and liquids. Generally a pill design is for swallowing intact or chewing to deliver a precise dosage of medication to patients. The pills, which include tablets and capsules, are able to retain their shapes under moderate pressure. However some patients particularly pediatric and geriatric patients have difficulty in swallowing or chewing solid dosage forms [298]. Many pediatric and geriatric patients are unwilling to take these solid preparations due to fear of choking. Oral fast dissolving drug delivery system (OFDDS) is one such novel approach to increase consumer acceptance by virtue of rapid disintegration, self administration without water or chewing [299].

It is estimated that 50% of the population is affected by dysphasia which results in high incidence of non-compliance and ineffective therapy [300]. To overcome this problem, Oral Disintegrating Tablets (ODTs) were developed which are also known as fast dissolve, rapid dissolve, rapid melt and quick disintegrating tablets. ODTs have been defined as "A solid dosage form containing medicinal substances which disintegrates rapidly, usually within a matter of seconds, when placed upon the tongue".

United States Food and Drug Administration (US FDA) further defines ODTs as solid oral preparations that disintegrate rapidly in the oral cavity, with an in-vitro disintegration time of approximately 30 s or less, when based on the United States Pharmacopeia (USP) disintegration test method or alternative [301]. Oral drug delivery technology has improved from conventional dosage forms to modified release dosage forms to oral disintegrating tablet to the recent development of oral disintegrating films (ODF). Most ODTs are fragile and brittle, which need special package for protection during storage and transportation. But the films are flexible, they are not as fragile as ODTs, easy transportation, handling and storage [298].

Oral disintegrating film or strip can be defined as a dosage form that employs a water dissolving polymer which allows the dosage form to quickly hydrate by saliva, adhere to mucosa, and disintegrate within a few seconds, dissolve and releases medication for oromucosal absorption when placed on the tongue or oral cavity. The sublingual mucosa is relatively permeable due to thin membrane and large veins [302].

Dissolvable oral thin films (OTFs) or oral strip (OS) or rapid disintegrating films (RDF) evolved over the past few years from the confection and oral care markets in the form of breath strips and became a novel and widely accepted form by consumers for delivering vitamins and personal care products.

RDFs are useful in patients, such as pediatric, geriatric, bedridden, or developmen-

tally disabled, who may face difficulty in swallowing conventional tablets or capsules and liquid orals or syrup, leading to ineffective therapy, with persistent nausea, sudden episodes of allergic attacks, or coughing for those who have an active life style [303,304]. RDFs are also applicable when local action in the mouth is desirable such as local anesthetic for toothaches, oral ulcers, cold sores, or teething [305,306]. Many drugs like cough/cold remedies, sore throat, erectile dysfunction drugs, antihistaminics, antiasthmatics, gastrointestinal disorders, nausea, pain and CNS drugs can be incorporated into these delivery systems. Other applications include the preparation of caffeine strips, multivitamins, sleeping aid snoring aid, etc.

Fast dissolving oral film when placed in the oral cavity, rapidly disintegrates and dissolves to release the medication without chewing and intake of water [317,318]. It gives quick absorption and bioavailability comparable to intravenous administration.

Bioadhesive sublingual formulations [319], such as tablets [320], patches, and films, have been developed using mucoadhesive polymers that can establish a strong adhesive contact with the mucosa, allowing for an increase in residence time of the delivery system and optimizing drug bioavailability [321]. The release kinetics of a given drug from a polymeric matrix could be governed predominantly by the polymer morphology and excipients present in the system [322].

5.1.2 Furosemide features

Furosemide (FUR) is a loop diuretic used orally in the treatment of edematous states associated with cardiac, renal, and hepatic failures and in the treatment of hypertension [307]. The usual dosage is 40–120 mg/day.

Data on solubility, oral absorption, and permeability are sufficiently exhaustive to classify FUR into Class IV of the Biopharmaceutics Classification System. Due to the carboxyl and sulfonamidic groups in the structure, with pKa of 3.8 and 9.6, respectively [308], FUR shows a very low solubility in water that increases as a function of pH from 0.01 mg/mL at pH 2 to 1.9 mg/mL at pH 7.4 [309], determining a higher absorption in the gastric rather than intestinal tracts. The bioavailability problems, reported as consequences of variable and erratic gastrointestinal absorption, are probably due to the low and pH-dependent solubility together with various existing polymorphic forms of FUR [310]. Indeed, FUR presents different polymorphic forms: four are true polymorphs (I, II, III, IV), two are solvates (IV-DMSO and V-dioxane) and one is an amorphous form [323,324].

It is well known that different polymorphic forms of an active administered in the oral or topical form can modify many properties like solubility, stability, color, compressibility, flowability, and workability and as a consequence can cause differences in bioavailability, toxicological safety, clinical effectiveness, and productive efficiency [311]. Different approaches have been proposed to enhance FUR absorption and bioavailability such as co-crystallisation [312,313], solid dispersion [314], microemulsification [315], and supramolecular complexes formation [316].

A number of techniques are employed to improve solubility of low solubility drugs. Supersaturation is, in fact, a reality; solubility enhancing techniques do not augment the solubility of insoluble drugs. Rather, these approaches present the drug in a form which is optimal to its solubility. These techniques include solid dispersion, solvent disposition, co-solvents, salt formation, pH control, micronization, co-grinding, use of surfactants, use of precipitation inhibitors, solid solution, selective adsorption on insoluble carriers and complexation [325,326].

In solvent disposition, solvent free solid dispersion are prepared for solubility enhancement where dispersion of drug takes place in a highly water soluble matrix whereby the drug is dispersed in a hydrophilic matrix and solid solution or eutectic mixture is formed [327–332].

In this work, the aim is to try to improve the solubilisation of a greater amount of furosemide using cyclodextrins that is able to make a complex. The release of furosemide

from erodible films HPMC5 based with and with cyclodextrins are carried out [360–362, 364].

The research in the Pharma Lux Lab in Oslo focused mainly on the study and analysis of releases from thin film HPMC5-based. Furosemide was the model drug used. Releases were performed using three different dissolution / analysis apparatus:

- Vertical diffusion cell (Franz cell);
- Millifluidic device;
- USP II Paddle dissolver (Sotax).

5.2 Materials and method

Potassium phosphate monobasic (KH_2PO_4), Sodium phosphate dibasic dehydrate (Na_2HPO_4) and Sodium chloride (NaCl) used for the preparation of simulated saliva were purchased from Merck, Darmstadt, Germany. For the preparation of mobile phase were used Methanol (MeOH, VWR BHD Prolabo, Singapore) and MQ water produced by dispenser Milli-Q Integral 3 Water Purification System, Merck Millipore, Billerica, MA, USA .

Release studies were carried out using a jacket Franz diffusion cell [270]. The cylindrical donor chamber (cross-section area 1 cm^2) was loaded with 0.1 ml of furosemide solution 0.5 mg/ml (or 0.5mg/ml furosemide +5%w/v CD). The donor chamber was separated by the receptor one with a dialysis membrane (*Spectra/Por*[®] 3, Standard RC Discs, MWCO 3.5 kDa, *Spectrum*[®] Laboratories, Rancho Dominguez, CA, USA) having an area of 1 cm^2 and thickness $L_m = 40\text{ }\mu\text{m}$.

The receptor chamber was filled with 7.9 ml of simulated saliva pH 6.7 (7.9mL receptor volume; PermeGear, Hellertown, PA, USA, at 37 °C) under constant stirring (500 rpm). Aliquots of 200 μl were withdrawn at fixed time intervals and replaced with equal volumes of fresh saliva.

All the samples were quantified by analysis carried out with HPLC system, Shimadzu, Kyoto, Japan, equipped with:

- Pump, LC-20AD;
- Auto injector, SIL-9A;
- Detector, SPD-10A;
- Plotter, Chromatopak C-R5A;
- Column oven, IGLOO-CIL HPLC column thermostat, SPC GmbH, Germany;
- Separation column, C18, 4 μm , 3.9 · 150 mm Cartridge *Nova – Pak*[®] Waters, USA with a *Nova – Pak*[®] Guard Column C18, 4 μm , 3.9 · 20 mm ;

Furosemide was analyzed using a mixture consisting of methanol and phosphate buffer (pH 6.8) (30:70, v:v), as the mobile phase, with a flow rate 1 ml/min and measuring the drug at 276 nm.

Sotax, Paddle apparatus (USP II Prolabo Dissolution Tester, France) in figure 5.1 was used to test the release at 37 °C and 50 rpm. Thin films was fixed at the bottom of the vessel and 500 ml of preheated simulated saliva was use to fill the vessel. Aliquots of 2 ml were withdrawn at fixed time intervals and replaced with equal volumes of fresh saliva. Tests are repeated in triplicate.

Drug release experiments are performed in the newly proposed continuous flow-through device [289,290]. Flow rates investigated in this work are in the range $Q \in [1–5]$ ml/min. Solution exiting the cell is sent to the UV/vis analyzer (UV-2401 PC, Shimadzu

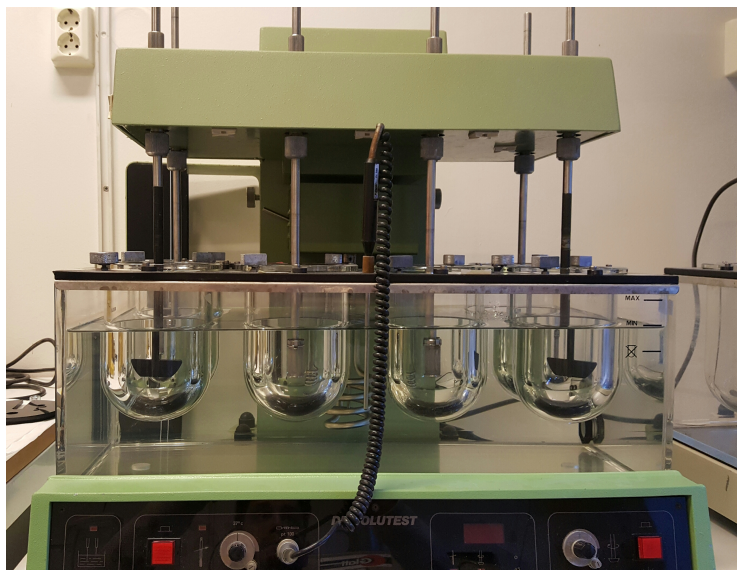


Figure 5.1: Sotax paddle apparatus for releases analysis.

Corporation, Kyoto, Japan, continuous flow cell, optical path 1 mm) in order to quantify the amount of active ingredient released from the swelling film. The amount of drug released is calculated with a calibration curve. Calibration curve for Furosemide reference standard (RS) is obtained by measuring the UV absorption ($\lambda = 276nm$) in dissolution medium (simulated saliva). Tests are repeated in triplicate.

To evaluate the swelling-erosion behaviour films were cut in square pieces (1.1 cm), weighted and inserted in a wet beaker. The system film+beaker was weighted. Then was add 1.5 ml of simulated saliva (pH 6.7) at $37^{\circ}C \pm 0,1^{\circ}C$ to allow thin films to swell and erode. At regular time intervals the excess of simulated saliva was removed, wet system film + beaker weighed and new fresh saliva was added to continue the test.

Films were produced by a casting/solvent evaporation technique using HPMC5 8% w/v (Hypromellose 5 (HPMC), 5 mPas (1 % w/w, 25 °C), NMD, Oslo, Norway) and the plasticizer Glycerol 2% w/v (Glycerol, NMD, Oslo, Norway) with or without cyclodextrins 5%w/v (Hydroxypropyl-beta-Cyclodextrins (2-hydroxypropyl- β -cyclodextrin), Cava-sol W7 HP Pharma, degree of substitution 0.6–0.9 mol per unit anhydroglucose, Mw: ~ 1396 g/mol, ISP, Koln, Germany).

HPMC5 and Glycerol and CD were dissolved in 100ml furosemide (Furosemide, Sigma Aldrich, Steinheim, Germany) solution 0.5 mg/ml previous done. The resulting solution was solubilized at 25 °C (room temperature), under magnetic stirring, for five hours. The mixture was coated onto Coatmaster 510 ERICHSEN GmbH and CO. KG, Germany (figure 5.2), equipped with the Wasag Model 288 Film Applicator System, then dried at room temperature for 15 hours. Thicknesses of OTFs are in the range 60 – 80 μm for OTFs without cyclodextrins and 80 – 100 μm for OTFs with cyclodextrins.

Thin films were detached from the coatmaster with a pocket knife and preserved in an alluminium sachet (furosemide need to be protected from the light).

5.3 Results and discussion

5.3.1 Preliminary analysis

Before starting the study of the releases, it is important to carry out a careful analysis of the system's swelling-erosion behavior. In fact, during the releases the films are able to absorb water and swelling as in the case of the Franz cell or swelling and dissolving as in the case of releases from Sotax and millifluidic device.



Figure 5.2: Coat master film applicator and drying.

Specifically in the figure 5.3 are shown swelling-erosion tests on films with and without cyclodextrins. At first the films tend to absorb water, they reach a maximum weight (equal to 3.5 times the initial one) and then begin to dissolve. The dissolution is very fast. In fact is complete in 5 min for film without cyclodextrin and 3 min for film with cyclodextrins .

The value of the maximum is very important and indispensable for the study of the Franz cell release. This is because the film absorbing water and increase thickness and hence the distribution domain of the drug in the donor chamber. In particular we can approximate the degree of swelling to 3.5 and consider it instantaneous. The following equation shows how the value of film thickness can be calculated as a result of swelling:

$$Th = Th_{dried-film} + Th_{water-uptake} = Th_{dried-film} + \frac{P_f^0(W/W_0 - 1)}{\rho_{water}A} \quad (5.1)$$

where $Th_{dried-film}$ is the initial thickness, P_f^0 is the initial weight, W/W_0 is the swelling degree (3.5 in this case), ρ_{water} the water density, and A the exposed section. The values are 0.45 mm for films without CD and 0.58 mm for CD films.

From the swelling-erosion test is possible to estimate the diffusivity coefficient of the solvent in the films ($D_s^G = 0.7 \cdot 10^{-8} m^2/s$) and the erosion factor (in this case the maximum value).

5.3.2 Release from Franz Cell

The Franz cell release studies started from the analysis of the blank (0.18 $\mu g/ml$ solution of furosemide with and without CD). The model used for the description of the release differs greatly from the classic model normally used that consider perfect mixing in the accepting chamber. In fact despite the presence of mechanical agitation, the geometry and the level of agitation, considering the diffusivity of the drug in the solvent, are not such as to obtain a perfect mixing within the accepting chamber. Strong gradients of concentrations are formed such that the approximation of the accepting department as homogeneous is not acceptable. Especially the area around the arm is characterized by great gradients of concentration compared to the rest of the room. So inside the cell there are real domains characterized by different fluid dynamics and transport conditions.

This is quite evident if you consider the images 5.4 and 5.5 showing the release from Franz cell of Eritrosin dye (1.46 mg / ml) loaded in the donor chamber, at different times. It is noted that during the 24h the arm cell is always less concentrate and therefore the department is not homogeneous overall.

The donor department is the first domain where we have a purely diffuse transport mechanism for the drug.

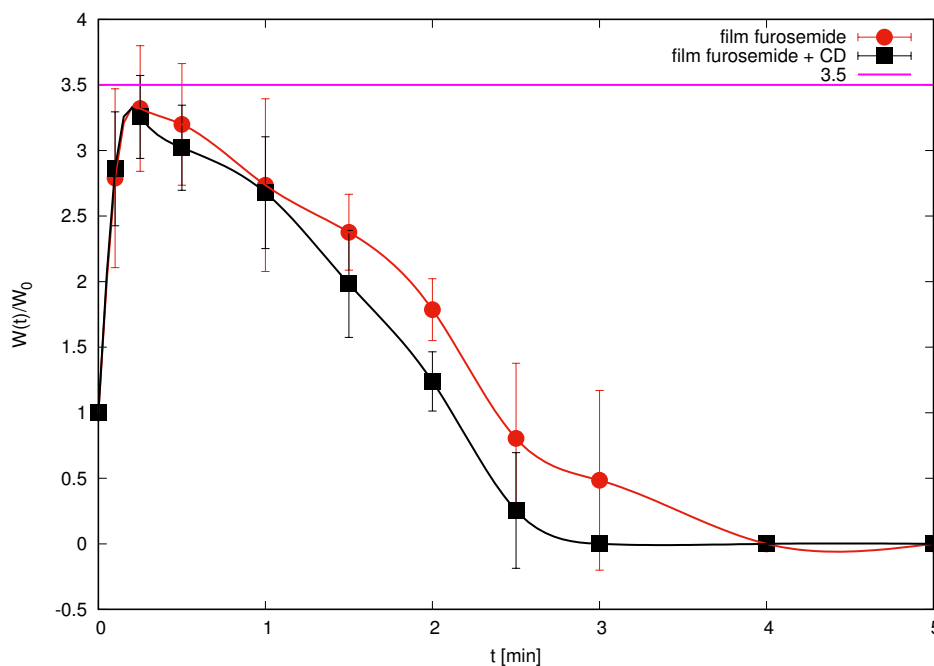


Figure 5.3: Swelling erosion tests. $W(t)/W_0$ represents the weight value of the film at time t with respect to the initial weight. The swelling degree is 3.5 in both cases (with and without cyclodextrins)

After passing the membrane (D), the drug is in the second domain (A) hypothesized to be the central body of the Franz cell where it can be assumed a perfect mix or at least a very high diffusivity space. So we have the arm area (C) of the cell in which the transport mechanism is purely diffuse. Here the drug comes with more difficulty and with longer times. The two zones are then connected by a fourth portion (B) of space, in which the samples comes out to be analyzed and fresh saliva reintegrated. In this area we have the largest gradients of concentration, and drug diffusivity passes from an almost infinite value to that physically detectable in the arm.

The figure 5.6 highlights this. The diffusivity decreases exponentially $D(s)$ from the great value in the acceptor department, perfectly blended with concentration C_{res} , to D_0 , the same as in the donor chamber.

In particular $D(s)$ has the following expression:

$$D(s) = (D_{res} - D_0)exp(-\beta s) + D_0 \quad \text{with} \quad \beta = 1000m^{-1}. \quad (5.2)$$

where $D_{res} \simeq 10^5 D_0$ represents the diffusivity coefficient in the reservoir (it can be approximated almost infinity), β a parameter and D_0 the real diffusion coefficient (in the donor chamber and in the arm).

The mathematical description of a model that takes account of these inequalities in the accepting department is necessary for a correct interpretation of the experimental data.

In fact the experimental data represent the concentration of domain B (this is the zone of the withdrawal) and therefore this value of concentration is not representative of all compartment. So considering an average concentration of the chamber is an interpretation error.

Of course, in addition to the physics illustrated, the mathematical model developed must also take into account the sampling (and therefore the withdrawals) carried out during the release tests.

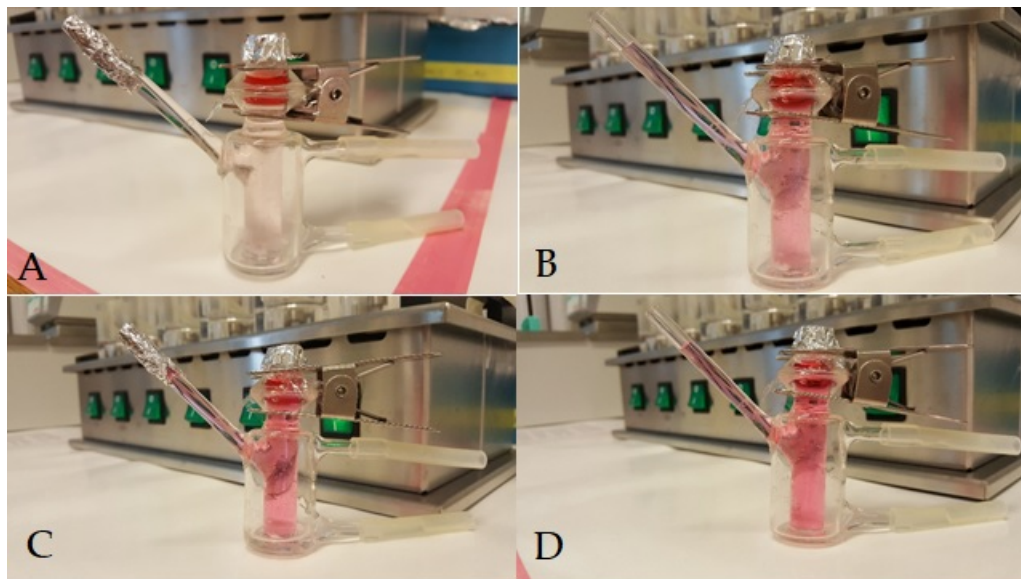


Figure 5.4: Eritrosin Franz cell release at different times: A) 10 min, B) 90 min, C) 4 h, D) 24 h.



Figure 5.5: Domains within the Franz cell. A) central body, B) connection zone, C) arm, D) membrane.

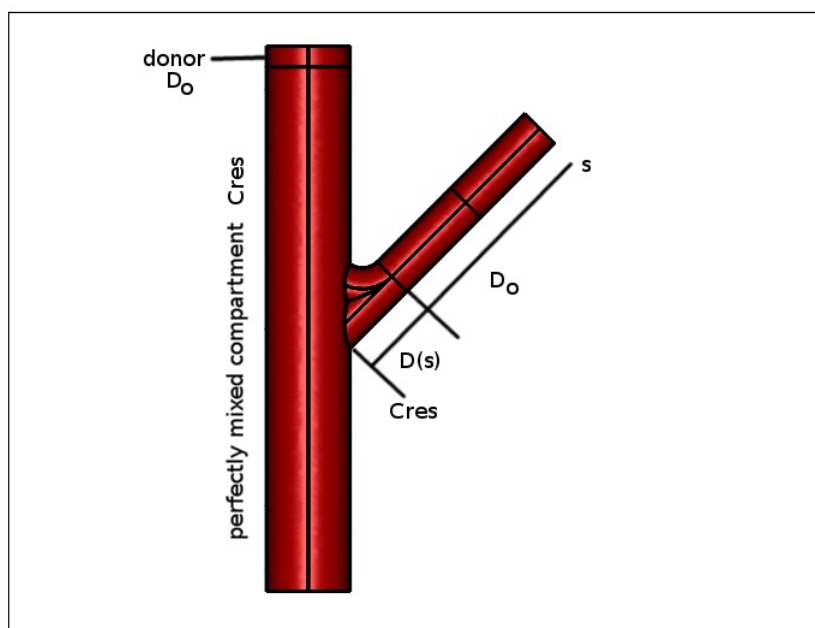


Figure 5.6: Geometric mapping of the concentration domains in the cell: s represents the curvilinear abscissa describing the arm. D_0 is the real diffusivity value of furosemide while $D(s)$ is the exponential decay from infinity value to real one D_0 .

Model of Franz Cell

The amount of drug released at time t will be:

$$M_t = V_d C_d^0 - \bar{C}_d V_d - \bar{C}_m V_m = \bar{C}_{res} V_{res} + \bar{C}_b V_b + \sum_{j=1}^{Ni} C_p(t_j) V_p \quad (5.3)$$

where V_d and C_d^0 are the volume and concentration of the loaded solution, \bar{C}_m and V_m average concentration and volume of the membrane, \bar{C}_d and V_d mean concentration and volume of the donor unit, \bar{C}_{res} and V_{res} concentration and volume of the reservoir, \bar{C}_b and V_b mean concentration and volume of the arm, C_p and V_p concentration and volume of the j th sample for a total of Ni samples.

So:

$$V_d C_d^0 = \bar{C}_d V_d + \bar{C}_m V_m + \bar{C}_{res} V_{res} + \bar{C}_b V_b + \sum_{j=1}^{Ni} C_p(t_j) V_p \quad (5.4)$$

and get it:

$$\bar{C}_{res} = \frac{V_d C_d^0 - \bar{C}_d V_d - \bar{C}_m V_m + \bar{C}_{res} V_{res} - \bar{C}_b V_b - \sum_{j=1}^{Ni} C_p(t_j) V_p}{V_{res}} \quad (5.5)$$

considering roughly:

$$\begin{cases} V_{arm} = 0.775ml \\ V_{res} = 7.12ml \end{cases}$$

Let us indicate with, D_f , and D_m the effective diffusion coefficients in the donor chamber and in the dialysis membrane, respectively. Considering $A=1cm^2$ the surface of the cell, $d=1.12cm$ the diameter of the cell, $H=1cm$ the height of the donor chamber and

$L_m = 40\mu m$ the thickness of the membrane, the mass transport within the donor chamber can be written as (for an isotropic Bi-dimensional problem):

$$\frac{\partial C_d}{\partial t} = (D_f \nabla^2 C_d), \quad \text{for } 0 < \chi < d, \quad 0 < \zeta < H, \quad C_d(t=0, \chi, \zeta) = C_d^0. \quad (5.6)$$

$$\left. \frac{\partial C_d}{\partial \chi} \right|_{0,\zeta} = \left. \frac{\partial C_d}{\partial \chi} \right|_{d,\zeta} = 0 \quad (5.7)$$

$$\left. \frac{\partial C_d}{\partial \zeta} \right|_{\chi,0} = 0 \quad (5.8)$$

$$D_f \left. \frac{\partial C_d}{\partial \zeta} \right|_{\chi,H} = D_m \left. \frac{\partial C_d}{\partial \zeta} \right|_{\chi,H} \quad (5.9)$$

taking in account the condition of insulation on the walls and on the top of the cell and the flow continuity condition at the membrane interface. For the membrane:

$$\frac{\partial C_m}{\partial t} = (D_m \nabla^2 C_m), \quad \text{for } 0 < \chi < d, \quad H < \zeta < H + L_m, \quad C_m(t=0, \chi, \zeta) = 0. \quad (5.10)$$

$$\left. \frac{\partial C_m}{\partial \chi} \right|_{0,\zeta} = \left. \frac{\partial C_m}{\partial \chi} \right|_{d,\zeta} = 0 \quad (5.11)$$

$$V_{res} \frac{\partial C_{res}}{\partial t} = D_m \frac{\partial C_m}{\partial \zeta} A. \quad (5.12)$$

For the arm considering $L_b = 6.5cm$ the length and $d_b = 0.4cm$ the diameter, using curviline axis (s and l) the mass transport is written:

$$\frac{\partial C_b}{\partial t} = D_f \left(\frac{\partial^2 C_b}{\partial s^2} + \frac{\partial^2 C_b}{\partial l^2} \right), \quad \text{for } 0 < s < L_b, \quad 0 < l < d_b, \quad C_b(t=0, s, l) = 0. \quad (5.13)$$

$$\left. \frac{\partial C_b}{\partial l} \right|_{s,0} = \left. \frac{\partial C_b}{\partial l} \right|_{s,d_b} = 0 \quad (5.14)$$

$$\left. \frac{\partial C_b}{\partial s} \right|_{L_b,l} = 0 \quad (5.15)$$

$$D_f \left. \frac{\partial C_b}{\partial s} \right|_{0,l} = D_{res} \left. \frac{\partial C_{res}}{\partial s} \right|_{0,l} \quad (5.16)$$

The picture (5.7) shows the physical domain for the mass transport within the Franz cell. This is just the visual or an easy way for the description of the equation that regulate the mass transport of furosemide in the Franz cell.

Is highlighted the presence of the membrane with concentration C_{res} at the interface with the reservoir with perfect mixing. Then the arm with diffusivity value equal to $D_0 = D_f$ as in the donor chamber and finally the zone for the transition of fluidodynamical condition, where the value of the diffusivity decrease with an exponential decay (as illustrated by equation (5.2)) from infinity value to $D_0 = D_f$ detectable in the arm.

The figure 5.8 reports the concentrations (differential curve) according to time. In this chart is even better evident as the perfect mixing model is not able to describe the physics of the release properly. In fact, the classic model fails to approximate quantitatively the release, even though the qualitative trend is similar. Quantities and concentrations are, however, quite different from those provided by the perfect mixing model, which therefore fails a more accurate quantitative analysis of the release.

In figure 5.9, the difference between a perfect mixing pattern and an unperfect mixing pattern is highlighted. In this picture the experimental data represents the integral value based on a perfect mixing model. However the continuous line M_t that represent the "unperfect mixing" theoretic model, shows how should be the release in the real case.

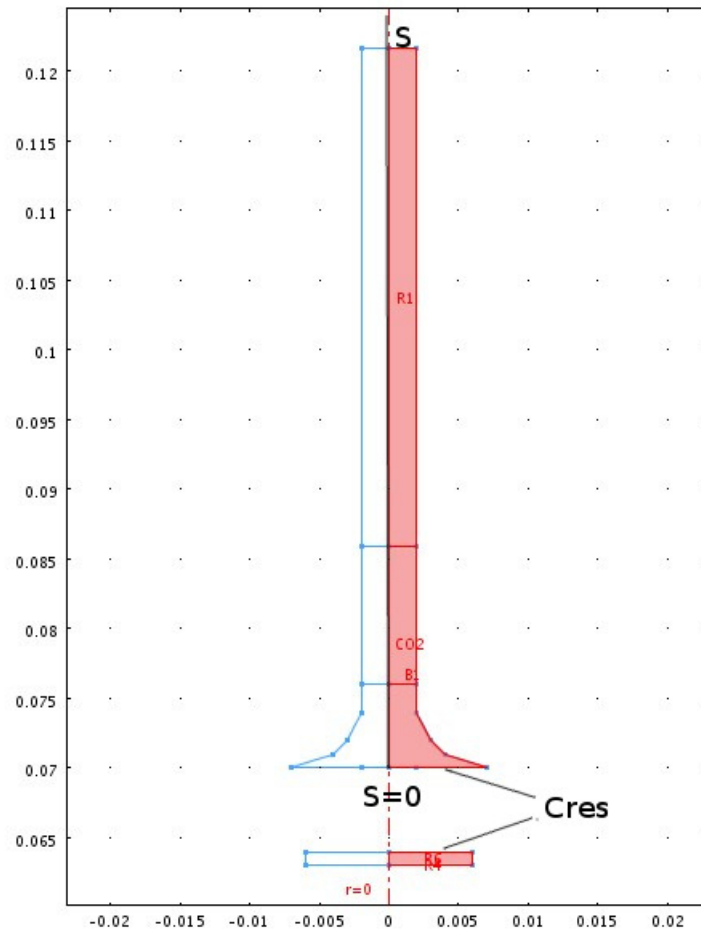


Figure 5.7: Domain for mass transport used from the numerical simulation. s is the curviline axis and C_{res} the reservoir concentration.

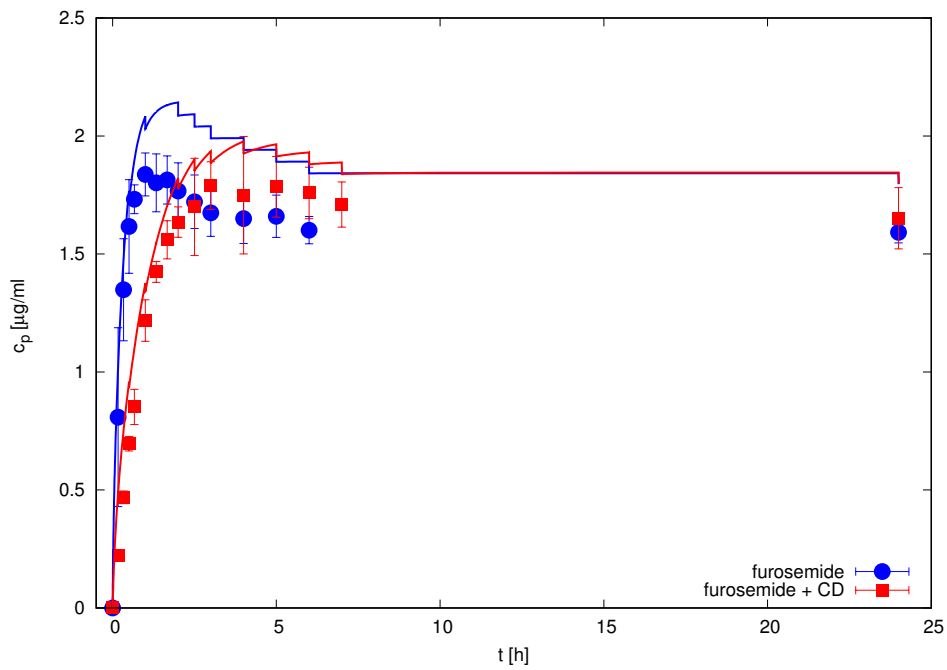


Figure 5.8: Differential release profile for modified model Vs experimental data. C_p is the punctual concentration of the sample.

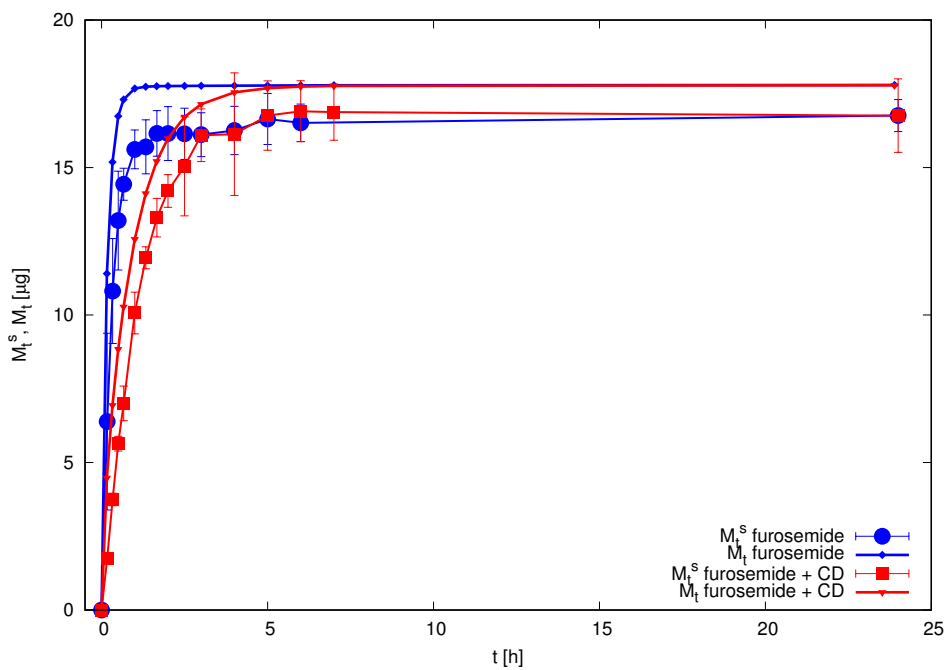


Figure 5.9: Difference in the release profile between perfect and UN perfect mixing. M_t^s represent the experimental data calculated respect to a perfect mixing model while M_t represent the theoretical "unperfect mixing" model developed.

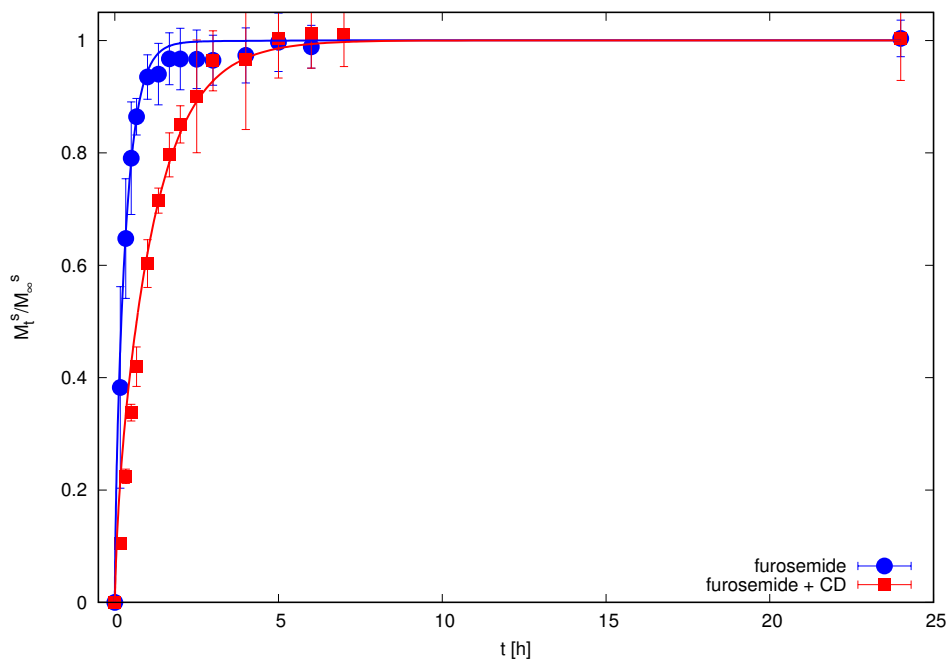


Figure 5.10: Normalization of integral curve for a classic release model.

Therefore, only in the case of a normalization of the release curves relative to the total amount released, the perfect mixing curve is capable of satisfying the experimental data, but only for diffusivity values lower than the real ones (figure 5.10).

From Wilke-Chang's relations (equation (3.8)) considering a $V_{LB} = 317.6$ for furosemide, we can estimate the diffusivity that is $5.78 \cdot 10^{-10} m^2/s$ ([274]).

From the analysis of blanks, considering a concentration of $C_0 = 180 \mu g/ml$ and $D_m = D_f \cdot \alpha$ we obtain the best fitting of the experimental data for $D_f = 5.78 \cdot 10^{-10} m^2/s$, $\alpha = 0.5$ and $D_{f+CD} = 1.73 \cdot 10^{-10} m^2/s$, $\alpha = 0.25$ in case with CD (Figure 5.11).

Therefore, assuming the same α values previously defined in the case with and without CD, we get a good approximation of the experimental data only for very low values of the diffusion coefficient. Specifically $D_f = 2.89 \cdot 10^{-10} m^2/s$, $D_{f+CD} = 0.867 \cdot 10^{-10} m^2/s$.

The non-homogeneity of the department, which is not considered by a classical model, is downloaded to the diffusivity value that becomes so much smaller than the real one. Then films were analyzed in Franz cell. The physics and the equations-model is the same defined before in this section. Of course the value of H change and becomes the thickness of the film and the donor chamber diffusivity become D_f^G or D_{f+CD}^G with cyclodextrins. Usually the average thickness is $67 \pm 12 \mu m$ for films without and $110 \pm 21 \mu m$ for films with cyclodextrins.

The amount of drug loaded in the film was calculated from content uniformity tests (figure 5.12).

The best fit of the data is obtained from the definition of the parameter φ , which is the ratio $P_{H20-residual}/P_{film-dry}$:

$$P_{film} = \frac{a}{1 - \varphi} P_{furosemide} \quad (5.17)$$

where a is a parameter could be 201 or 301, respectively without and with cyclodextrins. It is assumed that the amount of residual water is the same in both cases. So $\varphi = 0.123 \pm 0.006$. The superficial drug concentration for the films tested in the Franz cell is 70 ± 0.06 and $53 \pm 0.06 mg/cm^2$, respectively without and with cyclodextrins.

The concentrations considered thus give the releases illustrated in figure 5.13 and 5.14.

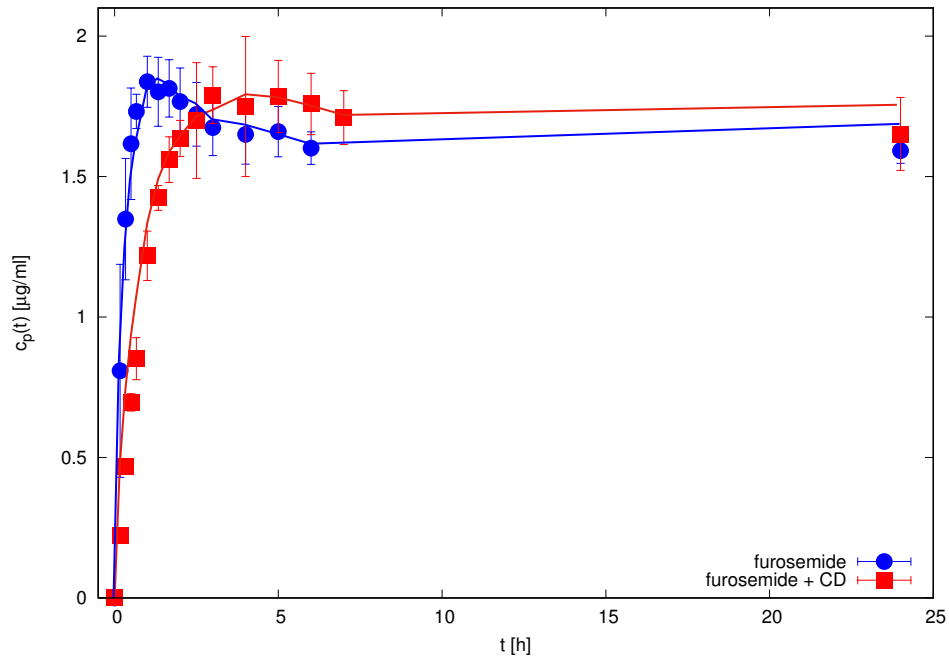


Figure 5.11: Release profile from blanks and "unperfect mixed" model. C_p is the punctual concentration of the sample

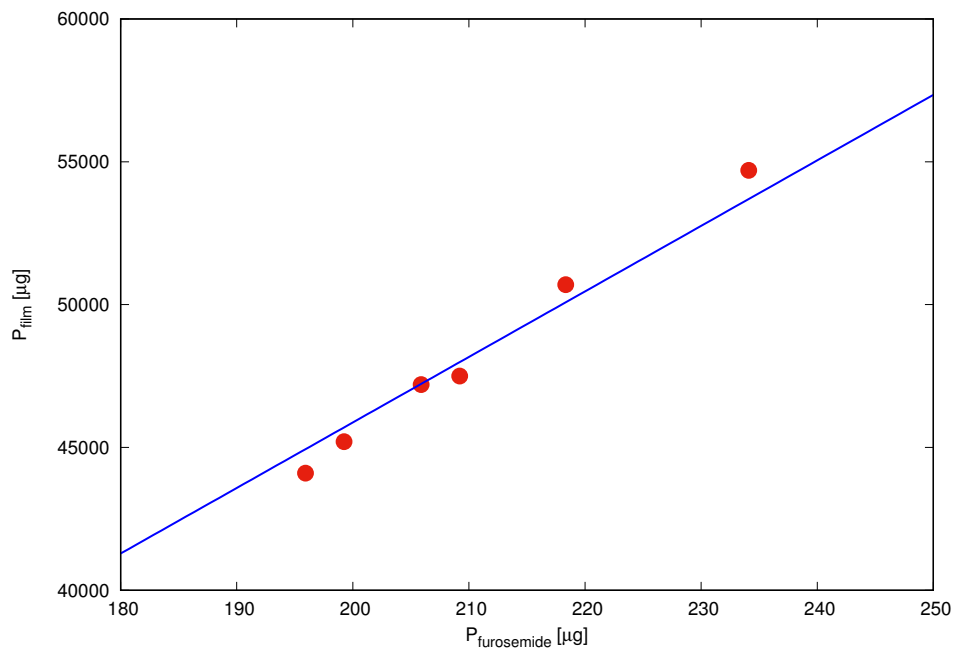


Figure 5.12: Uniformity content for film loaded with furosemide. P_{film} is the weight of the films and $P_{furosemide}$ the corresponding amount of drug loaded.

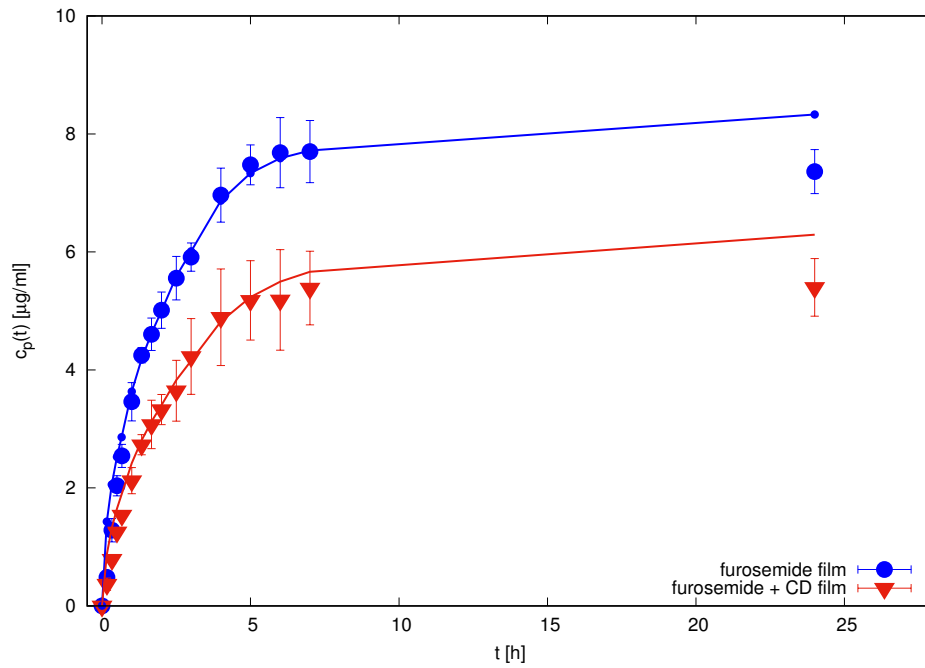


Figure 5.13: Release profile for film in Franz cell. Differential curve.

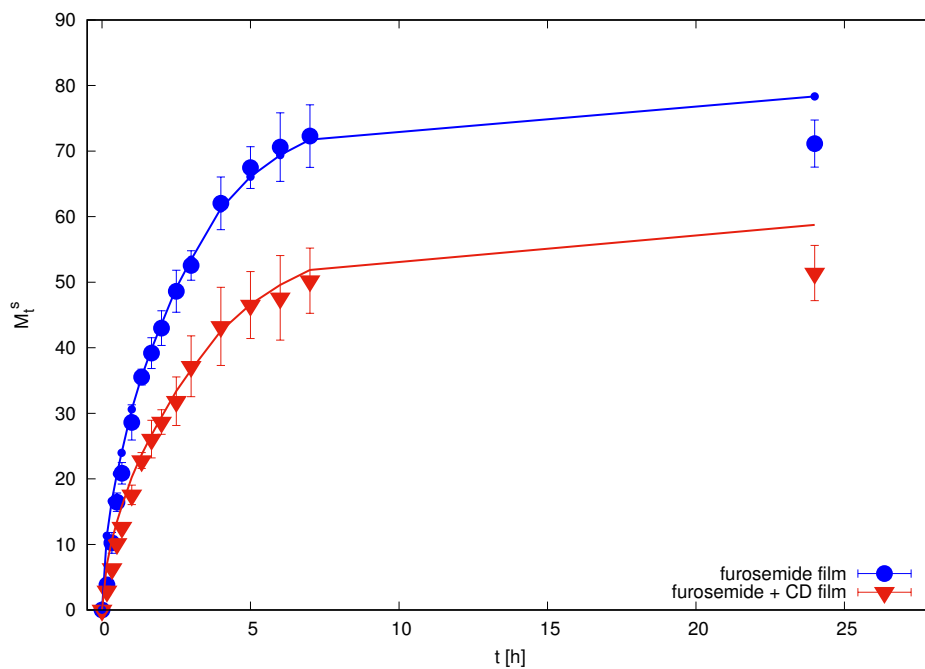


Figure 5.14: Release profile for film in Franz cell. Integral curve. M_t^s is the total amount of drug loaded in the film and released at time t .

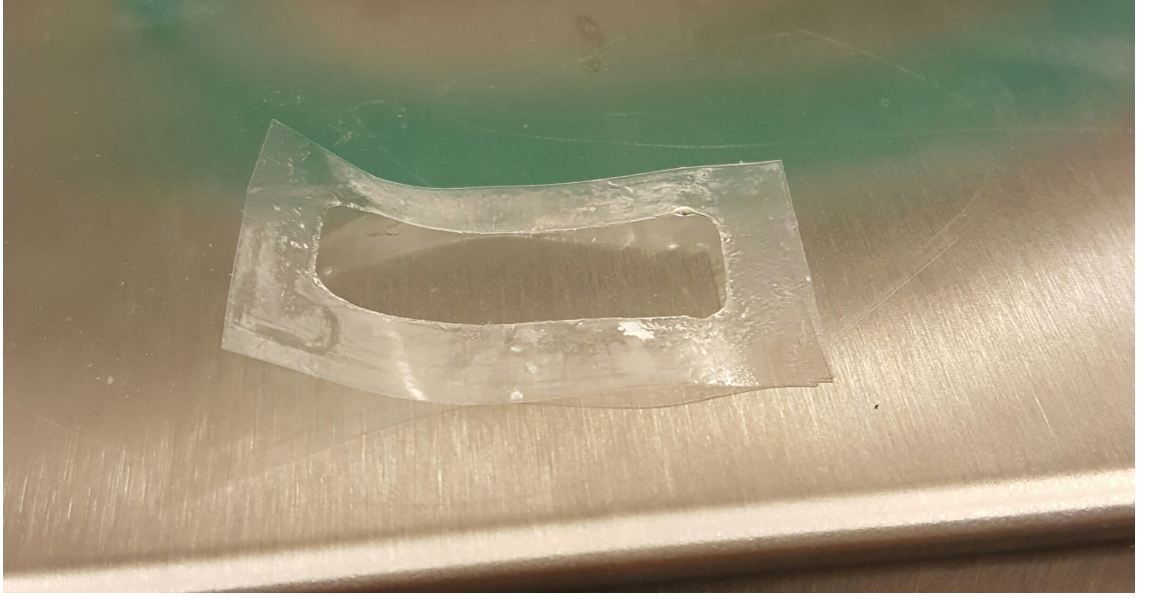


Figure 5.15: Example of film after release. Detail of erosion.

Experimental data and model are in agreement with each other and the best fitting diffusion values are:

$$\begin{cases} D_f^G = 0.65 \cdot 10^{-10} m^2/s \\ D_{f+CD}^G = 0.6 \cdot 10^{-10} m^2/s \end{cases}$$

where D_f^G and D_{f+CD}^G are respectively the diffusivity coefficient in the film of furosemide without and with cyclodextrin. The two values are quite close. In fact there is not so big difference in the two release profile and the time scale of the release is similar even if the amount released is different. In all cases with cyclodextrins, we made the hypothesis that the furosemide is completely complexed.

The diffusivity values D_f^S, D_f^G, D_{f+CD}^S and D_{f+CD}^G are necessary to describe the release into the millifluid device. D_f^S and D_{f+CD}^S are the diffusivity coefficients of furosemide in solution without and with cyclodextrins ($D_f^S = D_f$ and $D_{f+CD}^S = D_{f+CD}$).

However, the films in the device goes to swell and loseout erosion (as is possible to see in picture 5.15 that shows the film after release). These two effects should be taken into account during the release to avoid making mistakes in evaluating experimental data [291, 293, 357–359, 363].

5.3.3 Swelling-Erosion tests

The water up-take causes the matrix swelling, and the polymer disentanglement at the matrix surface causes the matrix erosion. Thus, these two phenomena, swelling and erosion, cause the matrix surface to be a moving boundary. Specifically before to write the drug release model, we must solve the swelling pattern associated with the film taking into account erosion [294], adding a term in the swelling equation (4.12):

$$\frac{dS}{dt} = -D_s^{SG} \frac{\partial \phi}{\partial t} - \frac{-C\phi^{1.625}}{M^{1.25}} \quad (5.18)$$

where C and M are two erosion constant. Using adimensional swelling time $\tau = t \cdot D_s^G / L_0^2$ becomes:

$$\frac{d\tilde{S}}{d\tau} = -\frac{\partial \phi}{\partial \tilde{z}} - C\phi^{1.625} \quad (5.19)$$

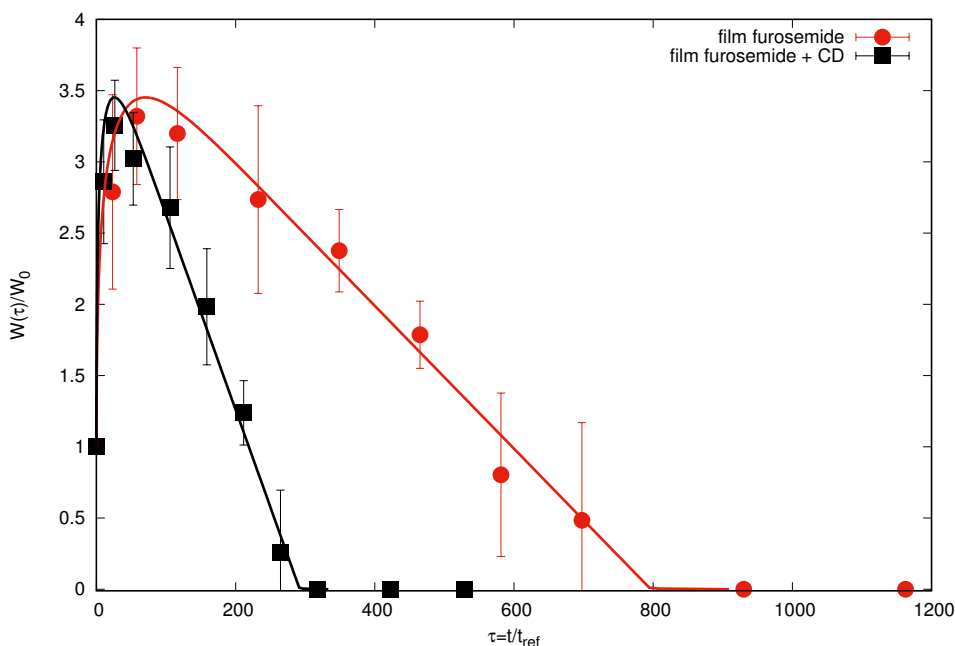


Figure 5.16: Swelling-erosion test for film with and without CD. $W(t)/W_0$ represents the weight value of the film at time t with respect to the initial weight. $t_{ref} = \frac{\bar{L}^2}{D_s^G}$ where \bar{L} is the thickness of dry films and D_s^G is the solvent diffusivity.

Figure 5.16, shows the results of the swelling/erosion tests from which it is possible to estimate D_s^{SG} and the erosion parameter C . In this picture is evident that erosion of films with cyclodextrin is significantly faster. In particular, the value of $P(t)/P_0$ (P_0 is the dry weight or the weight at time $t=0$) in function of the swelling time is reported to consider the effect of the thickness. In the first times, thin film swell and is able to retain water, but then the phenomenon of erosion and disintegration of the polymer with weight reduction prevails and subsequent complete dissolution.

The model is based on equation (4.10),(4.11),(4.13),(4.14),(4.15) defined in the previous chapter, plus the equation (5.19). Swelling/erosion tests are associated with an erosion rate that is assumed to be maximum. Obviously in the millifluidic device we will have erosion rates lower but increasing as the flow increase. The Sotax may be associated with the case of maximum erosion rates.

5.3.4 Sotax Vs Millifluidic device

By simultaneously solving the release model (equations (4.18),(4.20),(4.21),(4.22),(4.23),

(4.25),(4.26),(4.27),(4.28)) and the Swelling/erosion model we can describe the millifluidic curves for different flow rates $Q \in [1 - 5]$ ml/min (for $\frac{D_f^G}{D_s^G} \simeq 0.01$ and $\frac{D_f^s}{D_s^s} \simeq 0.1$ ratios values), going to fix the erosion parameter C which gives us the best fit of the data (figure 5.17 and 5.18). The values of parameter C in both cases (for different value of flow) are defined in table (5.1) and (5.2). From the these tables and figures is possible to understand again as the erosion increase with the flow. The release from Sotax are faster in both cases than the fastest release in the millifluidic device. Is also evident as the releases are erosion-controlled and films with cyclodextrins are associated with swift erosion and, as a consequence, swift release.

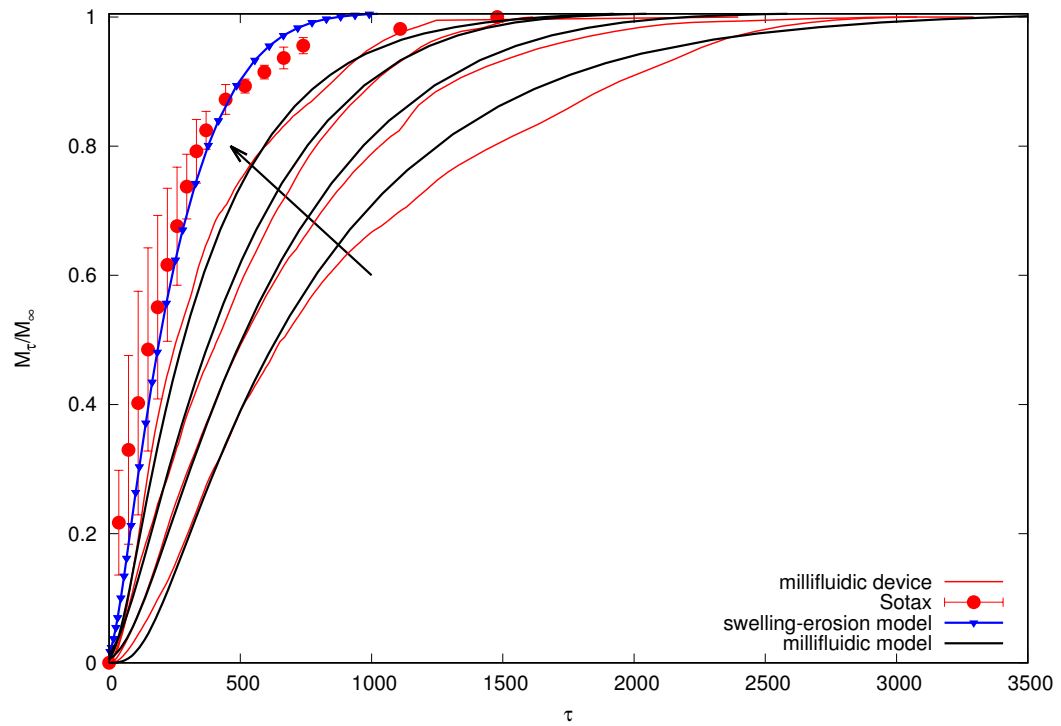


Figure 5.17: Release from millifluidic device and Sotax. Test for film without CD. $\tau = tD_s^G/L_{dry}^2$. Release curve for flow = 1, 2, 4, 5 ml/min and Sotax (50rpm), 37°C

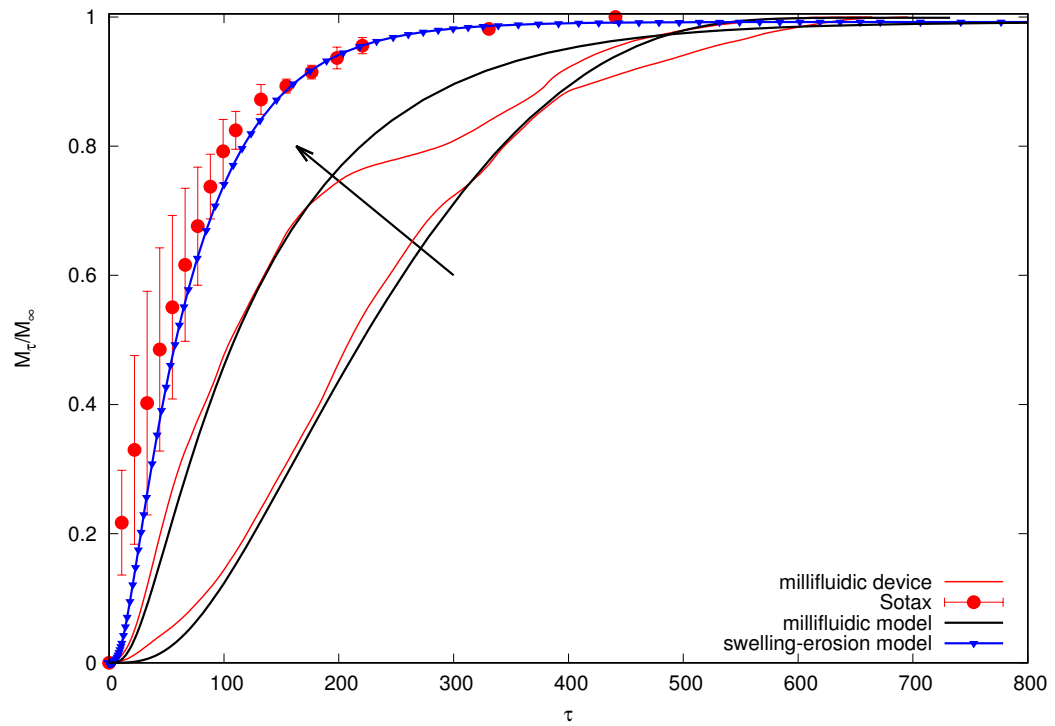


Figure 5.18: Release from millifluidic device and Sotax. Test for film with CD. $\tau = tD_s^G/L_{dry}^2$. Release curve for flow = 1, 3 ml/min and Sotax (50rpm), 37°C

Table 5.1: Erosion values for different flow values, without CD.

Q(ml/min)	C
1	0.01
2	0.015
4	0.03
5	0.08
<i>Sotax(50rpm)</i>	0.1

Table 5.2: Erosion values for different flow values, with CD.

Q(ml/min)	C
1	0.08
3	0.13
<i>Sotax(50rpm)</i>	0.25

5.4 Conclusion

HPMC5 based films were studied in this work. The releases were analyzed by 3 different devices: Franz cell, millifluid device and Sotax. An accurate Franz cell study has highlighted as release from Franz cell is far from being a "perfect mixing" release. Mathematical modeling has supported this thesis. In fact, a classical model can not approximate the experimental data, instead of a modified model that describes the release profile very well (even from a quantitative analysis).

Then the swelling-erosion kinetics of HPMC-based film was modeled, necessary to describe the release kinetics. Thus, the integral release profiles of the millifluid device and the Sotax were compared (release condition in Sotax corresponding to a maximum erosion rate).

Cyclodextrin releases appear to be slower (compared to those without) in the Franz cell, where no erosion phenomenon is associated, but only low diffusion. On the other hand, they are faster in the millifluid device and in the USP II, where instead the release kinetics is mainly controlled by film erosion.

Mucoadhesion test should be investigated to verify the residence time of the formulation required for drug transfer, but the analysis reported and the results obtained show that HPMC-based thin films represent a valid drug delivery solution and useful fast release formulations.

Chapter 6

Preventing drug crystallization in glycerol-plasticized gellan gum thin films

6.1 Introduction

The design of efficient films as carriers for drug delivery applications requires a proper selection of the polymer and excipients used for their fabrication as they can affect the ability of the films to swell, degrade and modulate the release of the therapeutic molecule included in the formulation [333,334]. The type of polymer can also influence the mechanical properties of the film produced that should be robust enough to ensure excellent resistance during handling, and application to the target site.

A large variety of film-forming polymers have been investigated over the last decade, and among them, gellan gum, an anionic and linear biopolymer produced by *Pseudomonas elodea*, presents a set of unique properties that make this polysaccharide a valid option for the fabrication of films. Specifically, gellan gum has attracted much attention in both academic and industrial research because of its biocompatibility as well as its gelling, texturizing, thickening, emulsifying, suspending, stabilizing and film-forming properties [335,336].

Gellan gum films have been investigated in a great variety of applications ranging from protective coatings to preserve the integrity of food [337–340] to more biomedical related fields. For instance, gellan gum-based films have been studied as protective and biodegradable film in wound healing [341,342] and bone regeneration [343]. The unique properties of gellan gum films should be particularly beneficial also for the design of drug delivery systems, however their application in this field is still almost unexplored. In fact, only few works have investigated the inclusion of an active principle in gellan gum films and their application as dosage forms [344].

These premises have motivated this study on gellan gum-based thin monolayered film as potential materials for drug delivery applications. Particular attention was focused on the homogeneous distribution of the active principle within the polymeric thin films, as it represents the main challenge for this type of formulation when used for drug administration [344]. In fact, both the reduced size and thickness characteristics of the thin films as well as the large number of excipients used in their formulation, including soluble polymers, plasticizers, preservatives, may severely limit the loading levels capacity of the dosage form. Uncontrolled crystallization of drug upon fabrication or storage is frequently described for this kind of delivery systems, especially in all that cases where a high dose of the active molecule is required. High drug loadings throughout the hydrophilic polymeric system may lead to aggregation processes with the formation of fractal-shaped aggregates randomly distributes within the matrix, which adversely affect

the uniformity of the resulting film [345, 346].

Moreover, considering that most of the polymers used for film fabrication are hydrophilic macromolecules, as it is the case for gellan gum, the always-troubling integration of drugs within polymeric films becomes particularly critical for lipophilic molecules [347]. Upon fabrication and storage, uncontrolled crystallization and crystal growth of the drug are frequently facilitated by the short diffusion distances of molecules embedded within thin films, therefore the resulting fractal patterns formed in thin polymer films are often related to diffusion-controlled growth processes. If the active pharmaceutical ingredient is not freely soluble in the polymer and is present at a supersaturated concentration, then it may phase-separate from the polymer and subsequently crystallize. Such effects potentially cause inhomogeneous drug distribution within drug-loaded films affecting uniformity of the system as well as drug release kinetics and physical stability during storage.

Casting, solidification processing and drying conditions as well as the right drug-polymer-plasticizer combinations can have a significant impact on the homogeneous distribution of the drug in the dried final product [348]. Therefore, from a pharmaceutical perspective, the stability of the film and the investigation of strategies aimed to avoid drug nucleation and crystal growth as well as inhomogeneous distribution of the therapeutic molecule within the matrix deserve special attention as these aspects are of critical importance for the development of commercially viable formulations.

To this end, process conditions and bulk materials characteristics, such as the viscosity of the polymeric systems prior to drying as well as the drying conditions, need to be deeply investigated as they have a contribution in preventing inhomogeneous drug distribution in the final dry product. These critical aspects have motivated a study on gellan gum based thin monolayered film as potential materials for drug delivery applications. Film casting method was used as preliminary screening technique to determine the optimum ratio among drug, polymer and plasticizer in order to overcome diffusion limited aggregation (DLA) phenomena during fabrication and storage.

Fluconazole (F) and glycerol (Gly) were used as BCS I model drug and plasticizer, respectively. The manufacturing process was optimized monitoring some critical parameters including the rheological properties of the starting polymeric solutions, air bubbles entrapped, residual water in the final films and drying rate. The physical appearance, thickness, mechanical and release properties of the resulting films were thoroughly investigated.

6.2 Materials and method

6.2.1 Materials

Fluconazole [$C_{13}H_{12}F_2N_6O$, 1*H*-1, 2, 4-*Triazole*-1-*ethanol*, α -(2, 4-*difluorophenyl*)- α -(1*H*-1, 2, 4-*triazol*-1-*methyl*)], gellan gum and glycerol used in the present study were purchased from Sigma Aldrich. Cellulose membrane filters were obtained from Medicell International. Methanol (CH_3OH), glacial acetic acid (CH_3COOH), bidistilled water (for HPLC), potassium dihydrogen phosphate (KH_2PO_4), di-sodium hydrogen phosphate dehydrate (Na_2HPO_4), sodium chloride (NaCl) and hydrochloric acid (HCl), (used to prepare simulated saliva, pH= 6.7), were supplied by Carlo Erba Reagents. *HP* - β - *CD* was purchased from Roquette.

6.2.2 Preparation of polymeric films

Films were produced by casting polymeric solutions (6 ml) containing constant concentration of GG (2% w/v) and different amounts of the glycerol, ranging from 0.5% to 6% w/v. In specific, the following GG:Gly weight ratios were investigated: 1:0; 1:0.25; 1:0.5; 1:1; 1:1.5; 1:2; 1:2.5 and 1:3 (w/w). For film preparation, GG and glycerol were dissolved in double distilled water and solubilized at 60 °C, for 5 hours under mild mag-

netic stirring to avoid air bubble incorporation. The hot polymeric mixtures were poured onto leveled silicone plates (diameter = 5.6 cm), let set and then dried in an oven at the constant temperature of $40\text{ }^{\circ}\text{C} \pm 2\text{ }^{\circ}\text{C}$ for 15 hours.

The same procedure was followed to prepare fluconazole-loaded thin films and, in this case, 6 ml of 9.25 mM fluconazole solution in water were used to dissolve the different GG:Gly mixtures, before the drying process.

All the samples were labelled as OTF_X , where X indicate the amount of Gly used for film preparation respect to GG. Instead, OTF_{XF} was used for films containing also fluconazole. Other samples were prepared including $HP-\beta-CD$ in the formulation. An equimolar amount of the selected cyclodextrin and fluconazole was used for the preparation of OTF_{CD} films.

6.2.3 Preparation of inclusion complex cyclodextrins-drug

Binary complexes between fluconazole and $HP-\beta-CD$ are prepared by the kneading technique or lyophilization. In the first case, equimolar amounts of the two components are triturated in mortar until a homogeneous mixture is obtained. To this, 0.5 ml of a 50:50 (v / v) ethanol-water mixture is added and the mixture obtained, after mixing in a mortar for another 30 minutes, is placed in a stove for 24 hours at temperature of $70\text{ }^{\circ}\text{C}$. The product obtained, after complete drying, is again reduced to powder.

Binary system fluconazole/ $HP-\beta-CD$ were produced even for lyophilization. A stoichiometric amount of drug was added to a $HP-\beta-CD$ solution in order to obtain an equimolar solution 1:1 of this two component. The solution obtained was mixed for 24h at $25\text{ }^{\circ}\text{C}$ and then freezed at $-30\text{ }^{\circ}\text{C}$. At the end the solution was lyophilized for the time that the operation need to complete.

6.2.4 Rheological studies

Rheological experiments were carried out with a Haake Rheo Stress 300 Rotational Rheometer (Germany) equipped with a Haake DC10 thermostat. Flow curves of all the polymeric solutions were obtained with a cone-plate geometry in the range of 0.01–1000 Pa, working at $60\text{ }^{\circ}\text{C} \pm 0,1\text{ }^{\circ}\text{C}$. The effect of temperature on the viscoelastic properties of the polymeric mixtures was also investigated through temperature sweep analysis in the range $60\text{ }^{\circ}\text{C} - 30\text{ }^{\circ}\text{C}$. All the experiments were carried out at least in triplicate.

6.2.5 Thickness measurements

Thickness of dry films was measured by means of a Mitutoyo Digimatic Micrometer, characterized by an instrument error $\pm 2\mu\text{m}$. Measurements were taken at least at three different points of each film.

6.2.6 Thermogravimetric analysis

Thermogravimetric analyses were carried out using a Q600 TGA (TA Instruments). Samples of the films (30mg) were put in open aluminum pans and submitted to three heating/cooling cycles in the temperature range from $25\text{ }^{\circ}\text{C} - 120\text{ }^{\circ}\text{C}$ under nitrogen atmosphere (5ml/min). Thermograms were recorded at the constant heating rate of $5\text{ }^{\circ}\text{C}/\text{min}$.

6.2.7 Differential scanning calorimetry

Calorimetric measurements were carried out using a DSC131 (Setaram, France) differential scanning calorimeter. Samples (5mg) of anhydrous dust fluconazole, freeze-dried fluconazole, buccal film of fluconazole, gellan and glycerol with different concentrations were weighted in sealed aluminum pans. Then were examined at three heating/cooling cycles in a temperature range from $25\text{ }^{\circ}\text{C} - 170\text{ }^{\circ}\text{C}$, flowing nitrogen atmosphere (20 ml/min). Thermograms were recorded at the constant heating rate of $5\text{ }^{\circ}\text{C}/\text{min}$. An empty aluminum pan was used as reference.

6.2.8 Tensile tests

Tensile tests were performed with a ZWICK-ROELL-Z010 mechanical testing machine, using a normal load of 1kN and a strain rate of 1mm/min. Ten specimens of opportune dimensions were cut from each film, mounted between the grips of the machine and tested to fracture. Specimens were cut in three different directions (angle 0°, 45°, 90°) of the film, in order to verify the isotropy of the material. Stress-strain diagrams were recorded and Young's modulus, strain and stress at break were acquired. Results were reported as mean values \pm standard deviation.

6.2.9 Swelling studies

Films were cut in square pieces (2.2 cm), weighted and inserted in beaker containing simulated saliva (pH 6.7) at $37^\circ\text{C} \pm 0,1^\circ\text{C}$. At regular time intervals, wet films were drained to remove excess water and weighed. The water-uptake capacity (Q) was expressed as:

$$Q = \frac{W_s(t) - W_0}{W_0} \quad (6.1)$$

where $W_s(t)$ and W_0 are the weight of the swollen film at time t and that of the starting dry film, respectively. Alternatively, the Q value was calculated according to Eq.2.

$$Q = \frac{W_s(t) - W_d}{W_d} \quad (6.2)$$

where $W_s(t)$ and W_d are, respectively, the weight of the swollen film after 2h in simulated saliva and that of the film recovered at the end of the swelling study and dried to constant weight. Eq. 2 enables considering the amount of glycerol lost during the swelling process. To this end, portions of the investigated films were kept for 2h in simulated saliva at $37^\circ\text{C} \pm 0,1^\circ\text{C}$, then they were removed from the medium and oven-dried at 70°C to constant weight, in order to calculate the amount of glycerol leached out the films. Each test was repeated in triplicate and the results reported as mean \pm SD.

6.2.10 Mucoadhesion tests

The mucoadhesive properties of GG:Gly films were evaluated in vitro, measuring the force required for detaching the films from a mucin tablet. The measurements were carried according to an already reported method, based on an in-house pulley system apparatus [349]. Briefly, a mucin tablet (diameter 12.5 mm, thickness 1.34 mm) was stucked onto a holder connected to one arm of the pulley system. Then, round-shaped portions of the films (diameter 12.5 mm) were attached to the mucin tablets, previously wetted with simulated saliva (pH 6.7). The mucoadhesiveness of the film was measured by adding water to a container connected to the second arm of the pulley system until the film was separated from the tablet. The weight of water needed to separate the film from the mucin tablet was recorded and introduced in the following equation for the calculation of the detachment force:

$$N = V\rho g \quad (6.3)$$

where V is the volume of added water, ρ is the density of water and g is the acceleration due to gravity.

6.2.11 Uniformity of drug content tests

The uniformity of drug content within the films was assessed by dividing a sample of fluconazole-loaded $OTF_{2.5}$ in three parts. Each individual part of the film was weighted and then it was extensively extracted with distilled water. The concentration of fluconazole in the obtained solutions was evaluated by HPLC analysis, carried out with a Perkin

Elmer system composed of a Series 200 LC pump, a 235 Diode Array Detector, a Total Chrom data processor and equipped with a RP-18 (250-4.5 μm) Merck Hibar LiChrocart column. The analyses were carried out under isocratic conditions, using a mobile phase composed of a methanol, bidistilled water and glacial acetic acid mixture in proportion of 50:48:2 (v:v:v). The flow rate of the mobile phase was maintained at 0.8 ml/min and the drug was monitored at $\lambda = 260\text{nm}$. Under these conditions, fluconazole retention time was about 6 minutes. All experiments were carried out in triplicate.

6.2.12 In vitro release studies

Dissolution tests were carried out in a conventional USP type II paddle apparatus and the millifluidic device. For the dissolution test in the paddle apparatus samples of round shape fluconazole-loaded OTF (surface area 98.5 cm^2) were placed in different part of the vessel: a) taped on the side wall; b) taped on the bottom; c) anchored to the bottom with a wire mesh. All the release studies were carried out in 500 mL of simulated saliva (phosphate buffer, pH 6.7, containing 0.137M NaCl) at $37^\circ\text{C} \pm 0,1^\circ\text{C}$ with a rotation rate of 50 rpm. Aliquots of the release medium (2 mL) were taken at appropriate time intervals from 1 to 30 min and immediately replenished with the same volume of fresh simulated saliva. Fluconazole concentrations were assayed by HPLC analysis. Tests were repeated in triplicate and the results were expressed as mean values \pm the standard deviation.

6.3 Results and discussion

6.3.1 Preparation of GG:Gly thin films

Deacylated gellan gum easily forms films for casting of its aqueous solutions. In this work, film forming solutions of the polymer were casted in round-shaped silicone molds, in order to obtain strips with defined dimensions and shape. In the solvent casting process, film fabrication involves the initial deposition of a liquid polymeric film on an opportune surface of a solid support and the subsequent evaporation of the solvent with conversion of the viscous liquid polymeric film into a solid polymeric film. The quality and characteristics of the final product are critically dependent on several physical properties of the initial film-forming solution, as well as the manufacturing conditions, such as the rate of solvent evaporation from the liquid film [350–352]. For this reason, both the rheological properties of the starting gellan gum solutions and their temperature-induced modification during casting of the liquid film and the evaporation step, were evaluated in the present work as they have a significant impact on the final properties of the film produced. In particular, absence of entrapped air bubbles or uniform distribution of active pharmaceutical agents within the medicated strips represent the most important and desired characteristics of polymeric films for drug delivery application, because they critically affect the performance of the formulation as pharmaceutical products.

All that considered, the first step of the experimental work involved the rheological characterization of the film-precursor polymer solutions, which were obtained stirring gellan gum at 60°C for five hours to enable the polymer to dissolve completely and obtain a homogeneous solution. Figure 6.1 and 6.2 shows the viscosity curves of gellan gum, at three different polymer concentrations 2.0, 2.5, 3.0% w/v, at 60°C . As expected, all the solutions in the concentration range under investigation can be described as non-Newtonian fluids, with a shear thinning behavior. Depending on the polymer concentration, the viscosities of the investigated systems ranged from 100 to 10.000 Pa·s at 60°C and shear rate of 10^{-4}s^{-1} .

Gellan gum solutions with a concentration 2.5% w/v resulted in non-uniform deposition of the polymer in a thin layer, probably as a consequence of their viscosity. Therefore, in order to avoid casting defects within the dried products, 2%w/v gellan gum solutions were selected for further studies. According to the literature, casting of

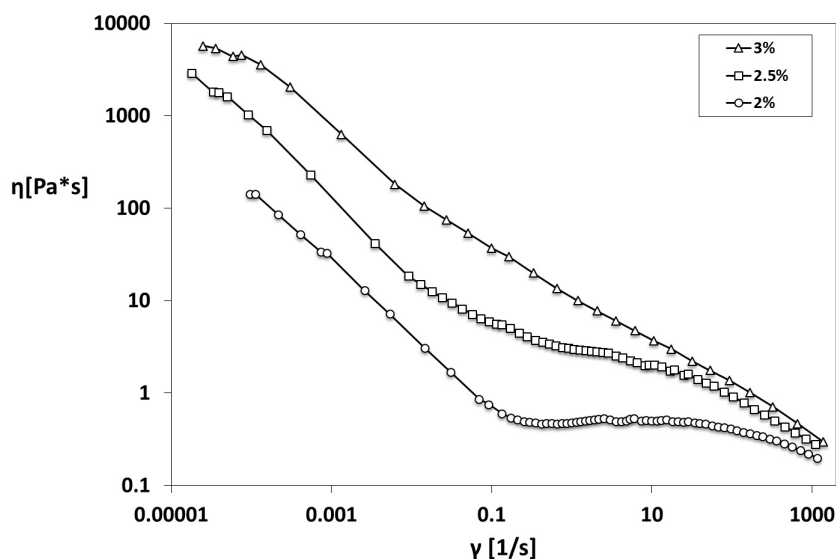


Figure 6.1: Flow curves of GG solutions at 60 °C: effect of polymer concentration on solution viscosity.

gellan gum solutions resulted, after the drying process, in the formation of very brittle films, which were hardly removed from the silicon molds used for the casting process [338]. Without at least a minimal concentration of a plasticizer, pure gellan gum films show interactions among the polymeric chains, which resulted in high rigid structures with poor mechanical properties. For this reason, different amounts of glycerol ranging from 0.5% to 6% w/v were added to 2% (w/v) gellan gum solutions. Glycerol was selected on the basis of the results reported by Yang L. and coworkers [338], who evaluated the effect of different plasticizers on the mechanical properties of gellan gum films, observing that glycerol-plasticized films were more stretchable and transparent, than PEG 400, sorbitol, propylene glycol or ethylene glycol - plasticized films.

The addition of a plasticizer to gellan gum solutions may lead to a decrease in intermolecular forces along the macromolecular chains as glycerol penetrate the polymeric network, and, in this way, it may influence both the flowing behavior of the film forming solutions, through the development of polymer-plasticizer hydrogen bonds, and the film formation process.

Therefore, preliminary experiments aiming to study the effect of glycerol concentration on the viscosity properties of 2% w/v gellan gum solutions, were carried out. Flow curves of gellan gum-glycerol mixtures at different polymer to glycerol ratio were recorded and the results reported in figure 6.2. It can be observed that, irrespective from the amount of plasticizer used, all gellan gum-glycerol mixtures showed almost the same flowing behavior when shear stress was applied and linearly increased from 0.01 to 1000 Pa.

Besides investigating the flow behavior of gellan gum/glycerol mixtures, also the effect of the plasticizer on the gelation process of the polymer was studied. The experimental conditions for the formation of polymeric films with appropriate properties should be optimized considering a low difference between the temperature of the polymer solution before casting and the gelation point of the systems. Therefore, the behavior of storage modulus and loss modulus (G' and G'') and the relationship between gelation temperature and plasticizer concentration were investigated through temperature sweep measurements from 60 °C down to 37 °C. The results reported in table 6.1 show that the crossover point

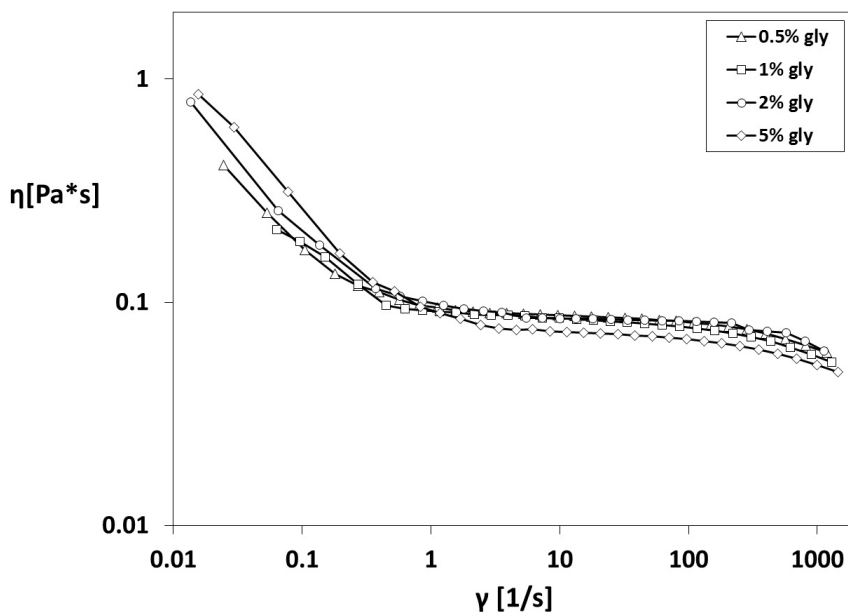


Figure 6.2: Flow curves of GG solutions at 60 °C: effect of glycerol concentration on GG (2% w/v) viscosity.

Table 6.1: Effect of glycerol concentration on the gelation temperature of gellan gum solutions, 2% (w/v).

% Glycerol(w/v)	% Gellan gum (w/v)	Gelation temperature (°C)
0	2	49.3 ± 1.5
0.5	2	51.9 ± 0.4
1	2	51.0 ± 1.0
2	2	52.4 ± 0.2
5	2	51.7 ± 1.4

of G' and G'' slightly shifted toward higher temperature when glycerol was added to GG solutions, with almost no differences for the different polymer-plasticizer combinations analyzed. At 60 °C all the systems behave like solutions, as the loss modulus G'' is, in all the cases, higher than the corresponding storage modulus G' .

Therefore, in the film formation process, all the GG:Gly mixtures behave like solutions when poured in the silicon molds, then they formed thin liquid layers, which experienced a rapid temperature modification, due to the reduced thickness, and consequent sol-gel transitions with the inversion of the G' and G'' moduli.

After the casting step, all the systems were dehydrated at the constant temperature of 40 °C until polymeric films were obtained and easily peeled off from the molds. TGA was used to monitor residual water content in the plasticized films during the drying step. Residence time lower than 15 hours in the drying oven, did not produce films of acceptable flexibility; instead clear and transparent films were obtained and easily peeled off from the support, when the residual water content in the final plasticized film, was in the range 9.4-11.5%, depending on the glycerol percentage. Such residual water content was obtained keeping the systems at the constant temperature of 40 °C for 15 hours.

Therefore, the maximum drying time for complete film formation was set at 15 h,

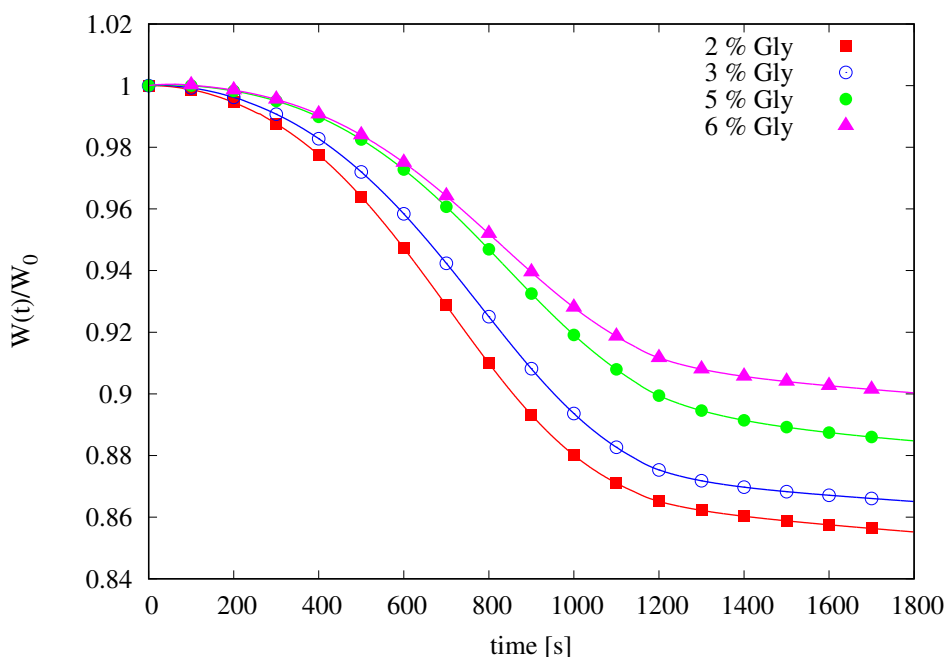


Figure 6.3: Thermogravimetric curves of OTF containing 2,3,5 and 6% (w/v) of glycerol.

because prolonging any further the drying process brought to excessive dehydration of the films, which resulted in poor mechanical properties, even in high-plasticized systems. In fact, beside glycerol, also the presence of water molecules within the constrained polymeric networks is able to increase the macromolecular mobility, while reducing the system rigidity. As expected, to higher percentages of glycerol in the film-forming solutions corresponded higher amounts of residual water within the dried films, when same drying times were applied, as observed from the thermogravimetric curves (figure 6.3).

Under the adopted experimental conditions (drying at 40 °C for 15 hours), films with mean thickness values varying from 25.8 ± 2.8 to $157.7 \pm 6.6 \mu\text{m}$ were obtained (table 6.2). Considering that the amount of gellan gum was maintained constant, the increase of plasticizer concentration in the film-forming solutions rises the total mass of solids casted in the molds and, consequently, an almost linear increase of the thickness of the corresponding dried films was observed. Two different film formulations can be defined: mucoadhesive buccal films and orodispersible films [353].

This classification is operated on the basis of the release rate of the drug included in the formulation, whereas no specification about the thickness of film is reported. Anyway, it is generally accepted that ultra-thin films for buccal delivery have a thickness comprised in the range $50\text{-}150\mu\text{m}$ [333]. Therefore, irrespective from the amount of glycerol used, all the systems prepared almost falls within the limits for ultra-thin film classification.

6.3.2 Mechanical properties of GG:Gly thin films

The mechanical properties of the final films were influenced by glycerol concentration. For the dried films, the values of Young's modulus suggest that the flexibility increased linearly when plasticizer concentration increased from 0.5 to 6% w/v. A progressive reduction of Young's modulus and a corresponding increase in the percentage of deformation at break can be observed in figure 6.4B-C for increasing amount of glycerol. The high number of hydroxyl groups and carboxyl groups along gellan chains are responsible for the formation of numerous hydrogen bonds and extensive intra- and inter-molecular interactions, which may contribute to the high mechanical strength and low flexibility of unplasticized or low plasticized gellan films.

Table 6.2: Effect of glycerol concentration on the gelation temperature of gellan gum solutions, 2% (w/v).

Sample	% Glycerol(w/v)	% Gellan gum (w/v)	Weight ratio GG:Gly	Total mass(mg)	Thickness(μ m)
<i>OTF</i> ₀	0	2	1 : 0	120	25.8 \pm 2.8
<i>OTF</i> _{0.25}	0.5	2	1 : 0.25	150	45.5 \pm 7.7
<i>OTF</i> _{0.5}	1	2	1 : 0.5	180	57.5 \pm 4.9
<i>OTF</i> ₁	2	2	1 : 1	240	76.9 \pm 6.3
<i>OTF</i> _{1.5}	3	2	1 : 1.5	300	93.9 \pm 4.8
<i>OTF</i> ₂	4	2	1 : 2	360	96.4 \pm 7.7
<i>OTF</i> _{2.5}	5	2	1 : 2.5	420	142.5 \pm 10.6
<i>OTF</i> ₃	6	2	1 : 3	480	157.7 \pm 6.6

When small quantities of glycerol are used, a strong interaction might occur between the polymer and the plasticizer, producing a "cross-linker" effect, which decreases the free volume and the molecular mobility of the polymer, thus reducing the flexibility of the films. Instead, incorporation of at least 50% w/w of glycerol within these systems probably replaces some of the gellan–gellan hydrogen bonds with glycerol–gellan hydrogen bonds, increasing the intermolecular separation of the gellan chains, with consequent increase in the chain segmental mobility. This effect results in a reduction of the mechanical strength of the films, whereas their flexibility was enhanced (figure 6.4A-B). Beside glycerol, also the residual water influences gellan gum mobility contributing to the elasticity of the films. No preferential orientation of the polymeric chains was evidenced along one specific direction of the films. In fact, tensile tests carried out on specimens of each OTF cut in three different directions failed to evidence differences among the obtained results, thus suggesting that all the films were completely isotropic in terms of tensile properties.

6.3.3 Swelling studies

All the OTFs were studied for their swelling ability. In a first attempt, the swelling degree of the thin films was calculated as the ratio between the weight of the swelled and the starting dry film. The obtained results are reported in figure 6.5. It can be observed a progressive reduction of the equilibrium Q values as the amount of glycerol in the films was increased. However, considering the presence of glycerol, its small dimension and its high solubility in water, it was subsequently evaluated whether a loss of the plasticizer may occur during the swelling study and in what extent this eventual loss may affect the results of the swelling measurements. In fact, as the OTFs prepared in this work did not undergo any degradation process in the time frame of the swelling study, glycerol may diffuse toward the swelling medium enabling water penetration within the polymeric film.

All that considered, it was evaluated the rate of glycerol loss from the OTFs. To this end, samples of the different films were let to swell in simulated saliva, then, at regular time intervals, the films were removed from the swelling medium, weighted and dried to constant weight. It was found that the plasticizer diffused out the films almost completely within 20 minutes of contact with simulated saliva. In fact, the weight of the samples, recovered at the end of this study and dried, almost corresponds to the value expected for a film made only of gellan gum (figure 6.7).

Therefore, the equilibrium swelling data were corrected considering the loss of the plasticizer towards the swelling medium and the results are reported in figure 6.6. An opposite trend in the swelling capacity of the different OTF can be observed in this case. In fact, the amount of water taken up by the films at equilibrium increases with the percentage of glycerol originally present in the polymeric strip. In view of these results, plasticized OTFs, specially those designed for sustained drug release, should be evaluated considering that a loss of the plasticizer may occur within time, with consequent possible effects on some of the properties of the films, such as the swelling capacity, the mechanical properties and the release rate.

6.3.4 Evaluation of the mucoadhesive properties of GG:Gly thin films

The mucoadhesive properties of GG:Gly films were evaluated in vitro measuring the force required for detaching the films from a mucin tablet. The obtained results are reported in table 6.3. A progressive reduction of the force required for detaching the OTFs from mucin was observed when the increasing amounts of glycerol were used in the formulation of the polymeric films. In particular, a marked drop in the mucoadhesive properties of the films was measured for OTF_1 containing equal amounts of polymer and plasticizer. It is likely that the excess of plasticizer prevents GG from interpenetrating

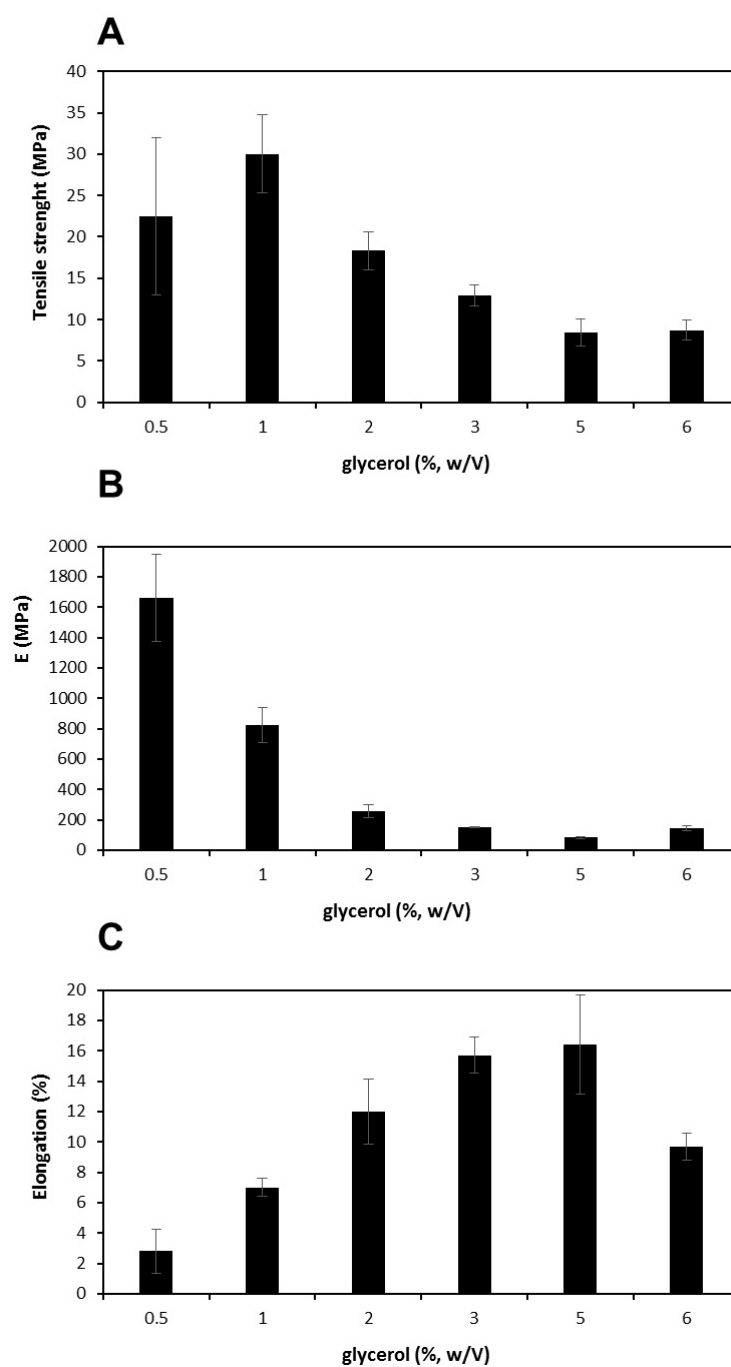


Figure 6.4: Mechanical properties of gellan based OTF containing different amount of the plasticizer glycerol: A) tensile strength and break; B) Young modulus and C) elongation at break.

and interacting with mucin thus negatively affecting the mucoadhesive properties of the final formulation.

6.3.5 Drug loaded films

Glycerol-plasticized films were loaded with a BCS I model drug, namely fluconazole. Although fluconazole is slightly soluble in water [354], uniform distribution of the drug

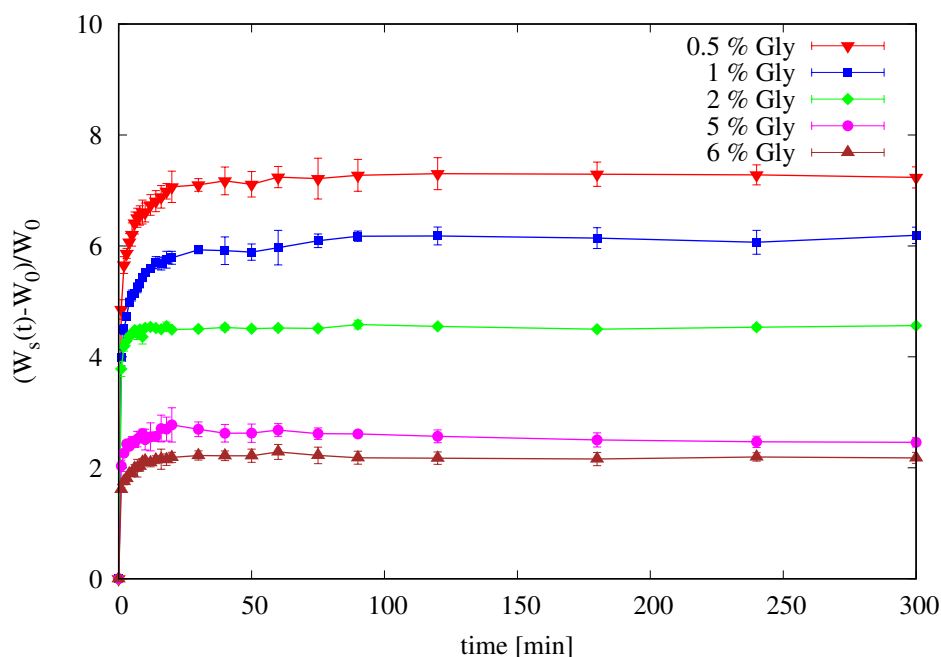


Figure 6.5: Dynamic swelling study. Evaluation of the variation of the swelling capacity within time for the gellan based OTFs containing different amount of the plasticizer glycerol.

Table 6.3: Mucoadhesive properties of GG:Gly thin films.

Sample	Weight ratio GG:Gly	Force(N)
$OTF_{0.25}$	1 : 0.25	0.71 ± 0.03
$OTF_{0.5}$	1 : 0.5	0.58 ± 0.01
OTF_1	1 : 1	0.13 ± 0.01
$OTF_{2.5}$	1 : 2.5	0.05 ± 0.01

within gellan gum films was critically dependent on the amount of glycerol used, when $0.64mg/cm^2$ of fluconazole was included in the formulation. In fact, strips containing concentration of the plasticizer lower than 70% w/w resulted in separation of white aggregates within the polymeric matrix, probably due to phenomena of limited diffusion aggregation of the drug molecules (figure 6.8).

After the drying process, all the systems showed an initial homogeneous appearance with no presence of aggregates, as evidenced by visual observation and confirmed by DSC analysis. In fact, no melting peaks of fluconazole were observed in the corresponding thermograms. However, films containing an amount of glycerol 50% w/w shown the appearance of some aggregates of fluconazole within few days from the preparation. It was observed that fluconazole aggregation depends on glycerol concentration within the films. In fact, a faster appearance of drug aggregates was observed in strips with lower amount of the plasticizer, maybe because of the different ability of fluconazole to diffuse within the differently plasticized systems. Low mobility of the drug may cause segregation of fluconazole within drug-rich regions of the film where local concentration may exceed its saturation limit, thus promoting its nucleation and crystallization, according to the general believing that branch-structured dendritic crystallization is a result of phase separation from supersaturated states [355,356].

In contrast, a more homogeneous drug distribution could be achieved when high amount of the plasticizer were added to the formulation. According with the effect of

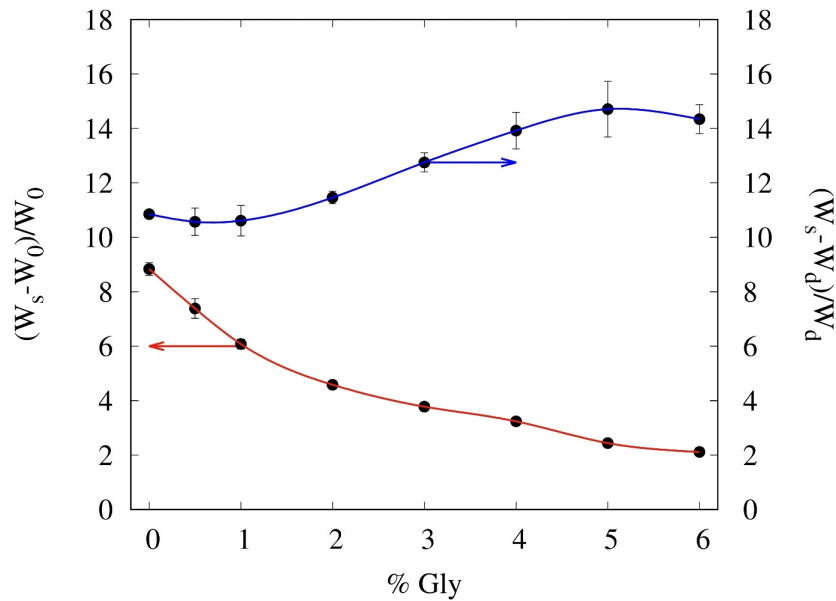


Figure 6.6: Effect of glycerol content on the swelling capacity of gellan based OTFs. The swelling degree was calculated as the weight ratio between the swollen film (W_s) and the weight of the film before swelling (W_0) (red line) or as the weight ratio between the swollen film (W_s) and the weight of the dried residual film recovered after 2 h in simulated saliva at $37^\circ\text{C} \pm 0,1^\circ\text{C}$ (blue line).

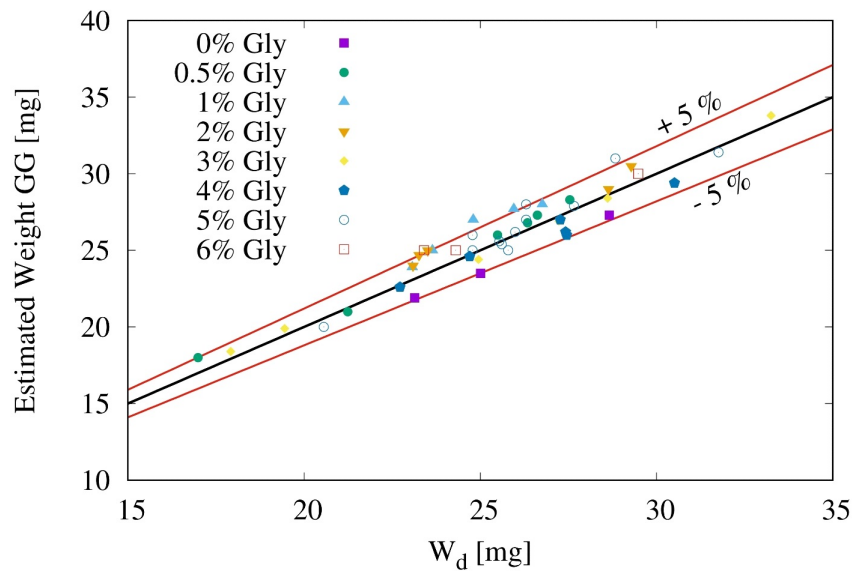


Figure 6.7: Analysis of the composition of the OTFs recovered after 2h in simulated saliva (pH 6.7) at $37^\circ\text{C} \pm 0,1^\circ\text{C}$ and dried to constant weight.

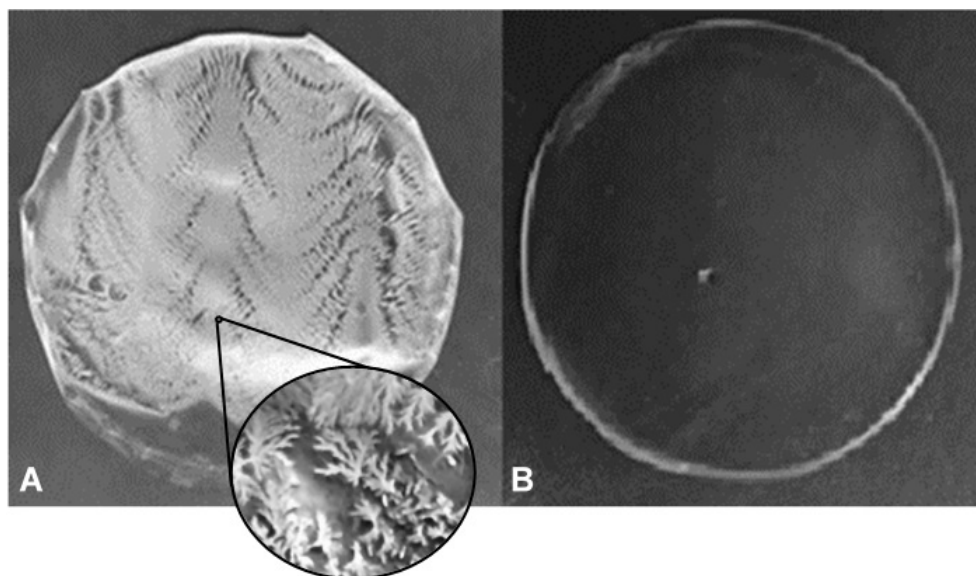


Figure 6.8: Photographs of (A) low-plasticized gellan based OTF containing 50% w/w of glycerol and (B) high-plasticized films containing 70% w/w of glycerol. The presence of crystals of fluconazole is well visible in low plasticized OTFs.

glycerol on the tensile properties of gellan films, it is likely that the presence of glycerol reduced the intermolecular interaction among gellan gum chains producing the formation of a less tight matrix, where fluconazole could be distributed more uniformly (figure 6.9).

According with this hypothesis, no signs of drug crystallization were observed when equimolar amounts of fluconazole and $HP - \beta - CD$ were introduced in the formulation. The presence of $HP - \beta - CD$ was able to suppress drug nucleation and further crystal growth even in glycerol-free films. A quite low amount of $HP - \beta - CD$ (76 mg, 0.055 mmoles) was used in the formulation, therefore the observed effect is more likely due to an altered disposition of the drug in the final film caused by cyclodextrin, than to a modified interaction between gellan gum chains. In fact, $HP - \beta - CD$ may produce a preferential localization of fluconazole in its internal cavity during the OTF formation, thus preventing drug aggregation, with a minimal interference in the arrangement of the polymeric chains in the dried film.

The presence of drug aggregates was confirmed by DSC analysis. The thermograms reported in figure 6.10 show the presence of an endothermic peak, which can be attributed to drug recrystallization within the polymeric matrix. It can also be observed a shift of the melting temperature of fluconazole toward lower values and the progressive broadening of the peak with increasing glycerol concentrations maybe due to certain amount of plasticizer, which remains within the crystal lattice, introducing defects in the structure during the crystallization process. The presence of fluconazole crystals was put into evidence with thermal analysis for concentration of glycerol lower than 50% w/w, whereas no endothermic peak of fluconazole could be observed in films containing 50% w/w of plasticizer (OTF_1), even though white aggregates were well visible within the strips.

It is likely that the inclusion of glycerol within fluconazole lattice first reduces the degree of crystallinity of the drug, and then it converts the solid into a complete amorphous structure. Similar results were already reported for felodipin loaded thin films [345]. An alternative explanation may also be proposed for this behavior. In specific, considering the relatively high amount of glycerol employed in OTF_1 , the disappearance of the melting peak of fluconazole may be consequent to drug solubilization in the excess of plasticizer present in the film. In fact, as solubility increases with temperature, dissolution of fluconazole in glycerol may occur during the heating phase of the DSC analysis which, for this reason, fail to evidence the presence of the drug in the sample [345].

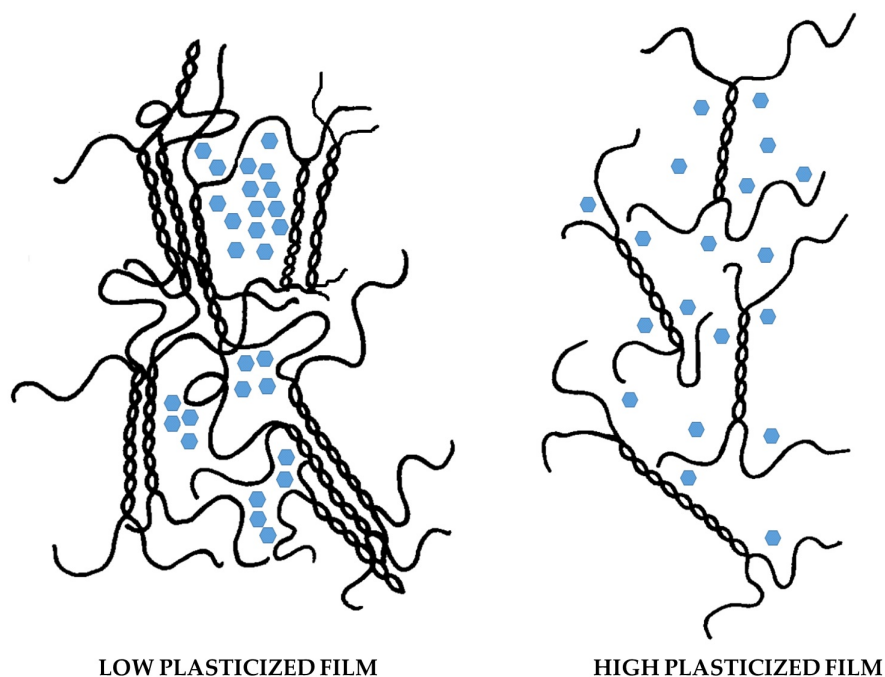


Figure 6.9: Schematization of the different distribution in low and high plasticized gellan based OTFs.

Based on these results, high amounts of plasticizer need to be used in the formulation of fluconazole loaded GG based OTFs in order to have a stable and homogeneous molecular dispersion of the drug within the polymeric matrix. In specific, at least 70% w/w of glycerol have to be present in the final formulation in order to avoid any drug aggregation within the thin film.

Fluconazole loaded thin films containing a 1:2.5 (w/w) GG:Gly ratio were selected for further investigation, because systems containing lower amounts of glycerol resulted in fast drug aggregation within few days from the preparation. $OTF_{2.5}$ were further characterized in order to evaluate the effect of fluconazole on the main properties of the OTFs and investigate their possible use as drug delivery systems.

The residual water content and the correlated tensile properties were not significantly affected by the presence of fluconazole within the films with values similar to plain formulation (data not shown).

6.3.6 Release studies

After evaluation of the uniform distribution of fluconazole within $OTF_{2.5}$ and OTF_3 films, these samples were studied for the release profile of the drug in simulated saliva (pH 6.7) at $37^\circ\text{C} \pm 0,1^\circ\text{C}$ using a USP type II apparatus. The results showed almost no difference between films containing 70 or 75% w/w of glycerol (data not shown). In both cases, fluconazole was completely release from the film within 15 min, in agreement with the results of the swelling studies which evidenced similar Q values for $OTF_{2.5}$ and OTF_3 .

On the contrary, a slower release was observed from films containing $HP - \beta - CD$ (figure 6.11). These results can be explained assuming the formation of an inclusion complex of fluconazole. The drug is free in $OTF_{2.5}$ and OTF_3 samples. This may explain the faster release rate of the drug compared with OTF_{CD} where fluconazole is, at least partially, complexed and bonded in the cavity of the $HP - \beta - CD$ and is able to diffuse in the medium just with a low value of the diffusion coefficient due to the great steric volume.

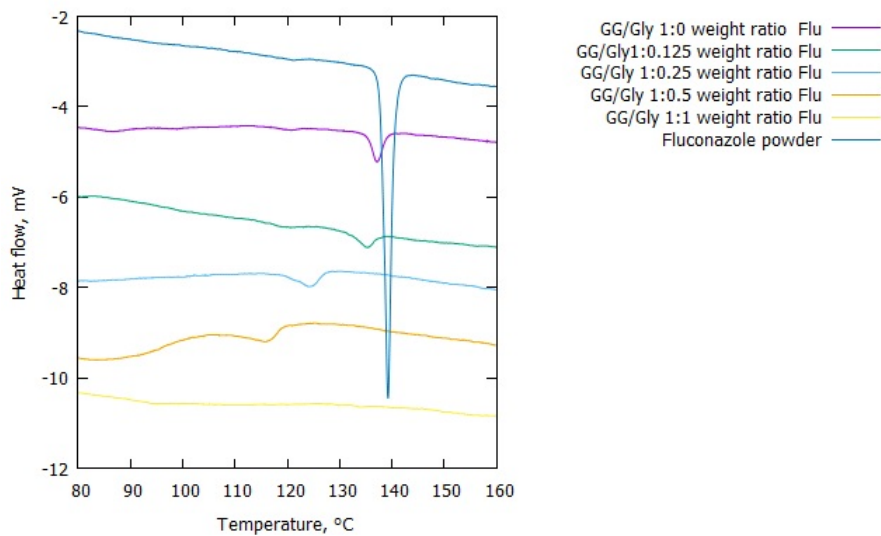


Figure 6.10: Thermograms of free fluconazole and drug loaded OTFs containing different amount of glycerol.

The release analysis were carried out also in the millifluidic device in the range of $Q \in [1 - 5]$ ml/min and 37°C . Even in this case the release of fluconazole with cyclodextrins is slower than the case without, as it's possible to verify in figure 6.12

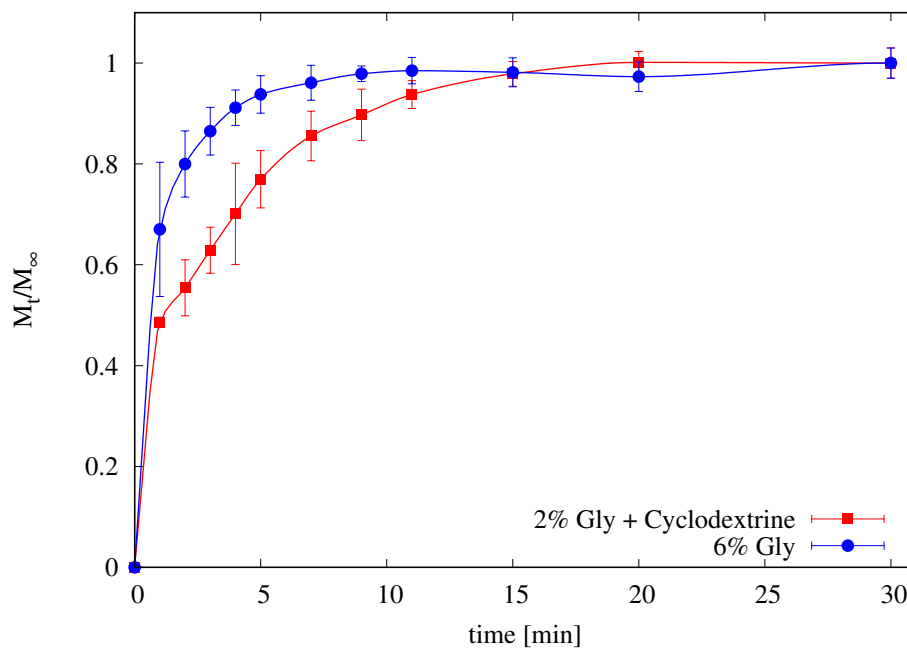


Figure 6.11: Release profile of fluconazole from OTF_3 and OTF_{CD} in simulated saliva (pH 6.7) at $37^\circ\text{C} \pm 0,1^\circ\text{C}$ (USP II).

In the figures 6.13 and 6.14 the same releases are shown on the basis of the adimensional time. It is important to consider a reference time that takes into account the different film thickness and the solvent diffusivity in the films. In particular, an average thickness of $70\mu\text{m}$ and $100\mu\text{m}$ respectively for the film at 6% glycerol and with cyclodextrins were considered, and a diffusivity of solvent in the film $D_s = 5.25 \cdot 10^{-11}$

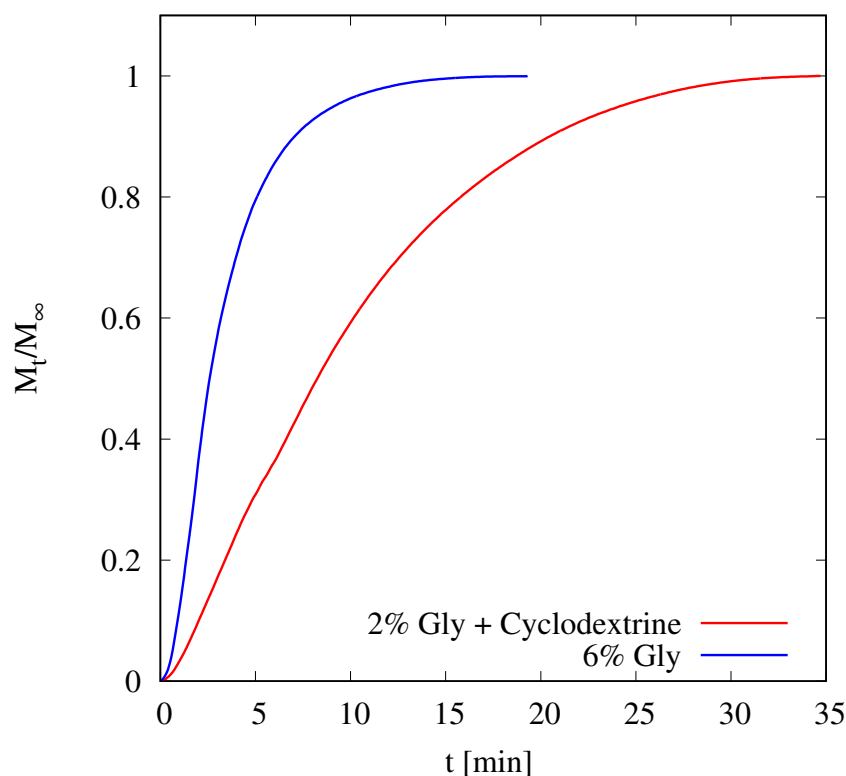


Figure 6.12: Release profile of fluconazole from OTF_3 and OTF_{CD} in simulated saliva (pH 6.7) at $37^\circ\text{C} \pm 0,1^\circ\text{C}$, $Q=2\text{ml}/\text{min}$ (millifluidic device).

m^2/s .

The adimensional analysis is very important as it highlight as the profiles are very close. Then even lowering the amount of glycerol we can get good mechanical and mucoadhesive properties while maintaining the same time scale for the release of the same amount of loaded drug .

6.4 Conclusion

The potential of deacylated gellan gum thin films for drug delivery was investigated. The addition of a plasticizer was required to improve the poor mechanical properties of the polymer formulated as a thin film. It was observed that, while low amount of the plasticizer glycerol were sufficient to increase the resistance and strength before rupture of the films, they resulted to be completely inadequate to have the model drug fluconazole homogeneously distributed within the polymeric matrix. In fact, much higher percentages of glycerol were needed to prevent drug nucleation and crystallization within the film, at least within a short timescale.

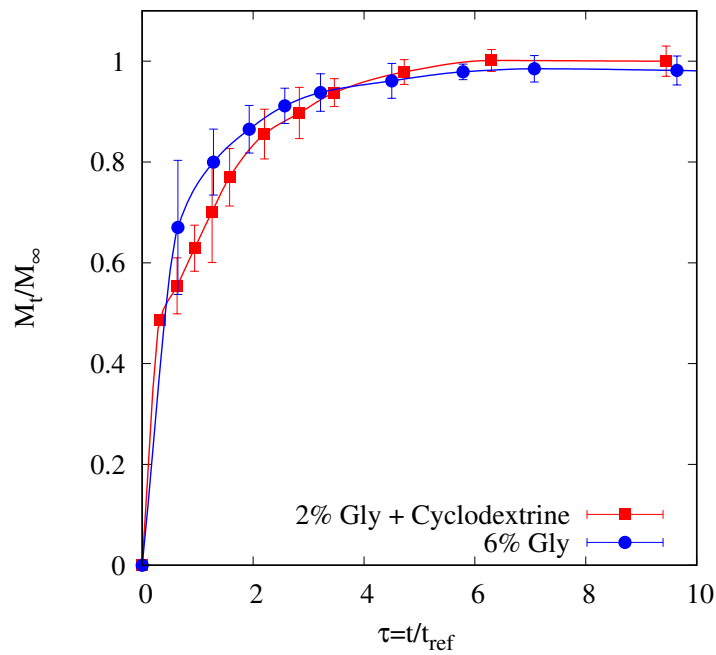


Figure 6.13: Release profile of fluconazole from OTF_3 and OTF_{CD} in simulated saliva (pH 6.7) at $37^\circ\text{C} \pm 0,1^\circ\text{C}$ (USP II). $t_{ref} = \frac{\bar{L}^2}{D_s}$ where \bar{L} is the average thickness and D_s is the solvent diffusivity.

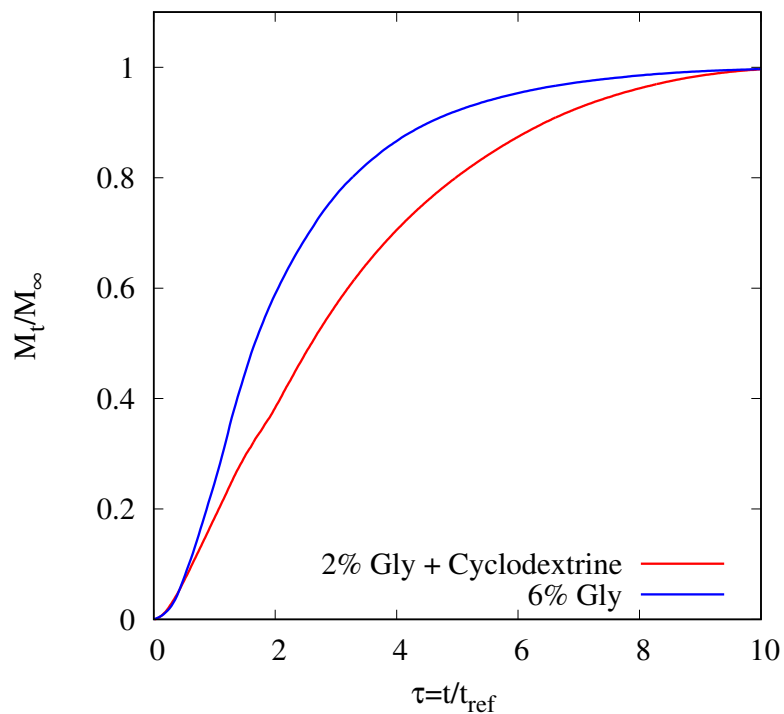


Figure 6.14: Release profile of fluconazole from OTF_3 and OTF_{CD} in simulated saliva (pH 6.7) at $37^\circ\text{C} \pm 0,1^\circ\text{C}$, $Q=2\text{ml/min}$ (millifluidic device). $t_{ref} = \frac{\bar{L}^2}{D_s}$ where \bar{L} is the average thickness and D_s is the solvent diffusivity.

Chapter 7

General conclusions

The main results presented in this research work can be summarized as follows:

- the design and preparation of hydrogels and OTFs based on natural and biocompatible polysaccharides for topical and buccal drugs delivery and the optimization of concentrations of the main components (polymer, plasticizer and / or cyclodextrins) to provide the best performances for an effective utilization of the formulation;
- a proper estimate of release time-scales from OTFs for buccal release by means of the recently proposed millifluidic flow-through device;
- the development of mathematical models able to properly describe the experimental data and release kinetics in different apparatuses. In particular:
 - a double-moving boundary model describing swelling and release from OTFs in the millifluidic device;
 - a polymer-drug interaction model for describing diffusion and release from hydrogels in a vertical Franz cell;
 - a new approach to the description and interpretation of Franz cell release data including the effects of the "unperfect mixing" chamber and withdrawal position.

Bibliography

- [1] Vishwkarma, D.K.Tripathi, A.K., Yoshev, P., et Maddheshiyab, B.(2011). Review article on mouth dissolving film. *Journal of global pharma Technology*, 3(1), 1-8.
- [2] Hearnden, V., Sankar, V., Hull, K., Juras, D. V., Greenberg, M., Kerr, A. R., et Thornhill, M. H. (2012). New developments and opportunities in oral mucosal drug delivery for local and systemic disease. *Advanced drug delivery reviews*, 64(1), 16-28.
- [3] Puratchikody, A.,et Mathew, S.T.(2011). Buccal Drug Delivery: Past, Present and Future-A Review. *International Journal of Drug Delivery*, 3(2), 171-184.
- [4] Asane, G.S. Nirmal, S.A., Rasal, K.B., Naik, A.A., Mahadik, M.S., et Rao, Y.M.(2008). Polymers for mucoadhesive drug delivery system: A current status. *Drug development and industrial pharmacy*, 34(11), 1246-1266.
- [5] Smart,J.D. (2005). The basic and underlying mechanisms of mucoadhesion. *Advanced drug delivery reviews*, 57(11), 1556-1568.
- [6] Serra, Laura, Josep Dom, and Nicholas A. Peppas. "Engineering design and molecular dynamics of mucoadhesive drug delivery systems as targeting agents." *European journal of pharmaceuticals and biopharmaceutics* 71.3 (2009):519-528.
- [7] Kharenko, E.A.,N. I. Larionova, and N. B. Demina. "Mucoadhesive drug delivery systems: quantitative assessment of interaction between synthetic and natural polymer films and mucosa." *Pharmaceutical Chemistry Journal* 42.7 (2008):392-399.
- [8] Collins,L. M. C., and C. Dawes. "The surface area of the adult human mouth and thickness of the salivary film covering the teeth and oral mucosa." *Journal of dental research* 66.8 (1987): 1300-1302.
- [9] Watabane, S., and C. Dawes. "Salivary flow rates and salivary film thickness in five-year-old children." *Journal of Dental Research* 69.5 (1990):1150-1153.
- [10] C. Dawes, Salivary flow patterns and the health of hard and soft oral tissues, *Journal of american dental association* 139 (suppl.2) (2008) 18S-24S.
- [11] Wolff, M., and I. Kleinberg."oral mucosal wetness in hypo-and normosaliva-tors." *Archives of oral biology* 43.6 (1998):455-462.
- [12] Verma, S., Kaul, M., Rawat, A., et saini, S. (2011). An overview on buccal drug delivery system. *International Journal of Pharmaceutical Sciences and Research*, 2(6), 1303-1321.
- [13] Patel, Viralkumar F., Fang Liu and Marc B. Brown. "Advanced in oral transmucosal drug delivery." *Journal of Controlled Release* 153.2 (2011):106-116.
- [14] Mamatha, Y., selvi, A., Prasanth, V. V., Sipai, M., et Yadav, V. (2012). Buccal drug delivery: a technical approach. *journal of Drug Delivery and Therapeutics*, 2(2).

- [15] Andersen, O., Zweidorff, O.K., Hjelde, T., et Rodland, E. A. (1995). Problems when swallowing tablets. A questionnaire study from general practice.
- [16] Bhyan, B., Jangra, S., Kaur, M., et Singh, H. (2011). Orally fast dissolving films: innovations in formulation and technology. *Int J Pharm Sci Rev Res*, 9,9.
- [17] Yajaman Sudhakar, Ketousetuo Kuotsu, A.K. Bandyopadhyay. "Buccal bioadhesive drug delivery - A promising option for orally less efficient drugs. *Journal of controlled release*, 114(2006), 15-40.
- [18] Nazila Salamat-Miller, Montakarna Chittchang, Thomas P. Johnston. The use of mucoadhesive polymers in buccal drug delivery. *Advanced drug delivery reviews*, 57(2015), 1666-1691.
- [19] N.Vidyasagar, K.MallikarjunaRao, K. Gnanaprakash, A. Divya, A.Sowjanya, M. Gobinath. "A review on buccal drug delivery system". *Journal of Pharmaceutical Research and Development*, 2012.
- [20] Chinna Reddy P, Chaitanya K.S.C., Madhusudan Rao Y. "A review on bioadhesive buccal drug delivery systems: current status of formulation and evaluation methods", *DARU Journal of Pharmaceutical Sciences* Vol. 19, No. 6 2011.
- [21] R. Jagadeeshwar Reddy , Maimuna Anjum and Mohammed Asif Hussain, "A Comprehensive Review on Buccal Drug Delivery System", *American Journal of Advanced Drug Delivery*, 2013.
- [22] N. G. Raghavendra Rao, B. Shravani, Mettu Srikanth Reddy, "Overview on Buccal Drug Delivery Systems", *J. Pharm. Sciences and Research*. Vol.5(4), 2013, 80 - 88
- [23] Jasvir Singh and Pawan Deep, "A REVIEW ARTICLE ON MUCOADHESIVE BUCCAL DRUG DELIVERY SYSTEM", *International journal of pharmaceutical sciences and research*, 2013; Vol. 4(3): 916-927
- [24] Radhakisan, Udhan Ravindra, Vijayalaxmi Chavan, and Nitin Tribhuvan. "MOUTH DISSOLVING FILM AND THEIR PATENT: AN OVERVIEW." *International Research Journal of Pharmacy* 3.
- [25] Bala, R., Pawar, P., Khanna, S., et Arora, S. (2013). Orally dissolving strips: A new approach to oral drug delivery system. *International Journal of Pharmaceutical Investigation*, 3(2), 67.
- [26] Siddiqui, MD Nehal, Garima Garg, and Pramod Kumar Sharma. "A short review on "A novel approach in oral fast dissolving drug delivery system and their patents"." *Advances in Biological Research* 5.6 (2011): 291-303.
- [27] E.M. Hoffmann, A. Breitenbach, J. Breitreutz, *Expert Opinion on Drug Delivery*, March 2011, Vol. 8, No. 3 : Pages 299-316
- [28] Schiraldi et al., US Patent 4,713,243, December 1987
- [29] Raval, K. M. (2013). OVERVIEW ON ORAL STRIP. *Journal of drug discovery and therapeutics*, 1(03).
- [30] Apoorva Mahajan et al, *Der Pharmacia Lettre*, 2011, 3(1):152-165
- [31] Arun Arya et al /*Int.J. ChemTech Res.*2010,2(1)
- [32] Shimoda, H., Taniguchi, K., Nishimura, M., Matsuura, K., Tsukioka, T., Yamashita, H., ... et Itoh, Y. (2009). Preparation of a fast dissolving oral thin film containing dexamethasone: a possible application to antiemesis during cancer chemotherapy. *European journal of pharmaceuticals and biopharmaceutics*, 73(3), 361-365.

- [33] Nishigaki, M., Kawahara, K., Nawa, M., Futamura, M., Nishimura, M., Matsuura, K., ... et Itoh, Y. (2012). Development of fast dissolving oral film containing dexamethasone as an antiemetic medication: Clinical usefulness. *International journal of pharmaceutics*, 424(1), 12-17.
- [34] Dixit, R. P., et Puthli, S. P. (2009). Oral strip technology: Overview and future potential. *Journal of controlled release*, 139(2), 94-107.
- [35] Thin film drug delivery, From Wikipedia, the free encyclopedia
- [36] Morales, Javier O., and Jason T. McConville. "Manufacture and characterization of mucoadhesive buccal films." *European Journal of Pharmaceutics and Biopharmaceutics* 77.2 (2011): 187-199.
- [37] Cremer K., Life cycle management using orally disintegrating dosage forms, International Association for pharmaceutical technology, Issue 01/2005
- [38] Reeta et al., *Journal of Drug Delivery and Therapeutics*; 2012, 2(3): 87-96
- [39] Vollmer et al., Rapid film: Oral Thin Film (OTF) as an Innovative Drug Delivery System and Dosage Form. *Drug Delivery Report*. Spring/Summer 2006.
- [40] R. C. Mashru et al., *Drug Development and Industrial Pharmacy*, 31:25-34, 2005
- [41] Y.I. Muzib, K.S. Kumari, *International Journal of Pharmaceutical Investigation*, 2011, Vol 1, 1
- [42] M. Semalty et al. *International Journal of Pharmaceutical Sciences and Nanotechnology* Volume 1, Issue 2, July-September 2008
- [43] Sane, *Novel Science International Journal of Pharmaceutical Science* (2012), 1(7): 452-456
- [44] Sournac et al., US Patent 20100041703A1, Feb. 2010
- [45] A. B. Bogue et al., EP 2461796 A2, June 2012
- [46] B. Assmussen and J. Moorman EP 1656112 B1, Feb. 2010
- [47] M. Mencherif, EP 2112923 A1, Nov. 2009
- [48] A. Breitenbach and N. Schwier, EP 2486913 A1, Aug 2012
- [49] Fuisz et al., US20120328688A1, Dec 2012
- [50] Panda et al., *Int J Pharm Sci Nanotech*, Vol 5; Issue 2, July-September 2012
- [51] S.L. Patil et al, *IJRRPAS*, 2(3).482-496, 2012
- [52] Sievens-Figueroa, L., Bhakay, A., Jerez-Rozo, J. I., Pandya, N., Romanach, R. J., Michniak-Kohn, B., ... et Dave, R. N. (2012). Preparation and characterization of hydroxypropyl methyl cellulose films containing stable BCS Class II drug nanoparticles for pharmaceutical applications. *International Journal of Pharmaceutics*, 423(2), 496-508.
- [53] Mishra. A., Ramteke.S. "Formulation and Evaluation of Mucoadhesive Buccal Film of Flurbiprofen" *International Journal of PharmTech Research*, Vol.3, No.3, pp 1825-1830, July-Sept 2011
- [54] Perioli, L., Ambrogi, V., Angelici, F., Ricci, M., Giovagnoli, S., Capuccella, M., et Rossi, C. (2004). Development of mucoadhesive patches for buccal administration of ibuprofen. *Journal of controlled release*, 99(1), 73-82.

- [55] Sandeep Karki, Hyeongmin Kim, Seon-Jeong Na, Dohyun Shin, Kanghee Jo, Jaehwi Lee, "Thin films as an emerging platform for drug delivery", *Asian journal of pharmaceutical sciences* 11(2016) 559–574.
- [56] Renukuntla J, Vadlapudi AD, Patel A, et al. Approaches for enhancing oral bioavailability of peptides and proteins. *Int J Pharm* 2013;447:75–93.
- [57] Khairnar GA, Sayyad FJ. Development of buccal drug delivery system based on mucoadhesive polymers. *Int J PharmTech Res* 2010;2:719–735.
- [58] Juluru N. Fast dissolving oral films: a novel drug delivery system. *Int J Pharm Sci Rev Res* 2013;2:108–112.
- [59] Irfan M, Rabel S, Bukhtar Q, et al. Orally disintegrating films: a modern expansion in drug delivery system. *Saudi Pharm J* 2015;2015:1–10.
- [60] Liew et al., *Drug Development and Industrial Pharmacy* 0 (2013): 1-10.
- [61] P. Sakellariou, R.C. Rowe, Interactions in cellulose derivative films for oral drug delivery, *Prog. Polym. Sci.* 20 (1995) 889-942.
- [62] Shweta Kalyan et al /*Int.J. PharmTech Res.*2012,4(2)
- [63] S. Malke et al., *The Internet Journal of Pediatrics and Neonatology.* 2010 Volume 11 Number 2
- [64] Karen et. al., *American Journal PharmTech Research* 2012; 2(3)
- [65] Landová H, Vetchý V, Gajdziok J. Evaluation of the influence of formulation and process variables on mechanical properties of oral mucoadhesive films using multivariate data analysis. *Biomed Res Int* 2014;2014:1–9.
- [66] Smart JD, Kellaway IW, Worthington HEC. An in-vitro investigation of mucosa-adhesive materials for use in controlled drug delivery. *J Pharm Pharmacol* 1984;36:295–299.
- [67] Ludwig A. The use of mucoadhesive polymers in ocular drug delivery. *Adv Drug Deliv Rev* 2005;57:1595–1639.
- [68] J. Guo, Bioadhesive polymer buccal patches for buprenorphine controlled delivery: formulation, in-vitro adhesion and release properties, *Drug Development and Industrial Pharmacy* 20 (1994) 2809–2821.
- [69] D. Chickering, E. Mathiowitz, Definitions, mechanisms, and theories of bioadhesion, in: E. Mathiowitz, D. Chickering, C. Lehr (Eds.), *Bioadhesive Drug Delivery Systems: Fundamentals, Novel Approaches, and Development*, Marcel Dekker, Inc., New York, 1999.
- [70] N.A. Peppas, J.J. Sahlin, Hydrogels as mucoadhesive and bioadhesive materials: a review, *Biomaterials* 17 (1996) 1553–1561.
- [71] B. Derjaguin, V. Smilga, *Adhesion: Fundamentals and Practice*, McLaren, London, 1969.
- [72] A.J. Kinloch, The science of adhesion. I: Surface and interfacial aspects, *Journal of Materials Science* 15 (1980) 2141–2166
- [73] L.L. Hench, E.C. Ethridge, *Biomaterials: An Interfacial Approach*, Academic Press, New York, 1982.
- [74] A. Baszkin, J.E. Proust, P. Monsenego, M.M. Boissonnade, Wettability of polymers by mucin aqueous solutions, *Biorheology* 27 (1990) 503–514.

- [75] S. Prager, The healing process at polymer–polymer interfaces, *Journal of Chemical Physics* 75 (1981) 5194
- [76] H.W. Kammer, Adhesion between polymers. Review, *Acta Polymerica* 34 (1983) 112–118.
- [77] J. Smart, The role of water movement and polymer hydration in mucoadhesion, in: E. Mathiowitz, D. Chickering, C. Lehr (Eds.), *Bioadhesive Drug Delivery Systems: Fundamentals, Novel Approaches, and Development*, Marcel Dekker, Inc, New York, 1999, pp. 11–23.
- [78] A.J. Kinloch, The science of adhesion. Part 1: Surface and interfacial aspects, *Journal of Materials Science* 15 (1980) 2141–2166.
- [79] A.G. Mikos, N.A. Peppas, Systems for controlled release of drugs. V: Bioadhesive systems, *STP Pharma Sciences* 2 (1986) 705–716.
- [80] S. Voitskii, *Autohesion and Adhesion of High Polymers*, Wiley-Interscience, New York, 1963.
- [81] J. Smart, The basics and underlying mechanisms of mucoadhesion, *Advanced Drug Delivery Reviews* 57 (2005) 1556–1568.
- [82] J. Guo, Bioadhesive polymer buccal patches for buprenorphine controlled delivery: formulation, in-vitro adhesion and release properties, *Drug Development and Industrial Pharmacy* 20 (1994) 2809–2821.
- [83] Nitesh S Chauhan et al., *Int. J. Drug Dev. and Res.*, April-June 2012, 4 (2): 408-417
- [84] F. Cilurzo et al. / *European Journal of Pharmaceutics and Biopharmaceutics* 70 (2008) 895-900
- [85] Rotta et al, *Cienc. Tecnol. Aliment.*, Campinas, 31(2): 450-455, abr.-jun. 2011
- [86] Peh, Kok Khiang, and Choy Fun Wong. "Polymeric films as vehicle for buccal delivery: swelling, mechanical, and bioadhesive properties." *J Pharm Pharm Sci* 2.2 (1999): 53-61.
- [87] Kulkarni A.S. et al., *Journal of Current Pharmaceutical Research* 2010; 2(1): 33-35
- [88] Dhagla Ram Choudhary et al /*Int.J. ChemTech Res.*2011,3(2)
- [89] N.L Prasanthi et al, *Der Pharmacia Lettre*, 2011, 3(1): 382-395
- [90] Dhere P.M. et al. /*International Journal Of Pharmacy and Technology*, 2011 3 (4),1572-1585
- [91] Dhanikula et al., *The AAPS Journal* 2004; 6 (3) Article 27
- [92] Murata et al., *Pharmacology and Pharmacy*, 2011, 2, 194-198
- [93] C. Eouani et al., *European Journal of Pharmaceutics and Biopharmaceutics* 52 (2001) 45-55
- [94] Nep and Conway, *Trop J Pharm Res*, August 2011;10 (4): 389
- [95] Boateng et al., *Drug Development and Industrial Pharmacy*, 2012; 38(1): 47-54
- [96] Sievens-Figueroa, L., Pandya, N., Bhakay, A., Keyvan, G., Michniak-Kohn, B., Bilgili, E., et Dave, R. N. (2012). Using USP I and USP IV for Discriminating Dissolution Rates of Nano-and Microparticle-Loaded Pharmaceutical Strip- Films. *AAPS PharmSciTech*, 13(4), 1473-1482.

- [97] V. A. Perumal, T. Govender, D. Lutchman, I. Mackraj, Drug Development and Industrial Pharmacy, 34:1036-1047, 2008.
- [98] Wong CF, Yuen KH, Khiang peh K. An in vitro method for buccal adhesion studies: importance of instrument variables. Int.J.Pharm.1999; 180: 47-57.
- [99] Julie Mariam Joshua, R Hari, Fithal K Jyothish, Saritha A Surendran, Fast Dissolving Oral Thin Films: An Effective Dosage Form for Quick Releases. Int. J. Pharm. Sci. Rev. Res., 38(1), May – June 2016; Article No. 50, Pages: 282-289.
- [100] Prasanna P. Ghodake, Kailas M. Karande, Riyaz Ali Osmani, Rohit R. Bhosale, Bhargav R. Harkare, Birudev B. Kale. Mouth Dissolving Films: Innovative Vehicle for Oral Drug Delivery. International Journal of Pharma Research et Review, Oct 2013; 2(10):41-47.
- [101] Naga Sowjanya Juluru, Fast Dissolving Oral Films: A Review, INTERNATIONAL JOURNAL OF ADVANCES IN PHARMACY, BIOLOGY AND CHEMISTRY, Vol. 2(1), Jan- Mar, 2013.
- [102] Muhammad Hanif, Muhammad Zaman and Vesh Chaurasiya, Polymers used in buccal film: a review , Designed Monomers and Polymers, 2015 ,Vol. 18, No. 2, 105–111.
- [103] Ms. Prakruti M. Amin, Prof. A. B. Gangurde, Ms. Pranali V. Alai, Oral Film Technology: Challenges and Future Scope for Pharmaceutical Industry, International journal of pharmacy et pharmaceutical research, June 2015 Vol.:3, Issue:3.
- [104] Rajni Bala, Pravin Pawar, Sushil Khanna, Sandeep Arora, "Orally dissolving strips: A new approach to oral drug delivery system", International journal of Pharmaceutical Investigation, April 2013, Vol3(2).
- [105] Preis M, Knop K, Breitzkreutz J. Mechanical strength test for orodispersible and buccal films. Int J Pharm 2014;461:22–29.
- [106] Hoffmann EM, Breitenbach A, Breitzkreutz J. Advances in orodispersible films for drug delivery. Expert Opin Drug Deliv 2011;8:299–316.
- [107] Anroop B.Nair, Rachna Kumria, Sree Harsha, Mahesh Attimarad, Bandar E. Al-Dhubiab, Ibrahim A. Alhaider, In vitro techniques to evaluate buccal films, Journal of Controlled Release 166(2013), 10-21.
- [108] Mishra, Renukra, and Avani Amin. "Quick API delivery." (2007).
- [109] U. Siemann, Progr Colloid Polym Sci (2005) 130: 1-14
- [110] Mishra and Avani, PHARMACEUTICAL TECHNOLOGY, 2011, Volume 35, Issue 1, pp. 70-73
- [111] Maniruzzaman, Mohammed, et al. "Hot-Melt Extrusion (HME): From Process to Pharmaceutical Applications." (2012).
- [112] Saini et al., Pharmacologyonline 2: 919-928 (2011)
- [113] Varun Rathi, et al. "A brief review on oral film technology." International Journal 2 (2011).
- [114] Guidance for Industry. Orally Disintegrating Tablets. U.S. Department of Health and Human Services, FDA Center for Drug Evaluation and Research (CDER), 2007.
- [115] G.L. Amidon et al., Pharmaceutical Research, Vol.12, No. 3, 1995

- [116] J.L. Cohen et al., *Pharmaceutical Research*, Vol. 7, No. 10, 1990
- [117] Carli et al., *Ann. Ist. Sup. Sanita'*, Vol. 18, N. 3 (1982), pp. 551-558
- [118] FIP/AAPS Guidelines for Dissolution/In Vitro Release Testing of Novel/Special Dosage Forms AA.VV. *Dissolution Technologies*, 2003
- [119] Brown, C. K., Friedel, H. D., Barker, A. R., Buhse, L. F., Keitel, S., Cecil, T. L., ... et Shah, V. P. (2011). FIP/AAPS joint workshop report: dissolution/in vitro release testing of novel/special dosage forms. *AAPS PharmSciTech*, 12(2), 782-794.
- [120] *Dissolution Toolkit Procedures for Mechanical Calibration and Performance Verification Test Apparatus 1 and Apparatus 2, Version 2.0*, March 2010, www.usp.org
- [121] 711 Dissolution, Revision Bulletin Official February 1, 2012, The United States Pharmacopeial Convention
- [122] S. M. A. Frost, *Introduction to the Validation of a Dissolution Apparatus*, *Dissolution Technologies* | FEBRUARY 2004
- [123] AA. VV., *In Vitro Dissolution Testing for Solid Oral Dosage Forms Technical Brief 2010 Volume 5*, Particle science Drug development services.
- [124] Kukura et al., *The AAPS Journal* 2006; 7 (4) Article 83
- [125] J. Kukura et al., *International Journal of Pharmaceutics* 279 (2004) 9-17
- [126] E. Kaunisto et al., *AIChE Journal* October 2011 Vol. 57, No. 10
- [127] G. Bai et al., *Journal of Pharmaceutical sciences*, vol. 96, no. 9, 2007
- [128] G. Bai et P. Armenante, *Journal of Pharmaceutical sciences*, vol. 98, no. 4, 2008
- [129] K. Asare-Addo et al. / *Colloids and Surfaces B: Biointerfaces* 81 (2010) 452-460
- [130] M. Kakhi, *International Journal of Pharmaceutics* 376 (2009) 22-40
- [131] M. Kakhi, *European Journal of Pharmaceutical Sciences* 37 (2009) 531-544
- [132] Fotaki, *Flow-Through Cell Apparatus (USP Apparatus 4): Operation and Features*, *Dissolution Technologies* | NOVEMBER 2011
- [133] Gao, Zongming. "In Vitro Dissolution Testing with Flow-Through Method: A Technical Note." *AAPS PharmSciTech* 10.4 (2009): 1401-1405
- [134] Shah VP, Maibach HI, *Topical Drug Bioavailability, Bioequivalence, and Penetration*, 1, Springer, USA, 1993, 369-391.
- [135] Kaur J, Singh G, Saini S, *Aspects Related To the Solid Lipid Nanoparticles Delivery through the Topical Route*, *Journal of Drug Delivery and Therapeutics*, 2(6), 2012, 111-116
- [136] Gisby J, Bryant J, *Efficacy of a new cream formulation of mupirocin: Comparison with oral and topical agents in Experimental skin infections*, *Antimicrobial agents and chemotherapy*, 44(2), 2000, 255- 260.
- [137] Ashni Verma, Sukhdev Singh, Rupinder Kaur, Upendra K. Jain, *Topical Gels as Drug Delivery Systems: A Review*, *Int. J. Pharm. Sci. Rev. Res.*, 23(2), Nov – Dec 2013; n. 60, 374-382
- [138] B.W. Barry, *Dermatological Formulations: Percutaneous Absorption*, Marcel Dekker, New York, NY, 1983.

- [139] H. Schaeffer, A. Zesch and G. Stüttgen, *Skin Permeability*, Springer Verlag, Berlin, 1982.
- [140] G.L. Flynn, Topical drug absorption and topical pharmaceutical systems, in: G.S. Banker and C.T. Rhodes (Eds.), *Modern Pharmaceutics*, Marcel Dekker, New York, 1979, pp. 263-327.
- [141] Richard H. Guy and Jonathan Hadgraft, TRANSDERMAL DRUG DELIVERY: A PERSPECTIVE, *Journal of Controlled Release*, 4 (1987) 237-251
- [142] Sherwood L, *Human Physiology: From cells to systems*, 6, Thomson Brooks, Stamford, 2007.
- [143] Noble WC, *The skin microflora and microbial skin disease*, University of Cambridge, Cambridge.
- [144] Mackie RM, *Clinical dermatology*, 5, Oxford University Press, Oxford, 2002.
- [145] Maghraby GM, Barry BW, Williams AC, Liposomes and skin: From drug delivery to model membranes, *European Journal of Pharmaceutical Sciences*, 34(4), 2008, 203-222.
- [146] Nino M, Calabro G, Santoianni P, Topical delivery of active principles: The field of dermatological research, *Dermatology online Journal*, 16(1), 2010, 4.
- [147] Khurram Rehman and Mohd Hanif Zulfakar, Recent advances in gel technologies for topical and transdermal drug delivery, *Drug Development and Industrial Pharmacy*, 2014; 40(4): 433-440.
- [148] Kamal Saroha, Sarabjeet Singh, Ajay Aggarwal and Sanju Nanda, TRANSDERMAL GELS - AN ALTERNATIVE VEHICLE FOR DRUG DELIVERY, INTERNATIONAL JOURNAL OF PHARMACEUTICAL, CHEMICAL AND BIOLOGICAL SCIENCES, 2013, 3(3), 495-503.
- [149] Tahsildar Apeksha Ganesh, Shinkar Dattatraya Manohar, Saudagar Ravindra Bhanudas, HYDROGEL-A NOVEL TECHNIQUE FOR PREPARTION OF TOPICAL GEL, WORLD JOURNAL OF PHARMACY AND PHARMACEUTICAL SCIENCES, Volume 2, Issue 6, 4520-4541.
- [150] Anita Devi, Ujjwal Nautiyal, Sarabjot kaur, Komal, Hydrogels: a smart drug delivery device, *Asian Pac. J. Health Sci.*, 2014; 1(4S): 92-105
- [151] Allan SH. Hydrogels for biomedical applications. *Adv Drug Deliv Rev* 2012;64:18-23.
- [152] Otto W, Drahoslav L. Hydrophilic gels in biologic use. *Nature* 1960; 185:117-18.
- [153] Shapiro YE. Structure and dynamics of hydrogels and organogels: an NMR spectroscopy approach. *Prog Polym Sci* 2011;36: 1184-253.
- [154] Peppas NA, Bures P, Leobandung W, Ichikawa H. Hydrogels in pharmaceutical formulation. *Eur J Pharm Biopharm* 2000;50:27-46.
- [155] Gupta A, Mishra AK, Singh AK, et al. Formulation and evaluation of topical gel of diclofenac sodium using different polymers. *Drug Invention Today* 2010;5:250-3.
- [156] Martinez RMA, Julian LVG, Maria MdB, et al. Rheological behavior of gels and meloxicam release. *Int J Pharm* 2007;333: 17-23.
- [157] Davide C, Patrick D, Marco R, et al. Semisynthetic resorbable materials from hyaluronan esterification. *Biomaterial* 1998;19: 2101-27.

- [158] Ansel HC, Popovich NG Loyd VA, Pharmaceutical Dosage Forms and Drug Delivery Systems, 9, B. I. Publications, New Delhi, 2005, 407-408.
- [159] Jain NK, Misra AN, Controlled and Novel Drug Delivery, 1, CBS Publishers and Distributors, New Delhi, 2005.
- [160] Vyas SP, Khar K, Controlled Drug Delivery, 1, Vallabh Prakashan, New Delhi, 2002.
- [161] Pandey S, Badola A, Bhatt GK, Kothiyal P, An Overview on Transdermal Drug Delivery System, Int Journal of Phr and Chemical Sciences, 2(3), 2013, 1171-1180.
- [162] Thakar B, Soni S, Patel, T, Pandya V, Bharadia PD, Transdermal drug delivery systems: A Review, International Journal of Universal Pharmacy and Life Sciences, 2(2), 2012, 374-393.
- [163] Jalwal P, Jangra A, Dahiya L, Sangwan Y, Saroha R, A review on transdermal patches, The Pharma Research, 3, 2010, 139-149
- [164] Balasubramanian R, Gopal RV, Design and In Silico Analysis Of Ring-Amonosubstituted Chalcones As Potential Anti-Inflammatory Agents, Bulletin of Pharmaceutical Research, 2(2), 2012, 70-77.
- [165] Patel H, Patel U, Bhimani B, Daslaniya D, Patel G, Transdermal drug delivery system as prominent dosage forms for the highly lipophilic drugs, Int journal of Phr Research and bio science, 1(3), 2012, 42-65.
- [166] Finnin BC, Morgan TM, Transdermal penetration enhancers: applications, limitations, and potential, Journal of pharmaceutical sciences, 88(10), 1999, 955-958.
- [167] Sandhu P, Bilandi A, Kataria S, Middha A, Transdermal drug delivery system (patches), Application in present scenario, International Journal of Research in Pharmacy and Chemistry, 1(4), 2011, 1139-1151.
- [168] Kumar SKP, Bhowmik D, Jaiswal J, Transdermal Iontophoresis Technique-A Potential Emerging Drug Delivery System, Indian Journal of Research in Pharmacy and Biotechnology, 1(1), 2013, 38-45.
- [169] Prabhakar D, Sreekanth J, Jayaveera KN, Transdermal Drug Delivery Patches: A Review. Journal of Drug Delivery and Therapeutics, 3(4), 2013, 213-221.
- [170] Bhowmik D, Pusupoleti KR, Duraivel S, Kumar KS, Recent Approaches in Transdermal Drug Delivery System, The pharma-Innovation Journal, 2(3), 2013, 99-108.
- [171] Barry BW, Dermatological Formulations: Percutaneous Absorption, 1, Marcel Dekker Inc, New York, 1983, 49-94.
- [172] Pfister WR, Hsieh DS, Permeation enhancers compatible with transdermal drug delivery system Part I Selection and formulation considerations, Medical Device Technology, 1(5), 1990a, 48-55.
- [173] Finnin BC, Morgan TM, Transdermal penetration enhancers: application limitations and potential, Journal of Pharmaceutical Sciences, 88(10), 1999, 955-958.
- [174] Liron Z, Cohen S, Percutaneous absorption of alkanolic acids II: Application of regular solution theory, Journal of Pharmaceutical Sciences, 73(4), 1984, 538-542.
- [175] Songkro S, An overview of skin penetration enhancers: penetration enhancing activity, skin irritation potential and mechanism of action, Songklanakarin J Sci Technol, 31(3), 2010, 299-321.

- [176] Lambert WJ, Kudla RJ, Holland JM, Curry JT, A biodegradable transdermal penetration enhancer based on N-(2-hydroxyethyl)-2-pyrrolidone I. Synthesis and characterization, *International Journal of Pharmaceutics*, 95(1), 1993, 181-192.
- [177] Hori M, Satoh S, Maibach HI, Classification of percutaneous penetration enhancers: A conceptual diagram, *Journal of Pharmacy and Pharmacology*, 42(1), 1990, 71-72.
- [178] Swarbrick J, Boylan JC, *Encyclopedia of pharmaceutical Technology*, 3, Marcel Dekker, New York, 1995, 449-493.
- [179] Pfister WR, Hsieh DS, Permeation enhancers compatible with transdermal drug delivery system. Part I. Selection and formulation considerations, *Medical Device Technology*, 1(5), 1989, 48-55.
- [180] Pfister WR, Hsieh DS, Permeation enhancers compatible with transdermal drug delivery system. Part II. System design considerations, *Medical Device Technology*, 1(6), 1990, 28-33.
- [181] Smith W, Maibach EW, *Percutaneous Penetration Enhancers*, 2, CRC Press, Florida, 1995, 5-20.
- [182] Asbill CS, Michniak BB, Percutaneous penetration enhancers: local versus transdermal activity, *Pharmaceutical Science et Technology Today*, 3(1), 2000, 36-41.
- [183] Osborne DW, Henke JJ, Skin penetration enhancers cited in the technical literature, *Pharmaceutical Technology*, 21(11), 1997, 58-66.
- [184] Peppas N.A.; *Hydrogels in Medicine and Pharmacy*, Vol. 1. Fundamentals, CRC Press, Boca Raton, FL, 1986, 180
- [185] Malcolm B. Huglin, M.B.Z., Swelling properties of copolymeric hydrogels prepared by gamma irradiation. 1986. p.457-475.
- [186] Sperinde, J.J. and L.G. Griffith, Control and Prediction of Gelation Kinetics in Enzymatically Cross- Linked Poly(ethylene glycol) Hydrogels. 2000. p. 5476-5480.
- [187] Peppas N.A., Crystallization of polyvinyl alcohol-water film by slows dehydration.
- [188] Carter SJ, Disperse system In: Cooper and Gunn's Tutorial Pharmacy, 6, CBS Publishers and Distributors, New Delhi, 2000, 68-72.
- [189] Lieberman HA, Rieger MM, Banker GS, *Pharmaceutical dosage form: Disperse system*, 2, Marcel Dekker, New York, 2005, 399-421.
- [190] Byrne ME, Park K, Pappas NA. A review on molecular imprinting within hydrogels. *Advanced Drug Delivery Reviews* 54.2002; 149–161.
- [191] Khaled MH, Majd M. Tayeb, Osama MF, Aladdin A, Motaz S. Preparation and Evaluation of Ketorolac Tromethamine Hydrogel. 2013;20(2):269-274.
- [192] Peppas NA, Bures P, Leobandung W, Ichikawa H. Hydrogels in pharmaceutical formulation. *Eur J Pharm Biopharm* 2000;50:27–46.
- [193] Naryan B, Jonathan G, Miqin Z. Chitosan-based hydrogels for controlled, localized drug delivery. *Adv Drug Deliv Rev* 2010;62: 83–99.
- [194] Saima Amin, Saeid Rajabnezhad and Kanchan Kohli, Hydrogels as potential drug delivery systems. *Scientific Research and Essay*. Nov 2009; 3:1175- 1183.
- [195] Satish CS, Satish KP, Shivakumar. A review on hydrogel as controlled drug delivery system. Synthesis, crosslinking, water and drug transport mechanism. *International Journal of Pharmaceutical Sciences*. 2006; 60(2):133-140.

- [196] Lin, C.C. and Metters A.T., Hydrogels in controlled release formulations: Networkdesign and mathematical modeling, *Advanced Drug Delivery Reviews*, 2006, 58(12-13), p. 1379-1408.
- [197] Bindu Sri. M, Ashok. V and Arkendu chatterjee, As A Review on Hydrogels as Drug Delivery in the Pharmaceutical Field, *INTERNATIONAL JOURNAL OF PHARMACEUTICAL AND CHEMICAL SCIENCES*, Vol. 1 (2) Apr – Jun 2012
- [198] Johannes P. Venter, Douw G. Muller, Jeanetta du Plessis, Colleen Goosen, A comparative study of an in situ adapted diffusion cell and an in vitro Franz diffusion cell method for transdermal absorption of doxylamine, *European Journal of Pharmaceutical Sciences* 13 (2001) 169–177.
- [199] Shiow-Fern Ng, Jennifer J. Rouse, Francis D. Sanderson, Victor Meidan, and Gillian M. Eccleston, Validation of a Static Franz Diffusion Cell System for In Vitro Permeation Studies, *AAPS PharmSciTech*, Vol. 11, No. 3, September 2010.
- [200] Joseph Scalfani, James Nightingale, Puchun Liu and Tamie Kurihara-Bergstrom, Flow-Through system effects on in vitro analysis of transdermal system, *Pharmaceutical research*, vol.10, N.10,1993.
- [201] Pil H. Lee, Robert Conradi, Veerabahu Shanmugasundaram, Development of an in silico model for human skin permeation based on a Franz cell skin permeability assay, *Bioorganic et Medicinal Chemistry Letters* 20 (2010) 69–73.
- [202] Yuliya Levintova, Fotios M. Plakogiannis, Robert A. Bellantone, An improved in vitro method for measuring skin permeability that controls excess hydration of skin using modified Franz diffusion cells, *International Journal of Pharmaceutics* 419 (2011) 96-106.
- [203] Matthew Alexander Miller and Gerald Kasting, A measurement of the unstirred aqueous boundary layer in a Franz diffusion cell, *Pharmaceutical Development and Technology*, 2012; 17(6): 705–711.
- [204] David R. Friend, In vitro skin permeation techniques, *Journal of controlled release*, 18 (1992) 235-248.
- [205] Bartek MJ, LaBudde JA, Maibach HI (1972) Skin permeability in vivo: comparison in rat, rabbit, pig and man. *J Invest Dermatol* 58:114–123.
- [206] Maibach HI (1975) *Animal models in dermatology*. Churchill-Livingstone, Edinburgh.
- [207] Wester RC, Maibach HI (1976) Relationship of total dose and percutaneous absorption in Rhesus monkey and man. *J Invest Dermatol*. 67:518–520.
- [208] Chow C, Chow AYK, Downie RH, Buttar HS (1978) Percutaneous absorption of hexachlorophene in rats, guinea pigs and pigs. *Toxicology* 9:147–154.
- [209] Wester RC, Noonan PK (1980) Relevance of animal models for percutaneous absorption. *Int J Pharm* 7:99–110.
- [210] Itoh T, Xia J, Magavi R, Nishihata T, Rytting JH (1990) Use of shed snake skin as a membrane for in vitro percutaneous penetration studies. *Pharm Res* 7:1042–1047.
- [211] Roberts ME, Mueller KR (1990) Comparisons of in vitro nitroglycerin (TNG) flux across Yucatan pig, hairless mouse and human skins. *Pharm Res* 7:673–676.
- [212] Sato K, Sugibayashi K, Morimoto Y (1991) Species differences in percutaneous absorption of nicorandil. *J Pharm Sci* 80:104–107.

- [213] Lin SY, Hou SJ, Hsu THS, Yeh FL (1992) Comparisons of different animal skins with human skin in drug percutaneous absorption studies. *Meth Find Exp Clin Pharmacol* 14:645–654.
- [214] Harada K, Murakami T, Kawasaki E, Hagashi Y, Yamamoto S, Yata N (1993) In vitro skin permeability to salicylic acid of human, rodent and shed snake skin. *J Pharm Pharmacol* 45:414–418.
- [215] Young CD, Wu JR, Tsou TL (1998) Fabrication and characteristics of polyHEMA artificial skin with improved tensile properties. *J Mem Sci.* 146:83–93
- [216] Berger A, Tanzella U, Machens HG, Liebau J (2000) Use of Integra in burn wounds and unstable scars. *Chirurgia* 71:558–563.
- [217] Machens HG, Berger AC, Mailaender P (2000) Bioartificial skin. *Cells Tissue Organs* 167:88–94.
- [218] Mizunuma M, Yanai A, Seno H, Hirabayashi S (2000) Experience in repair utilizing artificial skin for exposed bone surfaces. *Eur J Plast Surg* 23:305–308.
- [219] Moss GP, Gullick DR, Cox PA, Alexander C, Ingram MJ, Smart JD, Pugh WJ (2006) Design, synthesis and characterisation of captopril prodrugs for enhanced percutaneous absorption. *J Pharm Pharmacol* 58:167–177.
- [220] Stott PW, Williams AC, Barry BW (2001) Mechanistic study into the enhanced transdermal permeation of a model β -blocker, propranolol, by fatty acids: a melting point depression effect. *Int J Pharm* 219:161–176
- [221] Esposito E, Zanella C, Cortesi R, Menegatti E, Nastruzzi C (1998) Influence of liposomal formulation parameters on the in vitro absorption of methyl nicotinate. *Int J Pharm* 172:255–260.
- [222] Minghetti P, Casiraghi A, Cilurzo F, Montanari L, Marazzi M, Falcone L, Donati V (1999) Comparison of different membranes with cultures of keratinocytes from man for percutaneous absorption of nitroglycerine. *J Pharm Pharmacol* 51:673–678.
- [223] Franz TJ (1975) On the relevance of in vitro data. *J Invest Dermatol* 64:190–195.
- [224] Martin A, Swarbrick J, Cammarata A (1983) *Physical pharmacy*, 3rd edn. Lea et Febinger, Philadelphia.
- [225] Anissimov YG, Roberts MS (1999) Diffusion modelling of percutaneous absorption kinetics. 1. Effects of flow rate, receptor sampling rate and viable epidermal resistance for a constant donor concentration. *J Pharm Sci* 88:1201–1209.
- [226] Roberts MS, Cross SE (1999) A physiological pharmacokinetic model for solute disposition in tissues below a topical application site. *Pharm Res* 9:1392–1398.
- [227] Bronaugh RL, Maibach HI (1999) *Percutaneous absorption*, 3rd edn. Marcel Dekker, Inc. CRC Press, New York.
- [228] Morris, E. R.; Nishinari, K.; Rinaudo, M. *Food Hydrocolloid* 2012, 28, 373–411.
- [229] Ferris, C. J.; Gilmore, K. J.; Wallace, G. G.; in het Panhuis, M. *Soft Matter* 2013, 9, 3705–3711.
- [230] Doner, L. W.; Douds, D. D. *Carbohydr. Res.* 1995, 273, 225–233.
- [231] CP Kelco Product Information: KELCOGEL gellan gum; 2007.
- [232] Smith, A. M.; Shelton, R. M.; Perrie, Y.; Harris, J. J. J. *Biomater. Appl.* 2007, 22, 241–254.

- [233] Oliveira, J. M.; Caridade, S. G.; Oliveira, J. T.; Sousa, R. A.; Mano, J. F. J. *Tissue Eng. Regen. Med.* 2011, 5, 97–107.
- [234] Oliveira, J. T.; Santos, T. C.; Martins, L.; Picciochi, R.; Marques, A. P.; Castro, A. G.; Neves, N. M.; Mano, J. F.; Reis, R. L. *Tissue Eng. Part A* 2010, 16, 343–353.
- [235] Ferris, C. J.; Gilmore, K. J.; Beirne, S.; McCallum, D.; Wallace, G. G.; in het Panhuis, M. *Biomater. Sci.* 2013, 1, 224–232.
- [236] Sun, W.; Darling, A.; Starly, B.; Nam, J. *Biotechnol. Appl. Biochem.* 2004, 39, 29–47.
- [237] Doner, L. W. *Carbohydr. Polym.* 1997, 32, 245–247.
- [238] Camelin, I.; Lacroix, C.; Paquin, C.; Prévost, H.; Cachon, R.; Divies, C. *Biotechnol. Prog.* 1993, 9, 291–297.
- [239] O'Neill, M. A.; Selvendran, R. R.; Morris, V. J. *Carbohydr. Res.* 1983, 124, 123–133.
- [240] Chandrasekaran, R., Radha, A., Thailambal, V.G., 1992. Roles of potassium ions acetyl and L-glycerol groups in native gellan double helix: an X-ray study. *Carbohydrate Research* 224, 1–17.
- [241] Bengt Wittgren, and Anette Larsson. "Investigation of critical polymer properties for polymer release and swelling of HPMC matrix tablets." *European Journal of Pharmaceutical Sciences* 36.2 (2009): 297-309.
- [242] Larsson, Mikael, et al. "The influence of HPMC substitution pattern on solidstate properties." *Carbohydrate Polymers* 82.4 (2010): 1074-1081.
- [243] Sasa, Baumgartner, et al. "Analysis of surface properties of cellulose ethers and drug release from their matrix tablets." *European journal of pharmaceutical sciences* 27.4 (2006): 375-383.
- [244] L.S. Cheong Wan et al, *International Journal of Pharmaceutics* 116 (1995),159-168
- [245] Kavanagh, Nicole, and Owen I. Corrigan. "Swelling and erosion properties of hydroxypropylmethylcellulose (Hypromellose) matrices-influence of agitation rate and dissolution medium composition." *International journal of pharmaceutics* 279.1 (2004): 141-152.
- [246] S. Chirico, A. Dalmoro, G. Lamberti, G. Russo, G. Titomanlio, *Journal of Controlled Release* 122 (2007) 181-188.
- [247] J. Pajander et al. , *International Journal of Pharmaceutics* 427 (2012) 345-353.
- [248] J. Tritt-Goc, N. Pislewski , *Journal of Controlled Release* 80 (2002) 79-86
- [249] Gafourian, Taravat, et al. "A drug release study from hydroxypropylmethylcellulose (HPMC) matrices using QSPR modeling." *Journal of pharmaceutical sciences* 96.12 (2007): 3334-3351
- [250] Ioannis, G., Harvey, L. M., et McNeil, B. (2005). Scleroglucan. In *Biopolymers Online*.Wiley-VCH Verlag GmbH et Co. KGaA. <http://dx.doi.org/10.1002/3527600035.bpol6002>
- [251] Palleschi, A., Bocchinfuso, G., Coviello, T., et Alhaique, F. (2005). Molecular dynamics investigations of the polysaccharide scleroglucan: first study on the triple helix structure. *Carbohydrate Research*, 340, 2154–2162.

- [252] Guo, B., Stokke, B. T., et Elgsaeter, A. (1996). Swelling of Sclerolucan gels in binary DMSO water solvents. *Colloids and Surfaces A: Physicochemical and Engineering Aspects*, 112, 185–191.
- [253] Coviello, T., Palleschi, A., Grassi, M., Matricardi, P., Bocchinfuso, G., et Alhaique, F. (2005). Scleroglucan: a versatile polysaccharide for modified drug delivery. *Molecules*, 10, 6–33.
- [254] Corrente, F., Matricardi, P., Paolicelli, P., Tita, B., Vitali, F., et Casadei, M. A. (2009). Physical Carboxymethylscleroglucan/Calcium ion hydrogels as modified drug delivery systems in topical formulations. *Molecules*, 14, 2684–2698.
- [255] Vignaranta, S. C., Franco, N. J., Daraio, M. E., Figueroa, L. I. C., et Farina, J. I. (2007). Sclerotium rolfsii scleroglucan: The promising behavior of a natural polysaccharide as a drug delivery vehicle: suspension stabilizer and emulsifier. *International Journal of Biological Macromolecules*, 41, 314–323.
- [256] Corrente, F., Abu Amara, H. M., Pacelli, S., Paolicelli, P., et Casadei, M. A. (2013). Novel injectable and in situ cross-linkable hydrogels of dextran methacrylate and scleroglucan derivatives: preparation and characterization. *Carbohydrate Polymers*, 92, 1033–1039.
- [257] Cerreto, A., Corrente, F., Botta, B., Pacelli, S., Paolicelli, P., Mannina, L., et Casadei, M. A. (2013). NMR investigation of carboxymethyl scleroglucan. *International Journal of Polymer Analysis and Characterization*, 18, 587–595.
- [258] Corrente, F., Paolicelli, P., Matricardi, P., Tita, B., Vitali, F., et Casadei, M. A. (2012). Novel pH-sensitive physical hydrogels of carboxymethyl scleroglucan. *Journal of Pharmaceutical Sciences*, 101, 256–267.
- [259] Touitou, E.; Alhaique, F.; Riccieri, F. M.; Riccioni, G.; Santucci, E. Scleroglucan sustained release oral preparations. Part I. In vitro experiments. *Drug Des. Deliv.* 1989, 5, 141.
- [260] M. E. Brewster, T. Loftsson, "Cyclodextrins as pharmaceutical solubilizers", *ScienceDirect*, 59, (2007), pp. 645-666;
- [261] S.S. Jambhekar, P. Breen, "Cyclodextrins in pharmaceutical formulations I, structure and physicochemical properties, formation of complexes, and types of complex", *Drug Delivery Today*, 21, (2016), pp. 356-362;
- [262] S.S. Jambhekar, P. Breen, "Cyclodextrins in pharmaceutical formulations II, solubilization, binding constant, and complexation efficiency", *Drug Delivery Today*, 21, (2016), pp. 363-368;
- [263] www.cyclodextrin.com, "Hydroxypropylbetacyclodextrin". An enabling Technology for challenging pharmaceutical formulations", (2009), pp. 36-39;
- [264] Adrover, A., Capparucci, C., De Filippis, P., Pedacchia, A., Scarsella, M., "Devices and method for testing pharmaceutical thin films and strips", Italian patent application N: RM2013A000163, filed on March 18th, 2013
- [265] Arnstein, P. M. (2012). Evolution of Topical NSAIDs in the Guidelines for Treatment of Osteoarthritis in Elderly Patients. *Drugs et Aging*, 29, 523–531.
- [266] Touitou, E. (2002). Drug delivery across the skin. *Expert Opinion on Biological Therapy*, 2, 723–733.
- [267] Caló, E., et Khutoryanskiy, V. V. (2015). Biomedical applications of hydrogels: A review of patents and commercial products. *European Polymer Journal*, 65, 252–267.

- [268] Trookman, N. S., et Rizer, R. L. (2011). Randomized Controlled Trial of Desonlde Hydrogel 0.05% versus Desonide Ointment 0.05% in the Treatment of Mild-to-moderate Atopic Dermatitis. *Journal of Clinical and Aesthetic Dermatology*, 4, 34–38.
- [269] Hoare, T. R., et Kohane, D. S. (2008). Hydrogels in drug delivery. Progress and challenges. *Polymer*, 49, 1993–2007.
- [270] Olejnik, A., Goscianska, J., et Nowak, I. (2012). Active compounds release from semisolid dosage forms. *Journal of Pharmaceutical Sciences*, 101(11),4032–4045.
- [271] Pobudkowska, A., et Domanska, U. (2014). Study of pH-dependent drugs solubility in water. *Chemical Industry et Chemical Engineering Quarterly*, 20, 115–126.
- [272] Moraes, L. A., Lerner, F. E., Moraes, M. E., Moraes, M. O., Corso, G., et De Nucci, G.(1999). Fluconazole Bioequivalence Study: Quantification by Tandem Mass Spectrometry. *Therapeutic Drug Monitoring*, 21, 200–207.
- [273] Gonzalo-Lumbreras, R., Santos-Montes, A., Garcia-Moreno, E., et Izquierdo Hornillos, R. (1997). High-Performance Liquid Chromatographic Separation of Corticoid Alcohols and Their Derivatives: A Hydrolysis Study Including Application to Pharmaceuticals. *Journal of Chromatographic Science*,35, 439–445.
- [274] Hayduk, W., et Laudie, H. (1974). Prediction of diffusion coefficients for non electrolytes in dilute aqueous solutions. *AIChE Journal*, 20, 611–615.
- [275] Adrover, A., Giona, M., Grassi, M., Lapasin, R., et Pricl, S. (1996). Controlled release of theophylline from water-swollen scleroglucan matrices. *Journal of Membrane Science*, 113, 7–20.
- [276] Singh, M., Lumpkin, J. A., et Rosenblatt, J. (1994). Mathematical modeling of drug release from hydrogel matrices via a diffusion coupled with desorption mechanism. *Journal of Controlled Release*, 32, 17–25.
- [277] Draize, J. H., Woodard, G., et Calvery, H. O. (1944). Methods for the study of irritation and toxicity of substances applied topically to the skin and mucous membrane. *Journal of Pharmacology and Experimental Therapeutics*, 82, 377–390.
- [278] Ng, S. F., Rouse, J., Sanderson, D., et Eccleston, G. (2010). A comparative study of transmembrane diffusion and permeation of ibuprofen across synthetic membranes using Franz diffusion cells. *Pharmaceutics*, 2, 209–223.
- [279] Coviello, T., Grassi, M., Lapasin, R., Marino, A., et Alhaique, F. (2003). Scleroglucan/borax: characterization of a novel hydrogel system suitable for drug delivery. *Biomaterials*, 24, 2789–2798.
- [280] Grassi, M., Colombo, I., Lapasin, R., et Pricl, S. (2001). Experimental determination of the theophylline diffusion coefficient in swollen sodium-alginate membranes. *Journal of Controlled Release*, 76, 93–105.
- [281] Coviello, T., Grassi, M., Rambone, G., et Alhaique, F. (2001). A crosslinked system from Scleroglucan derivative: preparation and characterization. *Biomaterials*,22, 1899–1909.
- [282] De Caro, V.; Giandalia, G.; Siragusa, M.G.; Sutura, F.M.; Giannola, L.I. New prospective in treatment of Parkinson’s disease: Studies on permeation of ropinirole through buccal mucosa. *Int. J. Pharm.* 2012, 429, 78–83.
- [283] Campisi, G.; Giannola, L.I.; Florena, A.M.; De Caro, V.; Schumacher, A.; Götttsche, T.; Paderni, C.; Wolff, A. Bioavailability in vivo of naltrexone following transbuccal administration by an electronically-controlled intraoral device: A trial on pigs. *J. Control. Release* 2010, 145, 214–220.

- [284] Giannola, L.I.; De Caro, V.; Giandalia, G.; Siragusa, M.G.; Campisi, G.; Wolff, A. Current status in buccal drug delivery. *Pharm. Technol. Eur.* 2008, 20, 32–39.
- [285] Zhang, H.; Zhang, J.; Streisand, J.B. Oral Mucosal Drug Delivery Clinical Pharmacokinetics and Therapeutic Applications. *Clin. Pharmacokinet.* 2002, 41, 661–680.
- [286] Madhav, N.V.S.; Shakya, A.K.; Shakya, P.; Singh, K. Orotransmucosal drug delivery systems: A review. *J. Control. Release* 2009, 140, 2–11.
- [287] Nibha, K.P. An Overview on: Sublingual Route for Systemic Drug Delivery. *Int. J. Res. Pharma. Biomed. Sci* 2012, 3, 913–923.
- [288] Coneac, G., Vlaia, v., Olariu, I., Mut, A. M., Anghel, D. F., Ilie, C., Popoiu, C., Lupuleasa, D., Vlaia, L., Development and Evaluation of New Microemulsion-Based Hydrogel Formulations for Topical Delivery of Fluconazole, *AAPS Pharm-SciTech*, Gennaio 2015, vol.16, n.4, p.889-904.
- [289] A. Adrover , A. Pedacchia, S. Petralito and R. Spera, *Chemical Engineering Research and Design* 95, 173-178 (2015)
- [290] A. Adrover , M. Nobili, *Chemical Engineering Research and Design* 98, 188-211 (2015)
- [291] J. Siepmann, N.A. Peppas, Modeling of drug release from delivery systems based on hydroxypropyl methylcellulose (HPMC), *Advanced Drug Delivery Reviews* 48 (2001) 139-157.
- [292] J.Siepmann et al./*International Journal of Pharmaceutics*165(1998)191-200.
- [293] Siepmann, J. "Mathematical modeling of bioerodible, polymeric drug delivery systems." *Advanced Drug Delivery Reviews* 48.2(2001): 229-24.
- [294] Papanu, D.S Soane, A.T. Bell and D.W. Hess,1989,Transport Models for swelling and dissolution of thin polymer films,*Journal of Applied Polymer Sciences*,Vol.38,859-885.
- [295] Adrover, A., Nobili, M., Release kinetics from oral thin films: theory and experiments, *Chemical Engineering Research and Design*, 2015, vol.98, p.188-201
- [296] Yih-O Tu,A. C. Ouano,1977,Model for the Kinematics of Polymer Dissolution
- [297] Vivek V.,Ranade and Ramesh A. Mashelkar,1995, Convective Diffusion from a dissolving Polymeric Particle,*AIChE journal* ,Vol.41,No.3
- [298] Dixit, R.P.; Puthli, S.P. Oral strip technology: Overview and future potential. *J. Control Release*, 2009, 139(2), 94-10.
- [299] Suresh, B.; Rajender, K. Mittapalli.; Ramesh Gannu.; Madhusudan, Rao Y. Oral dispersible tablets: An overview. *Asian. J. Pharm.*, 2008, 2(1), 2-11.
- [300] Barnhart, S.D.; Sloboda, M.S. Dissolvable films the future of dissolvable films. *Drug Dev. Tech.*, 2007, 1, 34- 35.
- [301] Guidance for Industry: Orally Disintegrating Tablets, Center for Drug Evaluation and Research (Centre for Drug Evaluation and Research, CDER) US FDA, Dec. 2008.
- [302] Barnhart, S.D.; Sloboda, M.S. Dissolvable films the future of dissolvable films. *Drug Dev. Tech.*, 2007, 1, 34-35.
- [303] Renuka, M.; Avaniamin. *Pharm. Technol.*, 2009, 33(2), 48- 56.
- [304] Ito, A.; Sugihara, M. *Chem. Pharm. Bull*, 1996, 44 (11), 2132-2136.

- [305] Chang, R.K.; Guo, X.; Burnside, B.A.; Couch, R.A. *Pharma. Tech.*, 2000, 24(6), 52-58.
- [306] Kuchekar, B.S.; Arumugam, V. *Indian J. Pharm. Edu.*, 2001, 35, 150.
- [307] Swedberg, K.; Cleland, J.; Dargie, H.; Drexler, H.; Follath, F.; Komajda, M.; Tavazzi, L.; Smiseth, O.A.; Gavazzi, A.; Haverich, A.; et al. Guidelines for the diagnosis and treatment of chronic heart failure: Executive summary (update 2005). *Eur. Heart J.* 2005, 26, 1115–1140
- [308] Berthod, A.; Carda-Broch, S.; Garcia-Alvarez-Coque, M.C. Hydrophobicity of ionizable compounds. A theoretical study and measurements of diuretic octanol-water partition coefficients by countercurrent chromatography. *Anal. Chem.* 1999, 71, 879–888
- [309] Devarakonda, B.; Otto, D.P.; Judefeind, A.; Hill, R.A.; de Villiers, M.M. Effect of pH on the solubility and release of furosemide from polyamidoamine (PAMAM) dendrimer complexes. *Int. J. Pharm.* 2007, 345, 142–153.
- [310] Granero, G.E.; Longhi, M.R.; Mora, M.J.; Junginger, H.E.; Midha, K.K.; Shah, V.P.; Stavchansky, S.; Dressman, J.B.; Barends, D.M. Biowaiver Monographs for Immediate Release Solid Oral Dosage Forms: Furosemide. *J. Pharm. Sci.* 2010, 99, 2544–2556.
- [311] Censi, R.; Di Martino, P. Polymorph impact on the bioavailability and stability of poorly soluble drugs. *Molecules* 2015, 20, 18759–18776
- [312] Nidhi, K.; Indrajeet, S.; Khushboo, M.; Gauri, K.; Sen, D.J. Hydrotropy: A promising tool for solubility enhancement: A review. *Int. J. Drug Dev. Res.* 2011, 3, 26–33.
- [313] Harriss, B.I.; Vella-Zarb, L.; Wilson, C.; Evans, I.R. Furosemide cocrystals: Structures, hydrogen bonding, and implications for properties. *Cryst. Growth Des.* 2014, 14, 783–791.
- [314] Siahi-Shadbad, M.R.; Ghanbarzadeh, S.; Barzegar-Jalali, M.; Valizadeh, H.; Taherpoor, A.; Mohammadi, G.; Barzegar-Jalali, A.; Adibkia, K. Development and Characterization of Solid Dispersion for Dissolution Improvement of Furosemide by Cogrounding Method. *Adv. Pharm. Bull.* 2014, 4, 391–399.
- [315] Zvonar, A.; Berginc, K.; Kristl, A.; Gašperlin, M. Microencapsulation of self-microemulsifying system: Improving solubility and permeability of furosemide. *Int. J. Pharm.* 2010, 388, 151–158.
- [316] Garnero, C.; Chattah, A.K.; Longhi, M. Improving furosemide polymorphs properties through supramolecular complexes of α -cyclodextrin. *J. Pharm. Biomed. Anal.* 2014, 95, 139–145.
- [317] Dixit, R.P.; Puthli, S.P. Oral strip technology: Overview and future potential. *J. Control. Release* 2009, 139, 94–107.
- [318] Chandra, A.; Arya, A.; Chandra, A.; Sharma, V.; Pathak, K. Fast Dissolving Oral Films: An Innovative Drug Delivery System and Dosage Form. *Int. J. ChemTech Res.* 2010, 2, 576–583.
- [319] Sudhakar, Y.; Kuotsu, K.; Bandyopadhyay, A.K. Buccal bioadhesive drug delivery - A promising option for orally less efficient drugs. *J. Control. Release* 2006, 114, 15–40.
- [320] Llabot, J.; Manzo, R.; Allemandi, D. Double-Layered Mucoadhesive Tablets Containing Nystatin. *AAPS PharmSciTech* 2002, 3, e22.

- [321] Abruzzo, A.; Bigucci, F.; Cerchiara, T.; Cruciani, F.; Vitali, B.; Luppi, B. Mucoadhesive chitosan/gelatin films for buccal delivery of propranolol hydrochloride. *Carbohydr. Polym.* 2012, 87, 581–588.
- [322] Mizrahi, B.; Domb, A.J. Mucoadhesive Polymers for Delivery of Drugs to the Oral Cavity. *Recent Pat. Drug Deliv. Formul.* 2008, 2, 108–119.
- [323] Matsuda, Y.; Tatsumi, E. Physicochemical characterization of furosemide modifications. *Int. J. Pharm.* 1990, 60, 11–26.
- [324] Latosinska, J.N.; Latosinska, M.; Medycki, W.; Osuchowicz, J. Molecular dynamics of solid furosemide (4-chloro-2-furfurylamino-5-sulfamoyl-benzoic acid) studied by NMR and DFT methods. *Chem. Phys. Lett.* 2006, 430, 127–132.
- [325] Karkhile VG, Karmarkar RR and Sontakke MA (2010). Formulation and evaluation of floating tablets of furosemide. *Int. J. Pharm. Res. Dev.*, 1: 1-9.
- [326] Vemula VR, Lagishetty V and Lingala S (2010). Solubility enhancement techniques. *Int. J. Pharm. Sci. Rev. Res.*, 5: 41-51.
- [327] Craig DQM (2002). The mechanisms of drug release from solid dispersions in water-soluble polymers. *Int. J. Pharm.*, 31: 131-144.
- [328] Sekiguchi K and Obi N (1961). Studies on absorption of eutectic mixture-I: A comparison of the behavior of eutectic mixture of sulfathiazole and that of ordinary sulfathiazole in man. *Chem. Pharm. Bull.*, 9: 866-872.
- [329] Jain P, Goel A, Sharma S and Parmar M (2010). Solubility enhancement techniques with special emphasis on hydrotropy. *Int. J. Pharm. Prof. Res.*, 1: 34-45.
- [330] Ahire BR, Rane BR, Bakliwal SR and Pawar SP (2010). Solubility enhancement of poorly water soluble drug by solid dispersion techniques. *Int. J. Pharm. Tech. Res.*, 2: 2007-2015.
- [331] Uekama K, Fujinaga T, Hirayama F, Otagiri M and Yamasaki M (1982). Inclusion complexations of steroid hormones with cyclodextrins in water and in solid phase. *Int. J. Pharm.*, 10: 1-15.
- [332] Sapkal NP, Kilor VA, Bhusari KP and Daud AS (2007). Evaluation of some methods for preparing gliclazide- β -cyclodextrin inclusion complexes. *Trop. J. Pharm. Res.*, 6: 833-840.
- [333] S. Karki, H. Kim, S.-J. Na, D. Shin, K. Jo, J. Lee, Thin films as an emerging platform for drug delivery, *Asian J. Pharm. Sci.* 11 (2016) 559–574.
- [334] A.F. Borges, C. Silva, J.F. Coelho, S. Simoes, Oral films: Current status and future perspectives I-Galenical development and quality attributes, *J. Control. Release* 206 (2015) 1–19.
- [335] V.D. Prajapati, G.K. Jani, B.S. Zala, T.A. Khutliwala, An insight into the emerging exopolysaccharide gellan gum as a novel polymer. *Carbohydr. Polym.* 93 (2013) 670-678.
- [336] T. Osmalek, A. Froelich, S. Tasarek, Application of gellan gum in pharmacy and medicine, *Int. J. Pharm.* 466 (2014) 328-340.
- [337] P.G. Leóna, A.M. Rojas, Gellan gum films as carriers of l-(+)-ascorbic acid, *Food Res. Int.* 40 (2007) 565–575.
- [338] L. Yang, A.T. Paulson, Mechanical and water vapour barrier properties of edible gellan films, *Food Res. Int.* 33 (2000) 563-570.

- [339] L. Yang, A.T. Paulson, M.T. Nickerson, Mechanical and physical properties of calcium-treated gellan films, *Food Res. Int.* 43 (2010) 1439–1443.
- [340] Y.C. Wei, C.H. Cheng, Y.C. Ho, M.L. Tsai, F.L. Mi. Active gellan gum/purple sweet potato composite films capable of monitoring pH variations. *Food Hydrocoll.* 69 (2017) 491-502.
- [341] M.W. Lee, H.J. Chen, S.W. Tsao, Preparation, characterization and biological properties of gellan gum films with 1-ethyl-3-(3-dimethylaminopropyl) carbodiimide cross-linker, *Carbohydrate Polymers* 82 (2010) 920–926.
- [342] N.A. Ismail, S.F. Mohamad, M.A. Ibrahim, K.A. Mat Amin, Evaluation of Gellan Gum film containing virgin coconut oil for transparent dressing materials, *Advances in Biomaterials* 2014 (2014) 1-12.
- [343] S.J. Chang, S.M. Kuo, W.T. Liu, C.C.G. Niu, M.W. Lee, C.S. Wu, 2010. Gellan gum films for effective guided bone regeneration, *J Medical and Biological Engineering* 30 (2010) 99–103.
- [344] V.A. Perumal, T. Govender, D. Lutchman, I. Mackraj, Investigating a new approach to film casting for enhanced drug content uniformity in polymeric films, *Drug Dev. Ind. Pharm.* 34 (2008) 1036–1047.
- [345] S. Qi, J.G. Moffat, Z. Yang, Early stage phase separation in pharmaceutical solid dispersion thin films under high humidity: improved spatial understanding using probe-based thermal and spectroscopic nanocharacterization methods. *Mol. Pharm.* 10 (2013) 918-30.
- [346] Y.C. Ng, Z. Yang, W.J. McAuley, S. Qi, Stabilisation of amorphous drugs under high humidity using pharmaceutical thin films, *Eur. J. Pharm. Biopharm.* 84 (2013) 555–565.
- [347] V.A. Perumala, D. Lutchmanb, I. Mackrajc, T. Govendera, Formulation of monolayered films with drug and polymers of opposing solubilities, *Int. J. Pharm.* 358 (2008) 184–191.
- [348] U.S. Kestur, L.S. Taylor, Role of polymer chemistry in influencing crystal growth rates from amorphous felodipine, *Cryst. Eng. Comm.* 12 (2010) 2390–2397.
- [349] A. Gupta, S. Garg, R.K. Khar, Measurement of bioadhesion strength of mucoadhesive buccal tablet: design of an in vitro assembly, *Ind. Drugs* 30 (1993) 152–155.
- [350] Y.-C. Huang, T.-Z. Wang, T.-J. Liu, C. Tiu, Operating window of solution casting. II. Non-Newtonian fluids, *J. Appl. Polym. Sci.* 132 (2015) 41411.
- [351] R. Krampe, J.C. Visser, H.W. Frijlink, J. Breikreutz, H.J. Woerdenbag, M. Preis, Oromucosal film preparations: points to consider for patient centricity and manufacturing processes, *Expert Opin. Drug Deliv.* 13 (2016) 493-506.
- [352] U. Siemann, Solvent cast technology -a versatile tool for thin film production, *Prog. Colloid Polym. Sci.* 130 (2005) 1–14.
- [353] European Pharmacopoeia Commission. Oromucosal Preparations. In: *European Pharmacopoeia*. 8th ed. Strasbourg: European Directorate for the Quality of Medicines (EDQM); 2014.
- [354] A.K. Dash, W.F. Elmquist, Fluconazole. *Analytical Profiles of Drug Substances and Excipients*, H.G. Brittain Ed., 27, 85-88.
- [355] S. Seif, L. Franzen, M. Windbergs, Overcoming drug crystallization in electrospun fibers—Elucidating key parameters and developing strategies for drug delivery. *Int. J. Pharm.* 478 (2015) 390-397.

- [356] M. Alhijja, J. Bouman, N. Wellner, P. Belton, S. Qi, Creating drug solubilization compartments via phase separation in multicomponent buccal patches prepared by direct Hot Melt Extrusion-Injection Molding, *Mol. Pharmaceutics* 12 (2015) 4349-4362.
- [357] Gaetano Lambertia, Ivan Galdi, Anna Angela Barba, Controlled release from hydrogel-based solid matrices. A model accounting for water up-take, swelling and erosion, *International Journal of Pharmaceutics* 407 (2011) 78–86.
- [358] Luciana Lisa Lao, Nicholas A. Peppas, Freddy Yin Chiang Boey, Subbu S. Venkattraman, Modeling of drug release from bulk-degrading polymers, *International Journal of Pharmaceutics* 418 (2011) 28-41.
- [359] Iosif-Daniel Rosca, Jean-Maurice Vergnaud, Evaluation of the characteristics of oral dosage forms with release controlled by erosion, *Computers in Biology and Medicine* 38 (2008) 668 – 675.
- [360] Sharad S. Darandale, Pradeep R. Vavian, Design of a gastroretentive mucoadhesive dosage form of furosemide for controlled release, *Acta Pharmaceutica Sinica B* 2012;2(5):509–517.
- [361] Nurten Ozdemir and Sefika Ordu, Improvement of Dissolution Properties of Furosemide by Complexation with β -cyclodextrin, *Drug Development and Industrial Pharmacy*, 24(1), 19-25 (1998).
- [362] R.M. AMIN KREAZ, E.Y. ABU-EIDA, I. EROS and M. KATA, Freeze-Dried Complexes of Furosemide with β -Cyclodextrin Derivatives, *Journal of Inclusion Phenomena and Macrocyclic Chemistry* 34: 39–48, 1999.
- [363] Muhammad U. Ghor, Gidion Ginting, Alan M. Smith, Barbara R. Conway, Simultaneous quantification of drug release and erosion from hypromellose hydrophilic matrices, *International Journal of Pharmaceutics* 465 (2014) 405–412.
- [364] Cheong-Weon Cho, Jun-Shik Choi, Sang-Chul Shin, Controlled release of furosemide from the ethylene-vinyl acetate matrix, *International Journal of Pharmaceutics* 299 (2005) 127–133.

Papers

- Adrover A., Casadei M. A., Paolicelli P., Petralito S., Varani G. (2016). *Swelling and drug release from oral thin films (OTFs)*. In: Volume 1736: VIII International Conference on “Times of Polymers and Composites” From Aerospace to Nanotechnology. vol. 1736, AIP publishing, ISBN: 9780735413900, Naples, Italy, 19–23 June 2016, doi: 10.1063/1.4949660.
- Patrizia Paolicelli, Gabriele Varani, Settimio Pacelli, Elisa Ogliani, Martina Nardoni, Stefania Petralito, Alessandra Adrover, Maria Antonietta Casadei, *Design and characterization of a biocompatible physical hydrogel based on scleroglucan for topical drug delivery*, Carbohydrate Polymers 174 (2017) 960–969.
- Patrizia Paolicelli, Gabriele Varani, Settimio Pacelli, Martina Nardoni, Stefania Petralito, Alessandra Adrover, Maria Antonietta Casadei, *Manufacturing and characterization of polymeric thin films for buccal delivery of drugs*. 10th world meetings on pharmaceuticals, biopharmaceuticals and pharmaceutical technology, Glasgow, April 2016.
- Patrizia Paolicelli, Stefania Petralito, Gabriele Varani, Martina Nardoni, Settimio Pacelli, Jacopo Tirillo', Cecilia Bartuli, Stefania Cesa, Maria Antonietta Casadei, Alessandra Adrover, *Drug crystallization in glycerol-plasticized gellan gum thin films*, not yet submitted.
- Settimio Pacelli, Patrizia Paolicelli, Michele Avitabile, Gabriele Varani, Stefania Petralito, Laura Di Muzio, Stefania Cesa, Jacopo Tirillo', Cecilia Bartuli, Martina Nardoni, Stefania Petralito, Alessandra Adrover, Maria Antonietta Casadei, *Design of a tunable nanocomposite double network hydrogel based on gellan gum for drug delivery application*, not yet submitted.

Acknowledgments

Partirò da tutte le persone che ho conosciuto in questi tre anni... e vorrei farlo in ordine cronologico. Sarà così come rivivere questi tre anni intensi e bellissimi.

E allora non posso che iniziare dalla mia prof. *Alessandra Adrover*. Neanche ci conoscevamo. Mi ha dato la possibilità di fare questa esperienza. Mi ha dato fiducia. La ringrazio per avermi dato questa possibilità, di essermi stata sempre vicina. La ringrazio perché senza di lei non ce l'avrei fatta. Senza chi mi spronava sempre e comunque, che non mi nascondeva mai niente e se c'era da rimproverare lo faceva. Grazie perché mi ha insegnato tanto. Oltre che dal punto professionale come persona. Era bello poter parlare con lei di tutto. Quando entravo nel suo studio sapevo che non era solo film, gel o articoli. Si poteva parlare di Roma di sport di qualsiasi cosa.

Ringrazio la professoressa *Casadei, Paolicelli e Petralito* che mi hanno accolto nel loro lab. Sono stato benissimo. Un lab in cui si lavorava, in cui si mangiava rideva scherzava. Ero sempre allegro lì. E questo per me era una cosa splendida, bellissima. Grazie per avermi dato la possibilità di usare tanti strumenti e di avermi insegnato tante cose, che neanche sapevo esistessero.

Grazie a *Settimio*. I primi giorni in lab insieme non si sa la quantità di cose che mi hai imparato. E mi stavi vicino. Io che non sapevo niente di quel mondo. Come si usa la pipetta? Sempre presente. E poi non so cosa è successo. Da amici a migliori amici. Così. Naturale. Non so bene come. E quante corse a villa torlonia insieme al direttore. Poi sei partito, ma non ci siamo mai spenti. Per me sei forte. Uno dei più forti in assoluto. Spero un giorno di arrivare ad essere un ricercatore bravo come te. Io lo so che dall'altra parte del mondo batte il cuore di una persona che si farebbe tagliare un braccio per me. Grazie per non avermi mai abbandonato. Sono triste...fammi chiama Settimio!

E poi ci sei te. *Giuseppe* non ci sono parole per descriverlo. E' difficile. Quando uno è tanto in tutto come fai. La forza senza la superbia e l'intelligenza senza la saccenza. La persona più pura e vera che abbia mai conosciuto. Così come sei. Un pagnottone pure te. Che bello stare insieme in lab. Non c'era un momento in cui non mi facevi ridere. Quando mancavi te il lab era spento. Bastava la tua presenza per mettere allegri tutti. Ti vedevo sempre come un esempio, come un fratello maggiore da imitare. Spero di rivederti presto. Di riabbracciarti e ridere ancora insieme. Solo il meglio per te.

E come avrei fatto se il primo giorno non ci fosse stato *Pierluigi* ad insegnarmi a fare i film. Certo c'era pure Claudia ma destino ha voluto fossi proprio te. Sono contento di averti conosciuto e spero di vederci ancora. Perché con te mi divertivo parecchio. Tenevi sempre banco con le tue storie e le tue avventure. I tuoi giudizi solenni e le tue osservazioni. Con te era tutta un'altra storia. Le risate e gli scherzi non mancavano. Sapevi sempre stare al gioco. Io te l'ho detto. Per me sei una persona fantastica. Non cambiare mai. Rimani sempre così. Perché sei splendido così. Solare e spensierato.

Quanto ci sarebbe da dire *Elisa*. Ci vorrebbe una tesi solo per te. Me e te era un discorso aparte. Te forse sei quella che mi ha cambiato di più. Come dici sempre...eri entrato che eri un pagnottone fagotto... adesso sei un ottacchiotto dottorato. Un po' più forte. Eh sì. Forse te mi ha aiutato ad uscire dal guscio più di tutti. Sei una persona splendida. In assoluto. Una pagnotta. Sei una persona altruista è dire poco. Il cuore più grande e luminoso del firmamento. Con il telescopio si vede bene lo sai?. Pensi agli altri e a te non ce pensi mai praticamente. E quanto mi hai aiutato in lab. Doveva essere il contrario. Ma eri sempre te che aiutavi me. Una passione per quello che fai sorprendente. Fortissima. Come montavi la cella di Franz te io non sono mai riuscito a farlo. Sono sicuro che arriverai ad essere una delle migliori ricercatrici del mondo. Perché sei forte. Tanto. E meriti di arrivare ai massimi livelli. Tei tempe la più baba.

Quando penso ai film non può non venirmi in mente *Giulia Carella*. Siamo entrati insieme ed abbiamo imparato insieme. Insieme a fare i film. Per un anno. Un anno in cui abbiamo fatto tanto. Non se sa quanti film. Grazie perché come dicevi te mi sgrullavi ogni tanto . E quante volte abbiamo litigato? Un botto. E quante risate ci siamo fatti insieme? Tantissime. Grazie per per avermi capito tante volte. Come mi tenevi testa te nessuno.

Grazie a *Cinzia ed Ilaria*. In particolare Cinzia il tuo buffet ha vinto il titolo come miglior buffet di laurea. Non c'è mai stata storia se proprio vuoi saperlo. Il top. C'era il buffet di Cinzia e poi tutti gli altri. Una vittoria schiacciante e clamorosa. Ancora me lo sogno guarda. Quei cornetti e quei tramezzini erano una cosa assurda per quanto erano boni. Che buffet cavolo!

Grazie Al professor *Tirillo'* e alla dottoressa *Veca* per la pazienza avuta nell' ospitarmi nel loro lab e per il tempo che mi hanno dedicato. E' stato un onore ed un privilegio poter lavorare con voi. Vi ringrazio della vostra disponibilità e della vostra gentilezza.

Ringrazio tanto *Claudio Capparucci*. Nel laboratorietto quanto ne abbiamo dette su dzeko ahah. Quanti rilasci. E quanti consigli. Grazie per avermi insegnato ad usare il dispositivo e tutto il circuito e per tutti i consigli prima della partenza in norvegia. Per ogni cosa sempre disponibile e gentile. Ti ringrazio per avermi guidato e aiutato durante tutto il percorso.

Come avrei fatto questi tre anni senza mia sorellina *Martina*. Quanti ricordi con te. Quanti caffè. Quanti periodi buii abbiamo passato insieme e ci siamo sostenuti a vicenda. E insieme a Glasgow è stato il viaggio piu' pazzo di mai. Gabry dai vatte a lavà daje un po'. Gabry dai rifai la valigia...ahahaha. Quando avevo bisogno c'eri sempre e so che ci sarai sempre. Anche ad Oslo non mi hai mai abbandonato. Non c'è bisogno di dimostrare niente. Io lo sapevo che andavo bene così come sono. Mia sorella mi voleva bene comunque vada. Grazie per essere stata la mia ancora.

E chi l'avrebbe detto che avrei conosciuto la mia migliore amica in lab. Questo sei per me *Valentina*. Quanti rilasci zi. Quante iniezioni all'HPLZI. Pure il sabato andavamo insieme. La mia spalla destra. Quanto tempo mi hai ascoltato. Io tra 2000 problemi. Tante cose , tanti pensieri. Ma zia stava li. E io pure non potevo che stare li. Perché sapevo che potevo contare su di te. E quella colonna e quel DD. Quei rilasci a zig-zag. Abbiamo pianto e riso insieme. E perché ci veniva una cosa ogni mille. Ma alla fine ce l'abbiamo fatta. Grazie per avermi sempre incoraggiato, perché so che ormai faccio parte della tua vita.

Poi c'era un pandino che faceva caramelle da schiacciare a forma di cubetto. Splendido *Michele*, una sensibilità di un livello stratosferico. Una bontà pazzesca. Un cuoco perfetto. Ancora mi sogno la frittata con i funghi e la verza con la salsiccia. Ti ho visto piangere, sorridere, gioire e soffrire. Ma ti vorrei sempre felice. Perché questo che meriti. E so che te vorresti lo stesso per me. Mi hai sostenuto quando per me sarebbe stato piu' facile lasciarsi andare. Sei il meglio che si può trovare in una persona. Non aver mai paura. Quella porchetta insieme ad ariccia dopo un giro imprevisto a zagarolo mi ha fatto sentire come fratelli.

La barbie girl del laboratorio non potevo scordarla. *Barabara* col suo trolley la riconoscevi prima dal rumore delle rotelle. Ogni tanto quando vedevo un trolley da lontano ti associavo sempre ahah. Avevi la capacità di essere sempre tranquilla e serena. In realtà un po' mascheravi quello che avevi dentro. Grazie perché abbiamo condiviso momenti divertenti insieme.

Nel lab ad un certo punto è entrata un' onda rossa. Così eri *Valeria Chiaula*. La tesi piu' folle di sempre. 4 mesi per fare tutto. So uscito fori de testa co te ahah. Però forse anche per questo è stato divertente fare la tesi insieme. Grazie per tutte le crostatine e i giorni di perdizione al reometro. Me ce so pure addormentato li ahah. Grazie per essere stata sempre sorridente e solare.

Grazie a *Marta Dionisi* . quante discussioni tra politica, rilasci, modelli e piastre. Ti ho sempre stimato per il tuo carattere forte. Anche se qualche volta non ci prendevamo. So però che anche te mi stimavi parecchio e ti ringrazio di questo.

Grazie a *Francesco Pardo*. Ci conosciamo dal primo anno. Tanti esami insieme. Tante cene e tante uscite. Grazie per la tua simpatia. Facevi sembrare tutto facile. Una calma olimpionica a tutti gli esami. Non so come facevi. Poi il dottorato insieme. Ad anacapri ce semo divertiti un sacco. Tra cene, sigari, funivie e foto, non c'era un momento che non ridevamo insieme. Certo ogni tanto siamo pure andati al convegno ahaha. Spero di continuare a vederci e frequentarci. Sei grande.

Grazie a *Laura Quintarelli*. Sei stata l'unica ingegnera a lavorar con me alla fine. Hai condiviso il millifluidico ed i rilasci con me. Sei stata forte con la tesi. Non hai sbagliato un colpo. Farai bene ovunque andrai perchè ho conosciuto una persona davvero brava.

Grazie ad *Alessandra*. Grazie per aver organizzato tutti quegli aperitivi e cene. Quelli si che mi facevano felici ahah. Anche se come ho detto posso dare un terzo posto al tuo buffet. Dopo medusa mi dispiace. Cinzia era irraggiungibile. Grazie per tutte le chiacchierate davanti alle macchinette.

Grazie *Flavia* . Guarda mi dispiace essermi scordato tutti i tuoi compleanni e per aver perso il tuo numero (in Norvegia ho cambiato numero). Il fatto è che sei nata a Luglio. Come me e quelli di luglio non me li ricordo mai, compreso il mio. Grazie per la tua dolcezza. Cavolo ogni volta che mi rivedevi eri contenta davvero. Lo vedevo dal volto. Non mi scorderò la faccia che hai fatto quando sono tornato da Oslo. Mi è rimasta impressa. Grazie per avermi voluto bene. Pure io te ne voglio . Ricordati che sei forte e finalmente è finita. Meriti un applauso per la forza che hai dimostrato. Mai come nel tuo caso. Tanto studio, tanta sofferenza e adesso festeggiamenti assoluti.

La migliore di tutti era però *Emily*. Te e valeria eravate sempre a 2000. Inarrestabili e instancabili. Sei una persona semplice umile e simpatica. Sono contento di averti conosciuto, davvero. Così come tutta la tua famiglia, fantastici. Mi facevi ridere quando mi chiamavi gabrio ahah, mi faceva pensare ad una macchinina. Mi mettevi allegria. Era bello stare con te in lab anche se ci siamo conosciuti quando la pompa da vuoto è esplosa. Un inizio col botto.

Una volta mi hai chiesto di ottimizzare la quantità di fotoiniziatore. *Giulia De angelis* io te l'avevo fatta. Sto aspettando che la usi ahah. Mesà che non verrà mai usata. Peccato era un modello fico tutto sommato. Grazie per la tua dolcezza e la tua comprensione. Mi infondevi tranquillità. Sei una bravissima ragazza e ti ringrazio di tutte le merendine insieme nella 12. Con i succhi di frutta che non ti mancavano mai. Anche io sono un appassionato di ACE.

Imma te stavi sopra a fare liposomi quindi non abbiamo mai lavorato insieme ma quell'Italia-Germania la ricorderò sempre. Con tutta quella frutta affettata. Grazie per il passaggio in macchina quella sera dai granai. Avrei perso il treno. Nonostante tutti gli scherzi e le battute so che mi volevi bene. Grazie di tutto.

Grazie a *Valeria Fortunati*. Se c'è una persona che aveva una forza di volontà di ferro eri te. Non hai mollato nonostante tutto girava male e ad un certo punto volevi buttare

tutto. Davvero la piu' determinata di tutti. Non ti sei mai arresa. Sono contento di averti conosciuto. Ti ringrazio di avermi coinvolto nel tuo lavoro. Questo vuol dire che mi stimavi. Sono sicuro che andrai alla grande. A te non ti ferma niente.

Poi c'era una beads girl. *Grazie Valeria de Carlo*. Anche se insieme abbiamo misurato solo lo spessore delle beads con lo spessimetro (cavolo era difficile, erano minuscole) era piacevole stare in tua compagnia. Mi dispiace aver legato con te solo alla fine. Fino a quando ero un punto interrogativo per te.

Una sera mi ritrovo una marea di chiamate perse ahaha. Vero *Silvia*? Ricordati che la valvola zigrinata dell'HPLZI va chiusa. Sempre impeccabile. Ma quella valvola quella sera ti ha fatto smaltire ahah.

Come non posso ringraziare la juventina piu' accanita di sempre. *Chiara Odri* mi dispiace per il tuo errore sportivo ma ti ringrazio per tutte le risate che ci siamo fatti insieme, per tue le discussioni su arbitri, rigori, roma, juve e tutti i litigi via wa con bomber. Mi hai fatto divertire. Spero che continueremo ad essere ancora amici. Grazie per esserti ricordato di me anche quando non c'ero. Ho sentito che mi volevi bene davvero.

Poco prima di partire ho avuto modo di conoscere *Mariangela*, per fortuna. Perché le tue parole mi hanno aiutato tanto. Te che hai avuto la pazienza di ascoltarmi e capirmi. Grazie per tutte le volte che sei venuta a trovarmi in lab. Grazie per avermi salvato a pasqua con le tue parole e durante il periodo norvegese. Non mi scordo quello che hai fatto per me. Auguro a te e tuo marito il meglio. Vedi col cuore veramente.

Ma la farmacista per eccellenza rimane sempre *Laura*. Quante te ne ho dette. Ahah invece quello che penso è che sei la piu' brava con cui ho lavorato. Davvero, ormai lo posso dire. Te sei forte. Un'intelligenza superiore. Sei felice di fare ricerca. Ti diverti in lab. Non ti pesa fare quello che fai. Ti ho visto sempre felice di entrare in laboratorio. Sono sicuro che andrai alla grande e farai un percorso 100 volte migliore del mio che non ho mai avuto la passione che hai tu e l'intelligenza che hai te. Per non parlare di te persona. Un'amica vera. Sempre vicina a chi ne ha bisogno. Grazie per avermi considerato sempre un grande dottorando anche se non lo sono affatto. Grazie per la stima che hai nei miei confronti e sappi che io ne ho la stessa per te. Davvero. Per qualsiasi cosa ci sono. Anche se ormai i periodi buii sei brava a superarli dasola.

Dicono che il reometro non funziona piu'. Te credo dico io. Lo usava medusa che faceva picassi e van gogh a tutto spiano. *Federica* apparte tutti gli scherzi e le battute grazie per tutte le risate che ci siamo fatti insieme. Stavi sempre al gioco. Sei grande. E sei forte. Lo so. Un po' come la tua amica. Ovunque andrai saprai cavartela e fare bene. E dimostrare quanto sei brava.

E stando su a fare liposomi ci siamo conosciuti poco. Poi sono partito. Ma per quel che ho visto sei in linea con le tue amiche *Manuel*. Un lavoratore instancabile. Sempre perfetto. Ma in fondo, alla festa di laurea, ho visto pure in te un pizzico di follia. In quel video con la farmacista ubriaca ce la semo tagliata. Pure te stavi un pezzo avanti. Mi hai fatto ride.

Ultimamente invece ho scoperto che se voglio fare discorsi scientifici devo cercare *Simone*. Pure sulla solubilizzazione dello zucchero finisce che parliamo di costanti e parametri termodinamici. Mi raccomando con la tesi. Io ci conto su di te. Sempre concentrato e vedrai che andrai forte. Una delle persone piu' curiose che ho conosciuto. Con il mouse del computer piu' grande mai visto. Sei pronto per la nasa. Grazie per avermi intrattenuto con decine di discorsi scientifici. Vai così.

Grazie ad *Alessia Mirone*. Anche se pochi giorni, mi sono bastati per scoprire una

persona seria ma allo stesso tempo divertente, a cui piace scherzare e giocare. Forse si eri da 13 e non da 254 ahah. Quell'aperitivo ha aperto il mondo ad un'alessia diversa, quella che non ti aspetti. Quella parte del carattere fantastica che è uscita fuori e che fa di te il top.

Grazie ad *Alessia Sangiuliano*. Sei tante cose messe insieme. Forse perché convivono in te piu' sfumature diverse. E allora ci ho visto una persona che sa scherzare, solare, divertente, a volte spensierata e a volte super affaccendata. Un carattere estroverso e particolare. Nonostante a volte ti sminuisci secondo me sei in gamba e vali molto di piu' di quanto pensi. Basta che credi in te stessa perché in fondo so che hai un cuore grande e una grande forza. E vedrai che non c'è niente che non puoi fare. Grazie perché comunque in tua compagnia sono stato bene e mi hai fatto sorridere.

Grazie a tizi. *Tiziana* è difficile da descrivere. Non si apre facilmente. Eppure una volta che sboccia tira fuori tutto quello che da fuori neanche si riesce ad immaginare. Introspettiva. Sa vedere oltre. Capisce prima degli altri quello che è difficile da comprendere e forse davvero sai vedere quello che gli altri non riescono a vedere. Forse perché hai una sensibilità superiore. Se i sensi sono 5 ed il sesto tipico dell'uomo è l'emozione, te ti sei evoluta perché ne hai sette. Grazie di tutti gli aperitivi. Anche se bisogna stare sempre attenti a dare buca sennò è finita ahah!

Chiara N., Chiara P., Jordan, Giulio, Marta P., Marta S. purtroppo ci siamo conosciuti tardi. Mi sarebbe piaciuto conoscervi bene anche a voi e perdermi nei test con voi ancora una volta. Ma è andata così. Vi auguro di finire gli studi nel modo migliore possibile e di seguire e realizzare tutti i vostri sogni. Tutti quelli per cui pensate vale la pena di addannarsi e che vi facciano sentire vivi.

L'esperienza ad Oslo è stata indimenticabile. Mi ha dato tanto sotto tutti i punti di vista. Dal punto di vista professionale, ma anche e soprattutto come crescita personale. Forse lì sono diventato piu' uomo. Una vera e propria tempra norvegese. E non si sa quante persone ho conosciuto.

Voglio ringraziare *Flavio* e *Giuseppe* i miei co-worker italiani che condividevano l'ufficio della little italy ad Oslo. Grazie perché con voi potevo riassaporare quello spirito e quel modo di fare tipico italiano e a mio parere unico nel modo. Ci siamo sostenuti a vicenda. Tra neve (tanta neve mamma mia) e freddo riuscivamo comunque a divertirci tra laboratorio, palestra, pub e musei. Flavio grazie perché te forse sei quello che piu' mi ha sostenuto nell'approccio a quel mondo che per me è stato difficile. Senza il tuo aiuto all'inizio forse non ce l'avrei fatta. Avevi capito come mi sentivo. Come stavo. Ed era bello ridere e scherzare con te. Con te mi sentivo a mio agio. Mi mettevi allegria nel gelo norvegese. Grazie di esserci stato vecchio scarpone. Nonostante la distanza Roma-Padova, spero di vederci ancora e di continuare questa amicizia.

Poi dopo pasqua ci siamo conosciuti meglio, zio peppe. Tra alti e bassi tra Stoccolma ed Helsinki abbiamo condiviso momenti bellissimi e litigate in mensa clamorose ahah. Però hai una grande forza ed un grande spirito di adattamento. Ti stimo tanto per questo. E una grande passione per la chimica farmaceutica. Quante discussioni per le rivalità tra ingegneri, chimici e farmacisti ahah. Ti ringrazio per tutte le cene a casa e tutti i piatti che hai preparato. Devo ammettere che la pizza fatta al tuo compleanno era veramente buona. Spero di vederci ancora anche con te.

I want to thank my supervisor *Ingunn Tho*. Thank you for welcoming me. I didn't miss anything. Thank you for giving me this chance. Staying with you was so beautiful. I learned so much from this experience that it was really important. Thank you for your comprehension and kindness. You are really a fantastic teacher.

Thanks to *Ivar Groove*. I knew that for any problem I could ask you. And every

time I did not find something or I needed something you were always ready and willing to help me. Thank you so much for all the help you gave me in the laboratory.

Thank you so much to *Bente* and *Tove* for helping me with the DSC measurement. It was nice to exchange opinions with you.

Thanks to *Krister*, *Julia* and *Anca*. You are fantastic and prepared Ph.D. Really. It was nice to meet you and exchange different opinions and ways of thinking about the most disparate topics. Not just scientific. Thanks for all the Friday meetings where it was nice to socialize with you in front of a good and tasty cake.

Obviously I can not forget my roommates. *Intann*, *Maik*, *Leonie*, *Victor*, *Anurag* and *Hakoon* thank you so much. Thanks for all the dinners together, for all the beers between pub and home (thanks Victor). For all the tacos on Friday evenings, the walks in Sognsvann and the party party. It was fun to get drunk together and forget my name ahahah. Thank you because you supported me by understanding how difficult it was for me. It was fun to go to the stadium together. I remember when we saw Norway Vs Sweden. Damn Sweden has eliminated us. This year worldcup without Italy. Thank you for May 17th. It was great. I hope to see you soon. I would to come back to visit Oslo.

Mentre ero ancora li a giugno te ne sei andato *Jerry*. Davanti al sole di mezzanotte e a pescatori norvegesi sulla riva del mare non si sa quanto ho pianto. Per non averti salutato ancora una volta. Per non esserci stato quando stavi morendo. Sei stato il cane piu' bello e piu' bravo di tutti. Non ci poteva essere uno migliore per me. Mi manca chi ogni sera al tramontare del sole viene a bussare per il wurstel. Quando ti venivi a mettere vicino a me ogni volta che mi sedevo in giardino e salutare ogni volta che tornavo a casa. Grazie per essere stato il cane del mio cuore.

Ed adesso è arrivato il momento degli amici di sempre. Che ci sono sempre stati, e che rappresentano la mia storia.

Grazie a Bomber e Rom. *Gianluca e Mattia* ci conosciamo da non so quanto tempo. Forse ringraziarvi non ha neanche molto senso perché tanto noi staremo sempre insieme. Forse non c'è bisogno di farlo. Ormai abbiamo passato così tanto tempo insieme che siete una parte di me. In qualunque posto ci trovavamo, qualunque lavoro facevamo eravamo sempre li, sempre insieme. Quante serate insieme, quante partite a tifare Roma insieme. Quanto ci siamo divertiti insieme e quanto ancora lo faremo. Grazie perché in questi tre anni anche grazie a voi riuscivo a riderci sopra ed allentare la tensione. Qualunque cosa succedeva sempre pronti per una birra dalla meravigliosa.

Grazie a *Giorgio*. Io l'ho sempre detto che eravamo un trio perfetto con Settimio. Ogni volta hai qualcosa da raccontare, qualcosa da fare. Con te non ci si annoia mai. Mi metti allegria. Pronti per un altro capodanno insieme.

Non posso dimenticarmi di *Ludovico* ed *Edoardo*. I miei compagni di banco per eccellenza. Mi dispiace vederci solo saltuariamente. Ma il ricordo di come eravamo insieme è sempre vivo. Da delvecchio a Costanzo ahah. Le classe di delvi e cette paole mita te coddanno fazimmente ahah. Al matrimonio del capitano me avete fatto ammazza da ride.

E allora adesso devo passare a ringraziare tutta la squadra. Dal capitano *Domenico* a *Tommaso*, *Luca*, *Daniele*, *Michele*, *Mirko*, *Fabio*, *Iacopo*, *Alessandrino*, *Franz*, *Wurz*. . . . Grazie a tutti. In quel di Borgonara quante botte, quante sconfitte ahah. Ma stare con voi, giocare con voi è sempre il massimo del divertimento. Grazie per tutte le cene e gli eventi di squadra in cui se sfonnamo. Poi dimo perché perdemo sempre ahahahah.

E alla fine mi sono sentito di ringraziare anche te *Marika*. Si penso sia giusto così.

Perché comunque rappresenti il mio passato. 5 anni insieme non si cancellano così. Anzi io non voglio nemmeno cancellarli. Perché sei stata importante per me in passato. Dispiace solo sia finita così male. Ma se sono arrivato a fare il dottorato è anche grazie a te che mi hai sostenuto durante gli anni universitari.

Ringrazio la mia famiglia: *Francesco, Daniela e Alberto*.

Ringrazio Mamma e Papà perché nonostante tante incomprensioni e alcuni che sembravano punti di non ritorno, è grazie a voi se sono arrivato fin qua. Mi avete dato tanto. Vi ringrazio di avermi dato la possibilità di studiare e intraprendere il percorso che desideravo. Vi ti stimo tanto, per quello che siete e quello che fate tutti i giorni tra casa e lavoro. Non c'è una mamma e un papà più forte di voi. Mi dispiace che a volte non ci capiamo. Forse perché siamo caratteri uguali. Forse perché siamo nervosi tutti quanti. Forse perché tutti vorremmo dare di più' e non ce la facciamo, forse perché abbiamo paura o forse perché vorremmo vedere andare le cose in modo diverso. Ma il vostro affetto non mi è mai mancato. Vi voglio bene.

Ringrazio mio fratello perché quando riesce ad essere calmo e tranquillo riusciamo ancora a giocare come un tempo in cui mi divertivo a passare del tempo insieme. Basterebbe poco. In fondo so che ce la puoi fare. Basta liberare la mente da pensieri e fantasmi inutili. Sei qui con noi va tutto bene.

Ringrazio *Nonna* perché sono cresciuto forse più' con lei e zio che con mamma. Quante merende, quanti pranzi da piccolo. Adesso quanti caffè ogni giorno. Ha sempre qualcosa da mangiare per il nipote ahah. Riempie il piatto in continuazione fino a scoppiare. In linea con la tradizione calabrese. Quando se magna se fa sul serio.

Ringrazio i miei cugini *Lorenzo e Jacopo, Raffaele e Tiziana* per tutte le chiamate skype durante il periodo Norvegese.

E se la tesi l'avevo dedicata a Nonno, il mio immenso Nonno, adesso questa tesi la dedico a *Ricky*. La mia forza, il mio amico, mio zio. Tutti i giorni. Ci sono tanti modi di amare. I primi 10 anni sono cresciuto mangiando insieme e giocando a carte con te. Dormivo con te. Facevo tutto con te. E come farei senza vederti sorridere ogni giorno. Senza vedere le partite della domenica insieme. Non si può. Mi basta vederti gioire per riprendere forza. Fare qualcosa per farti stare meglio. Portarti in tutti i posti che vorresti vedere. Per farti divertire. Quando guardi fuori dalla finestra lo so che pensi. Si vede negli occhi. Forse chi non ha mai viaggiato riesce a vedere luoghi magici. Perché l'immaginazione è libera di volare. Il tuo pensiero viaggia verso posti remoti. Che non si possono descrivere. Vorrei farti vivere la magia. Almeno una volta. Spero di riuscirci. Forse se Dio da una parte toglie dall'altra dona qualcosa di straordinario. Infatti solo te hai il dono di dare gioia a tutti quelli che ti guardano sorridere. Una forza della natura che ti fa rinvenire e capire come a volte essere tristi per della cavolate è davvero stupido.

Ringrazio il *laboratorio 254-11-13* ed ogni pipetta becker, matraccio, beuta o pallone con cui abbia lavorato. Rimarrò sempre affezionato a questi posti.

Sono stati tre anni intensi. Sono entrato in un modo ed esco totalmente cambiato. Nel carattere e nella tecnica. Sono stati tre anni tosti in cui ho alternato periodi buii (alcuni davvero darkness assoluto) e periodi positivi. Sono caduto e mi sono rialzato, per poi cadere di nuovo e rialzarmi ancora. Non se sa quante volte l'ho fatto sto ciclo. Ma anche grazie a tutti voi sono riuscito a farcela e ad andare avanti.

E allora sai che ti dico. . . .spero di continuare a cadere e rialzarmi. Perché in fondo è così' che deve andare. Se vuoi veramente una cosa rischia. Se senti che ne vale la pena prova. Certo chi non rischia non cade mai. Chi rischia può cadere. Ma se non ti butti mai non vedrai mai quello che c'è dietro. L'essenza vera. Rimane solo il rimpianto di non averci provato.

Spero in futuro di avere questa forza. Ancora e per sempre. Quella di non avere

paura mai. Di niente. Di provare sempre. Di seguire l'istinto. Di fare quello che sento di fare. In tutti i campi. E se mai cadrò, di avere ancora piu' forza a rialzarmi.

E se sei arrivato fin qui ti faccio i complimenti perchè io me sarei già stufato da un pezzo de legge.....